Mauro Ferrari
Series Editor
Donald K. Martin
Editor

Nanobiotechnology of Biomimetic Membranes

Springer

Nanobiotechnology of Biomimetic Membranes

Nanobiotechnology
of Biomimetic Membranes

DONALD K. MARTIN

$\textcircled{\tiny\heartsuit}$ Springer

Editor:
Donald K. Martin
Associate Professor
Faculty of Science
University of Technology, Sydney
Broadway N.S.W. 2007
Australia
donm@uts.edu.au

PREFACE

This book is focussed on the lipid membrane, since that structure is a key component of the way that living cells are able to maintain and organise their functions. Unlocking the secrets of those membranes provides important lessons that are valuable in guiding the construction of devices to be used for medical applications. That philosophy is a central theme for scientists and engineers working in the field of biomimetics. Indeed, throughout this book we emphasise that approach in order to define the discipline of nanobiotechnology.

We define nanobiotechnology to be an interdisciplinary field of research and development that integrates engineering, physical sciences, and biology through the development of very small physical and biological devices using biomimetically inspired nano-fabrication techniques. In that sense, biomimetically-inspired means that the fabrication processes are based on the way the natural systems are constructed, usually by self-assembly of molecules in an aqueous environment.

That approach is often termed bionanotechnology, rather than nanobiotechnology. However, it is more appropriate to term the discipline that we support in the pages of this book as being nanobiotechnology. We emphasise that a significant research outcome is to exploit an understanding of biological processes in order to guide and influence the creation of devices and processes for use in biomedical applications, and this is usually defined as biotechnology. The nano prefix is necessary to accurately describe the scale of the manipulations required of the proteins, lipids and other molecules in order to create those biomedical devices and processes.

We have not broadly included the myriad of aspects of nanobiotechnology that are often included in other books that describe this discipline. We deliberately focus on the lipid membrane due to its importance in the function of the natural cells of the living organisms. Indeed, the targets of the majority of drugs and pharmaceuticals are membrane-incorporated proteins. That targeting is not by chance, since nature utilises the membrane and membrane-incorporated proteins as key components in maintaining organisation and function in the body. The separation and compartmentalisation of electrolyte concentrations within the body is maintained by the lipid membranes

and the membrane-incorporated proteins. Amongst other vital functions, that separation of electrolyte concentrations provides the electrochemical driving force for propagation of electrical "action potential" signalling in nerves and muscles. Biomedical devices based around biomimetic lipid membranes will allow improved biocompatibility and connection of the devices with the natural cells of living organisms. Perhaps the practical realisation of Drexler's robots will not be built from metal and plastic, but rather from biomimetic components utilising the principles of lipid membrane nanobiotechnology described in this book.

The book develops the principles of membrane nanobiotechnology by discussing methods to produce lipid membranes, methods of characterising lipid membranes, and the application of membranes to produce biosensors. We have addressed those topics in some depth in order to produce a reference book that is useful for researchers and senior undergraduates. The chapters have been written by friends and colleagues who are expert in the disciplines of physics, engineering, chemistry, and biology. Nanobiotechnology is the interdisciplinary glue that unites us, and I am indebted to those friends and colleagues who have generously and enthusiastically contributed the ideas and concepts described within the pages of this book. On many occasions they have forgiven my indulgences with time.

Donald K. Martin
Sydney, Australia
August, 2006

CONTENTS

3. Liposome Techniques for Synthesis of Biomimetic
Lipid Membranes 75

Stella M. Valenzuela

CONTRIBUTORS

Loïc J. Blum
Laboratoire de Génie Enzymatique
  et Biomoléculaire
EMB2/UMR 5013 - CNRS/UCBL
Université Claude Bernard Lyon 1
  43 Bd du 11 novembre 1918
F-69622 Villeurbanne Cedex
France

Till Böcking
School of Chemistry and School of
  Physics
The University of New South Wales
Sydney, NSW 2052
Australia

Agnès P. Girard-Egrot
Laboratoire de Génie Enzymatique
  et Biomoléculaire
EMB2/UMR 5013 - CNRS/UCBL
Université Claude Bernard Lyon 1
  43 Bd du 11 novembre 1918
F-69622 Villeurbanne Cedex
France

J. Justin Gooding
School of Chemistry
The University of New South Wales
Sydney, NSW 2052
Australia

Donald K. Martin
Faculty of Science
University of Technology Sydney
Broadway, N.S.W. 2007
Australia

Adam I. Mechler
Monash University
School of Chemistry
Clayton, VIC 3800
Australia

Stella M. Valenzuela
Faculty of Science
University of Technology Sydney
Broadway, N.S.W. 2007
Australia

1
The Significance of Biomimetic Membrane Nanobiotechnology to Biomedical Applications

Donald K. Martin

1.1.   Introduction

The application of nanotechnology principles and methodology to problems in biotechnology is providing an exciting discipline that will generate a revolution of novel applications in several arenas. Applications of nanotechnology range from novel nanosensors, to novel methods for sorting and delivering bioactive molecules, to novel drug-delivery systems. The philosophical approaches to finding solutions to those application areas historically have relied on engineering and the physical sciences to produce materials and processes that are then tested for efficacy in the biological environment. The difficulty in that approach is that it relies on an entirely empirical process in testing new materials or processes for compatibility in biological systems, and then subsequently for ultimate testing of the new material or process in humans. Whilst our intention with this book is not to denigrate the philosophy of that approach, nor to make claims that biological systems are completely predictable and thus able to be entirely modelled, the alternative approach that this book aims to address is that of nanobiotechnology. Put simply, the alternative that nanobiotechnology offers is to more closely utilise biological principles in guiding and influencing the materials and processes that are developed from engineering and the physical sciences for use in medical applications.

At this point it is worth considering a forward-looking paper that was published in 2001. Prokop[1] made several pertinent statements that clearly embody the philosophy of nanobiotechnology. Those statements were made especially with regard to bioartificial organs which involve the design, modification, growth and maintenance of living tissues embedded in natural or synthetic scaffolds to enable them to perform complex biochemical functions. Those thoughts exemplify the essence of the nanobiotechnological approach that this book aims to convey. Prokop[1] thought that future research in the area of bioartificial organs would

necessarily abandon the traditional concept of trial-and-error optimisation of implants in favour of the rational production of precisely formulated nanobiological devices. In particular, he considered that the concepts required were:

1. the use of molecularly manipulated nanostructured biomimetic materials,
2. the application of microelectronic and nanoelectronic interfacing for sensing and control, and
3. the application of drug delivery and medical nanosystems to induce, maintain and replace a missing function that cannot be readily substituted with a living cell and to accelerate tissue regeneration.

It is clear that all of the successful technologies that are used currently for human medical applications have been influenced by an understanding of biological principles. However, our thesis is that commencing development from a nanobiotechnology perspective will be more time-efficient in reaching an appropriate material, device or process that will be biocompatible and functional in a medical application. It follows that nanobiotechnology can be defined as an interdisciplinary field of research integrating engineering, physical sciences and biology through the development of very small physical and biological devices using biomimetically inspired nano-fabrication techniques. In that sense, biomimetically inspired means that the fabrication processes are based on the way that natural systems are constructed.

So, why another book on lipid membranes? The reason for focussing this book on the nanobiotechnology of lipid membranes is that the lipid membrane is fundamental to the organisation of biological molecules within the body. Cells in the body are enclosed by a lipid bilayer membrane, and indeed the organelles within the cell are also enclosed by a lipid bilayer membrane. It is the membrane transport proteins in the lipid bilayer, especially ion channels, which provide the fundamental electrochemical signals to maintain cell functions, including the creation of action potentials that allow communication in the nervous system. The transmembrane diffusion of electrolytes through ion channels and other membrane transport proteins provides the energy for osmotically driven fluid balance in the body. This includes the fundamental driving forces for the serous component of fluid secretion from excocrine glands, and the control of urine production in the kidneys. Drugs need to cross the lipid bilayer of cells in order to be absorbed, enter the blood or other internal fluid compartments and then provide function by binding with biological target molecules, many of which are membrane-bound transport proteins and ion channels. Also, implanted medical devices interact with the extracellular environment, and are invariably enclosed in some form of membrane.

The success of technologies for human medical applications relies on a good understanding of the interaction and incorporation of macromolecules in membranes and, indeed, the fundamental properties of the membrane itself. There is already a large biological literature on the structure and function of lipid membranes in cells. The purpose of this book is not to reproduce that extensive biological

literature, but rather to focus on the ways in which lipid membranes are incorporated into technological solutions for biomedical applications. The book contains expert chapters on methods for production and analysis of lipid membranes, functionalising lipid membranes with proteins and other bioactive molecules, and the use of such functionalised lipid membranes in biosensor applications.

We emphasise the ways that technologists can measure and utilise the biomimetic functions of lipid bilayer membranes. One of the most important of those functions is the way that nature utilises the lipid bilayer as a selectively permeable barrier for cells in order to achieve control over flows of electrolytes. Those flows of electrolytes are crucial in generating and transmitting electrical signals by nerve and muscle cells, in generating electrochemical potentials in response to external cellular stimuli by specialised sensing cells, in maintaining volume control in cells, and in secreting fluids such as saliva and tears. The selectivity in controlling flows of electrolytes is achieved by the incorporation of transport proteins, sensing proteins and transduction proteins into the lipid bilayer. With those systems included in the lipid bilayer, nature has provided the cell with an elegant sensing and transduction system.

A central concept in the flow of electrolytes across a lipid membrane is the electrophysiology of ion channels. However, in this text we will not include a detailed description of ion channel physiology. There are several excellent books and a large literature on ion channels. We will concentrate on the interaction of ion channels with the lipid bilayer membrane, as this is the interaction that needs to be understood and controlled in order to create nanotechnological solutions based on the physiology of ion channels and lipid membranes.

1.2.   Interaction of Lipid Membranes with Transport Proteins

An early study investigated the interaction of immunoglobulins with model lipid membranes produced from lecithin and which were cholesterol and which were either positively or negatively charged with the incorporation of either stearylamine or dicetyl-phosphate respectively[2]. Weissman et al[2] reported that heat-aggregated immunoglobulins were capable of releasing anions and glucose from the liposomes. Soon after that publication Sakmann and Neher[3] published their landmark paper that described ion channel activity using patch-clamp electrophysiology. Since that paper, there has been a plethora of publications that describe the electrophysiology of ion channels.

Of most relevance to the utilisation of ion channels in nanobiotechnological devices is in understanding the role that ion channels have in the cellular transduction process and the physico-chemical interaction between the lipid membrane and ion channels. All of the sensing systems in the body utilise ion channels including the specialised cells for vision, smell, taste, hearing, touch and pain. Although the exact characteristics of the ion channels may differ amongst those different sensing systems, the unifying aspect is that the ion

channel remains incorporated in the lipid bilayer and spans across the bilayer in order to transport ions. Arguably, the physico-chemical interaction between the molecules in the lipid bilayer membrane and the ion channel protein is critical to maintain the ion channel protein in an appropriate configuration in order to reliably transport ions across the lipid bilayer membrane. The lipid membrane is a dynamic fluid structure and the external forces acting on the lipid membrane are constantly changing. Thus, we will examine the nanomechanical interaction of ion channel proteins and lipid bilayer membranes as fundamental to the role of ion channels in transducing external stimuli into electrochemical signals for the body. Of significance to nanobiotechnology is the role of ion channels in facilitating an electrochemical reaction of stresses felt by lipid bilayer membranes. This system provides nature with an elegant mechanotransduction system, and it is a system that could be emulated in biomimetic nanosensors for mechanical forces, for example.

1.3.   Reaction of Eukaryotic Cells to the Physical Environment

We will first examine briefly how eukaryotic cells react to forces experienced in their surrounding environment. This background in the biology of eukaryotic cells will provide a basis upon which to appreciate the role that lipid bilayer membranes and transport proteins may play in developing those cellular concepts into nanobiotechnological devices. The pathway that we will consider involves sensing and transduction of the deformation in the plasma membrane of the eukaryotic cell, transmission of that deformation to the cell nucleus and a response generated by the cell.

The structure of eukaryotic cells is controlled by a balance of the force exerted by the extracellular matrix (ECM) on the cell and the force generated by the cytoskeleton on the ECM. The cytoskeleton maintains the cell morphology in this force balance because of its network of filamentous proteins. Ingber[4] proposed that these filamentous proteins are under constant mechanical tension to create a tensegrity structure, which hardwires the plasma membrane to the nucleus. The tensegrity structure of the cytoskeleton physically couples the cytoskeleton to the ECM and to other cells and allows an immediate response to mechanical stresses impinging on the cell plasma membrane[a] and transduced by membrane proteins that function as cell surface receptors. This concept is supported by several elegant biomechanical experiments from his group[5]. Pourati et al[6] also support this concept of the tensegrity architecture in the cell, and demonstrated that mechanical tension in the cytoskeleton is a major determinant of cell deformability in adherent endothelial cells[6]. Furthermore, their data showed that neither ATP-sensitive nor Ca^{2+}-sensitive processes were responsible. A more recent

---

[a]The plasma membrane is the outermost lipid bilayer that encloses the cell.

paper[7] presents the modified hypothesis that strain in *individual* actin filaments, rather than continuous tension in *all* filaments (tensegrity), is responsible for cytoskeleton reorganisation following ECM deformation.

Interactions between the cytoskeleton and ion channels have been documented. Structural studies indicate that cytoskeleton proteins, such as actin and the various actin-binding proteins, couple to a variety of transmembrane proteins including most ion transport molecules. Ankyrin and spectrin, for example, co-localize with the band 3 anion[8,9]. Functional interactions between the cytoskeleton and ion channels (especially Cl^- channels) have been studied in various preparations, whereby cytoskeletal filaments such as actin can regulate ("gate") ion channel activity[10,11]. On the other hand, ion channels can modulate the cytoskeleton[12,13].

One of the major cellular functions for such a mechanical transduction pathway is to facilitate the adherence of a cell to other cells (e.g. in an organ of the body) or to the ECM. The principal means for cell adhesion is by specialised proteins called "cell adhesion molecules (CAM)" that are inserted into the plasma membrane from within the cell. However, the structural and functional relationship between CAMs and ion channels has not been reported in the literature although the regulation of cytoskeletal filament assembly and maintenance of cytoskeletal organization are crucial to many aspects of cellular function[14]. Interactions between the cytoskeleton and CAMs appear to be essential for a variety of cellular functions, including cell-cell and cell-extracellular matrix interaction, cell motility, receptor-ligand interactions, and receptor internalizations[15]. Considerable evidence suggests that both actin microfilaments and intermediate filaments attach to the membrane via cytoplasmic domains of various membrane proteins including CAMs[16,17]. Among CAMs that support the attachment of cytoskeletal filaments to their cytoplasmic domains are members of the integrin and cadherin families[18,19]. Recent reports from the Pauli group[20] strongly support the hypothesis that ion channels can regulate CAMs. They have found that lung-endothelial cell adhesion molecule-1 (Lu-ECAM-1), an endothelial cell surface molecule that mediates adhesion of metastatic melanoma cells to lung endothelium, is 88% identical to a calcium-activated chloride channel described in bovine tracheal epithelium. This suggests that a CAM may function as an ion channel, although there currently is no specific literature that documents the structural or functional relation between CAMs and ion channels.

1.3.1.   Example of the Influence of Membrane Ion Channels on the Biology of Endothelial Cells

In this section some previously unpublished experimental data[b] are presented to demonstrate the linkage between CAMs and ion channels. The reason for studying the mechanistic link between ion channels and cytoskeletal proteins has

---

[b]Data kindly provided by Dr. Guo Jun Liu, produced whilst working in Dr. Martin's laboratory at the University of Technology, Sydney.

arisen from our observations that cell adhesion to substrates and morphology is altered when ion channels are inhibited[12,13,21]. We have reported this in macrophages and lymphatic endothelial cells. Other authors support our observations, in macrophages[22], endothelial cells[23] and in neurons[24].

Most authors suggest that integrins are mainly responsible for cell adhesion to a substrate. We screened lymphatic endothelial cells with 11 antibodies directed against CAMs from the major subfamilies (immunoglobulins, integrins, selectins, cadherins) that are known to be expressed on other endothelial cells. These antibodies were against **CD31** (PECAM-1, immunogloblin), **CD54** (ICAM-1, immunoglobulin), **CD106** (VCAM-1, immunoglobulin), **CD36** (platelet glycoprotein), **CD34** (lymphatic endothelial cell marker, glycosylated membrane protein), **CD54** (binds to integrins LFA-1), **CD106** (binds to integrins Mac-1), **CD62e** (ELAM-1, selectin), **CD62p** (P-selectin), **E-cadherin** and **CD44** (HCAM, lymphocyte adhesion molecule).

Our screening immunochemistry experiments indicated there was strong positive staining with only 3 antibodies, including E-selectin (CD62E), CD34 and E-cadherin (Figure 1.1). The other 8 antibodies showed either weak or no staining.

The lack of positive staining for the antibodies we used against integrins could simply be that we didn't screen enough antibodies. However, it is known that lymphatic endothelial cells lack a complete basement membrane[25] and do not stain for basement membrane markers[5].

Despite lymphatic endothelial cells lacking a substantial basement membrane, our previous experiments indicate that these cells adhere strongly to substrates and show reversible changes in morphology with ion channel inhibiting drugs[12]. Ingber's tensegrity hypothesis suggests that mechanical signal transfer across the cell surface and to the internal cytoskeleton is mediated by both integrins[5]. The lymphatic endothelial cells provide a good model to allow us to contribute additional information to this literature about cell adhesion and mechanotransduction, since these cells may not strongly express integrins but do strongly express both cadherins and selectins and show reversible morphological changes
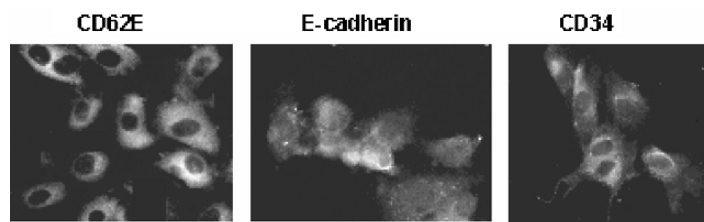
FIGURE 1.1. Fluorescence microscopy images of immunochemical binding of antibodies directed against CAMs expressed in lymphatic endothelial cells. The positive staining in the images indicates the expression of (a) CD62E, (b) E-cadherin, and (c) CD34 in the lymphatic endothelial cells (unpublished data from Dr G.J. Liu and Dr D.K. Martin).

when plated onto culture plastic. Previous authors have not studied whether the expression of CAMs is altered by disrupting the cytoskeleton.

We applied different ion channel blockers to cultures of lymphatic endothelial cells for 2 hours and measured whether the immunofluorescence of the CAMs expressed by the cells had changed. These experiments aimed to show whether the expression of E-selectin, E-cadherin or CD34 was regulated by particular ion channels. We found that 2 hours incubation with 5-nitro-2-(3-phenylpropylaminobenzoic acid (NPPB 100 μM, chloride channel blocker) **decreased** E-selectin immunostaining, but tetraethyl ammonium (TEA 10mM, potassium channel blocker) **increased** E-selectin immunostaining. As a positive control we incubated the cells with TNF-αs which is known to strongly induce CAM expression in endothelial cells[26], and found that E-selectin immunostaining was increased. Curiously, the immunostaining of both CD34 and E-cadherin was unaffected by either NPPB or TEA. Taken together, the results of these experiments suggested that the effect of the ion channel blockers was unlikely to be artifactual and that potassium and chloride channels may have different regulatory roles on CAM expression in the lymphatic endothelial cells.

In other experiments we found that NPPB 100μM applied to lymphatic endothelial cells disrupts the cytoskeletal intermediate filament vimentin. Cytochalasin D 1μM (actin-destabiliser) also disrupted vimentin probably through its actions on F-actin. The normally globular arrangement of vimentin, seen as the numerous white spots in control, was disrupted in response to either NPPB or cytochalasin D (Figure 1.2).

These results suggest an important role for intermediate filaments in linking the actin cytoskeleton with plasma membrane, and a regulatory role for chloride channels on the cytoskeleton. Previous authors have concentrated on F-actin and microtubules in studying this regulatory pathway[27].

Our earlier work with macrophages demonstrated that potassium channel inhibiting drugs disrupted the structure of F-actin, tubulin and vimentin[13]. In that publication, we also discovered that macrophages, like lymphatic endothelial cells, showed reversible changes in morphology induced by potassium channel inhibiting drugs.
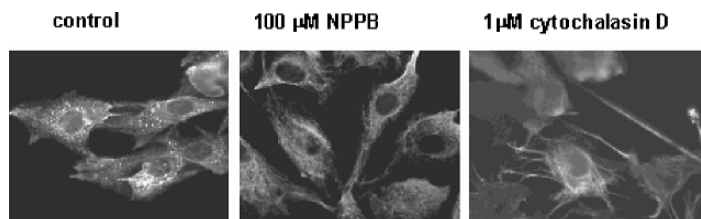
FIGURE 1.2. Fluorescence microscopy images of immunochemical binding of antibodies directed against the intermediate cytoskeletal filament vimentin in lymphatic endothelial cells. The normally globular arrangement of vimentin in the (a) control was disrupted by (b) the chloride channel blocker NPPB or (c) the actin-destabiliser cytochalasin D (unpublished data from Dr G.J. Liu and Dr D.K. Martin).

control
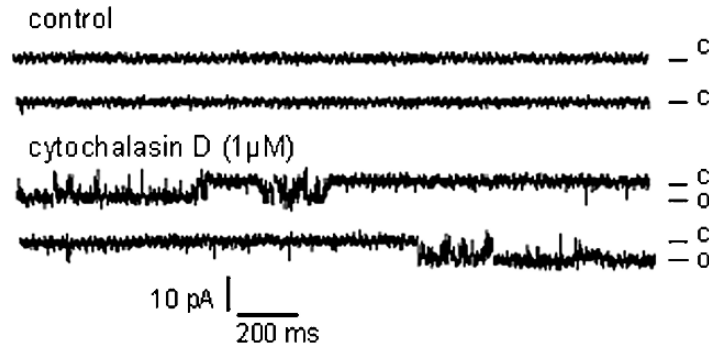
FIGURE 1.3. Inside-out patch-clamp recordings of chloride channels in lymphatic endothelial cells that were activated by the presence of cytochalasin D. The opening of the channels is indicated by downward steps (to **O**) from the closed state (from **C**, no current flow).

Most of the previous publications have reported that destabilising F-actin or microtubules affects ion channels when recorded in patch-clamp experiments[27]. In particular chloride channels are usually activated by cytochalasins. The data shown in the figure 1.3 confirm those reports, which shows activation of chloride channels in lymphatic endothelial cells by 1μM cytochalasin D. Opening of chloride channels is indicated by downward steps (to **O**) from the closed state (from **C**, no current flow).

1.3.2.   Mechanical Transduction of Stress in Lipid Bilayers

The other aspect of this mechanical transduction pathway for eukaryotic cells is the interaction of ion channels with the lipid bilayer cell membrane. Ion channels sensitive to mechanical deformation of the plasma membrane have been reported in many eukaryotic cell-types including skeletal muscle, nerve, epithelium, heart[28], macrophages[13], and smooth muscle[29]. In the specialized sensory organs, mechanosensitive ion channels are the mechanotransducers responsible for the sensations of hearing, touch and vibration, local gravity, kinesthesis, and probably osmoreception. In the viscera, such mechanoreception provides sensory feedback on organ volume and pressure. At the cellular level, mechanoreceptors are known to provide feedback for avoidance reactions in free-swimming protozoans and for the gravitational and tactile reactions of plants. Mechanotransducers are probably essential in regulating cell volume and cell division[30].

Several studies have been performed to investigate the fundamental mechanisms involved in mechanotransduction using the prokaryotic mechanosensitive ion channel MscL as a model system, since its sequence, structure and electrophysiological characteristics are well known[31]. Although MscL is derived from the *Eschericia Coli* bacterium and there is a great deal of diversity in

the conductance, selectivity and voltage dependence of mechanosensitive ion channels across species and genera[32], sequencing and structural similarities for the mechanosensitive ion channel proteins from different genera indicate that the mechanosensitive ion channels share a common ancestral origin and share a universal biophysical principle underlying the mechanosensitivity[33]. It would appear that all mechanosensitive ion channels share one distinctive gating mechanism which is governed by mechanical deformation of the lipid bilayer membrane[34].

In particular, the conducting state of such ion channels can be controlled by mechanical deformations of the cell membrane, such as due to cell division, growth and differentiation[34], thermal molecular agitation, or potentially destructive cell swelling caused by osmotic pressure gradients[35]. By considering the lipid membrane as a viscoelastic solid structure, force could be transferred to incorporated mechanosensitive ion channels via compression, expansion, thinning, bending, or extension of the lipid bilayer membrane[32]. The process of transduction of those forces to the incorporated mechanosensitive ion channel is thought to occur by a combination of global and local asymmetries in the transbilayer pressure profile at the lipid-protein interface. The two physical mechanisms that are potentially responsible for triggering the mechanosensitive ion channel gating are the energetic cost of protein-bilayer hydrophobic mismatches and the geometric consequences of bilayer intrinsic curvature[36].

The stability of the conformation of a mechanosensitive ion channel, MscS, incorporated in a lipid (POPC) bilayer was simulated using molecular dynamics modelling[37]. That molecular dynamics simulation, in a combined system of 224,340 atoms, showed that surface tension of 20 dyn/cm opened the channel for ion permeation, whereas the channel remained in a closed conformation under condition of constant pressure. Wiggins and Phillips[38] applied an analytical model for the forces and free energy generated by bilayer deformation and found support for the hypothesis that the competition between hydrophobic mismatch and tension could explain the function of the MscL channel and other transmembrane proteins[38]. Similarly, a steered molecular dynamics simulation of MscL showed that forces arising from membrane tension, especially from the cytoplasmic side of the membrane, induce an iris-like opening of the channel pore that was accompanied by tilting of the transmembrane helices[39].

A recent report suggested that the mechanosensitivity of MscL incorporated into artificial liposomes may be modulated by the influence of static magnetic fields[40]. Although the mechanisms of this effect were not clear to those authors, it appeared that the modulating effects of static magnetic fields may be mediated by changes in membrane properties due to anisotropic diamagnetism of lipid molecules. That conclusion confirmed an earlier publication, where the effects of a static magnetic field on the lipid membranes of neural cells were consistent with the slow reorientiation of diamagnetic domains within the lipid membrane and suggested tight coupling with the mechanism for neurotransmitter release[41]. The effect was limited by the mechanical constraints imposed by the interaction of the cytoskeleton with the membrane of the neural cells. It has also been reported

that lipid bilayer membranes are sensitive to electrical potential differences of as little at ± 10 mV across the membrane[42]. Such electrical potential differences caused movements of the lipid bilayer membrane of 0.5–15 nm. This effect has implications for the transduction of mechanical stimuli since this induced membrane bending will augment the gating of voltage-sensitive ion channels, especially for the case of excitable neural cells. In a subsequent study using non-excitable cells (HEK293), transmembrane electrical potential caused movement of the membrane of the HEK293 cells[43]. The magnitude and polarity of the movement was governed by cell stiffness and surface potentials. The significance of that electrically induced membrane motility is in understanding that the effect of electromagnetic forces on cells in the body could be a combination of the interaction with cellular proteins and with the lipid bilayer being able to provide a direct sensing function. Indeed, the effect of applied electrical potential can induce pore formation in lipid bilayers. Such a phenomenon is utilised in the patch-clamp technique to disrupt patches of lipid membrane in order to gain fluid and electrical access to the interior of the cell for whole-cell recording. A recent study utilised moleculr dynamics simulation to investigate this phenomenon in more detail[44]. One of the results that Tarek[44] reported was that an electric field applied to the lipid bilayer induced a significant lateral stress, which was manifested by surface tensions on the order of 1 mM/m.

1.4.   What is the Relevance of Lipid Bilayer Membranes to Nanotechnology?

The preceding sections investigated the role that the lipid bilayer membrane had in the biological function of cells. The relevance of that discussion is in being able to extract some guiding principles from nature in order to provide a basis for creating nanotechnological devices. This is the biomimetic approach. The bilayer self-assembles from lipid molecules, proteins and other molecules such as cholesterol, which is a principle that is utilised in some novel biosensors (see chapter 5). Supported planar bilayers have been used extensively in immunology to study molecular interactions at interfaces as a model for cell-cell interactions. The advantage of the supported planar bilayer system is in control of the bilayer composition and the optical advantages of imaging the cell-bilayer or bilayer-bilayer interface by various types of illumination[45]. A key question for nanobiotechnologists is why go to the trouble of attempting to replicate naturally occurring lipid bilayers?

The concept of designing phospholipid polymers to mimic the cell surface was considered more than 20 years ago. The hybrid qualities of biomembranes (polar surfaces, nonthrombogenic, low antigenic potential, and low permeability) and synthetic polymers (chemical and physical stability) suggest that polymeric phosphatidylcholines may serve as models for biomaterials design. For example, Hayward et al[46] considered that polymerization of diacetylenic phospholipids was easily attained by irradiation to produce a stable, crystalline array in which

membrane lipids could be linked covalently. Such a construction permitted the isothermal restriction in the motion of the membrane lipids, and thus was useful in basic studies of biomembranes[46]. However, in vitro experiments showed that that the polymeric phosphatidylcholines were thromboresistive, which may have been a consequence of the inability of phosphatidylcholines to participate in coagulation. The restricted lateral diffusion of proteins along a polymeric lattice will also inhibit the formation of coagulation complexes. Hayward et al[46] also suggested some other ways of exploiting polymeric phospholipids, in that:

1. existing polymers may be altered by a coating of polymeric lipid obtained by the Langmuir-Blodgett method,
2. polymerized vesicles display significant reductions in permeability and aggregation,
3. entrapment of soluble materials and reconstitution of membrane proteins may be exploited in controlled and site-directed drug delivery,
4. polymerization of cells in situ may produce "cellular capsules" with entrapped membrane and cellular components,
5. polymeric hemosomes may be capable of gas transport and may function as red cell surrogates.

The cell produces electrical signals from the diffusion of ions through ion channel proteins incorporated in the lipid bilayer. Such electrochemical signalling would allow for efficient two-way communication between cells and microelectronics, and offer exciting solutions to several problems of biosensing and implants to restore function. The microelectronics industry and human biology are separately well advanced. However, understanding the interface between a cell and the silicon chip well enough to produce reliable devices to restore or sense cell function remains a challenge.

Recent advances now offer solutions to create nanostructured surfaces on chips to improve the interface with cells and tissue. An example of such a device is a microfabricated chip that can measure the volume of small numbers of cells in real time with exceptional resolution[47]. The measurement of cell volume with this new device offers a means to quantify subtle changes in the overall metabolism of the cell, since the regulation of cell volume is one of the fundamental demands for life and it remains a universal measure of cell metabolism. For example, Ateya et al[47] have utilised their new device to screen natural compound and thus identify a peptide in spider venom that very sensitively inhibits eukaryotic volume regulation. Another application of such a novel biomimetically inspired high-throughput biosensor could be for the screening of candidate drugs for treating hypertension. It is known, for example, that the fluidity of the cell plasma membrane is lower in hypertension[48]. The volume response of cells to stimuli such as osmotic challenge would be modulated by the fluidity of the membrane. Thus, the real-time cell volume biosensor of Ateya et al[48] could provide a time-and-cost effective means of improving the drug discovery process for the pharmaceutical industry.

Indeed, identifying a cost-effective method of screening for candidate therapeutic and diagnostic drugs is a holy grail. Advances in nanotechnology can provide novel methods for efficient high-throughput systems for identifying biologically active compounds. However, these advanced systems at the nanoscale introduce several new technological challenges. The nanoscaled systems need to have appropriate microfluid flows and volumes, appropriate sensors, and appropriate interfaces between cells and silicon chips. Novel nanostructured systems are in development at major facilities in Europe, Australia, Asia, and North America and the guidance from an understanding of biomimetic systems would enhance those research efforts.

Although the incorporation of biomimetic lipid bilayers provides a significant enhancement to the biocompatibility of medical devices, there are significant concerns about the long-term stability of artificial biomimetic lipid bilayers. One of the challenges in utilising biomimetic lipid bilayers for diagnostic devices or medical implants us to improve the stability of the supported lipid bilayers. Halter et al[49] have reported that by using terminally reactive amphiphiles to build up supported lipid bilayers with cross-linked leaflets, bolaamphiphiles can be incorporated into asymmetric solid supported membranes to increase their stability in biosensor and medical implant applications[49]. Those authors demonstrated that the reactive lipids can cross-link within a lipid bilayer and are suitable for assembling supported lipid bilayers using Langmuir-Blodgett deposition (see chapter 2). A subtle modification to this strategy is through the use of crystalline bacterial cell-surface proteins (S-layer proteins) to provide a supramolecular scaffold on which to assemble lipid bilayers and other biomolecules, S-layers have proven to be suited as building blocks in a molecular construction kit involving all major classes of biological molecules[50].

A variation on utilising chemical means to strengthen the lipid molecules with cross-linking agents on a water surface is as is done in a Langmuir-Blodgett trough, is to form the supported bilayers over smaller holes in a solid substrate. This type of approach is adopted by several groups, including at the Centre d'Énergie Atomique (CEA)-LETI in Grenoble France for their Silipore® project. A recent publication exemplifed this type of approach[51]. Those authors utilised a micro-fluidic system to assemble a lipid bilayer over 100–200 μm pores in a substrate, for potential usage in an ion sensor chip or high-throughput screening device. A similar concept was utilised but with smaller pores, of 55 and 280 nm, in ordered porous alumina substrates[52]. Those nanopores in alumina allowed the formation of suspended lipid bilayers to incorporate gramicidin and alamethicin ion channels, from which there was a sufficiently high membrane resistance to make single-channel recordings.

In addition for the need to assemble stable lipid bilayers, there is the question of how well the artificial lipid bilayer can actually reproduce the conditions of the native lipid bilayer. The native lipid membrane is rarely as homogenous as the artificially assembled membranes. Some efforts have been made to create lipid bilayer membranes that incorporate phospholipid phase transitions, which renders an artificial membrane to better mimic the phase behaviour of a cell membrane

and create a more "native-like" lipid environment[53]. Shaw et al[53] created a system of nanoscale self-assembled particles called "nanodiscs", each of which contains a single phospholipid bilayer stabilised by an encircling membrane scaffold protein. A target membrane protein can be directly incorporated into a nanodisc. The nanodiscs are used to self-assemble to provide a bilayer that avoids the aggregation that often occurs in simpler bilayer systems[54].

The nanobiotechnology application of such lipid bilayers is to create nanodevices, with the most common being biosensors (see chapter 5). However, an interesting combination of layer-by-layer polyelectrolyte chemistry with lipid bilayers is in the self-assembly of virus-membrane complexes[80]. That system was a complex of cationic lipids and highly charged anionic M13 viruses, which had larger pore sizes than DNA-membrane complexes and could be used for packaging and organising large functional molecules (e.g. macroionic dyes). The applications of such virus-membrane complexes range from non-viral gene therapy to biomolecular templates for nanofabrication.

Since the first reported platform nanodevice that incorporated an ion channel in a supported lipid bilayer[55], there have been several variations on this same theme. However, the majority of such subsequent nanodevices have also relied on gramicidin[56] or alamethicin ion channels[57]. An interesting exception to that choice of channel has been the report of protein ion channels formed by the bacterial toxins Staphylococcus aureus hemolysin (alphaHL) and Bacillus anthracis protective antigen[58]. That system was produced using Langmuir-Blodgett techniques (see chapter 2), and no particular nanosensing application was investigated.

Recently, lipid bilayer membranes have been utilised as the platform for two different approaches to a nanodevice that responds to light. One nanodevice relied on lipid dyes incorporated into a Langmuir-Blodgett film, with the FRET (Forster resonance energy transfer) and FRAP (fluorescence recovery after photobleaching) to provide the readout[59]. The more recent nanodevice comprised a molecular valve embedded in a liposomal membrane and that can be opened by long wavelength UV (366 nm) light and closed by visible light. The valve consisted of the MscL ion channel that had been modified by attachment of synthetic compounds that undergo light-induced charge separation to reversibly open and close a 3 nm pore[60].

1.5. Can Biosensor Technology Benefit from Biomimetic Membrane Nanobiotechnology?

We have highlighted that one relevant application of biomimetic membranes for nanobiotechology is to construct biosensors. In the previous section we could see that the utilisation of lipid bilayer membranes in biosensors could allow the incorporation of membrane-incorporated transport proteins to provide the

transducing element. The question of how appropriate is the use of lipid bilayer membranes in the development of biosensors will be considered in greater detail in chapter 5. The purpose of this section is to highlight some concepts related to the use of lipid bilayers in biosensors.

The usage of lipid bilayers in the development of biosensors has been considered for some time. In 1988, Ligler et al[61] considered the following principles as necessary for the development of receptor-based biosensors:

1. develop asymmetric bilayer membranes with one monolayer adaptable to the particular receptor of interest and the other monolayer polymerized to enhance membrane stability,
2. introduce alamethicin and calcium channel complexes into the stabilized membrane and test for ion-channel function, and
3. fabricate a porous support for the receptor-containing membrane which is compatible with silicon technology.

Voltage-dependent anion channels were also considered as sensing elements to incorporate into lipid bilayers in order to develop a biosensor[62]. In particular, the incorporation of acetylcholine and glutamate receptors were considered as the ion channels to assist development of a new class of amperometric biosensor. That principle of utilising acetylcholine receptors was utilised in a biosensor that consisted of a stable bilayer membrane over a porous polyamide support[63]. Those authors reported that selective biosensors were made by incorporating nicotinic acetylcholine receptors (nAChRs) modified with bispecific antibodies. The nAChR channels are blocked when two bispecific antibodies that are attached to one nAChR encounter an antigen. Sensitivity to single antigen molecules would be possible by monitoring closure of individual nAChRs.

The first practical biosensor based on such principles was developed by Cornell et al[55] at the Australian Co-operative Research Centre for Molecular Engineering & Technology. That biosensor platform is being commercialised by AMBRI Pty Ltd. In that AMBRI biosensor, the conductance of a population of molecular ion channels is switched by the recognition event. The approach mimics biological sensory functions and can be used with most types of receptor, including antibodies and nucleotides. The technique is very flexible and even in its simplest form it is sensitive to picomolar concentrations of proteins. The sensor is essentially an impedance element whose dimensions can readily be reduced to become an integral component of a microelectronic circuit. It can be used in a wide range of applications and in complex media, including blood. These uses can include cell typing, the detection of large proteins, viruses, antibodies, DNA, electrolytes, drugs, pesticides and other low-molecular-weight compounds. That sensor has undergone continuing development[64], with either gramicidin or alamethicin channels incorporated into the tethered bilayer membranes[65].

Recent developments of ion-channel biosensors involve the use of gated artificial ion channels[66], engineering the transmembrane protein pore to detect

proteins[67], and investigating the use of gels such as agarose to support the lipid bilayer[68].

A slightly different approach to the development of a biosensor was based on the results of studies of cystic fibrosis, which implicated hydroxystearic acid as a contributing factor in altered biomembrane function[69]. The reason for discussing that biosensor was that the approach adopted was to guide the chemistry of the biosensor based on the biomimetics of cystic fibrosis. This approach adopted by Nikolekis et al[69] illustrates the nanobiotechnology principle. However, it was not completely understood at the time that biosensor was being developed that the pathology of cystic fibrosis is due to altered chloride ion channel function.

Around the same time as the development of the AMBRI ion-channel biosensor, a supported lipid bilayer was utilised in an acoustic wave biosensor to provide a direct immunosensing capability rather than to simply provide a support for ion channels[70]. That device was based on an acoustic waveguide geometry that supported a Love wave, with the biorecognition surface formed on a gold layer and consisting of a biotinylated supported lipid layer which specifically bound streptavidin and, subsequently, biotinylated goat IgG. The modified surface was used as a model immunosensor and successfully detected rabbit anti-goat IgG in the concentration range $3 \times 10^{-8} - 10^{-6}$ M.

In another deviation from the incorporation of ion channels in the supported lipid bilayers, a biosensor was developed that incorporated rhodopsin and transducin in a supported lipid bilayer[71]. That device served as a model system to show the feasibility to immobilize G protein-coupled receptors on solid supports and investigate receptor activation and interaction with G proteins by one-dimensional imaging surface plasmon resonance. Signal transduction by G-protein-coupled receptors (GPCRs) underpins a multitude of physiological processes. The GCPRs effectively amplify the intracellular signal that is produced after the extracellular binding of a ligand. This is an effective signalling system that has been studied extensively with both cell-based systems and assays comprising isolated signalling components. Several groups are developing biosensors based on isolated GPCRs, and the reader is directed to an excellent recent review for further details[72]. Interest and commercial investment in GPCRs in areas such as drug targets, orphan receptors, high-throughput screening, biosensors, and so on will focus greater attention on assay development to allow for miniaturization, ultra-high throughput and, eventually, microarray/biochip assay formats.

1.6. Does Biomimetic Membrane Nanobiotechnology Assist in Drug Delivery?

Lipid bilayers have been mainly used to assist in the biocompatibility of implanted drug-delivery pumps and devices. However, the more recent impacts of nanobiotechnology are to create nanocapsules to assist the delivery of drugs with low water solubility and low lipophilicity. An example of this is the

encapsulation of cisplatin, which is one of the most widely used agents in the treatment of solid tumors, but its clinical utility is limited by toxicity[73]. Those authors developed an encapsulation procedure that utilised negatively charged phospholipids to produce nanocapsules that have an unprecedented drug-to-lipid ratio and an in vitro cytotoxicity up to 1000-fold higher than free cisplatin.

However, a major problem still remains with targetting the nanocapsules to specific diseased organs to improve the efficacy and delivery of the encapsulated drug. A classical strategy is to utilise an antigen/antibody system, but that depends on identifying unique biomarkers on the target organ. Such an approach was adopted in the targetting of liposomes to infected macrophages[74]. In that example, the mannosyl-fucosyl receptors on macrophages were targetted by mannosylated or fucosylated liposomes containing the antileishmanial drug andrographolide to treat experimental leishmaniasis in the hamster model.

A nanobiotechnology approach is to encapsulate the drug in magnetic liposomes and then utilise a permanent magnet to attract the magnetic liposomes to the target organ or tumour. This approach was utilised to target magnetic liposomes with incorporated adriamycin to experimentally induced osteosarcoma in a hamster model[75]. The authors reported some success in achieving a higher concentration of adriamycon in the tumour compared to an intravenous injection of a solution of the drug. However, the clinical use of that approach would require the identification of all tumours and the implantation of permanent magnets into all of those identified tumours. Such applications of lipid bilayer nanobiotechnology will not be considered further in the subsequent chapters of this book.

1.7.   Can Implants Benefit from Biomimetic Membrane Nanobiotechnology?

We will introduce the concept of implants, but not discuss this in the following chapters. Implants and tissue engineering are well-developed applications that use several principles of nanobiotechnology. Many of the application areas are in arterial implants. Some of the early work in this field recognised the value of lipid bilayers to reduce coagulation for materials that were in contact with blood[76]. Those authors coated the surface of polymers with phosphatidylcholine polar groups to try and mimic the cell surface and improve the haemocompatibility of arterial implants. These principles of biomimicry were considered in the design of other types of arterial implants and tissue engineering, in order to provide a bioactive "living stent"[77].

With the recent advances in genetic engineering, there is considerable research in transplantation of pancreatic islet cells to treat diabetes. Such implanted tissue needs to be protected from immune rejection. The cell membrane establishes an important paradigm for the design of an effective biomimetic immunoisolation barrier for implanted islets, in addition to the capacity of the cell membrane to control interfacial mass transport[78]. Another area of implantation that will

become more significant is in neural implants. The use of nanobiotechnology to produce biomimetic surfaces for neural implants is an area of increasing research activity[79].

Whilst we will not dwell further on the detail of lipid bilayers and implants, it is clear that a lipid bilayer membrane provides a better biomimetic immunoisolation barrier and more sophisticated means of controlling mass transport into and out of the implant than would a polymeric material.

1.8.   Concluding Remarks

The remaining chapters of this book look more closely at the technical detail of the production of lipid bilayer membranes, the characterisation of lipid bilayer membranes, and how lipid bilayer membranes are relevant to the development of biosensor applications. The application of lipid bilayer membranes to biosensors provides a fundamental example of the principles of nanobiotechnology.

References

1. A. Prokop, Bioartificial ogans in the twenty-first century: nanobiological devices, *Ann N Y Acad Sci*. **944**, 472–490 (2001).
2. G. Weissmann, A. Brand, and E.C. Franklin, Interaction of immunoglobulins with liposomes, *J Clin Invest*. **53**, 536–43 (1974).
3. B. Sakmann, and E. Neher, Single-channel currents recorded from membrane of denervated frog muscle fibres, *Nature*, **260**,799–802 (1976).
4. D.E. Ingber, Tensegrity I Cell structure and hierarchical systems biology, *J. Cell Sci,*. **104,** 613–627 (1993).
5. N. Wang, J.P. Butler, and D.E. Ingber, Mechanotransduction across the cell surface and through the cytoskeleton, *Science,* **260**, 1124–1127 (1993).
6. J. Pourati, A. Maniotis, D. Spiegel, J.L. Scaffer, J.P. Butler, J.J. Friedberg, D.E. Ingber, D. Stamenovic, and N. Wang, Is cytoskeletal tension a major determinant of cell deformability in adherent endothelial cells, *Amer J. Physiol,* **274**, C1283–C1289 (1998).
7. J.H.C. Wang, Substrate deformation determines actin cytoskeleton reorganisation: a mathematical modelling experimental study, *J. Theor Biol*. **202**, 33–41 (2000).
8. P.L. Jorgensen, J. Petersen, and W.D. Rees, Identification of a Na^+, K^+, Cl^--cotransport protein of Mr 34 000 from kidney by photolabelling with [3H]bumethanide. The protein is associated with cytoskeleton components, *Biochim. Biophys. Acta*, **775**:105–110 (1984).
9. W.J. Nelson, and P.J. Veshnock, Ankyrin binding to (Na^+, K^+)ATPase and implications for the organisation of membrane domains in polarised cells, *Nature*, **328**:533–536 (1987).
10. H.F. Cantiello, J.L. Stow, A.G. Prat, and D.A. Ausiello, Actin filaments regulate epithelial Na^+ channel activity, *Amer J. Physiol*., **261**,C882–C888 (1991).
11. C.D. Lascola, D.J. Nelson, and R.P. Kraig, Cytoskeletal actin gates a Cl^- channel in neocortical astrocytes, *J. Neurosci.*, **18**, 1679–1692 (1998).

12. D.K. Martin, G.C. Boneham, B.L. Pirie, H.B. Collin, and T.J. Campbell, Chloride ion channels are associated with adherence of lymphatic endothelial cells, *Microvasc Res*, **52**, 200–209 (1996).

13. D.K. Martin, M. Bootcov, T.J. Campbell, P.W. French, and S.N. Breit, Human macrophages contain a stretch-sensitive potassium channel that is activated by adherence and cytokines. *J. Membr. Biol.*, **147**, 305–315 (1995).

14. D.E. Ingber, L. Dike, L. Hansen, S. Karp, H. Liley, A. Maniotis, H. McNamee, D. Mooney, G, Plopper, J. Sims et al, Cellular tensegrity: exploring how mechanical changes in the cytoskeleton regulate cell growth, migration, and tissue pattern during morphogenesis, *Int Rev Cytol,* **150**, 173–234, (1994).

15. D.E. Ingber, D. Prusty, Z. Sun, H. Betensky, and N. Wang, Cell shape, cytoskeletal mechanics, and cell cycle control in angiogenesis, *J. Biomech.* **28,** 471–1484 (1995).

16. E.J. Luna, and A.L. Hitt, Cytoskeleton-plasma membrane interactions, *Science*, **25,** 955–964 (1992).

17. A. Bretscher, Microfilaments and membranes, *Curr Opin. Cell Biol.* **5**, 653–660 (1993).

18. R.K. Andrews, and J.E. Fox, Identification of a region in the cytoplasmic domain of the platelet membrane glycoprotein Ib-IX complex that binds to purified actin-binding protein, *J. Biol Chem.* **167**, 18605–18611 (1993).

19. G.A. Rezniczek, J.M de Pereda, S. Reipert, and G. Wicke, Linking intregrin alpha6beta4-basal cell; adhesion to the intermediate filament cytoskeleton: direct interaction between beta4 subunit and plactin at multiple molecular sites, *J. Cell Biol,.* **141**, 209–225 (1998).

20. R.C. Elble, J. Widom, A.D. Gruber, M. Abdel-Ghang, R. Levine, D. Goodwin, H.C. Change, and B.U. Pauli, Cloning and characterisation of lung-endothelial adhesion molecule-1 suggest it is an endothelial chloride channel, *J. Biol Chem.*, **272**, 27853–27861 (1997).

21. D. Martin, J. Bursill, M.R. Qui, S.N. Breit, and T. Campbell, Alternative hypothesis for efficacy of macrolides in acute coronary syndromes. *Lancet* **351**, 1858–1859 (1998).

22. L.C. McKinney, and E.K. Gallin, Effect of adherence, cell morphology, and lipopolysaccharide on potassium conductance and passive membrane properties of murine J774.1 cells, *J. Membr Biol.* **116**, 47–56 (1990).

23. N. Wang, and D.E. Ingber, Control of cytoskeletal mechanics by extracellular matrix, cell shape, and mechanical torsion, *Biophys J.* **66**, 2181–2189 (1994).

24. D.L. Small, and C.E. Morris, Delayed activation of single mechanosensitive channels in Lymnaea neurons, *Amer J. Physiol.* **267**, C598–C606 (1994).

25. H.B. Collin, The ultrastructure of conjunctival lymphatic anchoring filaments, *Exp Eye Res.* **8**, 102–105 (1969).

26. M.P. Bevilacqua, J.S. Pober, D.L. Mendrick, R.S. Cotran, and M.A. Gombrone Jr., Identification of an inducible endothelial-leukocyte adhesion molecule, *Proc.Natl. Acad. Sci.* **84**, 9238–9242 (1987).

27. P.A. Jamney, The cytoskeleton and cell signaling: component localization and mechanical coupling, *Physiol Rev.*, **78**, 763–782 (1998).

28. F. Sachs, Biophysics of mechanotransduction, *Membr Biochem.*, **6**, 173–195 (1986).

29. G.L. Lyford, P.R. Strege, A. Shepard, Y. Ou, L. Ermilov, S.M. Miller, S.J.Gibbsons, J.L. Rae, J.H. Szurszewski, and G. Farruia, Alpha(1C) (Ca(V)1.2) L-type calcium channel mediates mechanosensitive calcium regulation, *Am J Physiol,*, **283,** C1001–C1008 (2002).

30. F. Sachs, Mechanical transduction in biological systems, *Crit Rev Biomed Eng.*, **16**, 141–169, (1988).

31. C. Norman, Z.W. Liu, P. Rigby, A. Raso, Y. Petrov, and B. Martinac, Visualisation of the mechanosensitive channel of large conductance in bacteria using confocal microscopy. *Eur Biophys J.***34**, 396–402 (2005).

32. O.P. Hamill, and B. Martinac, Molecular basis of mechanotransduction in living cells, *Physiol Rev.* **81,** 686–740, (2001).

33. A. Kloda, and B. Martinac, Common evolutionary origins of mechanosensitive ion channels in Archaea, bacteria and cell-walled eukarya. *Archaea,* **1**, 35–44, (2002).

34. B. Martinac, and A. Kloda, Evolutionary origins of mechanosensitive ion channels, *Prog. Biophys Mol Biol,,* **82,** 11–24, (2003).

35. B. Martinac, Mechanosensitive ion channels: molecules of mechanotransduction, *J Cell Sci.* **117**, 2449–2460, (2004).

36. E. Perozo, A. Kloda, D.M. Cortes, and B. Martinac, Physical principles underlying the transduction of bilayer deformation forces during mechanosensitive channel gating, *Nat Struct Biol*, **9,** 696–703, (2002).

37. M. Sotomayor, and K. Schulten, Molecular dynamics study of gating in the mechanosensitive channel of small conductance MscS, *Biophys J*, **87**, 3050–3065, (2004).

38. P. Wiggins, and R. Phillips, Analytic models for mechanotransduction: gating a mechanosensitive channel, *Proc Natl Acad Sci U S A.,* **101**, 4071–4076, (2004).

39. J. Gullingsrud, and K. Schulten, Gating of MscL studied by steered molecular dynamics, *Biophys J.*, **85**, 2087–2099, (2003).

40. S. Hughes, A.J. El Haj, J. Dobson, and B. Martinac B, The influence of static magnetic fields on mechanosensitive ion channel activity in artificial liposomes, *Eur Biophys J.* **34**, 461–468, (2005).

41. A.D. Rosen, Membrane response to static magnetic fields: effect of exposure duration, *Biochim Biophys Acta,* **1148**, 317–320, (1993).

42. J. Mosbacher, M. Langer, J.K. Horber, and F. Sachs, Voltage-dependent membrane displacements measured by atomic force microscopy, *J Gen Physiol.* **111**, 65–74, (1998).

43. P.C. Zhang PC, A.M. Keleshian, and F. Sachs, Voltage-induced membrane movement, *Nature*, **413**, 428–432, (2001).

44. M. Tarek, Membrane electroporation: a molecular dynamics simulation. *Biophys J*, **88,**4045–4053, (2005).

45. J.T. Groves, and M.L. Dustin, Supported planar bilayers in studies on immune cell adhesion and communication, *Immunol Methods*, **278**, 19–32, (2003).

46. J.A. Hayward, D.S. Johnston, and D. Chapman, Polymeric phospholipids as new biomaterials, *Ann N Y Acad Sci.* **446**, 267–281, (1985).

47. D.A. Ateya, F. Sachs, P.A. Gottlieb, S. Besch, and S.Z. Hua, Volume cytometry: microfluidic sensor for high-throughput screening in real time, *Anal Chem.* **77**, 1290–1294, (2005).

48. K. Tsuda, Y. Ueno, I. Nishio, and Y, Masuyama, Membrane fluidity as a genetic marker of hypertension, *Clin Exp Pharmacol Physiol Suppl*, **20,**11–16, (1992).

49. M. Halter, Y. Nogata, O. Dannenberger, T. Sasaki, and V. Vogel, Engineered lipids that cross-link the inner and outer leaflets of lipid bilayers, *Langmuir.* **20**, 2416–23, (2004).

50. B. Schuster, E. Gyorvary, D. Pum, and U.B. Sleytr, Nanotechnology with S-layer proteins, *Methods Mol Biol*, **300**, 101–123, (2005).

51. H. Suzuki, K. Tabata, Y. Kato-Yamada,H. Noji, and S. Takeuchi, Planar lipid bilayer reconstruction with a micro-fluidic system. *Lab Chip*, **4**, 502–505, (2004).

52. W. Romer, and C. Steinem, Impedance analysis and single-channel recordings on nano-black lipid membranes based on porous alumina, *Biophys J*, **86**, 955–962, (2004).

53. A.W. Shaw, M.A. McLean, and S.G. Sligar, Phospholipid phase transitions in homogenous nanometer scale bilayer discs, *FEBS Lett*, **556**, 260–264, (2004).

54. N.R. Civjan, T.H. Bayburt, M.A. Schuler, and S.G. Sligar, Direct solubilization of heterologously expressed membrane proteins by incorporation into nanoscale lipid bilayers, *Biotechniques*, **35**, 556–560, (2003).

55. B.A. Cornell, V.L. Braach-Maksvytis, L.G. King, P.D. Osman, B. Raguse, L.Wieczorek, and R.J. Pace, A biosensor that uses ion-channel switches, *Nature*, **387**, 580–583, (1997).

56. D. Anrather, M. Smetazko, M. Saba, Y. Alguel, and T. Schalkhammer, Supported membrane nanodevices, *J Nanosci Nanotechnol*, **4**, 1–22, (2004).

57. P. Yin, C.J. Burns, P.D. Osman, and Cornell BA, A tethered bilayer sensor containing alamethicin channels and its detection of amiloride based inhibitors, *Biosens Biolectron*, **18**, 389–397, (2003).

58. D.K. Shenov, W.R. Barger, A. Singh, R.G. Panchal, M. Misakian, V.M. Stanford, and J.J. Kasianowicz, Functional reconstitution of protein ion channels into planar polymerisable phospholipid membranes, *Nano Lett*, **5**, 1181–1185, (2005).

59. O. Worsfold, C. Toma, and T. Nishiya, Development of a novel optical bionanosensor, *Biosens Bioelectron*, **19**, 1505–1511, (2004).

60. A. Kocer, M. Walko, W. Meijberg, and B.L. Feringa, A light-actuated nanovalve derived from a channel protein, *Science*, **309**, 755–758, (2005).

61. F.S. Ligler, T.L. Fare, K.D. Seib, J.W. Smuda, A.M. Singh, O. Ahl, M.E.Ayers, A. Dalziel, and P. Yager, Fabrication of key components of a receptor-based biosensor, *Med Instrum*, **22**, 247–256, (1988).

62. D.A. Stenger, D.H. Cribbs, and T.L. Fare, Modulation of a gated ion channel admittance in lipid bilayer membranes, *Biosens Bioelectron* **6**, 425–430, (1991).

63. M. Eray, N.S. Dogan, S.R. Reiken, H. Sutisna, B.J. van Wie, A.R. Kodh, D.F.Moffett, M. Silber, and W.C. Davis, A highly stable and selective biosensor using modified nicotinic acetylcholine receptor (nAChR), *Biosystems* **35**,183–188, (1995).

64. G. Woodhouse, L. King, L. Wieczorek, P.D. Osman P, and B. Cornell, The ion channel switch biosensor, *J Mol Recognit*, **12**, 328–334, (1999).

65. P. Yin, C.J. Burns, P.D. Osman, and B.A. Cornell, A tethered bilayer sensor containing alamethicin channels and its detection of amiloride based inhibitors. *Biosens Bioelectron*, **18**, 389–397, (2003).

66. L. Husaru, R. Schulze, G. Steiner, T. Wolff, W.D. Habicher, and R. Salzer, Potential analytical applications of gated artificial ion channels, *Anal Bioanal Chem*, **382**, 1882–1888, (2005).

67. L. Movileanu, S. Howorka, O. Braha, and H. Bayley, Detecting protein analytes that modulate transmembrane movement of a polymer chain within a single protein pore, *Nat Biotechnnol*, **18**, 1091–1095, (2000).

68. Y. Matsuno, C. Osono, A. Hirano, and M. Sugawara, Single-channel recordings of gramicidin at agarose-supported bilayer lipid membranes formed by the tip-dip and painting methods, *Anal Sci*, **20**, 1217–1221, (2004).

69. D.P. Nikolelis, J.D. Brennan, R.S. Brown, G. McGibbon, and U.J. Krull, Ion permeability through bilayer lipid membranes for biosensor development: control by

chemical modification of interfacial regions between phase domains. *Analyst*, **116**, 1221–1226, (1991).

70. E. Gizeli, M. Liley, C.R. Lowe, and H. Vogel, Antibody binding to a functionalised supported lipid layer: a direct acoustic immunosensor, *Anal Chem*, **69**, 4808–4813, (1997).

71. S. Heyse, O.P. Ernst, Z. Dienes, K.P. Hofmann, and H. Vogel, Incorporation of rhodopsin in laterally structured supported membranes: observation of transducin activation with spatially and time-resolved surface plasmon resonance, *Biochemistry*, **37**, 507–522, (1998).

72. W.R. Leifert, A.L. Aloia, O. Bucco, R.V. Glatz, and E.J. McMurchie, G-protein-coupled receptors in drug discovery: nanosizing using cell-free technologies and molecular biology approaches, *J Biomol Screen*, **1–000**, October 18, doi: 1177/1087057105280517, (2005).

73. N. Burger, R.W. Staffhorst, H.C. de Vijlder, M.J. Velinova, P.H. Bomans, P.M. Frederik, and B. de Kruijff, Nanocapsules: lipid-coated aggregates of cisplatin with high cytotoxicity, *Nat Med* **8**, 81–84, (2002).

74. J. Sinha, S. Mukhopadhyay, N. Das, and M.K. Basu, Targeting of liposomal andrographolide to L. donovani-infected macrophages in vivo, *Drug Deliv*, **7**, 209–213, (2000).

75. T. Kubo, T. Sugita, S. Shimose, Y. Nitta, Y. Ikuta, and T. Murakami, Targeted delivery of anticancer drugs with intravenously administered magnetic liposomes in osteosarcoma-bearing hamsters, *Int J Oncol*. **17**, 309–315, (2000).

76. B. Hall, R.R. Bird, M. Kojima, and D. Chapman, Biomembranes as models for polymer surfaces. V. Thrombelastographic studies of polymeric lipids and polyesters, *Biomaterials*. **10**, 219–24, (1989).

77. R.S. Schwartz, W.J. van der Giessen, and D.R. Holmes Jr, Biomimicry, vascular restenosis and coronary stents, *Semin Interv Cardiol*, **3**, 151–156, (1998).

78. W. Cui, G. Barr, K.M. Faucher, X.L. Sun, S.A. Safley, C.J. Weber, and E.L. Chaikof, A membrane-mimetic barrier for islet encapsulation, *Transplant Proc*, **36**, 1206–1208, (2004).

79. W. He, and R.V. Bellamkonda, Nanoscale neuro-integrative coatings for neural implants, *Biomaterials*, **26**, 2983–2990, (2005).

80. L. Yang, H. Liang, T.E. Angelini, J. Butler, R. Coridan, J.X. Tang, and G.C. Wong, Self-assembled virus-membrane complexes, *Nat Mater*, **3**, 615–619, (2004).

2
Langmuir-Blodgett Technique for Synthesis of Biomimetic Lipid Membranes

Agnès P. Girard-Egrot* and Loïc J. Blum

Abbreviations:

A: Area per molecule	LB: Langmuir-Blodgett
AFM: Atomic Force Microscopy	LC: Liquid Condensed
DLPE: Dilauroylphosphatidylethanolamine	LE: Liquid Expanded
DMPC: Dimyristoylphosphatidylcholine	LS: Langmuir-Schaefer
DMPE: Dimyristoylphosphatidylethanolamine	MGDG: Monogalactosyldiglyceride
DOPC: Dioleoylphosphatidylcholine	DGDG: Digalactosyldiglyceride
DOPE: Dioleoylphosphatidylethanolamine	MLV: Multilamellar Vesicle
DPG: diposphatidylglycerol	OTS: Octadecyltrichlorosilane
DPPA: Dipalmitoylphosphatidic acid	PC: Phosphatidylcholine
DPPC: Dipalmitoylphosphatidylcholine	PE: Phosphatidylethanolamine
DPPE: Dipalmitoylphosphatidylethanolamine	PG: Phosphatidylglycerol
DPPS: Dipalmitoylphosphatidylserine	PI: Phosphatidylinositol
DSPC: Distearoylphosphatidylcholine	PS: Phosphatidylserine
DSPE: Distearoylphosphatidylethanolamine	R_D: Monolayer deposition Rate
ESP: Equilibrium Spreading Pressure	SAM: Self-Assembled Monolayer
FSB: Free Supported Bilayer	SFA: Surface Force Apparatus
GM1: Monosialoganglioside-GM1	π: Surface pressure
IgG: Immunoglobulin G	γ: Surface tension
incl.: included	SPM: Palmitoyl-Sphingomyeline

2.1. Introduction

One growing aspect of nanotechnology concerns the controlled elaboration of nanoscale systems. Generally speaking, nanobiotechnology requires the organization of atoms and molecules in a two- or three-dimensional space. The efficiency of the nanofabrication strategy and the recent development of methods allowing a direct characterisation at the molecular scale open a new way in the development of self-organized nanostructures. The analysis at the

---

*To whom correspondence should be addressed. E-mail: agnes.egrot@univ-lyon1.fr

molecular and supramolecular level of biological systems, like cell membranes, constitutes an outstanding model to devise "intelligent nanostructures" based on the self-molecular assembly of biological macromolecules. In this sense, biomimetic membranes, that can be self-assembled into lipid bilayers, provides the basic support structure for many applications in nanobiotechnology.

The concept of using biomolecules as an elementary structure to develop self-assembled superstructures of defined geometry has thus received considerable attention. In this way, the self-assembly ability of amphiphilic biomolecules such as lipids, to spontaneously organize into nanostructures mimicking the living cell membranes, appears as a suitable concept for the development of biomimetic membrane models. The potential of two-dimensional molecular self-assemblies is clearly illustrated by Langmuir monolayers of lipid molecules, which have been extensively used as models to understand the role and the organization of biological membranes[189] and to acquire knowledge about the molecular recognition process[44,67,82,165,190]. Langmuir-Blodgett (LB) technology allows building up lamellar lipid stacking by transferring a monomolecular film formed at an air/water interface – named *Langmuir monolayer* or *Langmuir film* – onto a solid support. When all parameters are optimized, this technique corresponds to one of the most promising for preparing thin films of amphiphilic molecules as it enables (i) an accurate control of the thickness and of the molecular organization, (ii) an homogeneous deposition of the monolayer over large areas compared to the dimension of the molecules, (iii) the possibility to transfer monolayers on almost any kind of solid substrate and (iv) to elaborate bilayer structures with varying layer compositions. Based on the self-assembled properties of amphiphilic biomolecules at the air/water interface, LB technology offers the possibility to prepare biomimetic layers suitable for immobilisation of bio-active molecules.

The development of biomimetic and functional proteo-lipidic nanostructures based on Langmuir-Blodgett technology and corresponding to highly organized molecular assemblies associating oriented biological compounds is of great interest in the nanobiotechnology field for many reasons. These reasons include, (i) used in contact with a chemical (or physical) device handling as a signal transducer, such molecular structures should open a new way in the biocatalysis investigations at a nanometric scale in a biomimetic situation. Indeed, the miniaturisation of the molecular recognition system must allow an analysis of organized biomimetic systems associating a biosensitive element; (ii) associated to microelectronic and optoelectronic devices, they should lead to the design of new bioelectronic hybrids and the development of novel nanobiosensors; (iii) deposited on an ovoid scaffold and integrating ion channels or pore proteins, they should be implied in the drug vectorisation and drug delivery.

This chapter will be concerned with the recent progress in the development of organized lipid bilayers based on the Langmuir-Blodgett technology. It focuses on the fundamental principles and practical aspects of the elaboration of biomimetic lipid bilayers through LB deposition. A brief overview on the different ways to incorporate biomolecules into LB membranes will also be presented.

2.2.   Langmuir Monolayer Formation

The Langmuir-Blodgett technology is based on the particular properties of organic molecules like lipids, phospholipids or glycolipids to orient themselves at an air/water interface between the gaseous and the liquid phase to minimise their free energy and form an *insoluble monolyer* called *Langmuir film* (Figure 2.1A). The classical materials forming Langmuir monolayers are insoluble amphiphiles, composed of two distinct molecular regions: a hydrophilic ("water loving") headgroup which is easily soluble in water, and a hydrophobic ("water-hating") tail which is soluble in nonpolar solvents. When drops of a dilute solution of an amphiphilic molecule in volatile and water-immiscible solvent such as chloroform are applied to a pure water surface, they rapidly spread over the interface to cover all the available area. After solvent evaporation, the interfacial film results in a monomolecular layer of one-molecule thick, with the headgroups immersed in the water and the tailgroups remaining outside (pointing towards the gas phase). This specific orientation is dictated by the amphiphilic nature of the molecules; also named *surfactants* for *surface active*, since they are located
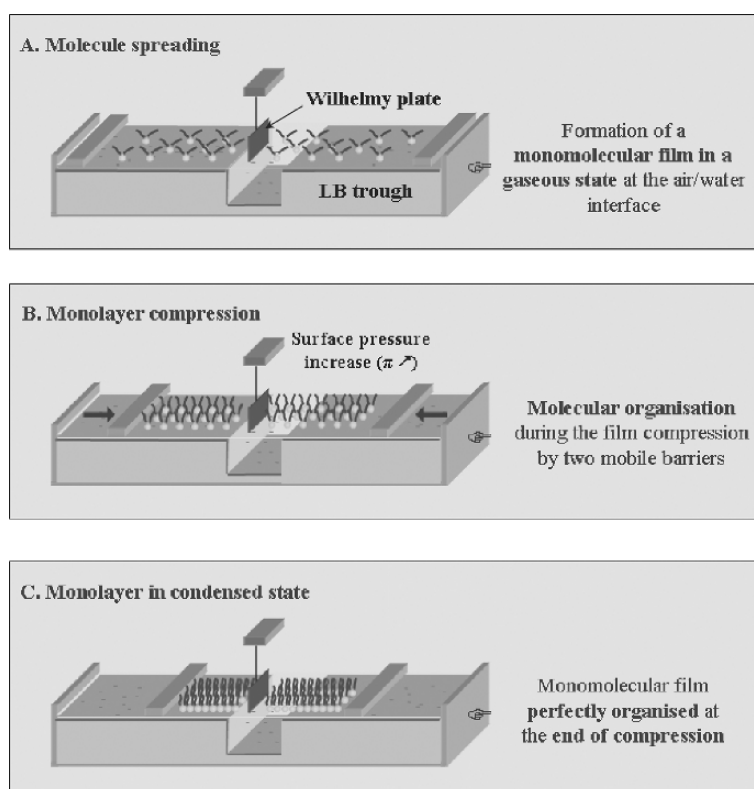
FIGURE 2.1. Langmuir monolayer formation.

at the air/water interface. The Langmuir monolayer represents an extreme case when considering adsorption to interfaces, because all the spread molecules are concentrated in a monomolecular interfacial film.

2.2.1. *Surface Tension*

The formation of an amphiphile monolayer is related to the particular thermo-dynamic properties of the air/liquid interface. The surface of a liquid has excess free energy due to the difference in environment between the surface molecules and those in the bulk. In the liquid, the molecules have a certain degree of attraction to each other. The degree of this attraction, also called *cohesion*, is dependent on the properties of the substance. In water, hydrogen bonding forces tend to set up loosely defined networks and the molecular interactions in the bulk are balanced by an equally attractive force in all directions (Figure 2.2). At the interface, a molecule is surrounded by fewer molecules than one in the bulk liquid and the equilibrium of forces is disrupted. The surface molecules experience an imbalance of forces due to unbalanced molecular attraction and a molecule at the air/water has a larger attraction towards the liquid than the gas phase. A net attractive force towards the bulk thus results from this situation and an air/water interface will spontaneously minimize its area and contract. Under this condition, the work done for extending a liquid surface is against this attractive force and consequently produces an increase of the free energy of the system. For an interface to be in equilibrium, as many molecules must leave the surface for the bulk of the liquid per time unit as diffuse from the bulk to the interface. However, due to the attractive force, more molecules will diffuse initially from the surface, thus increasing the mean atomic separation and therefore the intermolecular force between the surface molecules (Figure 2.2). The activation energy for a surface molecule escaping into the bulk will then increase until it is equal to that for molecules diffusing from the bulk to the surface, and a state of equilibrium is achieved[145]. The linear force acting on the surface molecules is the *surface tension* (γ). The thermodynamics of liquid surfaces has been initially reviewed by Birdi[19] and then by Gaines[53], and the surface tension of a plane interface can be expressed by the partial derivatives of free energy functions of the system with respect to the surface area S, as in equation 1.

$$\gamma \;=\; (\delta F/\delta S)_{T,V,ni} = (\delta G/\delta S)_{T,P,ni} \tag{1}$$

In equation 1, F and G are the Helmholtz or the Gibbs free energies of the system respectively, while temperature T, volume V, pressure P and amounts of all components n_i are held constant.

In the case of a *pure* liquid which is in equilibrium with its saturated vapour at the plane interface, the surface tension is also equal to the excess Helmholtz free energy per unit area, as in equation 2.

$$\gamma \;=\; F^s/A \tag{2}$$
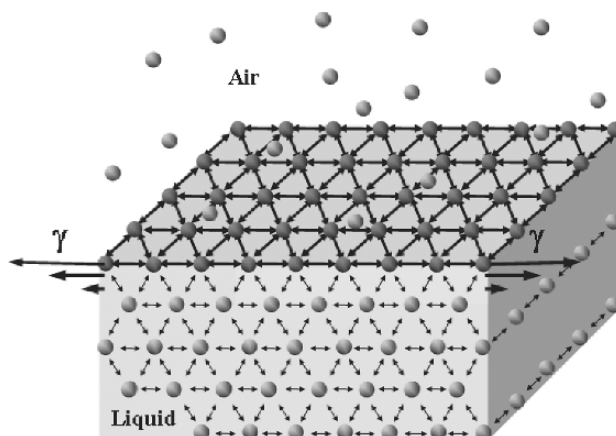
FIGURE 2.2. Surface tension at the air-water interface.

In equation 2, F^s refers to the surface excess free energy.

The common unit for surface tension is mM/m, since energy is usually expressed in $[J] = [N.m]$ and surface area in $[m^2]$. Therefore, the surface tension can also be defined in term of a force per length unit representative of the cohesive energy present at an interface. It should be noticed here that the surface tension remains constant at a constant temperature but decreases with increasing temperature.

Polar liquids, such as water, have strong intermolecular interactions and thus, high surface tension. The surface tension of water is 72.8 mN/m at 20˚C and atmospheric pressure. This is an exceptionally high value compared to most other liquids and consequently makes water as a pre-eminent subphase for monolayer studies.

2.2.2.   Surfactants

All the amphiphilic molecules are potentially surface active agents and substantially monolayer-forming materials. The reader may find a discussion on the range of a large variety of amphiphile compounds able (or previously used) to form insoluble monomolecular films in different reference books[53,145,158]. With the aim to synthesise biomimetic membranes, the most important types of amphiphilic molecules are *fatty acids*, *phospholipids* and *glycolipids*. *Cholesterol*, a type of steroid extremely abundant in the cell membrane, can also form insoluble monolayers but it is generally more studied mixed with other phospholipids[24,94,97,122,134,149,150,196,197,198] due to its implication in the formation of lipid microdomains or "*rafts*" in the cell membrane[2,26,168,169,170]. Figure 2.3 shows the principal structures of these different types of lipids and Table 2.1 gives the lipid composition of some characteristic biological membranes.

The amphiphilic nature of biological surfactants is responsible for their accumulation at the air/water interface. Their affinity for the air/water interface is

1. Phospholipids
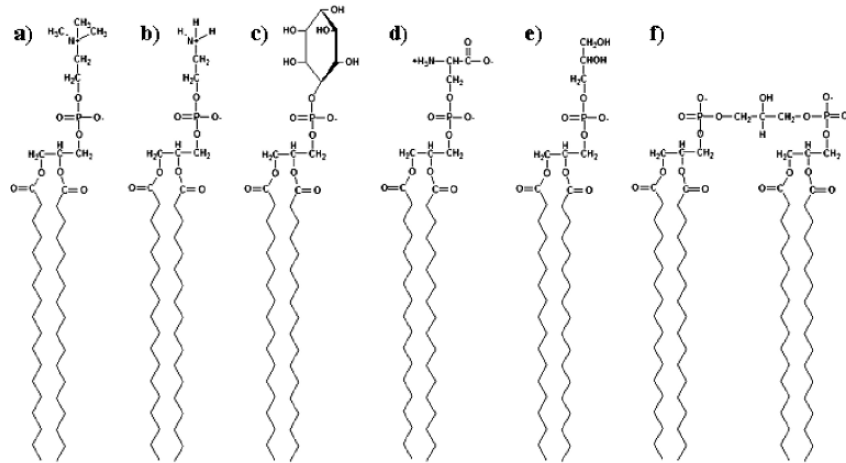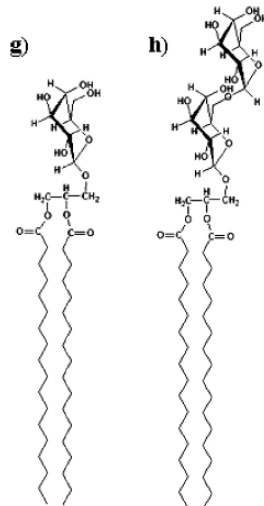
2. Glycolipids   3. Sphingolipids   4. Cholesterol
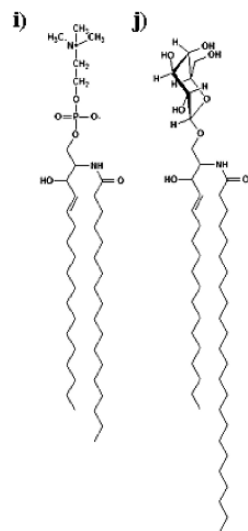
FIGURE 2.3. Structure of the main membrane lipids. 1) Phospholipids: a, phophatidyl-choline (PC); b, phophatidylethanolamine (PE); c, phophatidylinositol (PI); d, phophatidylserine (PS); e, phophatidylglycerol (PG); f, diphophatidylglycerol (DPG). 2) Glycolipids: g, monogalactosyldiglyceride (MGDG); h, digalactosyldiglyceride (DGDG). 3) Sphingolipids: i, sphingomyeline; j, galactosylceramide. 4) Cholesterol. Membrane lipids are characterized by two hydrocarbon chains per molecule (not necessarily of the same length). In the most common lipids, the fatty acid alkyl chains are usually unbranched and one of the two is often unsaturated. The double chains are essential to the correct solid geometry that allows lipids to form membranes while the unsaturated chain helps to maintain the lipid fluidity. All phospholipids have a negative charge on

TABLE 2.1. Lipid composition of some characteristic biological membranes.

	Myelin		Erythrocyte		Mitochondria		E. coli		Chloroplast	
Lipid/Protein (w/w)	3:1		1:3		1:3		1:3		1:1	
Phospholipid*	32		56		95		100		12	
incl. PC		11		23		48				
PE		14		20		28		80		
PI				2		8				
PS		7		11						
PG								15		12
DPG						11		5		
Glycolipid*									80	
incl. MGDG										41
DGDG										23
Sphingolipid*	40		18							
Sterol*	25		25		5					

* Composition given in % of total lipid amount.
Phospholipids: PC: Phosphatidylcholine, PE: Phosphatidylethanolamine, PI: Phosphatidylinositol, PS: Phosphatidylserine, PG: Phosphatidylglycerol, DPG: diposphatidylglycerol.
Glycolipids: MGDG: monogalactosyl diglyceride, DGDG: digalactosyl diglyceride.

determined by the physico-chemical properties of the hydrophilic and hydrophobic parts. The hydrophilic part confers water solubility while the hydrophobic part (most often hydrocarbon chains) prevents water solubility. The monolayer-forming abilities of the amphiphiles is dependent on the balance between these two opposite forces, which are determined by the size of the hydrophobic tailgroup (*i.e.* the alkyl chain length) and the strength of the hydrophilic headgroup (*i.e.* its size, its polarity, its charge and its hydration capacity). If the hydrocarbon chains are too short, or the polar group too strong, the material would simply "dissolve" in the subphase and could not form a stable monolayer.

For an amphiphile formed by only one alkyl chain, like the *long-chain fatty acids*, the hydrocarbon chain has to be long enough to form an insoluble monolayer (generally more than 12 hydrocarbon in the chain, $(CH_2)_n$, n>12), since the first one or two methylene groups are solubilised in the water. If the chain is shorter, these compounds are too "soluble" in water and the molecules spread on the water surface tend to form micelles above their critical micellar concentration. This formation of micelles, corresponding to water soluble entities, prevents the formation of a stable monolayer at the air/water interface. Conversely, if the hydrophobic part is dominant (chain length too long for

◀────────────────────────────

FIGURE 2.3. *(Continued)* the phosphate group at pH 7.0. The polar groups of phosphatidylcholine PC (a) and phosphatidylethanolamine PE (b) contain both positive and negative charges and are zwitterionic. The polar groups of phosphatidylinositol PI (c), phosphatidylserine PS (d), phosphatidylglycerol PG (e), contain a negative charge and are anionic. Glyco- (g, h) and sphingolipids (I, j) are neutral lipids (Petty 1996).

instance), these amphiphiles tend to crystallize on the water surface and they do not form a monolayer at the interface. In this case, a phase separation between the water and the lipid solid phase occurs. It is difficult to determine the optimal length for the hydrocarbon chain because the film-forming ability is also dependent on the polar part of the amphiphile.

Most of the lipidic cell membrane components are composed of a negatively charged or *zwitterionic* headgroup at pH 7.0 (*phospholipids*) or contain a highly hydrophilic polar group (*glycolipids*), and a hydrophobic part which is constituted by two hydrocarbon chains per molecule and drastically reduces the water solubility of the complete lipidic membrane molecule. Typically, their solubility in the form of monomers is between 10^{-12}– 10^{-10} M. Consequently, many components of cell membranes form insoluble monolayers at the air/water interface since the lipid concentration in the aqueous subphase is negligible, and some of them may be built up into multilayer films by Langmuir-Blodgett deposition (described in section 2.3).

2.2.3. Surface Pressure

As earlier mentioned, the air/liquid interface possesses an excess free energy originating from the difference in environment between the surface molecules and those in the bulk. The spontaneous formation of a monolayer when an amphiphilic surfactant is placed on a liquid surface will affect the surface tension. The surface tension can be viewed as a negative pressure due to the attractive interactions of the water molecules at the interface, which will be lowered by accumulation of the amphiphiles at the air/liquid interface. The presence of a monomolecular film on a liquid surface invariably results in a reduction of the free energy of the system due to the creation of interactions between the hydrophilic polar group and the water surface molecules, thus reducing the surface tension. The resulting effect of the reduction of the surface tension leads to an expansion of an air/water interface in the presence of surfactants.

When the area of surface available to the interfacial film is large and the amount of surfactants sufficiently low to limit the interactions between adjacent amphiphiles molecules, the monolayer has a minimal effect on the liquid surface tension. If the available surface area to the monolayer is reduced by a compression system comprised of mobile barriers (Figures 2.1B & 2.1C), the intermolecular distance decreases and the surface tension is lowered. The amphiphile molecules (mainly their hydrocarbon chains) start to interact and exert a repulsive effect on each other. The force exerted by the film per unit length, corresponding to a two-dimensional analogue of a pressure, is called *surface pressure* (π). It is equal to the reduction of the pure liquid surface tension by the presence of the interfacial film, as in equation 3.

$$\pi = \gamma_0 - \gamma \qquad (3)$$

In equation 3, γ_0 is the surface tension of the pure liquid and γ is the surface tension of the film-covered surface. It results from this equality that the maximum surface pressure for a monolayer on water surface at 20°C is 72.8 mN/m, and normally encountered values are much lower. The formation of a monolayer at the air/water interface is usually monitored by recording the surface pressure (π) – area (A) isotherm diagram, which will be discussed in the next section. Two fundamentally different approaches can be used to measure the surface pressure in the interfacial film during the monolayer compression: the *Langmuir balance* and the *Wilhelmy plate*.

The *Langmuir balance* method corresponds to the differential measurement of the force acting on a movable float separating a clean portion of the water (or aqueous) surface from the surface covered with the monolayer (Figure 2.4). The amplitude of the force exerted by the film, leading to a discrete displacement of the float (expansion of the monolayer-covered surface), is directly measured by a conventional balance connected to the float. The displacement of the float is usually small ($\sim$10 μm) and conveniently measured using a displacement transducer[158]. In this system, the force F acting on the float to move it a distance of dx and to expand the monolayer-covered surface of dS_m (*i.e.* reduce the clean water surface of dS_0) is related to the surface pressure π by equation 4.

$$F dx = \gamma dS_m - \gamma_0 dS_0 = (\gamma_0 - \gamma)dS = \pi \cdot l dx \qquad (4)$$

In equation 4, $dS_m = -dS_0$, and l is the width of the monolayer. Then, the surface pressure is obtained from equation 5.

$$\pi = F/l \qquad (5)$$
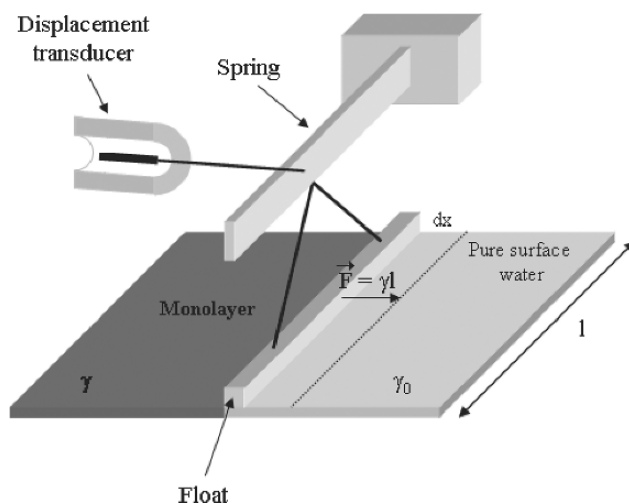
FIGURE 2.4. Principle of the Langmuir balance.

This technique was the first used by [101] to measure the surface pressure of a liquid covered by a thin film.

The *Wilhelmy plate* method is based on an absolute measurement of the force due to the surface tension on a plate, usually made of platinum or filter paper (ashless Whatman Chromatography paper Chr1), partially immersed in the subphase (Figure 2.5). The measurement is first performed on a clean surface and subsequently on the same surface covered by the monolayer. The variation due to the alteration in the surface tension is then converted into surface pressure with the help of the dimensions of the plate. Indeed, the forces acting on the plate consist of downward forces, such as gravity and surface tension, and upward force, such as the buoyancy due to the displacement of water. For a rectangular plate of dimensions L, w, and t, of material density ρ_p, immersed to a depth h in a liquid of density ρ_L, the net downward force, F_0, in the absence of a monolayer, is given by equation 6.

$$F_0 = \rho_p gLwt + 2\gamma_0(t+w)cos\theta_0 - \rho_L gtwh \tag{6}$$

In equation 6, g is the gravitational constant and θ_0 is the contact angle of the liquid on the solid plate [158].

With a monolayer-covered surface, the expression of the force, F_m, exerted on the plate is described by equation 7.

$$F_m = \rho_p gLwt + 2\gamma(t+w)cos\theta_m - \rho_L gtwh \tag{7}$$

In equation 7, θ_m is the contact angle of the liquid covered by the monolayer on the solid plate.
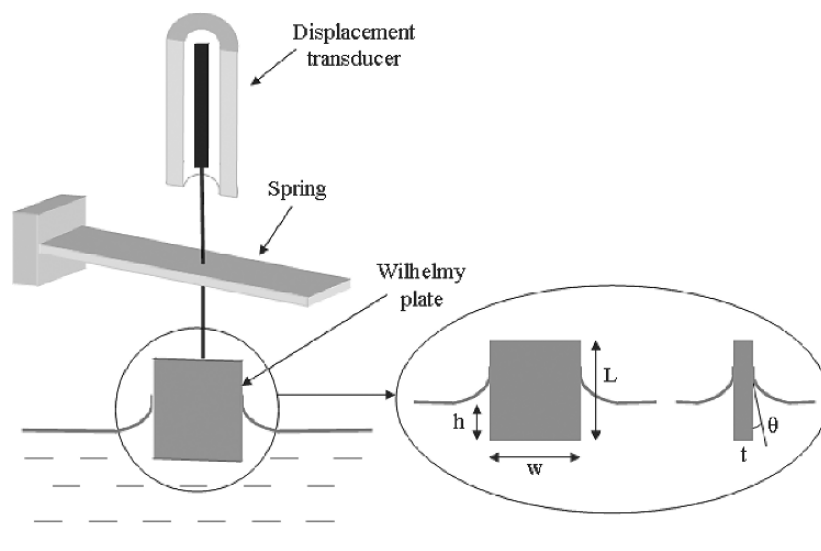
FIGURE 2.5. Principle of the Wilhelmy plate method.

The measurement of the change in the force exerted in the presence of the monolayer on a stationary plate (h maintained constant) is related to the change in surface tension by equation 8.

$$\Delta F = F_m - F_0 = 2(t + w)(\gamma cos\theta_m - \gamma_0 cos\theta_0) \qquad (8)$$

If the plate is completely wetted by the liquid, the contact angles equal zero, and if it is thin enough so that t«w, then the change in force can be expressed as in equation 9.

$$\Delta F = 2w(\gamma - \gamma_0) = 2w\Delta\gamma \qquad (9)$$

Thereby, the surface pressure, π, equal to the reduction of the pure liquid surface tension by the film, is related to the change in the force, ΔF, by equation 10.

$$\pi = -\Delta\gamma = -\Delta F/2w \qquad (10)$$

Most of available commercial systems are now equipped with a Wilhelmy plate. The forces are generally measured with a sensitive electrobalance directly coupled to the plate. The sensitivity is around 10^{-3} mN/m. Alternatively, the force exerted vertically on the plate by the surface tension can be transformed into a small displacement by means of a spring, which is conveniently measured using a displacement transducer (Figure 2.5). One important drawback of the Wilhelmy method is the change in contact angle when the plate is covered with monolayer material. It appears from equations (8) and (9) that the surface pressure measurement requires a precise knowledge of the contact angle value. A zero contact angle value is ensured when a freshly cleaned plate is immersed in the clean liquid surface and becomes perfectly wetted. However, a change in contact angle occurs if monolayer material is deposited on the plate. This artefact may be obviated by using a fresh, clean and appropriate material for each experiment. Other experimental deviations may nevertheless appear, especially for very rigid monolayers, owing to the movement of the Wilhelmy plate[35].

2.2.4.   *Surface Pressure (π) – Area (A) Isotherms*

The surface pressure (π) – Area (A) isotherm is a plot of the change in surface pressure as a function of the area available to each molecule on the aqueous subphase surface. This isotherm is the most common indicator of the monolayer formation and monolayer properties of an amphiphilic material. The isotherm is measured at constant temperature, usually under a pseudo-equilibrium condition, by continuously compressing the monolayer while monitoring the surface pressure. (Equilibrium values could be recorded by on a point-to-point compression process).

In a typical experiment, the amount of surfactants initially spread is sufficiently low so that the molecules are far enough apart on the water surface.

Under this condition, the molecules exert only small forces on one another and the resulting monolayer can be regarded as a *two-dimensional gas* due to the large distances between the molecules (Figure 2.1A). In the gaseous state, the monolayer has relatively little effect on the free energy of the aqueous subphase, even though the surfactant molecules have a natural tendency to aggregate. Therefore, the liquid surface tension remains unchanged and the surface pressure is very low (<1 mN/m). When the available area of the monolayer is reduced by a mobile compression barrier system the molecules become closer together, the intermolecular distance decreases and the surface tension diminishes. The hydrocarbon chains of the molecules begin to interact and the surface pressure start to increase (lift-off point). During the monolayer compression, the amphiphilic molecules self-organize and the monolayer will undergo several phase transformations analogous to the three-dimensional gaseous, liquid and solid states to finally form a floating monolayer perfectly ordered at the liquid surface. During this process, the hydrophilic and hydrophobic ends of the molecule ensure that the individual molecules are aligned in the same way (Figures 2.1B& 2.1C).

As the molecules forming Langmuir monolayers are insoluble amphiphiles, the total number of molecules unchanged during the whole compression. The a*rea per molecule*, which represents the mean area available to each molecule, is usually calculated by dividing the film area - determined by the barrier position during the compression - by the total number of molecules spread on the water surface. The *area per molecule*, A, is usually expressed in $Å^2$ or $nm^2.molecule^{-1}$. The continuous monitoring of the surface pressure as a function of the area per molecule gives rise to the surface pressure/area (π-A) isotherm diagram of the monolayer. Figure 2.6 depicts schematic π-A isotherms classically recorded for long-chain fatty acids (lipids with one alkyl chain) and phospholipids (natural membrane lipids presenting two alkyl chains). These diagrams are not meant to represent that observed for any particular substance, but shows most of the features obtained for these two classes of biological surfactants.

A number of distinct regions, named *phases*, can be distinguished on examining the isotherm. These phases are characteristic of different aggregation states that the molecules adopt in the monolayer during the compression and are identified as discontinuities in the isotherm. They correspond to various molecular organisations in which molecules have different degrees of freedom. They result from the molecular interaction forces occurring between the molecules in the floating film, and between the film and the subphase: the different monolayer states are both dependent on the van der Waals forces between the hydrocarbon chains, which are responsible for the cohesion within the film, and the magnitude of the attractive and repulsive forces existing between the headgroups. At a large area per molecule, the monolayer exists in the gaseous state (G, in Figure 2.6). The molecular interactions are small and there is no lateral adhesion in the interfacial film. The hydrophobic chains are distributed near the interface and present a large degree of freedom. This phase is generally encountered for a surface pressure lower than 0.5mN/m. As the gaseous phase is compressed, the hydrocarbon chains start to lift away and a first-order transition
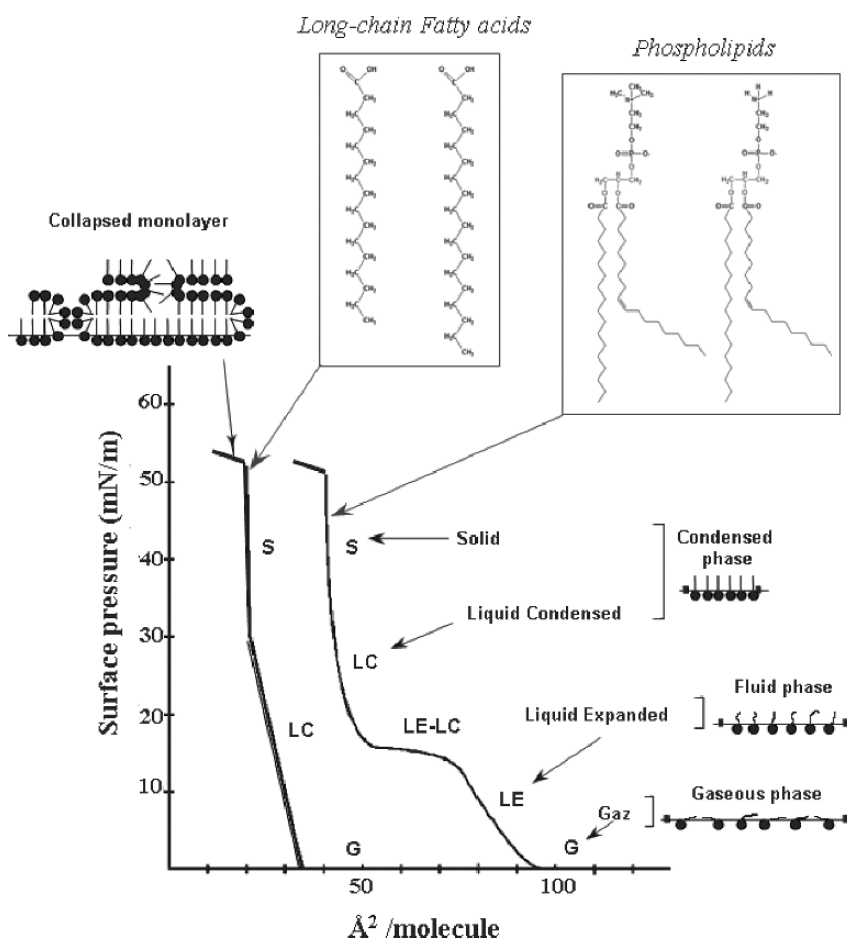
FIGURE 2.6. Schematic π-A isotherms of long-chain fatty acids or phospholipids. The overall shape of the isotherms mainly depends on the subphase temperature, the hydrocarbon chain length and the presence of unsaturated acyl chains.

from the "gas" to "liquid" state occurs. Usually, this is accompanied by a constant plateau region in the isotherm occurring at a surface pressure lower than 1mN/m owing to the weakness of interactions between the tailgroups. However, this portion of the isotherm is often not resolved by the Wilhelmy plate. As the surface area of the monolayer is further reduced, the liquid state, called "Liquid-Expanded" (LE) is formed. In the LE phase, the monolayer becomes coherent, but the molecules still possesses degrees of freedom. The hydrocarbon chains in such a film are randomly oriented and still present *gauche* conformations. In the expanded phase, the area per molecule varies considerably with the surface pressure and no relation between the observed molecular area and the dimensions of the constituent molecules is apparent: the area per molecule is larger than the area associated with the cross-section of cylindrical alkyl

chains (*i.e.* ≈0.19 nm^2 per unit). Under further compression, a second first-order thermodynamic transition from the liquid to the condensed states can occur in the monolayer. This Liquid Expanded - Liquid Condensed (LE-LC) transition phase is characterised by a second constant pressure region in the isotherm which occurs at area per molecule comprised between 0.6 and 0.8 nm^2.molecule^{-1} for phospholipid monolayers. In the LE-LC phase transition, condensed lipid domains appear in the expanded phase. The coexistence of both condensed and expanded phases may be directly observed in the floating monolayer by Brewster angle microscopy[188] or by fluorescence microscopy after incorporation a small fluorescent dye probe into the film[98,114]. As the molecular area is progressively reduced, condensed phases (*i.e.* Liquid Condensed, LC, or Solid, S, state) may appear (Figure 2.6). The terms "condensed phases" included in fact different monolayer states similar to mesophases found in the smectic liquid crystals and presenting a well-defined *in-plane* structure[145], which can be characterised by X-ray diffraction[95]. In the condensed phases, the monolayer presents a strong lateral cohesion. The molecules are closely packed. The hydrocarbon chains are crystallized and uniformly oriented. The area per molecule is approaching that of the molecular cross-section (≈0.2nm^2.molecule^{-1} for fatty acids and ≈0.4–0.5nm^2.molecule^{-1} for phospho- and glycolipid molecules), thus confirming the interpretation of the condensed monolayers as a two-dimensional solid. The various states of the condensed monolayers are assumed to be related to different interactions and to different arrangements of the polar and hydrocarbon chain groups. For fatty acid monolayers, the transition between the different condensed phases are characterised by a decrease of tilt angle of the alkyl chains from the normal to the interface and for the highest surface pressures, the chain axes are vertically oriented. Finally, if compression is further applied to the monolayer, the phenomenon of *collapse* occurs at smaller surface areas. It is due to mechanical instability at very high surface pressures and molecules are forced out of the interfacial film. The monolayer loses its integrity. Molecular layers are riding on top of each other and disordered multilayers are being formed (Figure 2.6). The onset of collapse depends on many factors including the rate at which the monolayer is being compressed and the history of the film (ageing time).

The phase behaviour of the monolayer is mainly determined by the physical and chemical properties of the amphiphile. As shown in Figure 2.6, the liquid expanded state cannot exist and a direct transition from the gas to the condensed phase can take place. This behaviour is generally obtained for fatty acids with a long hydrocarbon chain, for which van der Waals forces between the hydrocarbon chains are largely responsible for the phase transitions. For the phospholipid or glycolipid molecules, which contain two hydrocarbon chains per molecule, the size of the hydrophilic headgroup influences the hydrocarbon chain packing, and consequently, the molecular aggregation state in the condensed monolayer. In a general manner, because of their polarity, size, shape, interaction with water and/or the neighbouring headgroups, many polar groups strongly influence the arrangement of the hydrocarbon chains and hence the characteristics of the π-A isotherm. It must be stressed here that the shape of the isotherm also depends

on the experimental conditions (*e.g.* temperature, pH, subphase composition), the hydrocarbon chain length, and the presence of unsaturated alkyl chains (disruption in the chain ordering). For instance, different transition phases can be observed when the subphase temperature varies. Reducing the temperature or lengthening the chain both enhance the intermolecular (chain-chain) interactions, tending to make the film more coherent and ordered (extension of the LC phase with a clear fading of the LE-LC transition). Hence, an increase (or a reduction) in the saturated chain length can, to some extend, be traded for a reduction (or an increase) in temperature [10,158].

In a general manner, π-A isotherms provide information on the monolayer stability at the air/water interface, the reorientation of the molecules in the two-dimensional system, and the existence of phase transitions and conformational transformations [182]. For detailed discussions on π-A isotherms, Readers can refer to different books and reviews dedicated to Langmuir and Langmuir-Blodgett films [43,53,145,158,182].

2.2.5. *Monolayer Stability*

The monolayer stability and hence, the monolayer homogeneity is one of a prerequisite to elaborate organized lipid Langmuir-Blodgett films with a high structural quality. Monolayer stability mainly depends on the monolayer dissolution into the subphase and on the mechanical stability in order to resist overcompressions.

In most cases, when a lipid monolayer is compressed, it is not in a perfect stable thermodynamic equilibrium. To be in a stable equilibrium, the monolayer should not be compressed at surface pressures exceeding the *equilibrium spreading pressure, ESP*. This equilibrium surface pressure is defined as that spontaneously generated when a crystalline sample of the solid material is placed in contact with a pure water surface[93]; the monolayer formed by molecules detaching from the crystal surface and spreading over the subphase is, thereby, in equilibrium with the crystals themselves. In other words, the *equilibrium spreading pressure* corresponds to the equilibrium pressure between the monolayer, the two-dimension state, and the crystal, the three-dimension state. This means that at any surface pressure higher than this, the monolayer has a tendency to aggregate into crystals by a nucleation and crystalline growth process. This process can be understood by comparison with the formation of an equilibrium vapour over a bulk solid. An equilibrium vapour exists for the solid in presence of its vapour. If this vapour is exceeded, *i.e.*, the vapour becomes *supersaturated*, molecule deposition onto the solid surface can occur. This should be also the case for the compressed monolayers which are expected to form crystals at surface pressures greater than *ESP*[145]. On a practical point of view, the equilibrium state between the monomolecular film and the solid crystal is fortunately most often approached very slowly, and the *ESP* is generally not attained in the course of an experiment. In many experiments, seemingly stable surface pressures up to higher values than *ESP* may be reached. The practical benefit of such a situation is the possibility

to handle interfacial films over a long period of time (if the surface pressure is not too high) without discernible loss of monolayer integrity (*e.g.* without slow collapse occurrence).

As already mentioned, the stability of the monolayer also depends on the solubility of the amphiphile monomers in the subphase. However, for insoluble amphiphilic molecules, a barrier to dissolution exists and the equilibrium with saturated subphase concentrations may be approached very slowly. Noticeably, compressed monolayers made of biological amphiphile molecules are stable over a long period of time without noticeable effect of the material dissolution (section 2.2.2).

Even if the processes responsible for the monolayer instability take long periods of time, it is important to consider that a floating monomolecular film is in a *metastable state* rather than in an absolutely stable equilibrium state and consequently, monolayer homogeneity (integrity) can be lost if the monomolecular film is not cautiously handled. Several factors can enhance the monolayer stability prior its transfer. These factors include the presence of multivalent ions in the aqueous phase as well as the subphase pH, which were found to play a critical role in determining the stability and the transferability of ionised monolayers. The influence of mono-, di- and trivalent ions has been then widely investigated[17,23,27,52,55,99,109,111,195] and even if it appears difficult to draw a universal phenomenon, some generalities can be highlighted. The interaction of divalent metal ions with the acid headgroup of fatty acids seems to depend on their electronegativity[41,151,164,203]. While metal ions with higher electronegativity interact covalently, those with lower electronegativity interact electrostatically. Such interactions affect the packing behaviour of the alkyl chains[164]. Complexes of metal ions with the acid headgroup of fatty acids generally causes the monolayer to be more condensed[103], and usually, more easily and more uniformly transferred. It can be noticed that the waiting times allowed for solvent evaporation prior to compression or after monolayer compression (*relaxation time*) can also influence the monolayer stability. In most cases, the monolayer is not completely stable after compression, but stabilises after some time. In a general manner, the monolayer stability can be checked either by measuring the decrease in surface pressure when the area is held constant, or by recording the decrease in film area when the surface pressure is kept constant[53]. Another way of checking monolayer stability corresponds to the dynamic cyclic π-A isotherms, also named *hysteresis experiments*. In such an experiment, the monolayer is successively compressed to a fixed surface pressure and then, relaxed to the original state. Some hysteresis phenomenon during the first compression/decompression cycle is normally observed, even for stable monolayers. It has been mainly ascribed to a difference in the *aggregation* (organisation of the molecules at the compression) and *relaxation* (disorganisation of the molecules at the decompression) processes, due to the 'non-return' of domains formed during the compression to their original state after decompression[177,92]. For poorly stable monolayers, a continuous shift of hysteresis loops towards lower mean molecular areas is observed in consecutive isotherms. This

can be attributed to a loss of film-forming molecules into the bulk (monolayer dissolution) or to molecular over-riding to form bi- and multilayer structures (monolayer collapse)[43]. As will see below, the stability of the floating monolayer is a crucial parameter to obtain high quality Langmuir-Blodgett films. Depending on the material being investigated, repeated compressions and expansions may be necessary to achieve a reproducible isotherm trace and produce a stable monolayer.

2.3.   Langmuir-Blodgett Technique

When the surface pressure is sufficiently high to ensure lateral cohesion in the interfacial film, the floating monolayer can be transferred, like a carpet, from the water surface onto a solid plate "substrate". There are a number of different ways in which the monolayer may be transferred. This section is concerned exclusively with the universally known Langmuir-Blodgett technique[20,21], involving the vertical movement of a solid substrate through the monolayer/air interface.

2.3.1.   *Vertical Film Deposition Principles*

Depending on the nature of the substrate, the first monolayer will be transferred as the substrate is respectively raised (*immersion*, or downstroke) or lowered (*emersion*, or upstroke) through the interfacial film (Figure 2.7). The monolayer is usually laid down during emersion of a hydrophilic substrate when the hydrophilic headgroups interact with the surface. If the substrate surface is hydrophobic, the monolayer will be transferred during immersion when the hydrophobic alkyl chains interact with it. For a hydrophilic surface, the substrate may be immersed into the subphase before the monolayer formation. After transfer of the first monolayer, a hydrophilic substrate becomes hydrophobic and a second monolayer will be deposited at the immersion. Conversely, a hydrophobic substrate becomes hydrophilic and the second monolayer will be transferred during the emersion. Subsequently, multilayers will build up by successive depositions of single layers on each traversal of the surface (*i.e.* the monolayer/air interface). Such a deposition mode called *Y-type* (Figure 2.7b) leads to a stack in head-to-head and tail-to-tail configuration, which is the most representative of the natural lamellar stacking of the biological membrane. Although this is the most frequently encountered situation, instances in which the floating monolayer is only transferred at the immersion (*X-Type* deposition, Figure 2.7a) or the emersion (*Z-type* deposition, Figure 2.7c) of the substrate have been reported. The type of deposition is mainly determined by the amphiphilic balance of the molecules and the nature of substrate (whether it is hydrophilic or hydrophobic) but it also depends on the dipping conditions (section 2.3.2). Surface pressure, deposition speed, pH, temperature and composition of the subphase, may affect the deposition mode[20,51,53,146]. Furthermore, mixed deposition types (*XY-type*) are sometimes encountered and the deposition

Vertical transfer onto solid support
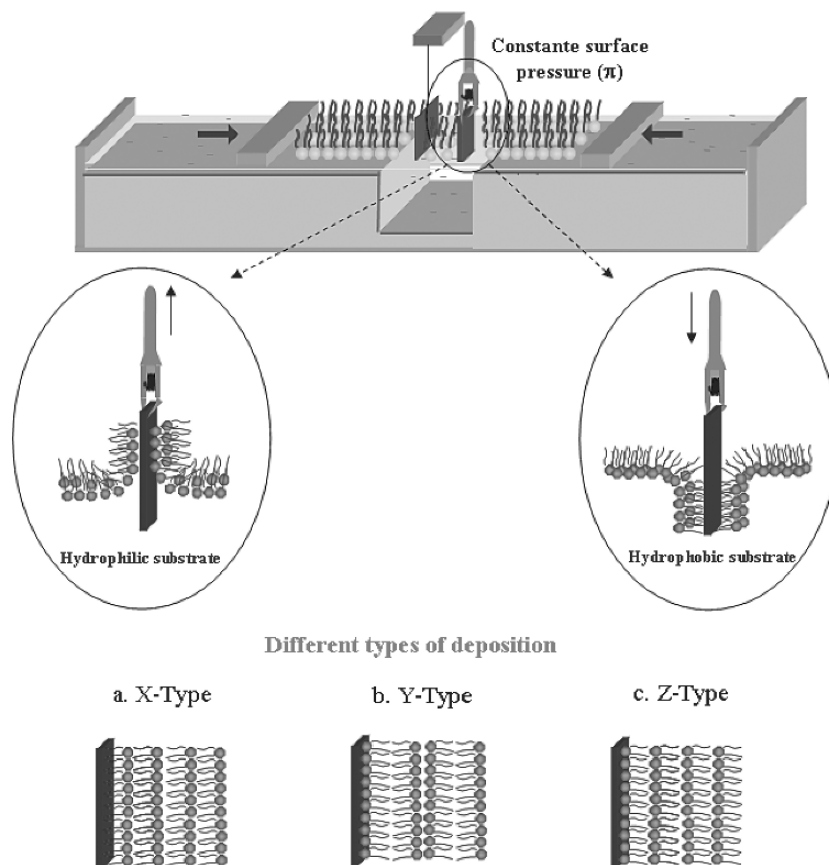
FIGURE 2.7. Langmuir-Blodgett deposition.

type can change as the LB films are built up. XY-type films refers to deposition in which monolayers are completely lay down each time the substrate is being lowered into the subphase, but partially transferred as the substrate moves up through the monolayer/air interface[77,79,85,161]. Despite extensive experimental evidence and a number of theoretical treatments of LB deposition[34], the detailed mechanisms by which the monolayers are transferred has never been completely explained[146]. Many phenomena noted by the original workers, including the different modes of film transfer and the variation at which different materials can be deposited remain not totally understood.

At this stage of the discussion, it must be emphasized that the diagrams shown in Figure 2.7 are simple sketches, which may not always accurately represent the real molecular arrangements on the substrate. For many fatty acid LB films in Y-type form, the long molecular axes can be inclined to the substrate

normal and the tilt angle will depend on the precise deposition conditions[139]; the molecular tilt may also change from layer to layer. In spite of suggested explanations[79,85], the molecular mechanism of the particular X-type transfer process (but also Z-type) is not yet clarified. Some reorganization may occur in the stacking during or shortly after the dipping process[74]. For instance, simple molecules would invert at some stage during the substrate immersion, when the film is inside the subphase water ('detach-turnover-reattach' mechanism), so that the structure finally produced is essentially identical to that of Y-films. For fatty acids, early experiments using X-ray diffraction revealed that the spacing between hydrophilic headgroups was nearly the same, and equal to twice the hydrocarbon chain length, whether they have been deposited as X-type or Y-type films[15,45,84]. It is noteworthy however that in a general manner, the lipids of biological interest normally deposit as Y-type films. The discussion in this chapter will therefore be restricted to the Y-type deposition.

2.3.1.1. Transfer Process Energy

The Y-type deposition is the most usual mode of multilayer formation for amphiphilic molecules in which the headgroup is very hydrophilic and the tailgroup is an alkyl chain. The transfer process energy during the deposition of a monolayer onto a substrate has been studied in detail by measuring the vertical force on the substrate during the dipping procedure[161]. This measurement has been performed by inserting a microforce transducer between the substrate and the dipping arm. This experiment is very similar to the Wilhelmy plate measurement of the surface tension. The vertical net force exerted onto the substrate during the transfer is the same as that measured by the Wilhelmy plate. However, the contact angle is not equal to zero during the transfer process. After subtraction of Archimedes flotation effects, the work of immersion and emersion of the substrate has been determined by integration of the immersion/emersion force cycle recorded during the transfer. Formal analysis shows that deposition during immersion will only occur if the interaction energy between the tailgroups per unit area is higher than the surface tension in the presence of the interfacial film. This implies that there exists a maximum value of the surface tension γ, that is to say a minimal surface pressure π value, beyond or below which deposition will not occur. Indeed, as we will see in the next section, monolayer transfer is often achieved in the condensed state since a minimum surface pressure is a necessary prerequisite to ensure sufficient cohesion in the interfacial film for an efficient transfer. The measurements of the integrated work of emersion indicate that emersion transfer process requires additional energy due to the headgroup dehydration between interlayers. Accordingly, the condition for deposition at emersion requires a high value for head-head interaction energy per unit area, which must be higher than twice the polar group dehydration energy (dehydration of both interfacing layers) in addition to the surface tension γ at the monolayer/air interface. Therefore, the Y-type film formation appears to be greatly dependent on the fact that head-head interactions are usually stronger than tail-tail interactions. For very hydrophilic headgroups, Y-type is the most

stable deposition mode, since the interactions between adjacent monolayers are either hydrophobic-hydrophobic or hydrophilic-hydrophilic. Hydrophilic interactions are, nevertheless, also dependant on pH variations and the presence of multivalent ions in the subphase. Hence, addition of divalent cations into the subphase and/or modification of pH can modify the type of deposition[8,9,79,136], by changing the extent of dehydration and/or the energy interaction between the interlayer headgroups.

2.3.1.2.   Contact Angle Values

The other point that must be highlighted and which modifies the nature of the deposition is the dynamic contact angle value between the liquid covered by the monolayer and the substrate coated by transferred layers (*i.e.* the contact angle value of the *meniscus*). As suggested in early reports for a successful deposition [18], the contact angle must be obtuse (>90°) for the downstroke and acute (<90°) for the upstroke. If the contact angle remains obtuse during the upward motion or acute in the downward direction, no layer will adsorb onto the substrate and the multilayers will built up as an X- or Z-film respectively. Such an hypothesis has been more recently verified by precise measurements of the forces[29], the work[161] of emersion and immersion during the transfer process, and by a precise analysis of the dynamic contact angle during deposition of docosanoic acid monolayers from $CdCl_2$ subphases as a function of pH[9]. The transfer efficiency effectively decreases when the contact angle increases form 0 to 90° on substrate emersion. By extrapolation, the authors determined that no transfer occurs if the contact angle equals 90°. However, as will seen in section 2.3.2, an optimal contact angle of 50°– 60° is required for an optimal deposition of a tightly bound monolayer to the substrate surface at the first upstroke (*reactive deposition*). To obtain an efficient transfer at the downstroke, the contact angle must be slightly higher than 90°. The optimal value is located in the range of 95° to 110°.

Numerous papers report contact angle measurement in order to get insight into the deposition process and to elucidate the molecular rearrangement mechanism arising from the XY- and X-type deposition[34,54,129,130]. Some results indicate that the dynamic contact angle on the upstroke is smaller for the first layer directly transferred on a hydrophilic surface than for the subsequent layers. For instance, the difference between the dynamic contact angles of the film-covered subphase on clean mica and during polar deposition on a lead stearate multilayer has been estimated to be approximately 18°[137]. On the other hand, the angle for the downstroke is established with the first layer. This means that one monolayer is sufficient to mask completely the substrate, and it is in agreement with the observation that the nature of the substrate influences the deposition of the first layer. Indeed, the molecular interactions involved in the deposition of the first layer may be quite different than those responsible for the transfer of the subsequent layers, especially for the hydrophilic interactions. Saint-Pierre and Dupeyrat[161] have reported that the values of the work at the first immersion or emersion according to the nature of the substrate are always different from the subsequent values. For the sake of completeness, we can mention that in some

cases, the difference between the immersion and withdrawal angles decrease with increasing the film thickness for the first 18 layers[159], which is coherent with the possible evolution of the deposition type as the LB films are built up. In a same way, Saint-Pierre and Dupeyrat[161] reported that the work of emersion and immersion transfer vary slowly when the number of transferred layers increases, even for Y-types films. Finally, it is important to notice that variations in the contact angle value that create instabilities in the height of meniscus during the substrate motion leads to a non-homogeneous deposition of the monolayer. Such instabilities have been however recently explored in the nanobiotechnology field for patterning lipidic LB film surfaces[68,117,125].

2.3.1.3.   Deposition Ratio

The transfer of the monolayer onto a solid substrate is usually characterised by the *deposition* (also named *transfer*) ratio. To be quantitatively transferred, the monolayer must be held at a constant surface pressure during the deposition process. To achieve this, the barrier advance compensates the surface pressure decrease. This allows the measurement of the *deposition ratio*, which is used as an indicator of the quality of deposition. The deposition ratio is defined as the decrease in the area occupied by the monolayer on the surface water divided by the coated area of the solid substrate. The transfer is the most efficient when the transfer ratio equals one. Such a transfer ratio of unity is often taken as a criterion for good deposition, and under most circumstances the orientation of the molecules on the substrate would be expected to be very similar to their orientation on the water surface[76]. An ideal Y-type film is in turn a multilayer system with a constant transfer ratio of one for both up and down directions[85]. However, it must be highlighted that the transfer ratio is sometimes higher (>1) for the first layer, because of the microscopic heterogeneities of the surface of the substrate. There are also cases where the transfer ratio is <1, but remains constant as the dipping proceeds. This consistent deviation from unity would point out the molecular orientation is changing during the deposition process. However, a value outside the range 0.8 to 1.20 suggests poor homogeneity of the transferred film. Variable transfer ratios are almost always a sign of unsatisfactory film deposition.

2.3.1.4.   Advantages and Caution

The LB technique offers the possibility to perfectly control each step of the LB film preparation (monolayer formation, substrate preparation, dipping procedure). The main advantage of the membranes obtained by LB deposition lies in the achievement of a molecular arrangement perfectly organized at the water surface, which can be maintained during the transfer onto the solid support when all the parameters are controlled and optimised. Stringent conditions are required for obtaining reproducible results with Langmuir and Langmuir-Blodgett films. Very subtle changes in the experimental conditions may result in dramatic changes in the deposition process. In this connection,

readers can find a detailed description of fundamental experimental require-
ments (*e.g.*material purity, selection of suitable spreading solvent of high
grade purity, accurate weighing of monolayer material, subphase quality made
of ultrapure water, precise subphase temperature control, surface cleaning,
trough environment, clean and vibration-free environment for carrying out the
experiments, monolayer spreading, substrate preparation) in different reference
books[145,158]. The Y structure makes LB films ideal candidates for developing
biomimetic models of natural membranes.

2.3.2.   *Elaboration of Organised Lipidic LB Films*

As mentioned above, the Langmuir-Blodgett technique is an attractive method
for preparing well-organized and structured films as lipid bilayers. However, the
development of highly sensitive methods of surface analysis has revealed some
defects in lipid LB films, including disclinations[180], in-homogeneous crystalline
domains[133], pinholes [13,14,42,107,156], local collapse[36], vacancies[162], transbilayers
and lateral heterogeneities[157]. These defects can be harmful for some appli-
cations such as molecular electronic devices which have specific functions at
the molecular level. Conversely, some applications, like patterned surfaces, are
not disadvantaged by generating discontinuous structures in LB films to create
nanoscale stripes and channel patterns in LB bilayers[68,117,124,125]. However, the
achievement of biomimetic membranes and their applications in nanobiotech-
nology, particularly in the development of novel nanobiosensors, cannot be
performed if lipid LB films are not perfectly structured and homogeneous.

The molecular organization in the LB film depends greatly on the quality
of the floating monolayer. Many types of defects found in the LB films can
occur before transfer. Such defects are due to the structure and the loss of
monolayer integrity during the time elapsed between the spreading and dipping
of the monolayer (ageing time)[11,91,192]. Therefore, as mentioned earlier, the first
and obvious crucial parameters will be the homogeneity and the stability of
the monolayer at the air-water interface. Once the stability of the interfacial
monolayer has been fully studied (section 2.2.5) the transfer process can be
addressed.

Additionally, the interfacial changes from an air/water to an air/solid interface
can impose some strong attractive interactions between the molecules and
the hydrophilic (or less often hydrophobic) substrate, which can modify the
molecular packing[71,155,172,173,175]. For some materials, a liquid to solid phase
transition can occur in the meniscus region at surface pressures lower than that
of the LE-LC transition indicated by the π-A isotherm[154]. Distinct phase changes
from a LC phase on the water surface to a closer-packed solid crystalline form
on the solid substrate have been also reported[112,113,140,141]. In the same way, some
fatty acid monolayers transferred in the LE region often condense to form close-
packed LC islands on the substrate[166,167,185]. Consequently, a growth of solid
domains can occur in the monolayer that is being transferred or immediately after
deposition. This change in the molecular arrangement will sometimes generate

defects, which will then grow up in the multilayer structure if the deposition is epitaxial[107]. In the case of fatty acids, electron diffraction experiments have shown each monolayer has the same local orientation of its molecular lattice as that of the underlying layer [143].

The adhesion of the first layer to the underlying substrate is particularly critical and will determine the quality of subsequent layers. This adhesion depends on the nature of the substrate and the attraction forces between the lipid head (or tail) group and the hydrophilic (or hydrophobic) substrate. Pre-treatment of the substrate (*e.g.* silanization, vacuum metal deposition, metal oxidation, lipid pre-coating) can favour the attachment of the first monolayer. Onto metallic substrates, for instances, there may be an ion exchange between ionisable polar group (like those of fatty acid salts) and the thin oxide layer on the substrate surface[144]. Consequently, a strong chemical bond can anchor the polar groups of the first layer to the substrate surface, creating adhesion so strong that only chemically destructive treatments can remove it. It is likely that under such a condition, the chemical and physical structure of the first monolayer will be different to that of subsequent layers. However, for subsequent monolayers transferring onto existing film, the deposition will be homogenous[145].

Mainly two parameters have been identified to be crucial for a high quality deposition: the *deposition speed*, from which depends the quality of the molecular interactions between the substrate and the layers, and the *transfer surface pressure*, from which depends the lateral cohesion of monolayer, but also its homogeneity.

The speed at which the substrate is moved through the monolayer can be different between the up- and down-stroke, and between the first layer and the subsequent ones. As the substrate is lowered into the subphase, it can be moved quite rapidly without affecting the monolayer transfer. In this case, the deposition of the monolayer mainly depends on the hydrophobic interactions and consequently on the transfer surface pressure (section 2.3.1). Conversely, the rate at which a substrate can be withdrawn from the water partly depends on the dynamic properties of the floating monolayer and partly on the rate at which the liquid subphase drains from the monolayer/solid interface[76]. For example, a highly viscous monolayer will be unable to adjust itself so as to maintain a homogenous film in the neighbourhood of a rapid moving substrate. The drainage of the subphase, not only due to gravity, is the result of the adhesion of the monolayer onto the solid material acting along the contact line with the monolayer and driving out the water film (headgroup dehydration). A *reactive deposition* thus occurs when molecules can adsorb spontaneously onto the substrate at the same speed as a new clean area becomes available during the withdrawal of the substrate. In this case, the transfer is accompanied by draining of the subphase, no subphase entrainment occurs and the monolayer becomes tightly bound to the solid, expelling the water layer rapidly. Under this condition, the dynamic contact angle formed by the water meniscus against the solid substrate as it is withdrawn from the subphase (referred as the "zipper angle" by Langmuir in 1938) is around 50°–60°[53] as earlier observed by Langmuir[102].

If the speed at which a new clean substrate area is created during the substrate removal is higher than the rate of the process of this molecular adsorption, the monolayer is practically forced onto the substrate and subphase entrainment occurs (*non-reactive deposition*). Under this condition, the meniscus is distorted and advances faster than the precursor film in the front of the monolayer can adsorb on the substrate. The value of the dynamic contact angle decreases and the substrate comes out wet when it is near to zero[53]. In this case, the monolayer shows a poor adhesion to the substrate and waiting for a complete drying of the water-supported monolayer is necessary to avoid the transferred layer to be re-spread at the subsequent substrate dipping. Then, it appears that the rate at which LB films can be built-up is mainly limited by the rate at which ascending substrate sheds water. In molecular terms, it means that the interactions of the molecules in the monolayer frontier with the substrate determine the success of the deposition at a given rate. The rate at which the water layer is expelled during the transfer process has been referred as the deposition speed[53]. It is important therefore to not raise the substrate faster than the speed at which water drains from the solid. The withdrawal velocity of the substrate must be lower than (or identical to) the adsorption process of the monolayer. The drainage speed depends both on the crystallised state (which increases with the time that the monolayer remains on the subphase water, *i.e.* the ageing time),[142] and on the intrinsic viscoelasticity properties of the floating monolayer[28]. Indeed, the surface viscosity must be below an optimal value for successful deposition. If the viscosity is too high the monolayer will be brittle easily broken on withdrawal (or insertion) of the substrate. Such a rigid monolayer presents a lack of flexibility to ensure the torsion necessary for the meniscus formation during the transfer process. A typical speed of $10\mu m/s$ to a few mm/s can be used for the transfer of the first layer onto a hydrophilic substrate. Once the first layer is adhering to the substrate, faster speeds can be applied to deposit the subsequent layers (up to several cm/s).

The optimal value of the surface pressure to produce the best results depends on the nature of the monolayer and is often established empirically[76]. However, the LB deposition is traditionally carried out in the condensed phase since it is generally believed that the transfer efficiency increases when the monolayer is in a close-packed state. In that condition the surface pressure is sufficiently high to ensure a strong lateral cohesion in the monolayer (section 2.2.4), so that the monolayer does not fall apart during the transfer process. Although the optimal surface pressure depends on the nature of the material constituting the film, biological amphiphiles can seldom be successfully transferred at surface pressures lower than 10 mN/m and at surface pressures above 40 mN/m, where collapse and film rigidity (brittle monolayers) often pose problems.

For fatty acids, the condensed state is reached for a surface pressure considerably higher than the equilibrium spreading pressure, ESP (section 2.2.5). So, the transfer of the monolayer is often achieved with an overcompressed monolayer, which does not represent an absolutely stable equilibrium system with respect to the bulk crystal phase. Therefore, it must be keep in mind that even if the

monolayer remains in this *metastable* state for an extended period of time, enabling meaningful experiments to be performed, the monolayer integrity must be preserved during the time elapsed for the transfer process (ageing time). In order to develop a highly organized biomimetic LB structure, a rational approach was first proposed in our group to avoid defect appearance in the condensed monolayer as it gets old (ageing). This approach mainly focuses on the method used to achieve the compression. Indeed, the nucleation crystal growth which occurs when a floating fatty acid monolayer ages has been demonstrated to not only depend on the surface pressure but to be also directly related to the compression procedure[126]. The compression procedure defines the early stages of the monolayer compression which affects the monolayer integrity. It is now well-known that aggregation of the solid condensed domains can start in the gaseous phase[43,188]. Thus, in order to obtain homogeneous LB films, the monolayer must be slowly compressed in order to avoid any surface local overcompressions that would be responsible for the crystal defect appearance through a slow collapse mechanism[126]. The precise compression speed depends on the nature of the lipid molecule and its equilibrium surface pressure. Moreover, to improve the monolayer stability during the time necessary for the transfer process, the transfer surface pressure must be poised at the beginning of the solid phase. This optimizes the compromise between the quantitative transfer of the monolayer, which needs a sufficient lateral cohesion, and the number of crystal defects, which can appear in the ageing floating monolayer.

Finally, a new parameter, referred as the *monolayer deposition rate* (R_D), has been introduced so as to preserve the monolayer integrity during the transfer process. This parameter has been defined as the lipid area deposited onto the substrate within one minute. The parameter R_D takes into account not only the dipping rate but also the coated area of the substrate, and it corresponds to the actual velocity at which the monolayer is removed from the water surface. Consequently, R_D controls the monolayer compression rate during the transfer process, which directly modulates the kinetics of the crystal defect appearance in the floating monolayer[57]. Finally, by adding divalent cations and adjusting the pH value of the subphase accordingly, both the stability and the integrity of the floating fatty acid monolayer can be successfully increased to form LB films of very high quality[106]. By using such an optimal transfer procedure, highly organized behenic acid LB films have been obtained on different hydrophilic or hydrophobic substrates[59].

2.3.3.   *Phospholipid LB Films*

In the context of biomimetic studies, LB films made of phospholipids or glycolipids will be more relevant since they are the essential components of biological membranes. Those molecules are complex lipids conmprising two hydrocarbon chains per molecule (not necessarily of the same length) and a large hydrophilic polar headgroup that is more or less hydrated (Figure 2.3). The primary hydration shell surrounding the phospho- and the glycolipid headgroup

is in rapid exchange with the bulk phase. This shell is constituted of 5 to 20 water molecules for phosphatidylethanolamines (PE) and phosphatidylcholines (PC) respectively[56]. The sugar headgroups of monogalactosyldiglycerides have much higher degrees of hydration than phosphatidylethanolamines[164]. Hence, some difficulties have been encountered to transfer phospholipid and glycolipid monolayers. Since the phospholipid and the glycolipid headgroup may have a stronger affinity for the water subphase than for the hydrophilic substrate[153], the first layer can be transferred at the upstroke by wetting of the substrate and slipping of the monolayer[161]. However, a poor adhesion of the first layer on a hydrophilic support leads the monolayer to peel off the substrate and to respread on the water surface at the second immersion in the subphase. A forced-deposited film will be easy to remove due to the lack of adsorption of the monolayer (lack of polar headgroup dehydration). Consequently, this first deposited phospholipid layer may be then stripped off during the subsequent immersion, as it has been once again recently reported by Hughes *et al.* for the transfer of the dimyristoylphosphatidylcholine (DMPC) monolayer[87]. Under such circumstances, despite the repeated dipping, only one monolayer will be deposited on the slide. To solve this problem, Tamm and McConnell[176] have proposed a combined approach to elaborate phospholipid bilayers on hydrophilic substrate, in which the first layer is transferred by vertical Langmuir-Blodgett (LB) deposition and the second one by horizontal Langmuir-Schaefer (LS) method (Figure 2.8). In this latter method, the substrate horizontally oriented with the face coated by the first layer lying parallel to the air-water interface is slowly lowered until the whole face is in contact with the floating monolayer, allowing tail-to-tail interaction. The substrate is then pushed through the interface for the deposition of the second layer[40,72,83,193].

Many phospholipids including phosphatidylcholines[30,87,89,115,128,133,138,156,171,179], phosphatidylethanolamines[13,14,78,89,163,171,179,207], and phosphatidic acids[37,38,73,116,118,121,179,183] have been examined for LB deposition. Depending on the nature of the phospholipid and on the experimental transfer conditions (*e.g.* cations, nature of the substrate, surface pressure, transfer speed) different types of phospholipid LB films have been described (Y- or Z-deposition). However, as the interactions between the phospholipid headgroups in the multilayer structure are often weaker than the interactions between the polar groups and the water subphase, the forces implied during the transfer process are not sufficient to pull up the monolayer from the water surface, and only few phospholipids such as phosphatidic acids, can form LB multilayers of more than five layers. To overcome such a difficulty, the mixture of different types of phospholipids (phosphatidylcholines and phosphatidic acids for instance) or of phospholipids with fatty acids can sometimes favour the transfer of phospholipidic monolayers[58,78]. Moreover, it must be emphasised that the transfer ratio value for the deposition of the second layer after transfer of the first one onto a hydrophilic substrate (*i.e.* the outer leaflet of the bilayer) is generally lower than the desired value of unity. A typical deposition ratio value for the transfer (at the downstroke) of a second phospholipid monolayer,
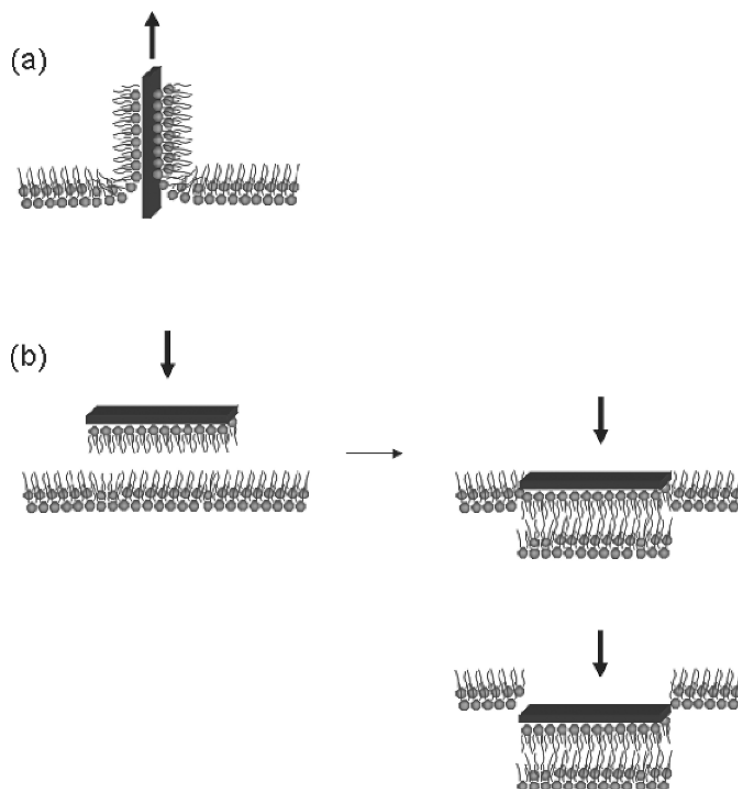
FIGURE 2.8. Mixed monolayer-deposition mode. The first layer is deposited by vertical Langmuir-Blodgett (LB) deposition (a); the second layer is deposited horizontal Langmuir-Schaefer (LS) procedure.

when hydrocarbon chains of the first phospholipidic layer are pointed outside, is often between 0.5 and $1.0^{13,30,87,121,125,156}$. A possible explanation for this experimental observation has been proposed by Bassereau and Pincet[13]. By using transfer ratio measurements and tapping mode atomic force microscopy (AFM) experiments, these authors suggest that during the deposition of the second monolayer, some lipid molecules of the first monolayer can desorb from the substrate and move over to the interfacial monolayer. This desorption phenomenon has been related to the balance between the adsorption energy of the molecules on the solid substrate and their energy at the air-water interface. In this case, the transfer ratio will reflect the balance between molecules of the interfacial film being transferred onto the substrate and molecules desorbing from the substrate. Therefore, the fact that the transfer ratio value differs from the unit is not a proof (under this condition) for a low transfer quality but it could be equally well interpreted as desorption from the substrate of some phospholipid molecules.

Desorption of lipids of the first monolayer during the transfer of the second monolayer has been shown to be responsible for the origin of the subnanometre bilayer-deep holes in different phospholipid LB bilayers[13,125,156,162] The incoming phospholipids thus cover only the hydrophobic surface of the first monolayer, resulting in lipid-bilayer-covered regions in contact with water that coexist with bare mica. The hole defects range in size from 30 nm (the order size of the AFM tip radius) up to 500 nm[13] and depend on the film transfer pressure, the deposition speed, the number of defects in the lower layer, the type of lipids used and the phase state of the lipids transferred[13,156]. Indeed, it has been reported that the shape of the defects is influenced primarily by the constituents of the first leaflet[156]. The density and the size of the holes decrease as the transfer velocity and the deposition surface pressure increase[13]. Fewer defects appear when the second leaflet is transferred at higher surface pressures[14,128,156]. The percentage of uncovered substrate in bilayers with a second leaflet deposited at a high surface pressure (monolayer in a more condensed phase, typically Liquid Condensed phase) is lower than in bilayers with a second monolayer deposited at a low surface pressure (loosely packed monolayer, typically Liquid Expanded phase). Generally speaking, a higher transfer surface pressure (but see section 2.3.2) leads to the formation of more uniform and tightly packed phospholipid bilayers with fewer pinhole defects[128,199]. Recently, the quantity of the defects (holes of $\leqslant 0.5\,\mu$m) has been correlated to the stability of the bilayers measured by surface force apparatus (SFA)[14]. The condensation state of the floating monolayer that has to be transferred likely determines how many lipids molecules of the first layer leave the substrate during deposition (determining the amount of defects in the bilayers). Since the desorption depends on the balance between the adsorption energy onto the hydrophilic substrate and the affinity for the air/water interface, the decrease of the surface tension when the floating monolayer is compressed limits the affinity of the polar group for the water interface and favours the adsorption onto the hydrophilic substrate[13].

The presence of defects tunnelling both leaflets (holes perforating) in the supported phospholipid bilayers appeared surprising at first because the same lipid systems self-assemble in aqueous solution into tightly sealed vesicular bilayers. But, as reported by Bassereau and Pincet[13], the desorption phenomenon is probably common in any supported bilayer system and has been observed previously by different groups. However, as recently described by Benz *et al.* [14], the formation of holes in supported membranes may be related to the existence of pores in free bilayer membranes[200].

To circumvent this problem of desorption and to improve the transfer characteristics of the phospholipids, it is necessary to enhance the adhesion of the first layer to the substrate. By adapting the procedure optimised for the transfer of a fatty acid monolayer (*i.e.* by adjusting the *monolayer deposition rate* (R_D) according to the size of the immersed substrate area and by positioning the transfer surface pressure at the beginning of the steep rise of the LC phase in the π-A isotherm diagram), dipalmitoylphosphatidic acid (DPPA) and

dipalmitoylphosphatidic acid – dipalmitoylphosphatidylcholine (DPPA-DPPC) mixed monolayers (molar ratio 2:1) have been efficiently transferred in the Y-type form from a pure water subphase onto different hydrophilic substrates[58]. However, depending on the nature of the substrate (fluorine, glass or silicon), an evolution of the deposition type from the Y- (for the two or three first bilayers) to the Z-type has been observed as the number of deposited layers increased. Such an evolution occurs through an intermediate type, now referred as "*YZ-type*". By analogy with the XY-type, "*YZ structure*" is defined to describe the multilayers obtained with a transfer ratio at the withdrawal always close to 1 and a transfer ratio at the downstroke clearly lower than the transfer ratio obtained at the upstroke[58]. This evolution has been directly related to the strength of the interaction between the headgroups of the first layer and the hydrophilic surface. Depending on the type of the substrate, the deposited molecules may adopt different orientations, and as the layers are progressively deposited, the interactions between the tails of the molecules become less efficient, thus decreasing the transfer efficiency during the down-stroke.

Silicon has been demonstrated to be an adequate substrate for the transfer of phospholipid monolayers. In our group, by using the optimal procedure mentioned above, we have transferred up to 21 layers of DPPA and 5 layers of DPPA: DPPC (2:1) in the Y-type form onto a silicon substrate with a transfer ratio of 1.1 ± 0.1 for each of the deposited layers. The role of the substrate mediated condensation (SMC) previously described by Riegler and Spratte for silicon wafer[155,172] had provided a possible explanation for such results. These authors reported that additional adhesive interactions on the substrate can induce some local morphological and constitutional modifications by a variation of the internal pressure, explaining why the first deposited layer was in a more condensed state than the floating monolayer. Therefore, such a SMC effect may enhance the quality of the deposition of the first phospholipid monolayer onto a silicon substrate and the good adhesion of this first layer may orient the molecules in a position favouring the effectiveness of further multilayer stacking. The same denser effect has been recently reported to explain the deposition ratio value slightly higher than the unit for the transfer of phosphatidylcholine (PC) monolayers on silicon surfaces[30]. It must be pointed out that the more hydrophilic the substrate, the better the interaction with the substrate, because a strong hydrophilicity may compensate the strong affinity of the headgroup for the water subphase interface. The difference in the surface hydrophilicity of the different kinds of substrates used for LB deposition can explain the discrepancies between the various behaviours observed during the transfer of phospholipid monolayers. Such behavous include the formation of Y-type bilayers on silicon, and desorption of lipid of the first layer during the deposition of the second monolayer on mica. In fact, the substrate hydrophilicity can favour the adsorption of the molecules on the solid substrate rather than the respreading on the subphase surface and thereby prevent (or not) the partial desorption phenomenon. For this reason, silicon substrates are suitable for obtaining high-quality phospholipid LB films in the Y-form, which constitute an excellent model of the bilayer

structure of biological membranes. In the nanobiotechnology field, elaboration on silicon substrates of phospholipid bilayers as biomimetic lipid membranes appears very attractive to achieve miniaturised bio-electronic hybrids after their functionalisation with proteins or other biological molecules.

The transfer of a phospholipid bilayer system onto a hydrophilic substrate is so far the more relevant approach to elaborate biomimetic membranes. However, it must be emphasised that the transferred bilayers or a part of them (outer layer) can be partially or totally removed from the substrate when the bilayer-covered system crosses vertically a pure air/water interface. This 'detaching' phenomenon is once again due to the balance of the interaction energy between the polar groups on the substrate and their affinity for the air-water interface, and the strength of hydrophobic forces between the hydrocarbon chains. Consequently, a bilayer membrane system deposited on a hydrophilic surface needs to be carefully handled after LB deposition in order to prevent any dewetting problem[13] and to maintain the stability of the outer monolayer[14]. The best way preserve the integrity of the bilayer structure and to avoid any molecular desorption is to keep the supported bilayer under water. After the last transfer at the downstroke, the lipid-covered substrate can be plugged into a small container previously immersed in the subphase, prior to spreading the monolayer[13,14,156,162,163,197,199]. In addition, this produces fully hydrated bilayers, which is the most representative biological situation compare with LB films transferred in dry state (last layer deposited at the upstroke).

2.3.4.   Free Supported Phospholipid LB Films

The strong interaction between the first layer and a hydrophilic substrate such as silicon may modify some characteristics of the biomimetic membrane compared with those of the biological one. An example is the fluidity of the supported bilayers. A natural biomembrane is a dynamic, fluid system, where the component molecules have considerable translational freedom and this fluidity is essential for the behaviour of the membrane. The presence of the substrate may constrain the freedom of the component phospholipid molecules within the plane of the membrane, in a manner which may significantly affect the interaction of the membrane system with other biological agents. The supported systems may have structural similarities with a bilayer membrane, but their behaviour may be affected by the tethering effects. Depending on the nature of the biomolecules that will be associated with the bilayer system, these tethering effects may become a major problem. Whereas a single lipid bilayer system is helpful in the studies or in the association of peripheral proteins or proteins residing in the outer leaflet, the global loss of the lipid mobility may be especially harmful in the case of the integration of transmembrane proteins. For this reason, some authors have been interested to deposit a 'double' bilayer of dipalmitoylphosphatidylcholine (DPPC) or distearylphosphatidylcholine (DSPC) onto a silicon wafer (Figure 2.9a). This multi-bilayer configuration has been obtained using the combined Langmuir-Blodgett/Langmuir-Schaefer approach: the three first layers
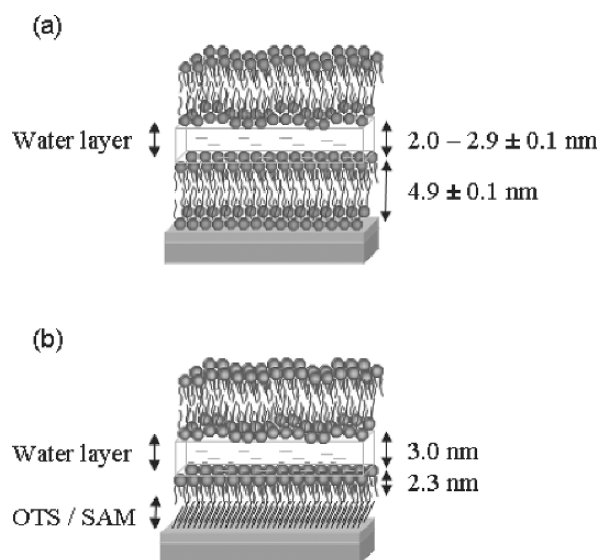
FIGURE 2.9. Schematic diagram of different 'free supported bilayers' (FSB) on silicon wafer. (a) Monolayers 1, 2, 3 were deposited by the Langmuir-Blodgett method; the monolayer 4 was deposited by Langmuir-Schaefer method. The second bilayer, more free to fluctuate, was significantly rougher (0.5–0.6 nm) than the first one[30]. (b) The three outermost phospholipid layers were deposited by Langmuir-Blodgett technique under octadecyltrichlorosilane self-assembled monolayer (OTS/SAM)[88].

have been deposited by vertical LB transfer and the fourth one by horizontal LS deposition, leading the substrate to be immersed in the subphase water at the end of the transfer (section 2.3.3). In this system, the double bilayers retain an intermediate thick hydration layer necessary to limit any substrate tethering affects. The second bilayer, called "*free bilayer*", corresponds to a highly hydrated membrane floating at 2 to 3 nm above the first one[30]. Those authors have obtained some evidence that the thermotropic phase behaviour of the 'free bilayer' mimics that of the vesicle system[48]. More recently,[87] have improved that initial system by using a hybrid self-assembled monolayer (SAM)/double bilayer system, where the lower phospholipid monolayer has been replaced by an octadecyltrichlorosilane (OTS) SAM (Figure 2.9b). As this substrate enhances the transfer ability of dimyristoylphosphatidylcholine (DMPC), it enables formation of a free hydrated bilayer with phospholipid in a fluid state at room temperature. DMPC is a phospholipid which presents a chain melting temperature value (*i.e.* a *phase transition temperature* (T_c) of 24°C lower than those of DPPC (41.5°C) or DSPC (51°C)[22]. Consequently, DMPC forms a Liquid Expanded monolayer at air/water interface. The characterisation of this "*free supported bilayer*" (FSB) by neutron and X-ray reflectivity has clearly demonstrated that the upper bilayer, *i.e.* the '*free bilayer*', is separated from the substrate with a water layer approximately

3 nm thick. Additionally, it presents thermotropic phase behaviours comparable to those observed for DMPC multilamellar vesicles (MLV). Mainly, the authors were able to detect the transition to a ripple phase (P_{β}'), which is an intermediate phase between the crystalline ordered solid phase (gel phase, L_{β}') obtained at temperature lower than the melting temperature and the disordered fluid phase (liquid crystalline phase, L_{α}) in which the chain melts with apparition of *gauche* conformations, obtained at temperature higher than the melting temperature[56]. In the ripple phase, the bilayer adopts a rippled, undulating structure. Therefore, the detection of the transition to the ripple phase is highly significant of the freedom of molecules in that it cannot occur if there is appreciable tethering of the phospholipid molecules to substrate since the ripple phase requires that the phospholipid molecules are able to move normal to the substrate plane[87]. Finally, these authors demonstrate that the structure of this "*free supported bilayer*", in term of area per molecule (A) and bilayer thickness, is identical to that of DMPC vesicles in the gel phase (low temperature). In going from the gel phase to the fluid phase, the bilayer thickness decreases and the area per molecule increases due to the chain melting. The thickness of the intervening water layer decreases across the main transition in the same way as it is seen in multilamellar systems[88].

Hence, it appears that the free supported phospholipid bilayer deposited onto a first bilayer LB film or another mixed bilayer structure (OTS SAM/ LB films) represents a realistic fluid biomimetic membrane. Even if these membranes are not constituted by only one bilayer, they will be able, however, to find applications in the nanobiotechnology field for molecular systems based on membrane fluidity. These applications could include systems incorporating integral proteins like pores or ion channels, design of drug delivery vehicles requiring membrane fusion with the target cell, or molecular recognition of ligands by cell-membrane receptors.

2.3.5.   *Asymmetric Phospholipid LB Bilayers*

Another interesting aspect of the LB film deposition is the possibility to elaborate asymmetric phospholipid bilayers, termed *alternate-layer LB films*. Indeed, in animal and bacterial cells the lipid composition differs from the inner to the outer faces of the plasma membranes. For instance, the inner lipid layer of the human erythrocyte membrane contains most of the phosphatidylethanolamine and phosphatidylserine, whereas the outer leaflet contains most of phosphatidyl-choline and sphingolipide[105]. Beside the specific variation which can be encountered in the total lipid composition, asymmetric lipid distribution is a common aspect of the different types of biological membranes.

LB deposition allows building up films containing more than one type of monomolecular layer. In the simplest case, alternate-layer films may be produced by raising the substrate through a monolayer of one material (consisting of molecules of compound A) and then, lowering the substrate through a monolayer of a second substance (compound B). A multilayer structure consisting of
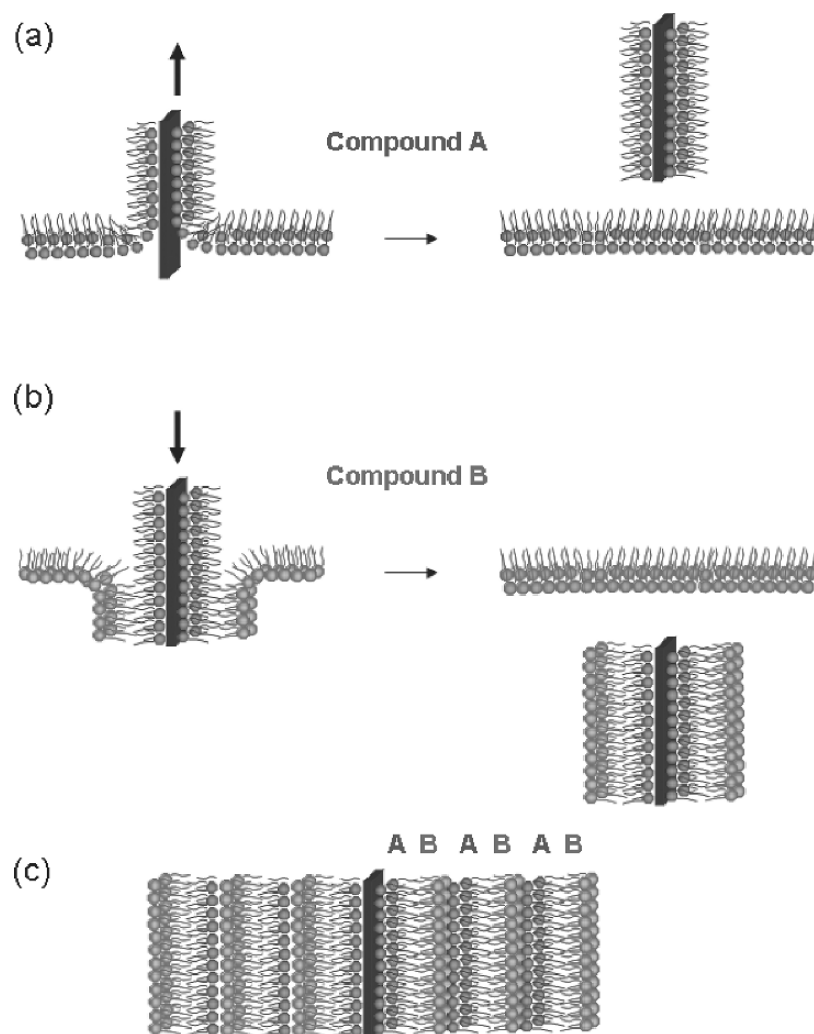
FIGURE 2.10. Alternate-layer Langmuir-Blodgett films. The alternate multilayers were obtained by (a) raising the substrate through the monolayer of compound A; (b) lowering the substrate through the monolayer of compound B, etc… (c) Structure of ABABAB alternate LB multilayers.

ABABAB… layers will be produced (Figure 2.10). In particular, *alternate-bilayer* structures are of great interest in the study of the membrane asymmetry and may find applications in the development of biomimetic bilayer structure. In this case, one monolayer is transferred in emersion (A) and the other in the immersion mode (B).

Production of asymmetric membranes (*i.e.* hybrid supported bilayers) by LB deposition can be helpful for the analysis of lipid phase-separation

and lipid domain formation in mixed bilayers[162,197]. Despite the traditional view of a lipid bilayer as a dynamic, fluid environment, there is increasing evidence that organization of lipids and other membrane components into microdomains, named rafts, plays a crucial role in many cellular functions[2,169,170]. In another respect, asymmetric bilayers can be produced with the first leaflet formed by zwitterionic phospholipids and the second one by anionic phospholipids. Such bilayer structures may have potential applications for protein incorporation, since many of them associate with membranes *via* interactions with anionic phospholipids[156]. A number of recent publications deal with the formation and the characterization of phospholipidic asymmetric LB bilayers of different phospholipid combinations, including DMPE/DOPC[13], PC/PG or PC/PE[156], DSPE/DOPE, DSPE/DOPE-DSPE-MGDG mixture,[162,163], DPPE/DPPC, DPPE/DPPC-GM1 mixture, DPPC/DPPC-Cholesterol-GM1 mixture[197], DPPE/SPM-DOPC, DPPE/SPM-DOPC-Cholesterol mixture, DPPE/SPM-DOPC-Cholesterol-GM1 mixture[199], DPPE/ DLPE[14]. These different types of combinations has been mainly characterized in terms of structural homogeneity and lipid phase-segregation. An interesting point is that the asymmetric bilayer is more homogeneous (with fewer defects) when the first layer is composed of phosphatidylethanolamine (PE) compared with phosphatidylcholine (PC)[13,156,197]. As mentioned above (section 2.3.3), this result is partially due to the lower number of defects in the original PE monolayer and to a resulting lower probability of losing some molecules of the bottom monolayer on second transfer[197]. Specific properties of PC cause polygonal patterns in supported bilayers[156]. PC is known to have a bulky headgroup with a larger cross-sectional area than that occupied by two saturated acyl chains. In hydrated bilayers (in condensed phase) this causes packing constraints, resulting in tilted acyl chains[80]. Hence, supported PC monolayers consist of multiple ordered domains with lipids in a tilted conformation in different directions from one domain to another, thus creating disordered line defects on the borderlines between the different domains. From these weak line defects, PC molecules preferentially desorb upon passing through the second monolayer, generating more defects in the bilayers[156]. This does not occur with PE which has a smaller headgroup and for which the acyl chain is straightforward.

The success of the biomimetic membrane applications in nanobiotechnology relies on the understanding of the fundamental properties of the membrane itself. The production of phospholipidic asymmetric membranes will be an innovative way to develop a new kind of biomimetic membranes that may open new opportunities to integrate recognition biological systems. Finally, it can be mentioned that asymmetric membrane composed of biological molecules can additionally possess some specific properties due to the non-centrosymmetric (*i.e.* no plane of symmetry)[182]. A pyroelectric effect has been reported by developing alternate-layers LB films of different phospholipids (DPPA, DPPS, DPPC, DPPE), long-chain fatty amine (docosylamine) and fatty acid (22-tricosenoic acid)[147].

2.4.   Functionalisation of Lipidic LB Films: Specific Features

The functionalisation of the structural biomimetic membranes by association or incorporation of macromolecules presenting specific biological activities such as enzymes, antibodies or specific ligands is one of crucial steps for multiple applications in nanobiotechnology. This section will be concerned with a brief overview of methods enabling functionalisation of LB membranes, based on specific features of the Langmuir-Blodgett technology.

Due to the fact they are transferable on various types of substrate, LB films present great advantages for the development of novel nanobiosensors. Like the other systems mimicking the biological membrane, their structural organization (highly ordered molecular array) and their ultrathin thickness (few nanometers) are the main criteria for the design of ultra-rapid micronic sensors operating at the molecular level and of further developments of "smart" sensors and biochips. However, the interest of LB films is not limited to these structural aspects. Specific advantages include (i) the ability to achieve in a one-step procedure the elaboration of a bioactive sensing layer and its association with the transducer, *(ii)* the low enzyme amount needed for the membrane preparation, *(iii)* the possibility to work at ambient pressure and temperature avoiding thermic treatments arising in the micronic system design (which can denature the biological compounds), and *(iv)* the ability to modulate the sensor performances (detection limit, sensitivity, dynamic range) in varying the number of the deposited proteolipidic layers[6,31,108,127,135,194].

The successful incorporation of biological compounds retaining their activity in LB films remains the crucial step as well. Several approaches to build up supported lipid LB bi(multi)layers containing proteins have been reported. Principles, advantages and inconveniences of such specific methods based on LB technology are briefly listed in the following sections.

2.4.1.   *Protein Association with the Floating Monolayer before LB Deposition*

One of the most commonly used approaches derives from the procedure developed to study protein-lipid interaction with a Langmuir monolayer[25,39,49,184,206]. It corresponds to the adsorption of the protein from the subphase onto the interfacial film before transfer of the mixed proteo-lipidic monolayer (Figure 2.11). For 25 years, several bioactive protein-lipid LB films have been produced by using this approach[12,33,46,50,109,123,148,152,160,176,191,205,206] and some of them have been studied with regard to their potential applications in biosensing devices[6,7,31,47,127,174,194,201,202,204]. However, additionally to the relatively large amount of proteins required in the Langmuir trough, some drawbacks must be pointed out[81]. If the monolayer is prepared on a subphase containing the dissolved protein, a layer of denatured protein may
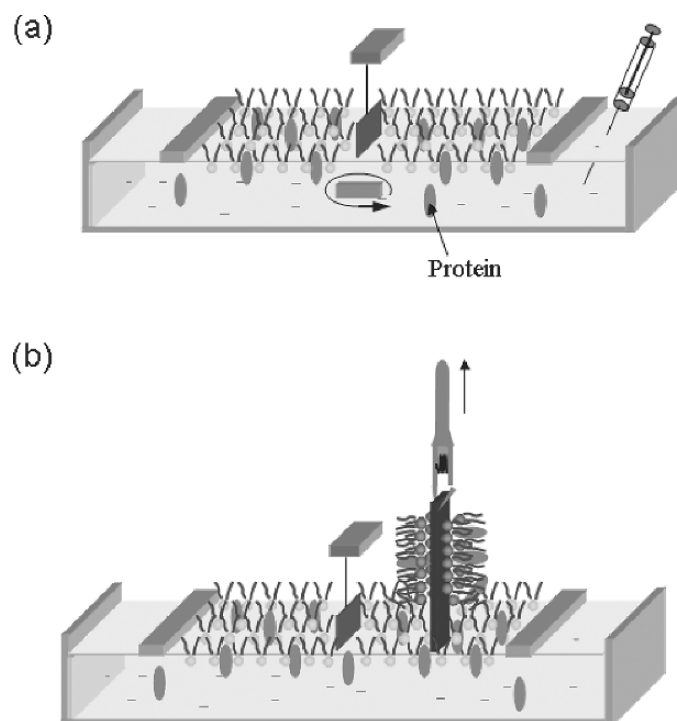
FIGURE 2.11. Protein insertion in the floating monolayer before Langmuir-Blodgett deposition.

form on the water surface and may mix with the lipid layer. If the protein is injected into the subphase after lipid monolayer formation, the protein may penetrate the monolayer close to the injection point and hence, may not distribute homogeneously in the interfacial film. In this case, multipoint injections or injecting the protein progressively under the monolayer may circumvent this disadvantage.

In order to avoid protein denaturation at the air-water interface, the possibility to directly spread the enzyme or a protein/detergent mixture on the surface of a floating lipidic monolayer has been reported[81,108,135]. Using these techniques, homogeneous proteo-lipidic monolayers have been formed. The formation of a protein/synthetic dialkyl amphiphile complex, soluble in an organic solvent (benzene or chloroform) and directly spreadable at the air-water interface, has been also used to prepare active and stable proteo-lipidic monolayers that preserve the enzyme activity and are transferable onto an electrochemical transducer[131,132].

Finally, the presence of the enzyme in the mixed monolayer could modify its transferability properties[31,191,206]. The surface pressure needed for the transfer procedure is not always adapted for the enzyme association. The expulsion of the

protein is often encountered at high surface pressures. Furthermore, the presence of the protein can induce a poor monolayer adhesion on the substrate, which can lead to a peeling-off at the subsequent immersion.

2.4.2.   *Protein Association onto Preformed-Lipidic LB Films*

Another approach consists in the adsorption of the enzyme onto pre-formed LB films[3,4,32,61,62,104,119,128]. The main advantage of this procedure lies in the possible interaction of the enzyme with a hydrophobic or hydrophilic surface depending on the number of the deposited layers, thus allowing the control of the enzyme environment. Likewise, this approach allows the control of the thickness and the homogeneity of the LB films harbouring the enzymes. Nevertheless, the release of protein molecules due to the weakness of their association with the lipidic surface remains a major drawback[120] and is often the main reason which explains the poor reproducibility of responses of LB membrane-based sensors[5]. In order to avoid desorption, some authors have proposed to covalently immobilise the enzyme on LB film surfaces by the use of crosslinking agents[178,181]. The stabilisation of the proteo-lipidic LB films by reticulation after transfer with glutaraldehyde vapour has been also investigated[191,204]. However, covalent attachment to the lipid structure may induce changes in the protein conformation, which can lead sometimes to a loss of its biological activity.

Another alternative to limit protein desorption and avoid covalent immobilisation is to cover the protein molecules by transfer of an outermost layer after enzyme adsorption. This procedure referred as "*inclusion process*" allows the sandwiching of the enzyme in a hydrophobic or a hydrophilic environment while keeping the homogeneity of the supporting layers[60]. Alternate-layer LB films such as monolayer 1/adsorded protein layer/lipid monolayer 2, have been also considered[16]. The specific features of these latter methods are the possibility to easily vary the types of monolayers, the conditions of their deposition and of protein adsorption during the film preparation process. The control of these parameters allows improving the stability of the mixed LB films to preserve the protein activity[16].

Finally, the appropriate choice of the monolayer onto which protein should be adsorbed can advantageously limit the protein detachment. The use of asymmetric LB bilayers of zwitterionic and anionic phospholipids may present an advantage for an efficient protein association (section 2.3.5). Moreover, an appropriate monolayer may prevent the protein denaturation, which can occur by adsorption onto high-surface tension hydrophilic surfaces.

Whether the protein is associated to the LB membrane before or after the monolayer deposition, it stays randomly adsorbed on the surface of the lipid layer. The control of the protein incorporation in a defined orientation similar to the biological membrane, where the protein association in/on the lipidic leaflets determines their own orientation for an optimal functionality, remains a

crucial challenge to achieve functionalized biomimetic membranes. The building-up of proteo-lipidic LB bilayers possessing properly oriented recognition sites constitutes a promising model for further developments in biomimetic sensing applications.

2.4.3. Oriented Protein Association in Lipidic LB Films

In order to overcome the problem of protein orientation associated with biomimetic membranes in general, and with lipidic LB films in particular, several attempts have been recently performed. These include the covalent coupling of antibody fragments through disulphide bridges to a lipid linker embedded in phospholipid monolayers[90,186,187], or the immobilisation of histidine-containing proteins onto metal ion chelating lipid monolayers[96]. However, in this latter case, several defined binding orientations could be obtained depending on the spatial distribution of histidine units on the surface of the protein. With the aim of designing functionalised biomimetic membranes with an unique recognition site orientation, another approach has been recently proposed, which involves the insertion of a non-inhibitory monoclonal antibody (IgG) in LB films as an anchor. This anchor is able both to sequester a hydrophilic protein (soluble enzyme) in an oriented position at the surface of the lipidic matrix (avoiding adsorbed protein denaturation) and to preserve biological (enzyme) activity over few months (Figure 2.12)[69,70].

In order to ensure the functional orientation of the antibody in the glycolipidic LB membrane, our group has developed an original strategy which is based on an adapted combination of liposome fusion at an air-buffer interface and Langmuir-Blodgett technology. This strategy exploits the possibility to spread proteo-lipidic liposomes at an air-buffer interface, which are able to disintegrate and to form a mixed proteo-lipidic monolayer[64]. After compression, the mixed monolayer can be transferred by LB deposition[65]. The main interest of forming proteo-lipidic vesicles prior the interfacial film formation is to favour the creation of optimal proteo-lipidic interactions in order to improve the protein retention both in the interfacial film and in the LB films, without implying covalent bonds. The governing idea of this method is to include the antibody (soluble protein) in pre-formed lipidic vesicle membranes able to carry it towards the air/buffer interface directly in a lipidic environment[63].

The building-up of the functionalised LB biomimetic membrane depicted in figure 2.12 has been explained by the strong interactions occurring between the fluid lipid matrix, which corresponds to a synthesised glycolipid having high hydrocarbon chain fluidity, and the immunoglobulin, which is a glycoprotein. On the one hand, weak (but favourable) carbohydrate/carbohydrate hydrophilic interactions could exist between the glycolipid headgroup and the glycan moiety of the IgG molecule (located in the hinge region). On the other hand, hydrophobic interactions could embed the hydrophobic Fc fragment of IgG in the lipid moiety of the glycolipid leaflets; this embedment is favoured by the high fluidity of the glycolipid hydrocarbon chains allowing their conformational adaptation[70].

These specific interactions initially formed in the vesicle membrane are preserved during the interfacial vesicle disintegration and lead in turn to a preferential orientation of the IgG molecules in the supported bilayer structure[70]. After immunoassociation, the enzyme will be retained at the surface of the bilayer structure in a well-defined orientation[69].

This functionalised biomimetic membrane has been shown to be structurally stable and able to retain enzyme activity for a long period of time (over a period of 82 days)[69]. To our knowledge, such a high stability has never been reported previously for an immobilised enzyme onto Langmuir-Blodgett films. Furthermore, the typical enzymatic behaviour of the enzyme retained at the surface of the biomimetic membrane has clearly demonstrated the potential
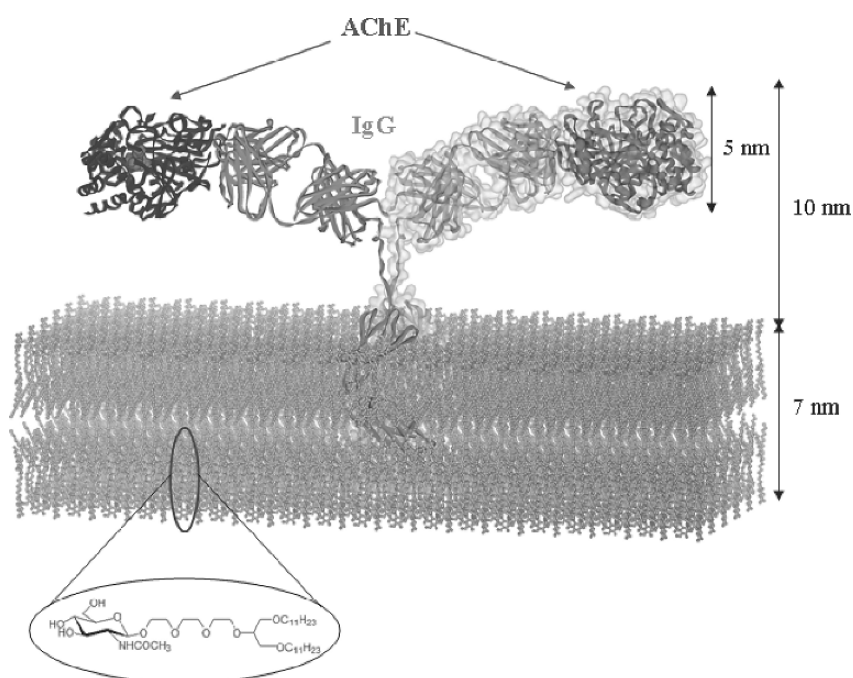
FIGURE 2.12. Functionalized bilayer Langmuir-Blodgett structure with unique recognition site orientation. This biomimetic membrane has been obtained by using an adapted combination of liposome fusion at an air/buffer interface and the Langmuir-Blodgett technology (see text). The lipidic bilayer is constituted of a neoglycolipid presenting highly-fluid hydrocarbon chains. The antibody is embedded in the bilayer structure by the way of (i) favourable carbohydrate/carbohydrate interactions between the glycan moieties of the antibody (IgG) molecule and the glycolipid head group and (ii) probable hydrophobic interactions between the Fc fragment of the immunoglobulin and the lipid moiety of the glycolipid leaflets. The acetylcholinesterase (AChE) is associated to the functionalized bilayer structure, after transfer, by immuno-association. This functionalized biomimetic LB membrane has been shown to be stable more than 3 three months[70].

usefulness of such a functional molecular assembly for biocatalysis investigations in a biomimetic environment[70].

Interfacial spreading of proteo-vesicle together with Langmuir-Blodgett technique appears thus to be an efficient method for developing functionalized biomimetic LB membranes with favourable orientation of recognition sites. The combination of these methods, based on the self-molecular assembly of biomolecules, allows both the insertion of the protein presenting specific recognition properties with a pre-determined orientation in the vesicle membranes and the enhancement of the proteo-lipidic organization by using lateral compression.

2.5.   Trends and Prospects

For several years, self-assembly properties of biomolecules received more and more attention because of their ability to spontaneously organize into nanostructures, which allows mimicking the living cell membranes. As attested by the number of recent papers quoted in this chapter, LB technology is a powerful method to elaborate functionalised biomimetic membranes. Different aspects of the biological membrane, like fluidity or asymmetry can be preserved, but the most promising outcome resides in the possibility to orient functional macromolecules in the bilayer structure. By the way to be directly prepared at the surface of different kinds of solid materials, LB membranes present some real advantages for applications in nanobiotechnology and applied nanobiosciences. A direct association with active surfaces constitutes an attractive opportunity for designing novel nanosensors. The intimate contact between LB membranes and effective transducers, allowing recognition and signal transduction events in a single device is without doubt, a very promising way for the development of biomimetic nanosensors and minute investigations of biological processes at the molecular level.

Finally, the possibility to incorporate amphipathic biomolecules in LB membranes offers the opportunity to diversify the number of new organized nanosensing bilayer which can be devised. Actually, a precise knowledge of the hydrophilic and hydrophobic domains of macromolecules will allow different kinds of molecular assemblies to be designed for fundamental and applied investigations.

References

1. Ancelin H., Zhu D.G., Petty M.C., Yarwood J. 1990. Infrared spectroscopic studies of molecular structure, ordering, and interactions in enzyme-containing Langmuir-Blodgett films. *Langmuir*, 6:1068–1070.
2. Anderson R.G.W. and Jacobson K. 2002. A role for lipid shells in targeting proteins to caveolae, rafts and other lipid domains. *Science*, 296:1821–1825.

3. Anzai J.I., Furuya K., Chen C.W., Osa T., Matsuo T. 1987. Enzyme sensors based on ion-sensitive field effect transistor. Use of Langmuir-Blodgett membrane as a support for immobilizing penicillinase. *Anal. Sci.*, 3:271–272.

4. Anzai J.I., Hashimoto J.Y., Osa T., Matsuo T. 1988. Penicillin sensors based on an ion-sensitive field effect transistor coated with stearic acid Langmuir-Blodgett membrane. *Anal. Sci.*, 4:247–250.

5. Anzai J.I., Lee S., Osa T. 1989. Enzyme-immobilized Langmuir-Blodgett membranes for biosensor application. Use of highly branched polyethyleneimine as a spacer for immobilizing α-chymotrypsin and urease. *Makromol. Chem., Rapid Commun.*, 10:167–170.

6. Arisawa S., Yamamoto R. 1992. Quantitative characterization of enzymes adsorbed on to Langmuir-Blodgett films and application to a urea sensor. *Thin Solid Films*, 210/211:443–5.

7. Arisawa S., Arise T., Yamamoto R. 1992. Concentration of enzymes adsorbed onto Langmuir films and characteristics of a urea sensor. *Thin Solid Films*, 209: 259–263.

8. Aveyard R., Binks B.P., Fletcher P.D.I. 1991. Effects of subphase pH on the successive deposition of monolayers of docosanoic acid onto mica. *Progr. Colloid Polym. Sci.*, 84:184–188.

9. Aveyard R., Binks B.P., Fletcher P.D.I., Ye X. 1992. Dynamic contact angles and deposition efficiency for transfer of docosanoic acid on to mica from $CdCl_2$ subphases as a function of pH. *Thin Solid Films*, 210–211:36–38.

10. Baret J.F., Hasmonay H., Firpo J.L., Dupin J.J., Dupeyrat M. 1982. The different types of isotherm exhibited by insoluble fatty acid monolayers. A theoretical interpretation of phase transitions in the condensed state. *Chem. Phys. Lipids*, 30:177–187.

11. Barraud A., Leloup J., Maire P., Ruaudel-Texier A. 1985. Microdefect decoration and visualization in Langmuir-Blodgett films. *Thin Solid Films*, 133:133–139.

12. Barraud A., Perrot H., Billard V., Martelet C., Therrasse J. 1993. Study of immunoglobulin G thin layers obtained by the Langmuir-Blodgett method: application to immunosensors. *Biosens. Bioelectron.*, 8:39–48.

13. Bassereau P., Pincet F. 1997. Quantitative analysis of holes in supported bilayers providing the adsorption energy of surfactants on solid substrate. *Langmuir*, 13:7003–7007.

14. Benz M., Gutsmann T., Chen N., Tadmor R., Israelachvili J. 2004. Correlation of AFM and SFA measurements concerning the stability of supported lipid bilayers. *Biophys. J.,* 86:870–879.

15. Bernstein S. 1938. Comparaison of X-ray photographs taken with X and Y built-up films. *J. Am. Chem. Soc.*, 60: 1511.

16. Berzina T.S., Piras L., Troitsky V.I. 1998. Study of horseradish peroxidase activity in alternate-layer Langmuir–Blodgett films. *Thin Solid Films,* 327–329:621–626.

17. Bettarini S., Bonosi F., Gabrielli G., Martini G., Puggelli M. 1992. Interactions between monolayers and metal ions at the water-air interface: conditions for the transferability as Langmuir-Blodgett multilayers.*Thin Solid Films*, 210–211:42–45.

18. Bikerman J.J. 1939. On the formation and structure of multilayers. *Proc. R. Soc. London, Ser. A*, 170:130–144.

19. Birdi K.S. 1989. Lipid and biopolymer monolayers at liquid interfaces. New York: Plenum Press.

20. Blodgett K.B. 1935. Films built by depositing successive monomolecular layers on a solid surface. *J. Am. Chem. Soc.*, 57:1007–1022.

21. Blodgett K.B., Langmuir I. 1937. Built-up films of barium stearate and their optical properties. *Phys. Rev.*, 51:964–982.

22. Blume A. 1983. Apparent molar heat capacities of phospholipids in aqueous dispersion. effects of chain length and head group structure?. *Biochemistry*, 22, 5436–5442.

23. Böhm C., Leveiller F., Jacquemain D., Möhwald H., Kjaer K., Als-Nielsen J., Weissbuch I., Leiserowitz L. 1994. Packing characteristics of crystalline monolayers of fatty acid salts, at the air-solution interface, studied by grazing incidence X-ray diffraction. *Langmuir*, 10:830–836.

24. Bonn M., Roke S., Berg O., Juurlink L.B.F., Stamouli A., Müller M. 2004. A molecular view of cholesterol-induced condensation in a lipid monolayer. *J. Phys. Chem. B*, 108:19083–19085.

25. Brockman H. 1999. Lipid monolayers: why use half a membrane to characterize protein-membrane interactions? *Curr. Opin. Struct. Biol.*, 9:438–443.

26. Brown D.A., London E. 2000. Structure and function of sphingolipid- and cholesterol-rich membrane rafts. *J. Biol. Chem.*, 275:17221–17224.

27. Budach W., Ahuja R. C., Mobius D. 1993. Metal ion complexation and electron donor properties of dioctadecyldithiocarbamate in monolayers at the gas/water interface and in organized monolayer systems. *Langmuir*, 9:3093–3100.

28. Buhaenko M.R., Goodwin J.W., Richardson R.M., Daniel M.F. 1985. The influence of shear viscosity of spread monolayers on the Langmuir-Blodgett process. *Thin Solid Films*, 134:217–226.

29. Buhaenko M.R., Richardson R.M. 1988. Measurements of the forces of emersion and immersion and contact angles during Langmuir-Blodgett deposition. *Thin Solid Films*, 159:231–238.

30. Charitat T., Bellet-Amalric E., Fragneto G., Graner F. 1999. Adsorbed and free lipid bilayers at the solid-liquid interface. *Eur. Phys. J. B*, 8:583–593.

31. Choi J.W., Min J., Jung J.W., Rhee H.W., Lee W.H. 1998. Fiber-optic biosensor for the detection of organophosphorous compounds using AChE-immobilized viologen LB films. *Thin Solid Films*, 327–329:676–680.

32. Choi J.W., Kim Y.K., Lee I.H., Min J., Lee W.H. 2001. Optical organophos- phorous biosensor consisting of aceytlcholinesterase/viologen hetero Langmuir- Blodgett film. *Biosens. Bioelectron.*, 16:937–943.

33. Chovelon J.M., Gaillard F., Wan K., Jaffrezic-Renault N. 2000. Influence of the surface pressure on the organization of mixed Langmuir-Blodgett films of octadecylamine and butyrylcholinesterase. 2. Film transferred onto silica support. *Langmuir*,16:6228–6232.

34. Clint J.H., Walker T. 1974. Interaction energies between layers of alkyl and partially fluorinated alkyl chains in Langmuir-Blodgett multilayers. *J. Colloid Interface Sci.*, 47:172–185.

35. Constantino C.J.L., Dhanabalan A., Oliveira, Jr. O.N. 1999. Experimental artifacts in the surface pressure measurement for lignin monolayers in Langmuir troughs. *Rev. Sci. Instrum.*, 70:3674–3680.

36. Cordero S.R., Weston K.D., Buratto S.K. 2000. Near-field microscopy of collapsed Langmuir-Blodgett films. *Thin Solid Films*, 360:139–144.

37. Cui D.F., Howarth V.A., Petty M.C., Ancelin H., Yarwood J. 1990. The deposition and characterization of phosphatidic acid Langmuir-Blodgett films. *Thin Solid Films*, 192:391–396.

38. d'Acapito F., Emelianov I., Relini A., Cavatorta P., Gliozzi A., Minicozzi V., Morante S., Solari P. L., Rolandi R. 2002. Total external reflection X-ray absorption spectroscopy reveals a zinc coordination shell in phospholipid Langmuir-Blodgett films. *Langmuir,* 18:5277–5282.

39. Demel R.A. 1994. Monomolecular layers in the study of biomembranes. *Subcell. Biochemistry*, 23:83–120.

40. Desmeules P., Grandbois M., Bondarenko V.A., Yamazaki A., Salesse C. 2002. Measurement of membrane binding between recoverin, a calcium-myristoyl switch protein, and lipid bilayers by AFM-based force spectroscopy. *Biophys. J.*, 82:3343–3350.

41. Dhanabalan A., Prasanth Kumar N., Major S., Talwar S. 1998. Variation of monolayer behaviour and molecular packing in zinc arachidate LB films with subphase pH. *Thin Solid Films*, 327–329:787–791.

42. Dufrêne Y.F., Lee G.U. 2000. Advances in the characterization of supported lipid films with atomic force microscope. *Biochim. Biophys. Acta*, 1509:14–41.

43. Dynarowicz-Latka P., Dhanabalan A., Oliveira O.N. Jr. 2001. Modern physico-chemical research on Langmuir monolayers. *Adv. Colloid Interface Sci.*, 91:221–293.

44. El Kirat K., Besson F., Prigent A.F., Chauvet J.P., Roux B. 2002. Role of calcium and membrane organization on Phospholipase D localization and activity. Competition between a soluble and an insoluble substrate. *J. Biol. Chem.*, 277:21231–21236.

45. Fankuchen I. 1938. On the Structure of "Built-Up" Films on Metals. *Phys. Rev.*, 53:909.

46. Fiol C., Valleton J.M., Delpire N., Barbey G., Barraud A., Ruaudel-Texier A. 1992a. Elaboration of a glucose biosensor based on Langmuir-Blodgett technology. *Thin Solid Films*, 210/211:489–491.

47. Fiol C., Alexandre S., Delpire N., Valleton J.M., Paris E. 1992b. Molecular resolution of enzyme-containing Langmuir-Blodgett films. *Thin Solid Films*, 215:88–93.

48. Fragneto G., Charitat T., Graner F., Mecke K., Perino-Gallice L., Bellet-Amalric E. 2001. A fluid floating bilayer.*Europhys. Lett.*, 53:100–106.

49. Fromherz P. 1971. A new technique for investigating lipid protein films. *Biochim. Biophys. Acta*, 225:382–387.

50. Fujiwara I., Ohnishi M., Seto J. 1992. Atomic force microscopy study of protein-incorporating Langmuir-Blodgett films. *Langmuir*, 8:2219–2222.

51. Fukuda K., Shiozawa T. 1980. Conditions for formation and structural characterization of X-type and Y-type multilayers of long-chain esters. *Thin Solid Films*, 68:55–66.

52. Furlong D.N., Scoberg D., Davy J., Pragert R.H. 1993. Ring substitution position and the monolayer and Langmuir-Blodgett multilayer properties of Heneicosa-2,4-diynyl carboxybenzoates. *Langmuir*, 9:766–770.

53. Gaines G.L. Jr. 1966. Insoluble monolayers at liquid-gas interfaces. NewYork: Interscience publishers, J Wiley & Sons, Inc.

54. Gaines G.L. Jr. 1977. Contact angles during monolayer deposition. *J. Colloid Interface Sci.*, 59:438–446.

55. Ganguly P., Paranjape D.V., Sastry M., Chaudhari S.K., Patil K.R. 1993. Deposition of yttrium ions in Langmuir-Blodgett films using arachidic acid. *Langmuir*, 9:487–490.

56. Gennis R.B. 1989. Biomembranes. Molecular structure and function. New York: Springer-Verlag.

57. Girard-Egrot A.P., Morélis R.M., Coulet P.R.. 1993. Dependence of Langmuir-Blodgett film quality on fatty acid monolayer integrity. 2. Crucial effect of the removal rate of monolayer during Langmuir-Blodgett film deposition. *Langmuir*, 9:3107–3110.

58. Girard-Egrot A.P., Morélis R.M., Coulet P.R. 1996. Direct influence of the interaction between the first layer and a hydrophilic substrate on the transition from Y- to Z-type transfer during deposition of phospholipid Langmuir-Blodgett films. *Langmuir*, 12:778–783.

59. Girard-Egrot A.P., Morélis R.M., Coulet P.R. 1997a. Bioactive nanostructure with glutamate dehydrogenase associated with LB films: protecting role of the enzyme molecules on the structural lipidic organization. *Thin Solid Films*, 292:282–289.

60. Girard-Egrot A.P., Morélis R.M., Coulet P.R. 1997b. Choline oxidase associated with behenic acid LB films. Reorganization of enzyme-lipid association under the conditions of activity detection. *Langmuir*, 13:6540–6546.

61. Girard-Egrot A.P., Morélis R.M., Coulet P.R. 1998a. Direct bioelectrochemical monitoring of choline oxidase kinetic behaviour in Langmuir-Blodgett nanostructures. *Bioelectrochem. Bioenerg.*, 46:39–44.

62. Girard-Egrot A.P., Morélis R.M., Coulet P.R. 1998b. Influence of lipidic matrix and structural reorganization on choline oxidase activity retained in LB films. *Langmuir*, 14:476–482.

63. Girard-Egrot A.P., Morélis R.M., Boullanger P., Coulet P.R. 2000. Immunological proteo-glycolipidic interfacial film obtained from spreading of liposomes including ascitic fluid. *Colloids Surf., B: Biointerfaces*, 18:125–135.

64. Girard-Egrot A.P., Chauvet J.-P., Boullanger P., Coulet P.R. 2001. Glycolipid and monoclonal immunoglobulin-glycolipidic liposomes spread onto high ionic strength buffers: evidence for a true monolayer formation.*Langmuir*, 17:1200–1208.

65. Girard-Egrot A.P., Chauvet J.-P., Boullanger P., Coulet P.R. 2002. IgG$_1$-glycolipidic LB films obtained by vertical deposition of an interfacial film formed through proteo-liposome spreading at the air/water interface. *Colloids Surf., B: Biointerfaces*, 23:319–25.

66. Girard-Egrot A.P., Godoy S., Chauvet J.-P., Boullanger P., Coulet P.R. 2003. Preferential orientation of an immunoglobulin in a glycolipid monolayer controlled by the disintegration kinetics of proteo-lipidic vesicles spread at an air-buffer interface. *Biochim. Biophys. Acta*, 1617:39–51.

67. Girard-Egrot A.P., Chauvet J.-P., Gillet G., Moradi-Améli M. 2004. Specific interaction of the antiapoptotic protein Nr-13 with phospholipid monolayers is prevented by the BH3 domain of Bax. *J. Mol. Biol.,* 335:321–331.

68. Gleiche M., Chi L.F., Fuchs H. 2000. Nanoscopic channel lattices with controlled anisotropic wetting. *Nature*, 403:173–175.

69. Godoy S., Chauvet J.-P., Boullanger P., Blum L.J., Girard-Egrot A.P. 2003. New functional proteo-glycolipidic molecular assembly for biocatalysis analysis of an immobilized enzyme in a biomimetic nanostructure. *Langmuir*, 19:5448–5456.

70. GodoyS., Violot S., Boullanger P., Bouchu M.-N., Leca-Bouvier B.D., Blum L.J., Girard-Egrot A.P. 2005. Kinetics study of *Bungarus fasciatus* venom acetylcholinesterase immobilised on a Langmuir-Blodgett proteo-glycolipidic bilayer. *ChemBioChem*, 6:395–404.

71. Graf K., Riegler H. 1998. Molecular adhesion interactions between Langmuir monolayers and solid substrates. *Colloids Surf., A: Physicochem. Eng. Aspects*, 131:215–224.

72. Grandbois M., Clausen-Schaumann H., Gaub H. 1998. Atomic force microscope imaging of phospholipid bilayer degradation by phospholipase A_2. *Biophys. J.*, 74:2398–2404.

73. Greenhall M.H., Lukes P.J., Petty M.C., Yarwood J., Lvov Y. 1994. The formation and characterization of Langmuir-Blodgett films of dipalmitoylphosphatidic acid. *Thin Solid Films*, 243:596–601.

74. Grundy M.J., Musgrove R.J., Richardson R.M., Roser S.J. 1990. Effect of dipping rate on alternating layer Langmuir-Blodgett film structure. *Langmuir*, 6:519–521.

75. Hanke Th., Wollenberger U., Ebert B., Scheller F., Zaitsev S. Yu. 1992. Glucose oxidase/lipid mixed LB films on a Pt electrode application as sensor model. In Scheller F, Schmid R.D., eds. Biosensors, Fundamentals, Technologies and Applications, Vol. 17, GBF monographs, New York:VCH Publishers. p 43–46.

76. Hann R.A. 1990. Molecular structure and monolayer properties. In Robert G.G., ed. Langmuir-Blodgett films. New York: Plenum Press. p 17–83.

77. Hasmonay H., Dupeyrat M., Dupeyrat R. 1976. Stearate thin film of adjustable refractive index and some practical applications. *Opt. Acta*, 23:665–677.

78. Hasmonay H., Caillaud M., Dupeyrat M. 1979. Langmuir-Blodgett multilayers of phosphatidic acid and mixed phospholipids. *Biochim. Biophys. Res. Commun.*, 89:338–344.

79. Hasmonay H., Vincent M., Dupeyrat M. 1980. Composition and transfer mechanism of Langmuir-Blodgett multilayers of stearates. *Thin Solid Films*, 68:21–31.

80. Hauser H., Pascher I., Pearson R.H., Sundell S. 1981. Preferred conformation and molecular packing of phosphatidylethanolamine and phosphatidylcholine. *Biochim. Biophys. Acta*, 650:21–51.

81. Heckl W.M., Zaba B.N., Möhwald H. 1987. Interactions of cytochromes b_5 and c with phospholipid monolayers. *Biochim. Biophys. Acta*, 903:166–176.

82. Higuchi M., Koga T., Taguchi K., Kinoshita T. 2002. Substrate-induced conformation of an artificial receptor with two receptor sites. *Langmuir*, 18:813–818.

83. Hollars C.W., Dunn R.C. 1998. Submicron structure in L-α-dipalmitoyl-phosphatidylcholine monolayers and bilayers probed with confocal, atomic force, and near-field microscopy. *Biophys. J.*, 75:342–353.

84. Holley C., Bernstein S. 1937. Grating space of barium-copper-Stearate films. *Phys. Rev.*, 52:525.

85. Hönig E.P. 1973. Molecular constitution of X- and Y-type Langmuir-Blodgett films. *J. Colloid Interface Sci.*, 43:66–72.

86. Hönig E.P., Hengst J.H. Th., Den Engelsen D. 1973. Langmuir-Blodgett deposition ratios. *J. Colloid Interface Sci.*, 45:92–102.

87. Hughes A.V., Goldar A., Gerstenberg M.C., Roser S.J., Bradshaw J. 2002a. A hybrid SAM phospholipid approach to fabricating a 'free' supported lipid bilayers. *Phys. Chem. Chem. Phys.*, 4:2371–2378.

88. Hughes A. V., Roser S.J., Gerstenberg M., Goldar A., Stidder B., Feidenhans'l R., Bradshaw J. 2002b. Phase behavior of DMPC free supported bilayers studied by Neutron reflectivity. *Langmuir*, 18:8161–8171.

89. Hui S.W., Viswanathan R., Zasadzinski J.A., Israelachvili J.N. 1995. The structure and stability of phospholipid bilayers by atomic force microscopy. *Biophys. J.*, 68:171–178.

90. Ihalainen P., Peltonen J. 2002. Covalent immobilization of antibody fragments onto Langmuir-Schaefer binary monolayers chemisorbed on gold. *Langmuir*, 18:4953–4962.

91. Iriyama K., Araki T. 1990. Local collapse of a monolayer on an aqueous subphase at a fairly high surface pressure lower than its collapsing pressure visualized by electron microscopy. *Chem. Lett.*, 1189–1192.

92. Ivanova Tz., Panaiotov I., Georgiev G., Launois-Surpas M.A.. Proust J.E., Puisieux F. 1991. Surface pressure - area hysteresis of surface films formed by spreading of phospholipid liposomes. *Colloid Surf.*, 60:263–273.

93. Iwahashi M., Maehara N., Kaneko Y., Seimiya T., Middleton S. R., Pallas N. R., Pethica B. A.. 1985. Spreading pressures for fatty-acid crystals at the air/water interface, *J. Chem. Soc., Faraday Trans. 1, 81:973–981.*

94. Kaladhar K., Sharma C.P. 2004. Supported cell mimetic monolayers and their interaction with blood.*Langmuir,* 20:11115–11122.

95. Kenn R. M., Biihm C., Bibo A.M., Peterson I.R., Mohwald H., Als-Nielsen J., Kjaer K. 1991. Mesophases and crystalline phases in fatty acid monolayers. *J. Phys. Chem.*, 95:2092–2097.

96. Kent M.S., Yim H., Sasaki D.Y., Majewski J., Smith G.S., Shin K., Satija S., Ocko B.M. 2002. Segment concentration profile of myoglobin adsorbed to metal ion chelating lipid monolayers at the air-water interface by neutron reflection. *Langmuir*, 18:3754–3757.

97. Kim K., Kim C., Byun Y. 2001. Preparation of a dipalmitoylphosphatidyl-choline/cholesterol Langmuir-Blodgett monolayer that suppresses protein adsorption. *Langmuir,* 17:5066 -5070.

98. Kjaer K., Als-Nielsen J., Helm C.A., Laxhuber L.A., Möhwald H. 1987. Ordering in lipid monolayers studied by synchrotron X-ray diffraction and fluorescence microscopy. *Phys. Rev. Lett.,* 58:2224–2227.

99. Klechkovskaya V., Anderle M., Antolini R., Canteri R., Feigin L., Rakova E., Stiopina N. 1996. Comparative analysis of high energy electron diffraction patterns from LB films of Cd- and Pb-stearates. *Thin Solid Films*, 284–285:208–210.

100. Krüger P., Schalke M., Wang Z., Notter R.H., Dluhy R.A., Lösche M. 1999. Effect of hydrophobic surfactant peptides SP-B and SP-C on binary phospholipid monolayers. I. Fluorescence and Dark-Field Microscopy. *Biophys. J.*, 77: 903–914.

101. Langmuir I. 1917. The constitution and fundamental properties of solids and liquids. II. Liquids. *J. Am. Chem. Soc.*, 39:1848–1906.

102. Langmuir I. 1938. Overtunrning and anchoring of monolayers. *Science*, 87:493–500.

103. Laxhuber L.A., Möhwald H. 1987. Thermodesorption spectroscopy of Langmuir-Blodgett films. *Langmuir*, 3:837–845.

104. Lee S., Anzai J.I., Osa T. 1993. Enzyme-modified Langmuir-Blodgett membranes in glucose electrodes based on avidin-biotin interaction. *Sens. Actuators B*, 12:153–158.

105. Lehninger A.L. 1982. Principles of biochemistry. New York: Worth publishers, Inc. p 322.

106. Léonard M., Morélis R.M., Coulet P.R. 1995. Linked influence of pH and cations on fatty acid monolayer integrity related to high-quality Langmuir-Blodgett films. *Thin Solid Films*, 260:227–231.

107. Lesieur P., Barraud A., Vandevyver M. 1987. Defect characterization and detection in Langmuir-Blodgett films. *Thin Solid Films*, 152:155–164.

108. Li J.R., Cai M., Chen T.F., Jiang L. 1989. Enzyme electrodes with conductive polymer membranes and Langmuir-Blodgett films. *Thin Solid Films*, 180:205–210.

109. Li J., Rosilio V., Boissonnade M.M., Baszkin A. 2003. Adsorption of glucose oxidase into lipid monolayers: effect of a lipid headgroup charge. *Colloids Surf., B: Biointerfaces*, 29:13–20.

110. Lin B., Bohanon T.M., Shih M.C., Dutta P. 1990. X-ray diffraction studies of the effects of Ca^{2+} and Cu^{2+} on Langmuir monolayers of heneicosanoic acid. *Langmuir*, 6:1665–1667.

111. Lindén D.J.M., Peltonen J.P.K., Rosenholm J.B. 1994. Adsorption of some multivalent transition-metal ions to a stearic acid monolayer. *Langmuir*, 10, 1592–1595.

112. Lösche M., Rabe J., Fischer A., Rucha B.U., Knoll W., Möhwald H. 1984. Microscopically observed preparation of Langmuir-Blodgett films. *Thin Solid Films*, 117:269–280.

113. Lösche M., Helm, C., Mattes H.D., Möhwald H. 1985. Formation of Langmuir-Blodgett films via electrostatic control of the lipid/water interface. *Thin Solid Films*, 133:51–64.

114. Lösche M., Duwe H.-P., Möhwald H. 1988. Quantitative analysis of surface textures in phospholipid monolayer phase transitions. *J. Colloid Interface Sci.*, 126: 432–444.

115. Lotta T.I., Laakkonen L.J., Vitanen, J.A., Kinnunen, P.K.J. 1988. Characterization of Langmuir-Blodgett films of 1,2-dipalmitoyl-sn-glycero-3-phosphatidylcholine and 1-palmitoyl -2- [10-(pyren-1-yl)decanoyl]-sn-glycero-3-phosphatidylcholine by FTIR-ATR. *Chem. Phys. Lipids*, 46:1–12.

116. Lozano P., Fernández A.J., Ruiz J.J., Camacho L., Martín M.T., Muñoz E. 2002. Molecular organization of LB multilayers of phospholipid and mixed phospholipid/viologen by FTIR spectroscopy. *J. Phys. Chem. B*, 106:6507 -6514.

117. Lu N., Gleiche M., Zheng J., Lenhert S., Xu B., Chi L., Fuchs H. 2002. Fabrication of chemically patterned surfaces based on template-directed self-assembly. *Adv. Mater.*, 14:1812–1815.

118. Lukes P.J., Petty M.C., Yarwood J. 1992. An infrared study of the incorporation of ion channel forming peptides into Langmuir-Blodgett films of phosphatidic acid. *Langmuir*, 8:3043–3050.

119. Marron-Brignone L., Morélis R.M., Coulet P.R. 1996a. Immobilization through adsorption of luciferase on Langmuir-Blodgett films. Influence of the hydrophilicity or hydrophobicity of the surface on the enzyme kinetic behaviour. *Langmuir*, 12:5674–5680.

120. Marron-Brignone L., Morélis R.M., Blum L.J., Coulet P.R. 1996b. Behaviour of firefly luciferase associated with Langmuir-Blodgett films. *Thin Solid Films*, 284–285:784–788.

121. Matuoka S., Asami H., Hatta I. 1989. Stability and characterization of phospholipid Langmuir-Blodgett films. *Thin Solid Films*, 180:123–127.

122. McConnell H.M., Radhakrishnan A. 2003. Condensed complexes of cholesterol and phospholipids. *Biochim. Biophys. Acta*, 1610:159–173.

123. Miyauchi S., Arisawa S., Arise T., Yamamoto R. 1989. Study of concentration of an enzyme immobilized by Langmuir-Blodgett films. *Thin Solid Films*, 180: 293–298.

124. Moraille P., Badia A. 2002. Highly parallel, nanoscale stripe morphology in mixed phospholipid monolayers formed by Langmuir-Blodgett transfer. *Langmuir,* 18:4414 -4419.

125. Moraille P., Badia A. 2003. Nanoscale stripe patterns in phospholipid bilayers formed by the Langmuir-Blodgett technique. *Langmuir*, 19:8041–8049.

126. Morélis R.M., Girard-Egrot A.P., Coulet P.R. 1993. Dependence of Langmuir-Blodgett film quality on fatty acid monolayer integrity. 1. Nucleation crystal growth avoidance in the monolayer through the optimized compression procedure. *Langmuir*, 9:3101–3106.

127. Moriizumi T. 1988. Langmuir-Blodgett films as chemical sensors. *Thin Solid Films*, 160:413–431.

128. Mou J., Yang J., Shao Z. 1995. Atomic force microscopy of cholera toxin B-oligomers bound to bilayers of biologicallyrRelevant lipids.*J. Mol. Biol.*, 248:507–512.

129. Neuman R.D. 1978. Molecular reorientation in monolayers at the paraffin-water interface. *J. Colloid Interface Sci.*, 63:106–112.

130. Neuman R.D., Swanson J.W. 1980. Multilayer deposition of stearic acid—calcium stearate monomolecular films. *J. Colloid Interface Sci.*, 74:244–259.

131. Okahata Y., Tsuruta T., Ijiro K., Ariga K. 1988. Langmuir-Blodgett films of an enzyme-lipid complex for sensor membranes. *Langmuir*, 4:1373–1375.

132. Okahata Y., Tsuruta T., Ijiro K., Ariga K. 1989. Preparations of Langmuir-Blodgett films of enzyme-lipid complexes: a glucose sensor membrane. *Thin Solid Films*, 180:65–72.

133. Okamura E., Umemura J., Iriyama K., Araki T. 1993. Microstructure of thin Langmuir-Blodgett films of dipalmitoylphosphatidylcholine: electron microscopic images replicated with plasma polymerized film by glow discharge. *Chem. Phys. Lipids*, 66:219–223.

134. Okonogi T.M., McConnell H.M. 2004. Contrast Inversion in the Epifluorescence of Cholesterol-Phospholipid Monolayers. *Biophys. J.,* 86:880–890.

135. Pal P., Nandi D., Misra T.N. 1994. Immobilization of alcohol dehydrogenase enzyme in a Langmuir-Blodgett film of stearic acid: its application as an ethanol sensor. *Thin Solid Films*, 239:138–143.

136. Peng J. B., Ketterson J.B., Dutta P. 1988. A study of the transition from Y- to X-type transfer during deposition of lead stearate and cadmium stearate Langmuir-Blodgett Films. *Langmuir*, 4:1198–1202.

137. Peng J.B., Abraham B.M., Dutta P., Ketterson J.B. 1985. Contact angle of lead stearate-covered water on mica during the deposition of Langmuir-Blodgett assemblies. *Thin Solid Films*, 20:187–193.

138. Peng J.B., Prakash M., Macdonald R., Dutta P., Ketterson J.B. 1987. Formation of multilayers of dipalmitoylphosphatidylcholine using the Langmuir-Blodgett technique. *Langmuir*, 3:1096–1097.

139. Peterson I. R. 1992. Langmuir-Blodgett films. In Ashwell G.J., ed. Molecular Electronics. New York: Research Studies Press. p 117–206.

140. Peterson I.R., Russell G.J. 1985a. Deposition mechanisms in Langmuir-Blodgett films. *Br. Polym. J.*, 17:364–367.

141. Peterson I.R., Russell G.J. 1985b. The deposition and structure of Langmuir-Blodgett films of long-chain acids.*Thin Solid Films*, 134:143–152.

142. Peterson I.R., Russell G.J., Roberts G.G. 1983. A new model for the deposition of ω-tricosenoic acid Langmuir-Blodgett film layers. *Thin Solid Films*, 109:371–378.

143. Peterson IR. 1990. Langmuir-Blodgett films. *J. Phys. D:Appl. Phys.*, 23:379–395.

144. Petty M.C. 1990. Characterization and properties. In Robert G.G., ed. Langmuir-Blodgett films. New York: Plenum Press. p 133–221.

145. Petty M.C. 1996. Langmuir-Blodgett films. An introduction. Cambridge: University press.

146. Petty M.C., Barlow W.A. 1990. Film deposition. In Robert G.G., ed. Langmuir-Blodgett films. New York: Plenum Press. p 93–132.

147. Petty M., Tsibouklis J., Petty M.C., Feast W.J. 1992. Pyroelectric behaviour of synthetic biomembrane structures. *Thin Solid Films*, 210–211:320–323.

148. Pillet L., Perez H., Ruaudel-Teixier A., Barraud A. 1994. Immunoglobulin immobilization by the Langmuir-Blodgett method. *Thin Solid Films*, 244: 857–859.

149. Radhakrishnan A., McConnell H.M. 2000. Electric field effect on cholesterol-phospholipid complexes. *Proc. Natl. Acad. Sci.*, 97:1073–1078.

150. Radhakrishnan A., Anderson T.G., McConnell H.M. 2000. Condensed complexes, rafts, and the chemical activity of cholesterol in membranes. *Proc. Natl. Acad. Sci.*, 97:12422–12427.

151. Rajagopal A., Dhanabalan A., Major S.S., Kulkarni S.K. 1998. The effect of different metal cation incorporation in arachidic acid Langmuir-Blodgett (LB) monolayer films *Appl. Surf. Sci.*, 125:178–186.

152. Ramsden J.J., Bachmanova G.I., Archakov A.I. 1996. Immobilization of proteins to lipid bilayers *Biosens. Bioelectron.*, 11:523–528.

153. Reicher W.M., Bruckner C.J., Joseph J. 1987. Langmuir-Blodgett films and black lipid membranes in biospecific surface-selective sensors. *Thin Solid Films*, 152:345–376.

154. Riegler J.E., LeGrange J.D. 1988. Observation of a Monolayer Phase Transition on the Meniscus in a Langmuir-Blodgett Transfer Configuration. *Phys. Rev. Lett.*, 61:2492–2495.

155. Riegler H., Spratte K. 1992. Structural changes in lipid monolayers during the Langmuir-Blodgett transfer due to substrate/monolayer interactions. *Thin Solid Films*, 210/211:9–12.

156. Rinia H.A., Demel R.A.,van der Eerden Jan P.J.M.,de Kruijff.B. 1999. Blistering of Langmuir-Blodgett bilayers containing anionic phospholipids as observed by atomic force microscopy. *Biophys J*, 77:1683–1693.

157. Rinia H.A., de Kruijff B. 2001. Imaging domains in model membranes with atomic force microscopy. *FEBS Lett.*, 504:194–199.

158. Robert G.G. 1990. Langmuir-Blodgett films. New York: Plenum Press.

159. Robinson I., Sambles J.R., Cade N.A. 1989. Variations in the surface free energy of fatty acid Langmuir-Blodgett multilayers. *Thin Solid Films*, 178:125–136.

160. Rosilio V., Boissonnade M.M., Zhang J., Jiang L., Baszkin A. 1997. Penetration of glucose oxidase into organized phospholipid monolayers spread at the solution/air interface. *Langmuir*, 13:4669–4675.

161. Saint Pierre M., Dupeyrat M. 1983. Measurement and meaning of the transfer process energy in the building up of Langmuir-Blodgett multilayers. *Thins Solid Films*, 99:205–213.

162. Schneider J., Dufrêne Y.F., Barger Jr. W.R., Lee G.U. 2000. Atomic force microscope image contrast mechanisms on supported lipid bilayers. *Biophys J.*, 79:1107–1118.

163. Schneider J., Barger W., Lee G.U. 2003. Nanometer scale surface properties of supported lipid bilayers measured with hydrophobic and hydrophilic Atomic Force Microscope probes. *Langmuir,* 19:1899–1907.

164. Schwartz D.K., Viswanathan R., Zasadzinski J.A.N. 1993. Commensurate defect superstructures in a Langmuir-Blodgett film. *Phys. Rev. Lett.*, 70:1267–1270.

165. Siegel S., Kindermann M., Regenbrecht M., Vollhardt D., von Kiedrowski G. 2000. Molecular recognition of a dissolved carboxylate by amidium monolayers at the air-water interface. *Progr. Colloid Polym. Sci.*, 115:233–237.

166. Sikes H.D., Woodward J.T., Schwartz D.K. 1996. Pattern formation in a substrate-induced phase transition during Langmuir-Blodgett transfer. *J. Phys. Chem.*, 100:9093–9097.

167. Sikes H.D., Schwartz D.K.. 1997. A temperature-dependent two-dimensional condensation transition during Langmuir-Blodgett deposition. *Langmuir*, 13:4704–4709.

168. Silvius J.R. 2003. Role of cholesterol in lipid raft formation: lessons from lipid model systems. *Biochim. Biophys. Acta*, 1610:174–183.

169. Simons K., Ikonen E. 1997. Functional rafts in cell membranes. *Nature,* 387:569–572.

170. Simons K., Ikonen E. 2000. How Cells Handle Cholesterol. *Science,* 290: 1721–1726.

171. Solletti J.M., Botreau M., Sommer F., Brunat W.L., Kasas S., Minh Duc T., Celio M.R. 1996. Elaboration and characterization of phospholipid Langmuir-Blodgett films. *Langmuir*, 12:5379–5386.

172. Spratte K., Riegler H. 1994. Steady state morphology and composition of mixed monomolecular films (Langmuir monolayers) at the air/water interface in the vicinity of the three-phase line: model calculations and experiments. *Langmuir*, 10:3161–3173.

173. Spratte K., Chi L.F., Riegler H. 1994. Physisorption instabilities during dynamic Langmuir wetting. *Europhys. Lett.*, 25:211–217.

174. Sriyudthsak M., Yamagishi H., Moriizumi T. 1988. Enzyme-immobilized Langmuir-Blodgett film for a biosensor. *Thin Solid Films*, 160:463–469.

175. Steitz R., Mitchell E.E., Peterson I.R. 1991. Relationships between fatty acid monolayer structure on the subphase and on solid substrates. *Thin Solid Films*, 205:124–130.

176. Tamm L.K., McConnell H.M.. 1985. Supported phospholipid bilayers. *Biophys. J.*, 47:105–113.

177. Taneva S.G., Keough K.M.W. 1994. Dynamic surface properties of pulmonary surfactant proteins SP-B and SP-C and their mixtures with dipalmitoyl-phosphatidylcholine. *Biochemistry*, 33:14660–14670.

178. Tatsuma T., Tsuzuki H., Okawa Y., Yoshida S., Watanabe T. 1991. Bifunctional Langmuir-Blodgett film for enzyme immobilization and amperometric biosensor sensitization. *Thin Solid Films*, 202:145–150.

179. Taylor D.M., Mahboubian-Jones M.G.B. 1982. The electric properties of synthetic phospholipid Langmuir-Blodgett Films. *Thin Solid Films*, 87: 167–179.

180. Tredgold R.H. 1994. Order in thin organic films. Cambridge: University press.

181. Tsuzuki H., Watanabe T., Okawa Y., Yoshida S., Yano S., Koumoto K., Komiyama M., Nihei Y. 1988. A novel glucose sensor with a glucose oxidase monolayer immobilized by Langmuir-Blodgett technique. *Chem. Lett.*, 1265–1268.

182. Ulman A. 1991. Langmuir-Blodgett Films. In An introduction to ultrathin organic films from Langmuir-Blodgett to self assembly. New York: Academic press Inc. p 101–219.

183. Vaughan M.H., Froggatt E.S., Swart R.M., Yarwood J. 1992. Fourier transform infrared spectroscopic studies on model biological membranes deposited by the Langmuir-Blodgett technique. *Thin Solid Films*, 210/211:574–576.

184. Verger R., Pattus F. 1982. Lipid-protein interactions in monolayers. *Chem. Phys. Lipids*, 30:189–227.

185. Vickery S.A., Dunn R.C. 2001. Direct observation of structural evolution in palmitic acid monolayers following Langmuir-Blodgett deposition. *Langmuir,* 17:8204–8209.

186. Vikholm I., Albers W.M. 1998. Oriented immobilization of antibodies for immunosensing. *Langmuir*, 14: 3865–3872.

187. Vikholm I., Viitala T., Albers W.M., Peltonen J. 1999. Highly efficient immobilisation of antibody fragments to functionalised lipid monolayers. *Biochim. Biophys. Acta*, 1421:39–52.

188. Vollhardt D. 1996. Morphology and phase behavior of monolayers. *Adv. Colloid Interface Sci.*, 64:143–171.

189. Vollhardt D. 2002. Supramolecular organization in monolayers at the air/water interface. *Mater. Sci. Eng.* C, 22:121–127.

190. Vollhardt D., Fainerman V.B. 2000. Penetration of dissolved amphiphiles into two-dimensional aggregating lipid monolayers. *Adv. Colloid Interface Sci.*, 86:103–151.

191. Wan K., Chovelon J.-M., Jaffrezic-Renault N. 2000. Enzyme-octadecylamine Langmuir-Blodgett membranes for ENFET biosensors. *Talanta*, 52:663–670.

192. Yamada S., Ishino F., Matsushita K., Nakadaira T., Kitao M. 1992. Conducting defects in Langmuir-Blodgett films of cadmium stearate. *Thin Solid Films*, 208:145–148.

193. Yang J., Kleijn J.M. 1999. Order in phospholipid Langmuir-Blodgett layers and the effect of the electrical potential of the substrate. *Biophys. J.*, 76:323–332.

194. (Yasuzawa M., Hashimoto M., Fujii S., Kunugi A., Nakaya T. 2000. Preparation of glucose sensors using the Langmuir-Blodgett technique. *Sens. Actuators B*, 65:241–243.

195. Yazdanian M., Yu H., Zografi G., Kim M.W. 1992. Divalent cation-stearic acid monolayer interactions at the air/water interface *Langmuir*, 8:630–636.

196. Yuan C., Johnston L.J. 2000. Distribution of ganglioside GM1 in L-α-dipalmitoylphosphatidylcholine/cholesterol monolayers. *Biophys. J.*, 79:2768–2781.

197. Yuan C., Johnston L.J. 2001. Atomic force microscopy studies of ganglioside GM1 domains in phosphatidylcholine and phosphatidylcholine/cholesterol bilayers. *Biophys. J.*, 81:1059–1069.

198. Yuan C., L. J. Johnston. 2002. Phase evolution in cholesterol/DPPC monolayers: atomic force microscopy and near field scanning optical microscopy studies. *J. Microscopy*. 205:136–146.

199. Yuan C., Furlong J., Burgos P., Johnston L.J. 2002. The size of lipid rafts: an Atomic Force Microscopy study of Ganglioside GM1 domains in sphingomyelin/DOPC/cholesterol membranes. *Biophys. J.*, 82:2526–2535.

200. Zahn D., Brickmann J. 2002. Molecular dynamics study of water pores in a phospholipid bilayer. *Chem. Phys. Lett.*, 352: 441–446.

201. Zaitsev S.Yu, Kalabina N.A., Zubov VP, 1991a. Biosensors based on glucose oxidase Langmuir films. *J. Anal. Chem. USSR*, 45:1054–1056.

202. Zaitsev S. Yu, Hanke Th., Wollenberger U., Ebert E., Kalabina N.A., Zubov V.P., Scheller F. 1991b Mono- and multilayer membranes with adsorbed glucose oxidase. *Bioorg. Khim.*, 17:767–772.

203. Zasadzinski J.A., Viswanathan R., Madsen L., Garnaes J., Schwartz D.K. 1994. Langmuir-Blodgett films, *Science*, 263, 1726–1733.

204. Zhang A., Hou Y., Jaffrezic-Renault N., Wan J., Soldatkin A., Chovelon J.M. 2002. Mixed urease/amphiphile LB films and their application for biosensor development. *Bioelectrochemistry*, 56:157–158.

205. Zhang J., Rosilio V., Goldmann M., Boissonnade M.M., Baszkin A. 2000. Adsorption of glucose oxidase into lipid monolayers. Effect of lipid chain lengths on the stability and structure of mixed enzyme/phospholipid films. *Langmuir*, 16:1226–1232.
206. Zhu D.C., Petty M.C., Ancelin H., Yarwood J. 1989. On the formation of langmuir-blodgett films containing enzymes. *Thin Solid Films*, 176:151–156.
207. Zhu D.G., Petty M.C., Ancelin H., Yarwood J. 1992. Molecular interactions in Langmuir-Blodgett films of phospholipid and fatty acid mixtures. *Langmuir*, 8:619–623.

3
Liposome Techniques for Synthesis of Biomimetic Lipid Membranes

Stella M. Valenzuela

3.1.   Introduction

The lipid bilayer is the universal basis for cell membrane structure. Historically, the formation of this bilayer into a closed, spherical vesicle, essentially a microscopic sac, resulted in the creation of a boundary separating the internal environment (lumen) from the external environment. This very basic vesicle structure with its semipermeable properties, has formed the basis for the development of life on earth as we know it.

The term used to describe these closed spherical structures is a liposome. These bilayer vesicles form spontaneously when phospholipids (containing 2 hydrocarbon chains and a hydrophilic polar head group) are exposed to an aqueous environment. This was first demonstrated in 1965 by Bangham and his colleagues[1] who were studying the diffusion of univalent ions across what they described as "spontaneously formed liquid crystals of lecithin". They reported that ions diffused across these artificial membranes in a manner highly analogous to that observed in biological membranes[1].

The liposome is the favoured structure adopted by the bilayer when in contact with water. This arises from the fact that it is a more energetically stable form, avoiding exposure of the hydrophobic tails of the phospholipids, to the aqueous milieu. In this configuration, the polar head groups are in contact with the watery interface, while the hydrocarbon tails remain buried in the bilayer, creating a hydrophobic inner layer. On the other hand, single chain lipids such as lysolipids and detergents, spontaneously aggregate into micelles rather than bilayers[2].

3.2.   Applications and Uses of Liposomes

Along with this highly convenient property of forming spontaneously, liposome self-assembly results in their trapping an aqueous inner environment. As such, these sealed compartments act as a highly useful transport vehicle in numerous

applications including the rapidly expanding field of drug delivery[3], gene therapy[4] and form one of the basic building blocks in the development and design of the artificial cell[5]. More fundamentally, liposomes have served as a workhorse over the last decades providing a model system for cell membranes in experimental studies and have been useful in our understanding of basic cell physiology.

A more recent application of liposomes is as "nanoreactors". This involves the encapsulation of enzymes within the vesicles, along with the presence of membrane channels to control the entrance of substrate and subsequent exit of the enzymatic reaction product[6,7]. Advancement in our understanding of intracellular processes is assisted by the use of liposomes. For example, in a paper by Roux et al[8], giant liposomes and kinesin molecules were used to demonstrate the formation of tubular networks such as those involved in transport events between cellular compartments in cells. Another application of liposomes is their use as food processing microcapsules[9]. An example of this is the entrapment of the enzyme neutrase within liposomes to accelerate the maturation of Cheddar cheese[10]. Liposomes are also used in the cosmetics industry where they are incorporated into such products as facial and skin creams. They have also been found to serve as adjuvants, enhancing the immunogenicity of small antigens[11−13], while other reports describe their use and incorporation into traditional immunoassays[14].

3.3.   Liposome Structure is Influenced by its Phospholipid Composition

The types of phospholipids used in the production of liposomes are crucial in determining the liposomal properties. One can use various combinations of charged or uncharged lipids, depending on the ultimate use of the liposome. Negatively charged acidic phospholipids include, dipalmitoyl phosphatidyl glycerol (DPPG), dipalmitoyl phosphatidic acid (DPPA), phosphatidyl serine (PS), phosphatidyl inositol (PI). Uncharged, neutral lipids commonly used include, phosphatidyl choline (PC), phosphatidyl ethanolamine (PE), sphingomyelin and alkyl ether lecithin. In addition, incorporation of sterols (such as cholesterol which is found in most naturally occurring membranes) is often used and their incorporation is known to impact on the membrane fluidity, permeability and stability[15−17]. There are also positively charged lipids, which are synthetically made molecules such as stearylamine. Most commonly these positively charged lipids are used in the preparation of liposomes for the purpose of transfecting DNA into mammalian cells. Examples of such positively charged lipids include DOTAP {1,2-dioleoyloxy-3-(trimethylammonio) propane}, DOTMA {N-(2,3-(dioleyloxy)propyl-N,N,N-trimethyl ammonium}[2,18] and DODAc (dioctadecyldimethylammonium chloride)[2].

Liposomes can vary in size, depending on how they are produced. The smallest liposomes range down to approximately 25nm[17], while the diameter of giant liposomes can span up to several hundred microns[19]. Lamellarity, which refers to the number of bilayers contained within a single liposome, is a property that is also controlled by the method of preparation. Some methods favour the production of unilamellar liposomes while others result in the formation of a population of liposomes with an onion like structure of multiple layers of concentric membranes, referred to as multilamellar vesicles. Multilamellar liposomes are generally more stable than unilamellar liposomes[20]. However, the presence of many internal compartments limits the use of multilamellar liposomes especially when such cellular processes such as endocytosis and exocytosis, transport mechanisms and permeability are to be studied[21,22].

3.4. Common Terminology Used in the Description of Liposome Structure

The following terms are commonly used in the literature to describe liposomes[17,21]

1. Multilamellar vesicles (MLVs)	these range in size between 0.1 to 10 μm in diameter each vesicle usually consists of 5 or more concentric lamellae
2. Small unilamellar vesicles (SUVs)	these have a diameter typically less than 100nm
3. Large unilamellar vesicles (LUVs)	these have diameters ranging between 100 to 500 nm
4. Giant liposomes (GUV)	these have diameters greater than 1 μm

3.5. Liposome Preparation

Liposomes can be obtained by several approaches which include the use of organic solvents, mechanical procedures, or by the removal of detergent from phospholipid/detergent micelle mixtures. As stated earlier, the structural properties of the liposomes produced, depend on such factors as the composition and concentration of the constituent phospholipids, liposomal size, membrane fluidity, surface charge, the ionic strength of the aqueous medium and the time allowed for hydration[2].

Numerous review papers and textbooks have been written on the preparation and characterisation of liposomes, to which the reader can refer for additional information. These include Hope et al.,[21], New[17], Szoka and Papahadjopoulos[23] and Gregoriadis[24]. The following sections aim to present some of the most commonly used liposome methods as well as, some of the latest advances in the methodology for the preparation and modification of liposomes.

3.5.1. Preparation of Multilamellar Vesicles

Multilamellar vesicles are the simplest of all liposomes to produce. The most direct method for their preparation involves dissolving a known quantity of lipid in organic solvent, followed by the drying of this mixture and its subsequent reconstitution. The following is a commonly used combination of lipids, it incorporates egg lecithin, cholesterol and phosphatidyl glycerol in a molar ratio of 0.9:1.0:0.1 respectively. The solvent most commonly used is chloroform or a mixture of chloroform and methanol in a typical ratio of 2:1 respectively.

   Each of the lipid components are initially dissolved in the organic solvent separately, then mixed in the required proportion with the other solubilized lipids. This is done to ensure an even distribution of the lipids in the mixture. The mixture is then dried under a stream of nitrogen to form a uniform film on the walls of a round-bottomed glass test tube or flask. The lipid film is then allowed to completely dry in an evacuated chamber for a minimum of 4–6 hours, in order to remove any last traces of organic solvent.

   The dry residue can be either stored at this point or reconstituted with water or buffer of choice, at a temperature above the lipid phase transition temperature. Typically, the rehydration step is allowed to proceed for a minimum time of 30 minutes to 1 hour with gentle agitation of the mixture. However, in order to increase encapsulation efficiency, a prolonged hydration time is required. Szoka and Papahadjopoulos[23] indicate that a similar lipid concentration can encapsulate 50% more of the aqueous phase per mole of lipid when allowed to hydrate for 20 hours with gentle shaking, compared to a sample allowed to hydrate for only 2 hours with gentle shaking. In addition they describe that a similar lipid preparation allowed to hydrate for only 30 minutes with vigorous shaking results in both a lower encapsulation volume of aqueous phase per mole of phospholipid, as well as, a smaller mean diameter of the resultant liposomes[23]. In order to achieve a smaller and/or more uniformly sized population of liposomes, vigorous vortexing, brief sonication, or extrusion through polycarbonate membranes can be employed[23].

   Other methods for increasing solute entrapment volume per mole of lipid and promoting equilibrium solute distribution between the aqueous compartments of multilamellar vesicles, is the process of freeze-thawing[21] or dehydration-rehydration[13,20]. Freeze-thawing involves several[4–5] cycles of quick freezing of the rehydrated liposomes in liquid nitrogen, followed by rapid thawing in warm water[21]. The process of dehydration-rehydration requires mixing of an aqueous solution containing the solute to be encapsulated, with a suspension of water-containing multilamellar liposomes. This mixture is then freeze-dried, which results in bringing the solute into close contact with the liposomal membrane structures. The freeze-dried mixture is then rehydrated in a controlled fashion[13,20], resulting in an increased encapsulation volume of the solute of interest.

3.5.2.   *Preparation of Unilamellar Vesicles*

The most popular type of liposome is the unilamellar vesicle. This liposome configuration allows for a uniform distribution of trapped agents within a single internal aqueous compartment, with large unilamellar vesicles providing an increased trapped aqueous volume per mole of phospholipid compared to multilamellar liposomes of comparable size[23].

3.5.2.1.   Ultrasonication

The preparation of small unilamellar liposomes up to 100nm in diameter using ultrasonication involves starting with a standard preparation of multilamellar liposomes, by a method such as that described in the previous section. These multilamellar liposomes can then be ultrasonicated using either a bath or probe sonicator. The vortexing or sonication is done in short bursts of several seconds duration interspersed over the rehydration period. Agitation can be increased by the addition of glass beads (sized between 0.5–3mm), which assists in the suspension of lipid clumps or thick regions of lipid dried on the glass vessel[17]. This procedure results in the production of small unilamellar liposomes, with their size generally being less than 30–60nm[2,25]. However, such liposomes tend to have defects and undergo aggregation and fusion[2] particularly if the physical agitation is done at a temperature below the lipid melting phase transition temperature[23]. An early publication by Huang in 1969[26], demonstrated the use of sonication to form unilamellar liposomes. The unilamellar morphology of the liposomes was demonstrated by transmission electron microscopy, with the liposomes estimated to have an average diameter of 23–25nm[26].

3.5.2.2.   Extrusion through Polycarbonate Filters

Larger sized unilamellar vesicles between 50–200nm can be achieved by pressure extrusion of multilamellar vesicles through membranes of known pore size[27]. This procedure can be used in combination with freeze-thaw protocols to produce unilamellar vesicles with diameters in the range 60–100 nm[27]. The advantages of this technique include the absence of organic solvents or detergents, the high lipid concentrations that can be used as well as achieving high encapsulation efficiencies (up to 30%)[27]. Liposomes prepared by extrusion therefore offer certain desirable properties such as a uniform size distribution, a high degree of unilamellar structure, long-term stability and controlled responsiveness to the milieu[28]. However, it has been reported that they do tend to possess an elongated elliptical shape rather than a truly spherical one, an important point to be considered especially for experimental work where quantitation is required[28].

3.5.2.3.   Freeze – Thawing

Freeze-thawing is a useful procedure in achieving an increased trapped volume within multilamellar liposomes as well as unilamellar liposomes. It is also another way of preparing small unilamellar liposomes. This approach for preparing
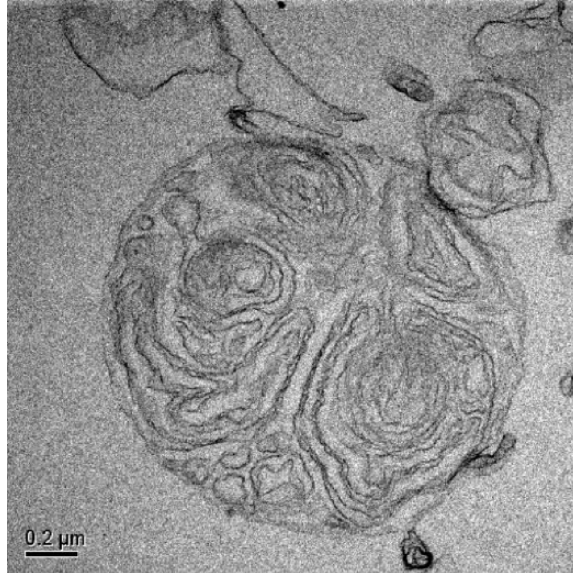
FIGURE 3.1. Transmission Electron Micrograph of a multilamellar liposome prepared by sonication (Image courtesy of Mr. Sabah Al Khazaaly, University of Technology Sydney, Australia).
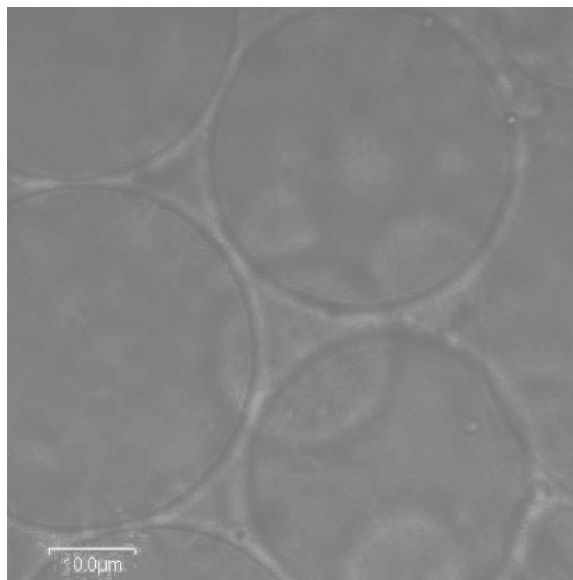

FIGURE 3.2. Unilamellar vesicles prepared by rehydration in the presence of sucrose. Viewed by phase contrast microscopy (image courtesy of Dr. Isabelle Di Maio, OzNano$_2$Life, University of Technology Sydney, Australia).

small unilamellar vesicles involves several rounds of freezing and thawing. An example of this procedure is taken from Singh et al.[29] The lipids used were dipalmitoylphosphatidyl choline (DPPC), dipalmitoylphosphatidic acid (DPPA) and diacetyl phosphate (DCP). The initial process involves drying a mixture of chloroform-solubilized lipids under a gentle stream of nitrogen. The sample is then further dried under high vacuum for up to 8 hours. Buffer solution is then added to the lipid film and the suspension is left for a minimum of 12 hours or overnight at +4°C. This is then heated to 65°C in a water bath for 10 minutes, vortexed for 15 seconds then cooled in an ice-water mixture for 15 minutes. This freeze–thaw process is repeated for a total of 3 times. The resulting suspension is then bath sonicated for 15 minutes above the lipid melting phase transition temperature, which leads to the formation of larger vesicles with a unilamellar morphology.

3.5.2.4.   Ethanol Injection

This method is particularly useful for incorporating hydrophobic and amphiphilic drugs into liposomes, and avoids use of detergents and sonication[2,23]. It simply requires that the lipids, which are dissolved in ethanol, be rapidly injected into a buffer solution where they spontaneously form small unilamellar vesicles. The major deficit of this approach is that the resulting liposomes are relatively dilute[23].

3.5.2.5.   Detergent Method

The use of detergents which have a high critical micelle concentration such as cholate (deoxycholate) or octylglucoside are employed for this approach, since this allows for their complete and rapid removal by such methods as dialysis[17,21]. The detergent removal approach has proven highly successful as a means of reconstituting transmembrane proteins in particular[2] and was first introduced by Kagawa and Racker[30]. The method involves the initial solubilization of dry lipid or pre-formed vesicles in the desired buffer with detergent, to form mixed micelles. Micelles containing 2 or more detergents or components in addition to detergent are referred to as mixed micelles[17]. The detergent is then removed by dialysis, column chromatography, Biobeads or other methods, resulting in the spontaneous formation of unilamellar vesicles[2,17,21], having a mean diameter in the range of 80–200nm[13].

   This detergent approach, has been modified by others such as, Rigaud et al., Le Dain et al., Kloda et al., and Park et al.,[31−34] to form giant liposomes incorporating transmembrane ion channel proteins that are suitable for patch clamping.

3.5.2.6.   Preparation of Sterile Large Unilamellar Vesicles

A novel method for the preparation of sterile submicron liposomes was described by Li and Deng[35]. Lipid is dissolved in *tert*-butyl alcohol, after which it is mixed with an aqueous sucrose solution. This mixture is then sterilized by filtration

through a 0.22 μm pore sized filter. The sterile mixture is then subjected to a process of freeze-drying. Several steps are involved with the mixture initially being frozen at -40°C for 8 hours, followed by drying at -40°C for 48 hours and then a further 10 hours of drying at 25°C. The lyophilized products are reported to be stable for prolonged periods if kept dry and well sealed. The lyophilised products are then reconstituted by the addition of an equal volume of sterile water, with gentle shaking, which results in the formation of an aqueous suspension of sterile liposomes[35].

3.5.3.   Preparation of Giant Unilamellar Liposomes

In the preparation of giant liposomes, many methods refer to the need to use only distilled water, non-electrolyte or zwitterions[17,36]. This is believed to be due to an increase in attraction between membranes caused by the presence of ions imparting a net charge, and thereby inhibiting the separation of the membrane sheets during the rehydration and swelling process[17]. However, more recently, Akashi et al.,[19] have demonstrated preparation of giant liposomes using physiological strength buffers, outlined below in section 3.5.3.3.

3.5.3.1.   Electroformation

Giant unilamellar vesicles (greater than 10 microns in diameter) can be prepared by the use of an AC electric field[25,37]. This method involves initial solubilization and mixture of the lipids in a chloroform-methanol mixture (9:1) to obtain the correct composition. The solvent is then evaporated under a stream of nitrogen, followed by a further evacuation under reduced pressure for at least 12 hours. The dry lipid residue is then dissolved in a mixture of diethylether and methanol in a ratio of 9:1 (v/v) yielding a final lipid concentration of 1mM. Approximately 1μl of this solution is then applied onto the surface of platinum electrodes. These are then dried with a stream of nitrogen, followed by evacuation in a vacuum for at least 1 hour.

The electrodes are then placed into a glass chamber with a quartz window bottom allowing the chamber to be viewed on an inverted microscope with a heated stage (temperature needs to be kept above the phase-transition temperature of the lipids used). An 0.2 V AC voltage is applied prior to the addition of water or a low ionic strength buffer, such as 0.5mM Hepes, pH7.4[25]. The voltage is then raised to 1-2V during the first minute of rehydration. Rehydration is allowed to proceed for 2 hours after which time, giant liposomes (diameters > 10μm) can be directly observed through the phase contrast objective of an inverted microscope[25,37]. Drawbacks of this method are the need to use low ionic strength buffers and ensuring that the voltage applied does not exceed 2 V[22,37].

3.5.3.2.   Rapid Preparation of Giant Liposomes

A method described by Moscho et al.,[22] results in the formation of giant unilamellar liposomes of up to 50μm in diameter, after only 2 minutes. The

ionic strength of the buffer is limited to a maximum of 50mM, but the advantage of this method is presented as the short preparation time which allows for the encapsulation of highly labile or enzymatically active substances[22]. The method essentially involves the initial dissolving of the lipids in chloroform (0.1M) followed by diluting 20µl of the dissolved lipid into a chloroform / methanol mixture (980µl chloroform + 100µl methanol) in a 50ml round-bottomed flask. A volume of 7mls water or low ionic strength buffer containing molecules to be entrapped into the liposomes is then added down the sides of the flask. The organic solvent is then removed using a rotary evaporator under reduced pressure for about 2 minutes. The remaining aqueous solution contains giant unilamellar liposomes in high concentration[22].

3.5.3.3.   Giant Unilamellar Liposomes Prepared in Physiological Buffer

Akashi et al.,[19] use a modified gentle hydration method to prepare giant unilamellar liposomes with diameters of 25–100 µm using various physiological salt solutions, such as 100mM KCl plus 1mM CaCl$_2$. Their preparation however requires the inclusion of 10–20% charged lipid such as phosphatidylglycerol, phophatidylserine, phosphatidic acid, or cardiolipin. The bulk lipid was a neutral lipid, either phosphatidylcholine or phosphatidylethanolamine. The lipid mixture is dissolved in a chloroform:methanol mixture (9:1). This is then dried down in a glass test tube at 45ºC using a rotary evaporator to form a thin film on the lower portion of the test tube. The film is further dried for a minimum of 6 hours in a vacuum drier. The resultant dehydrated film is then prehydrated at 45ºC with water saturated nitrogen for 15–25 minutes, followed by the gentle addition of 5–6ml of a nitrogen purged, aqueous solution, containing 0.1M sucrose and appropriate salts. This is refered to as the internal solution as it will remain entrapped in the liposomes. The tube is then sealed under argon and incubated at 37ºC overnight. During this time the film of lipid comes away from the glass tube surface and forms a bulky white mass floating in the middle of the solution. It is this bulky white mass which contains the giant unilamellar liposomes, which is then harvested (about 1ml) and can be stored in a plastic tube[19].

3.5.4.   Modified Liposomes

A paper by Hill and Zeidel[38] describes the design and preparation of "Leaflet-specific liposomes". The liposomes they constructed were designed to mimic either the exofacial leaflet or the cytoplasmic leaflet of Madin-Darby canine kidney (MDCK) cells. This was achieved by using specific combinations of lipids known to be located specifically on either of the 2 membrane leaflets. Differential sorting of lipids naturally occurs in these cells by the trans-Golgi network, directing lipids to either the outer or inner leaflet of the bilayer and then subsequently, restricting their intermingling[38]. Such an approach of tailoring liposomes is useful in elucidating cellular processes associated with specific lipid membrane compositions. A review paper by Spector and Yorek[39] describes the

various changes that can occur in membrane lipid composition under biological conditions and the functional consequences of these variations. For example the conformation or quaternary structure of transmembrane proteins is greatly influenced by their lipid micorenvironment, or the production of certain factors such as prostaglandins, is dependent on the availability of substrate fatty acids stored in the membrane phospholipids[39].

Other modifications of liposomes include entrapment of a gel such as agarose within the vesicle lumen[40] or, the incorporation of biotinylated lipids for such purposes as their purification[41,42], fluorescent labelling[43], and as a means of studying such properties as ligand-receptor binding, adhesion and spreading pressures[43,44]. The use of biotinylated phospholipids in unilamellar vesicles was described by Pignataro et al[44] in their study which addressed such questions as the function of adhesion energy in regards to changes in vesicle morphology. Their study utilized the binding properties of biotinylated liposomes to avidin / streptavidin coated surfaces, along with scanning force microscopy to observe vesicle rupture on solid substrates.

The use of liposomes in certain applications and their long-term storage has been limited by their relative instability due to such processes as chemical degradation including oxidation and hydrolysis, dehydration induced phase transition, thermodynamic instability, aggregation, membrane fusion and degradation *in vivo* by enzymic lipases. In a recently published paper by Raysschaert et al.,[7] they describe 3 different types of mechanically stable hollow capsules based
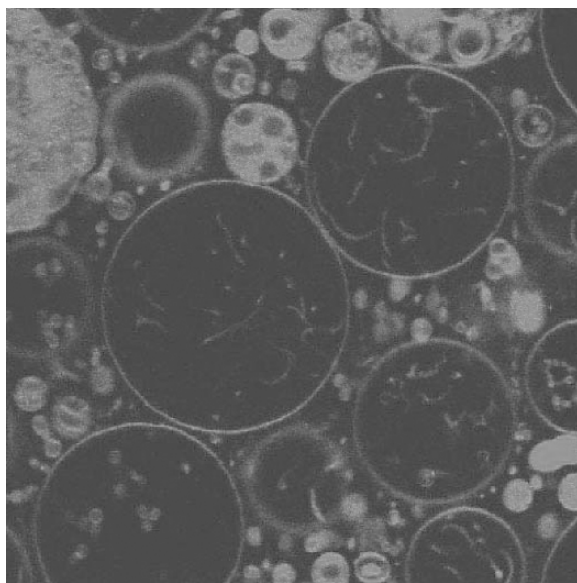

FIGURE 3.3. Liposomes prepared with the incorporation of 10% biotinylated phospholipid and stained with streptavidin-FITC conjugate (image courtesy of Dr Isabelle Di Maio, OzNano$_2$Life, University of Technology Sydney, Australia).

on liposomes. These liposome modification methods are designed to produce stable liposomes with many potential applications. The strategies they employed, included polymerisation of a 2-dimensional network in the hydrophobic core of the membrane, coating of the liposomes with a polyelectrolyte shell and adding surface active polymers to form mixed vesicular structures[7].

3.5.5.   Purification of Liposomes

The need to purify lipids away from their surrounding solution is often necessary in order to quantify the entrapped or lipid bound material. A number of approaches have been developed and used for this purpose[17]. Examples include gel filtration columns such as Sephadex G-50 columns (Sigma), dialysis, centrifugation through a discontinuous gradient of Ficoll[17] or sucrose[45]. The method of simple pelleting of liposomes by centrifugation can be difficult due to their size and low density[42]. A way around this is by the addition of streptavidin to vesicles containing trace amounts of biotinylated lipid. This causes the liposomes to aggregate, allowing them to then be pelleted by ordinary high speed centrifugation[42]. A drawback of this technique are the harsh conditions required to disrupt this interaction between the biotin and streptavidin which can potentially destroy the liposomes and any associated proteins[41]. A refinement of this method, devised by Peker et al.,[41], takes advantage of the fact that the biotinylated liposomes will reversibly bind to a monomeric avidin-functionalized resin. This therefore acts as a means of affinity purifying the liposomes, by their competitive elution from the column using a solution of free biotin. Thus providing a rapid, gentle method for liposome purification.

References

1. Bangham AD, Standish MM, Watkins JC. Diffusion of univalent ions across the lamellae of swollen phospholipids. J Mol Biol 1965;13(1):238–52.
2. Ulrich AS. Biophysical aspects of using liposomes as delivery vehicles. Bioscience Reports 2002;22(2):129–50.
3. Felnerova D, Viret JF, Gluck R, Moser C. Liposomes and virosomes as delivery systems for antigens, nucleic acids and drugs. Current Opinion in Biotechnology 2004;15(6):518–29.
4. Ropert C. Liposomes as a gene delivery system. Brazilian Journal of Medical & Biological Research 1999;32(2):163–9.
5. Pohorille A, Deamer D. Artificial cells: prospects for biotechnology. Trends Biotechnol 2002;20(3):123–8.
6. Nasseau M, Boublik Y, Meier W, Winterhalter M, Fournier D. Substrate-permeable encapsulation of enzymes maintains effective activity, stabilizes against denaturation, and protects against proteolytic degradation. Biotechnology & Bioengineering 2001;75(5):615–8.

7. Ruysschaert T, Germain M, Gomes JF, Fournier D, Sukhorukov GB, Meier W, et al. Liposome-based nanocapsules. IEEE Transactions on Nanobioscience 2004;3(1):49–55.

8. Roux A, Cappello G, Cartaud J, Prost J, Goud B, Bassereau P. A minimal system allowing tubulation with molecular motors pulling on giant liposomes. Proc Natl Acad Sci U S A 2002;99(8):5394–9.

9. Arshady R. Microcapsules for food. J Microencapsul 1993;10(4):413–35.

10. Fresta M, Wehrli E, Puglisi G. Neutrase entrapment in stable multilamellar and large unilamellar vesicles for the acceleration of cheese ripening. Journal of Microencapsulation 1995;12(3):307–25.

11. Gregoriadis G. Immunological adjuvants: a role for liposomes. Immunol Today 1990;11(3):89–97.

12. Alving CR. Liposomes as carriers of antigens and adjuvants. J Immunol Methods 1991;140(1):1–13.

13. Frezard F. Liposomes: from biophysics to the design of peptide vaccines. Braz J Med Biol Res 1999;32(2):181–9.

14. Rongen HA, Bult A, van Bennekom WP. Liposomes and immunoassays. J Immunol Methods 1997;204(2):105–33.

15. van den Bergh BA, Wertz PW, Junginger HE, Bouwstra JA. Elasticity of vesicles assessed by electron spin resonance, electron microscopy and extrusion measurements. International Journal of Pharmaceutics 2001;217(1-2):13–24.

16. Oldfield E, Chapman D. Dynamics of lipids in membranes: Heterogeneity and the role of cholesterol. FEBS Lett 1972;23(3):285–297.

17. New RRC. Liposomes - A Practical Approach. Oxford: IRL Press at Oxford University Press; 1994.

18. Chesnoy S, Huang L. Structure and function of lipid-DNA complexes for gene delivery. Annu Rev Biophys Biomol Struct 2000;29:27–47.

19. Akashi K, Miyata H, Itoh H, Kinosita K, Jr. Preparation of giant liposomes in physiological conditions and their characterization under an optical microscope. Biophys J 1996;71(6):3242–50.

20. Kirby C, Gregoriadis G. Dehydration-rehydration vesicles: a simple method for high yield drug entrapment in liposomes. Biotechnology 1984;2:979–984.

21. Hope MJ, Bally MB, Mayer LD, Janoff AS, Cullis PR. Generation of Multilamellar and Unilamellar Phospholipid Vesicles. Chemistry and Physics of Lipids 1986; 40:89–107.

22. Moscho A, Orwar O, Chiu DT, Modi BP, Zare RN. Rapid preparation of giant unilamellar vesicles. Proceedings of the National Academy of Sciences of the United States of America 1996;93(21):11443–7.

23. Szoka F, Jr., Papahadjopoulos D. Comparative properties and methods of preparation of lipid vesicles (liposomes). Annu Rev Biophys Bioeng 1980;9:467–508.

24. Gregoriadis G. Liposome Technology. 2nd Edition ed. Boca Raton, FL.: CRC Press Inc.; 1993.

25. Holopainen JM, Angelova MI, Soderlund T, Kinnunen PK. Macroscopic consequences of the action of phospholipase C on giant unilamellar liposomes. Biophys J 2002;83(2):932–43.

26. Huang C. Studies on phosphatidylcholine vesicles. Formation and physical characteristics. Biochemistry 1969;8(1):344–52.

27. Hope MJ, Bally MB, Webb G, Cullis PR. Production of large unilamellar vesicles by a rapid extrusion procedure. Characterization of size distribution, trapped volume and

ability to maintain a membrane potential. Biochimica et Biophysica Acta (BBA) – Biomembranes 1985;812(1):55–65.

28. Jin AJ, Huster D, Gawrisch K, Nossal R. Light scattering characterization of extruded lipid vesicles. European Biophysics Journal 1999;28(3):187–99.

29. Singh Y, Gulyani A, Bhattacharya S. A new ratiometric fluorescence probe as strong sensor of surface charge of lipid vesicles and micelles. FEBS Lett 2003;541(1–3):132–6.

30. Kagawa Y, Racker E. Partial Resolution of the Enzymes Catalysing Oxidative Phosphorylation. The Jouranl of Biological Chemistry 1971;246(17):5477–5487.

31. Le Dain AC, Saint N, Kloda A, Ghazi A, Martinac B. Mechanosensitive ion channels of the archaeon Haloferax volcanii. Journal of Biological Chemistry 1998;273(20):12116–9.

32. Kloda A, Martinac B. Molecular identification of a mechanosensitive channel in archaea. Biophysical Journal 2001;80(1):229–40.

33. Park KH, Berrier C, Martinac B, Ghazi A. Purification and functional reconstitution of N- and C-halves of the MscL channel. Biophysical Journal 2004;86(4):2129–36.

34. Rigaud JL, Levy D. Reconstitution of membrane proteins into liposomes. Methods in Enzymology 2003;372:65–86.

35. Li C, Deng Y. A novel method for the preparation of liposomes: freeze drying of monophase solutions. J Pharm Sci 2004;93(6):1403–14.

36. Needham D, Evans E. Structure and mechanical properties of giant lipid (DMPC) vesicle bilayers from 20 degrees C below to 10 degrees C above the liquid crystal-crystalline phase transition at 24 degrees C. Biochemistry 1988;27(21):8261–9.

37. Angelova MI, Dimitrov DS. Liposome Electroformation. Faraday Discuss. Chem. Soc., 1986;81:303–311.

38. Hill WG, Zeidel ML. Reconstituting the barrier properties of a water-tight epithelial membrane by design of leaflet-specific liposomes. Journal of Biological Chemistry 2000;275(39):30176–85.

39. Spector AA, Yorek MA. Membrane lipid composition and cellular function. Journal of Lipid Research 1985;26(9):1015–35.

40. Viallat A, Dalous J, Abkarian M. Giant lipid vesicles filled with a gel: shape instability induced by osmotic shrinkage. Biophys J 2004;86(4):2179–87.

41. Peker B, Wuu JJ, Swartz JR. Affinity purification of lipid vesicles. Biotechnology Progress 2004;20(1):262–8.

42. Tortorella D, Ulbrandt ND, London E. Simple centrifugation method for efficient pelleting of both small and large unilamellar vesicles that allows convenient measurement of protein binding. Biochemistry 1993;32(35):9181–8.

43. Noppl-Simson DA, Needham D. Avidin-biotin interactions at vesicle surfaces: adsorption and binding, cross-bridge formation, and lateral interactions. Biophysical Journal 1996;70(3):1391–401.

44. Pignataro B, Steinem C, Galla HJ, Fuchs H, Janshoff A. Specific adhesion of vesicles monitored by scanning force microscopy and quartz crystal microbalance. Biophysical Journal 2000;78(1):487–98.

45. Lee RJ, Huang L. Folate-targeted, anionic liposome-entrapped polylysine-condensed DNA for tumor cell-specific gene transfer. Journal of Biological Chemistry 1996;271(14):8481–7.

4
Characterization and Analysis of Biomimetic Membranes

Adam I. Mechler

Characterization and analysis of biomimetic membranes represent a challenge to the relatively young field of nanotechnology. Performing measurements on these few nanometers thick, soft, viscoelastic and moderately dynamic systems is close to the limits of the available tools and methods. It is thus important to understand the physics involved in the characterization process to be able to ask the right questions and deduce a correct interpretation of the answers. In this chapter, we provide an overview of the physical properties of biomimetic membrane systems, describe the tools that can measure these properties, and identify a few common errors and artifacts. At the end, we briefly discuss the possibilities and potentials in the emerging methods.

4.1.   Important Properties of Biomimetic Membranes

Before engaging ourselves in the discussion of the characterization of the biomimetic membranes, let us consider of what respect do we need to perform such measurements. The first and most important question one can ask about a biomimetic membrane system is why do we resort to use it. A biomimetic membrane is, by its nature, a necessary compromise; a testbed of selected processes, conveniently reducing the complexity of living organisms. Accordingly, it is not, and it cannot be, the the artificial version of a piece of a cell wall; it is less, but what makes it less, that makes it also more. Since the surface of the membrane can be easily accessed, the mechanism of selected membrane processes, related to signaling, regulation and metastasis of the cells can be studied in controlled conditions with high resolution. Changes in the chemical environment, membrane potential, mechanical stress as well as other perturbations can be precisely and systematically applied. The membrane can serve as an anchor bed for functionalised biomolecules used in biosensor applications. Accordingly, the target of characterization is not so much the membrane itself, but rather the membrane-inserted structures (practically, both) where the
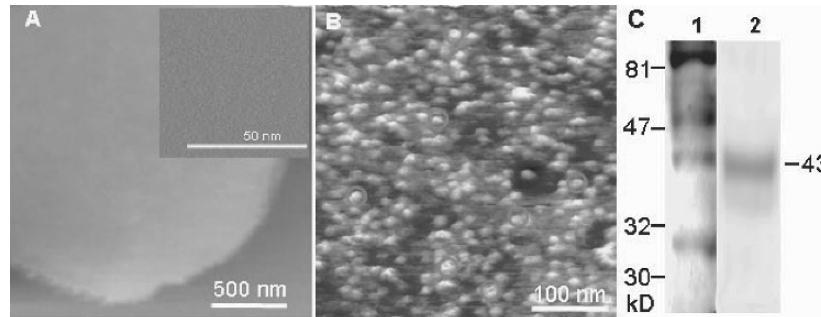
FIGURE 4.1. AFM morphology image of A) a phospholipid membrane patch without any proteins inserted, inset: a zoom into the membrane, B) a membrane surface with connexin hexamers (gap junctional hemichannels) fused into the membrane. Examples of open hemichannels are encircled. C) shows gel electrophoresis results of the analysis of the protein; the 43 kDalton band confirms the presence of the connexins. Reprinted from Thimm et al.[7]. Copyright (2005) by the American Society for Biochemistry and Molecular Biology.

requirements towards the method are set by the dimensions and properties of the membrane inserted structures under investigation (Figure 4.1). This requirement leads to the preferred selection of imaging or analytical methods of subnanometer resolution. Whereas it is disputed if studies of processes on artificial membranes *in vitro* have any relevance to the same processes *in vivo*, a number of well planned, comprehensive works proove the sceptics wrong. The key of performing such studies is a good understanding of the limits of a biomimetic system; the carefully drawn line between the general and the circumstancial characteristics of the observed phenomena.

It is crucial therefore to know and understand and well charcterize our system. When identifying the parameters that we need to know, the most obvious basis of comparison is the membrane involved in the biological process we aim to study. Composition of the membrane and the buffer solutions are key control parameters, which are however purposefully selected and thus known from the beginning; their relevance was discussed in other chapters. The properties of the membrane not known from the start, however, are just as important. First of all, the general mechanical descriptors of the system: the amount of lipid forming the membrane, that is, mass and thickness; the coverage of the surface, and the nature of the discontinuities in this coverage, simply said, morphology. Equally important are the properties describing the membrane in interactions: the stability against mechanical intrusions, shear and penetration, the rate of regeneration, the potential for incorporation of e.g. aminoacid structures: elasticity, viscosity and surface energetics. May be less obvious are the dielectric properties, which however closely relate to the electrical field around the membrane, held responsible for many aspects of protein-membrane interactions. Last but not least, we have to mention that most biomimetic systems are actually supported membranes: phospholipids deposited to a convenient—usually

atomically flat—substrate surface such as mica, single crystal gold or graphite. Nanoparticle films are also frequently used. The presence of the substrate can influence membrane properties by restricting the electrolyte flow, change the membrane potential and physically, or, in special cases, chemically bind to the membrane system. Thus substrate effects need to be identified and accounted for in the analysis of the system.

To categorize the available methods, we turn to the basic principles of operation. Two major groups can be distinguished by the interaction used for the measurements: optical and mechanical techniques. Optical techniques use intensity loss, polarization or reflection angle change of light to measure thickness, dielectric constant (change) and, eventually, mass of surface deposited thin layers. The optical techniques to be discussed here are Ellipsometry and Surface Plasmon Resonance. Mechanical techniques use different probes: static or oscillating tips, balls, cylinders and other force probes to measure morphology and a wide range of mechanical properties such as elasticity, viscosity and surface energetics of thin layers. We will discuss Quartz Crystal Microbalance (QCM), Surface Force Apparatus (SFA) and last but not least, Scanning Probe Microscopes, with a special emphasis on Atomic Force Microscopy (AFM). There are certainly other methods which could be used for the characterization of biomimetic membrane systems; however, our goal in this book is to focus on the commonly used and widely available techniques.

It is important to understand that on the nanometer scale, our methods are working at the limits of their capabilities, as is our science, too. A measurement is not a neutral, extraneous look at a system but a "brutal" interaction, where the presence of the measuring probe, let it be a laser beam, an oscillating quartz crystal or an ultrafine tip, might distort the original system beyond recognition. It is necessary therefore to be critical towards our results, and expose them to serious reality checks before believing any piece of information. In the followings, we will discuss the means of these reality checks, and the necessary and satisfactory conditions of performing measuremnts on the nanometer scale.

4.2.   Methods of Characterization and Analysis

4.2.1.   A Few Thoughts

As we discussed in the previous section, there exists a number of methods which *can* be applied to characterize thin layers such as biomimetic membranes. Before engaging in a detailed discussion of these methods, however, let us also consider which of these methods are *convenient* to use and thus defining where shall be the focus of the discussion directed. The first question to answer is whether a method provides high resolution (Hi-Res) or "bulk" results. Talking about the nanotechnological aspects of the biomimetic membranes, we ought to prefer the Hi-Res approach, although in certain cases, discussed in the folowings, bulk results can yield useful information, too.

The reason for using Hi-Res tools is to access the molecular dimensions directly. At first, this approach seem to prefer imaging techniques. However, all it means is that the probe size has to fall into the nanometer range; mapping the surface with this accuracy is not required (although useful). Since the main reason for using biomimetic membranes is to reconstruct/reproduce a biological process *in vitro*, in a well controlled test environment, it is a reasonable wish to follow up on the single events instead of examining averages of the plenty. In terms of the membrane itself, it is important to know whether the whole surface is covered, the coverage is monolayer or multilayer, are there discontinuities or not, what are the patterns and if the vesicles used to deposit the membrane have even ruptured. In terms of membrane inserted biomolecules, individual morphology, conformation, energetics, elasticity can reveal the molecular level cahnges and the environmental factors/reagents initiating those changes; provide a better statistics on the overall behaviour of the sample and allow for identifying possible structural differences responsible for the non-uniform behaviour of the sample, a common problem of biology that is impossible to address in any other way.

The diffraction limit of the resolution of optical methods is $\lambda/2$, where λ is the wavelength of the light. In practical terms, the resolution limit for red light ($\lambda \sim 650$–700 nm), a common solid state laser wavelength for e.g. laser pointers and CD writers, it is 320–350 nm. If we compare this resolution to the size of the vesicles used for membrane deposition, usually 200 nm in diameter, we must realise that we cannot even study an individual vesicle, not mentioning the membrane - inserting structures such as peptides and proteins, which fall into the few nm size range. Decreasing the wavelength towards ultraviolet can result in an improvement of a factor of ~3, which is still far from the resolution required. By employing near field techniques, when the light is emitted through a diaphragm much smaller than the wavelength (typically 20–50 nm), a further improvement can be achieved. The situation is much better with the *vertical* resolution. The methods can resolve not only nm size but also commonly atomic layer thicknesses; which, however, are measured as an average over a surface area equivalent to the probing beam cross section.

Mechanical methods, on the other hand, have no theoretical limits of resolution, at least not before reaching the single atom level. The limiting factors are in the design of the systems. Of the methods listed above, only AFMs are made for Hi-Res measurements. AFMs (with a few other SPMs) are the workhorses of nanotechnology, being able to record 3D maps of surface morphology, measure a number of physical properties, and modify surfaces with nm precision. Hence, we will discuss the AFM in the finest details.

4.2.2.   Atomic Force Microscopy

AFM[1], where a mechanical microprobe is used to image the sample surface, is a relatively new and rapidly developing tool, or rather, a research field by itself. The study of the physical processes involved in image acquisition, many of which

are not fully described yet, leads to new solutions, such as higher resolution, faster imaging, new analytical modes, etc. The working principle of the atomic force microscope doesn't differ much from that of the old-fashioned turntable. A sharp tip, mounted on a micro-cantilever (probe) is pushed against and scanned along the sample surface, while the bending of the cantilever is monitored. In case of the AFM, this monitoring is done by a laser reflection-based position sensor (Figure 4.2). If the bending of the cantilever, that is, the force exerted on the surface is maintained constant during scanning (the detector signal of this constant value is called *setpoint*), which can be achieved by a *feedback-control* of the height position of the clamped end of the cantilever (*z scanner*), is called contact mode. The trajectory followed by the z scanner is then interpreted as topography, while the torsion of the cantilever carries information about the tribological properties of the surface. This mode is simple and effective for hard surfaces but unsuitable for soft, poorly bound biological samples due to the appearing high shear forces. To overcome this problem, dynamical modes have been invented where the cantilever is driven close to its resonance frequency and the amplitude of the oscillation is monitored (Figure 4.3). If this resonating probe is moved into the vicinity of the surface, due to the tip-surface interactions the probe amplitude becomes the function of the probe-surface distance. Thus, the amplitude of the probe oscillation can be also used to trace the surface. This kind of operation is also called "tapping mode", since weak non-contact (attractive) forces can be sensed, and a light "tapping" of the sample can be established. The tapping is believed to minimize the imaging damage to the surface. Accordingly, the study of bioimaging problems detailed in this chapter will mainly concern dynamic modes.

In addition to morphological imaging, AFM is also an analytical tool. Electrical recording through the probe tip can be used to map the local charge transfer properties of the substrate as it was demonstrated[2]. The torsion of the probe provides information about the tribology, an approach-retract curve of the probe about the adhesion and elasticity. Furthermore, the phase lag between
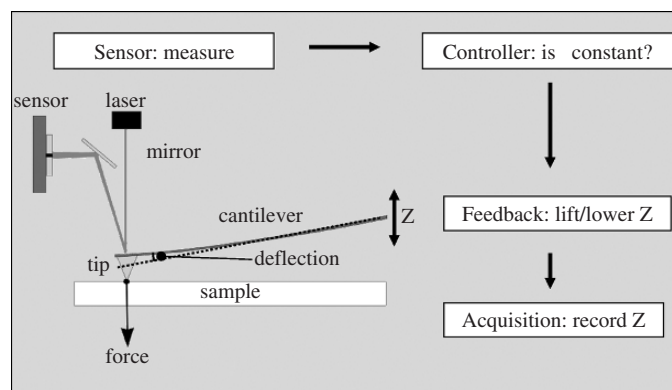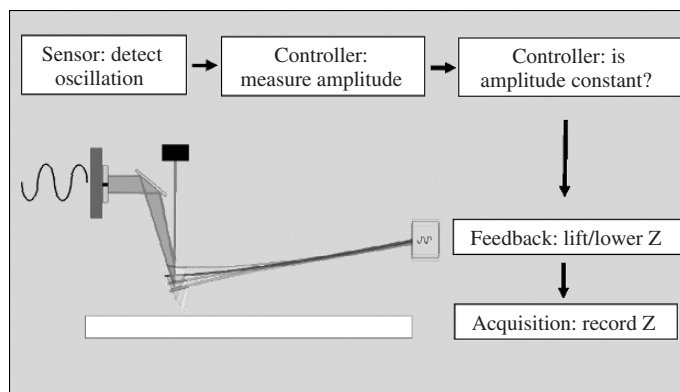

FIGURE 4.2. The schematics of AFM operation.

FIGURE 4.3. The schematics of the dynamic ("tapping") mode AFM operation.

the drive and the response signal in case of dynamical operation is a complex function of surface properties such as elasticity, surface energy, charge distribution and energy dissipation e.g.[3−5] and thus capturing a phase shift map parallel to the morphological measurements offers a secondary information channel. Phase imaging can be utilized to substract physical properties and thus identify different material qualities on the surface.

AFM imaging is routinely used to record morphology of crystalline or semi-crystalline hard structures, to substract hidden features by extensive image analysis e.g.[6] and to identify substructural features and physico-chemical properties through phase imaging[2,7]. However, the method is capable of doing even more than that. When studying a liquid-solid interface, adsorption, aggregation and surface bound conformation of nanoparticles and biomolecules, as a function of surface properties and ionic environment, can be also studied (for a review see[8]). Self-organising structures, (bio-)polymerization, dynamical processes could be also addressed if the dynamics is slow enough to allow for recording multiple pictures[9]. What is a major advantage of AFM imaging utilized to study interfacial processes, is also a major disadvantage of this method: it works only on surface confined systems. Many biological systems of interest, while being spatially confined (e.g. membrane proteins, ionchannels), are not particularly surface processes. The geometry therefore often prohibits *in vivo* studies.

It is debated whether *in vitro* studies have any relevance to living organisms at all; nevertheless, it was recently demonstrated in high profile articles that protein functions can be identified in carefully constructed biomimic systems e.g.[6,7,10]. In a recent work, Cx43 gap junctional hemichannels were fused into reconstituted phospholipid membranes, which provided the platform for studying the gating properties and identifying physiological function of these membrane protein structures[7]. The effect of Ca^{2+}, Mg^{2+} and Ni^{2+} cations on the conformation of the hemichannel was studied *in situ*, and the nature of extracellular Ca^{2+} gating was described. Such studies are only possible by combining traditional

macroscopic characterizing methods (e.g. fluorescent microscopy, electrophysiology) with nanotechnology, such as nanopatterning, high resolution imaging and spectroscopy. This approach offers a molecular level look at the mechanism in question, and allows for not only the *in situ* follow-up on the morphological changes involved in the protein function but also the identification of possible flaws in the macroscopic characterizing method employed.

There is some controversy, however, around the interpretation of high resolution imaging data; reported imaging conditions are inconsistent, the reproducibility is poor, and the resolution is often much lower than expected. Since these problems persist in spite of the extensive hardware development of the past few years, it is assumed that the problems stem from the imaging process itself; a revision of our view of the AFM is quite timely. Furthermore, all applications detailed above are based on a 3D morphological measurement so it is of central importance to know the accuracy of the height measurements. The AFM, however, is not free of imaging artefacts, especially when imaging on the nanometer range.

Determining the accuracy of the morphological measurements and distinguishing the real surface features from the imaging artifacts is a problem which reaches beyond common sense reasoning[11]. Analysis of high resolution morphology maps needs intensive image processing[6], and often numerical simulation of the imaging mechanism[7−16]. Another important problem is the control of imaging force, which is necessary for the non-destructive imaging of delicate biomolecules as well as for achieving better morphological resolution[17]. The dynamics of the AFM probe and the nature of interactions which the probe undergoes in close proximity to the surface determines the force exerted on the sample (e.g.[13,18]), accordingly, simulation of the imaging process is the solution in this case, too.

The evolution of AFMs has reached the point, where measurements in liquid phase, preferably *in situ* during characterisation by another, conventional method such as fluorescent microscopy, electrophysiology or electrochemistry became the major challenge. The physics of such measurements, however, are still not completely developed. The AFM liquid cell is a complex mechanical system where the cantilever oscillation is determined by the viscous medium and a coupled resonance scheme. The literature is scarce on the fluid dynamics of the oscillation in liquid[19], and therefore the experties of the AFM operator, based on mostly phenomenological observations, will determine the achievable results. In general, AFMs are considered hard to operate, providing inconsistent results and being "moody". Such assumptions were not made without any basis. When imaging micron scale objects in ambient environment, optimizing the system parameters is usually not a challenge. For imaging biological samples in their native hydrated state, however, a continuous control of a number of independent system parameters is essential. The parameters in question are the feedback gains, the setpoint, the scan rate, the drive frequency and drive amplitude. These are optimized at present in an iterative fashion, by hand, which is time-consuming and leads to an acceptable image

being acquired, at best, every 5 to 10 minutes. There have been few attempts made to improve this situation; a study of automatic setpoint selection[20] and a proposed self-optimizing feedback [21] were published; however, at this point, the commercial systems do require a continuous fine tuning. As we will see, however, the "moodiness" of the AFM can be easily backtraced to simple physical phenomena, and, based on the knowledge of the theoretical background, the method becomes a reliable and essential tool of nanoscale surface characterization.

4.2.3.   Quartz Crystal Microbalance

Quartz crystal microbalance is a simple tool to measure mass deposited to (or removed from) a surface. It is based on the simple principle that the mechanical resonance of an object, this case a piezoelectric disk, is a function of the mass of the object. Whereas the piezoelectric effect was known decades before, the theoretical description of the resonance shift as a function of added mass for such a system was not developed before 1959 when Sauerbrey published a simple formula[22]. Based on his theory, measuring the changes of the resonance frequency of the disk would provide information about mass change, and, depending on what is known of the deposited material, about surface coverage, density and layer thickness. Thus the methode of quartz crystal microbalance was born. Even before the age of high precision digital circuitry, QCM was a simple and accurate tool due to the simple principles it is based on. Recent improvements include measuring frequency shift at multiple harmonics of the fundamental resonance which are not only more sensitive than the fundamental resonance but also provide spatial information about the thickness and vertical mass distribution of the deposit (Figure 4.4). In addition, measuring the energy dissipation to the sample and the environment reveals information about viscoelastic properties of the deposit layer. The major use of QCM for the characterization of biomimetic membranes is at the deposition phase, where the formation of a layer from vesicles can be monitored, and the dynamics can be determined; however, it can be also used for measuring the rate and amount of e.g. peptide incorporation into the membrane.

4.2.4.   Surface Force Apparatus

The SFA is an extremly sensitive tool to measure interaction forces with a sub-nanometer spatial (e.g. normal) resolution. It creates a point contact between two materials, then slowly pulls the two apart, measuring the force as a function of distance. While this is a very simple principle, and it provides with only a force-distance curve, the SFA can yield high accuracy information about material properties such as elasticity, surface energy or Hamaker constant, depending on what sort of interaction model (atomistic, continuummechanical, simple or complex) is used when the results are analysed. The physics involved in the
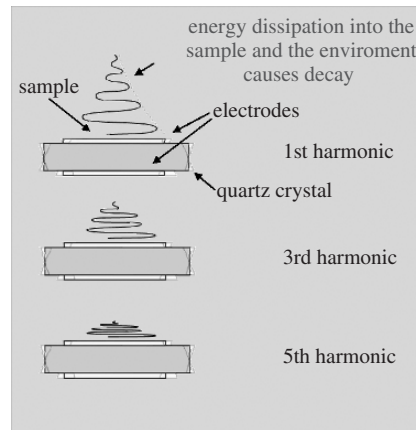
FIGURE 4.4. Schematics of the working principle of the quartz crystal microbalance. The crystal resonates in shear mode. The shear wave in the sample and the environment, generated by the motion of the crystal, decays in a short distance due to energy loss via dissipative processes (the idea of representation kindly provided by Q-SENSE).

SFA analysis is identical to the problem of AFM imaging, therefore we do not include a separate discussion. It is however important to point out that the accuracy of the AFM force measurements is yet to procure the accuracy achieved with SFA.

4.2.5. *Ellipsometry*

Ellipsometry is based on the polarization of light. In the physical optics (as opposed to geometrical optics) it is known that on an interface of two materials of different optical density (practically, this means different index of refraction), both refraction and reflection occur. In a coordinate system of H and V where H is the plane of the surface whereis the V is the normal plane in the incident light path, the polarization of the light can be described in terms of H and V polarized components. For any angle of incidence between 0 and 90 degrees these two components reflect differently and this difference is a function of the properties of the reflecting surface. Thus, ellipsometry measures the polarization of the reflected beam to identify material properties such as the complex index of refraction. Depending on what is known about the material, layer thickness, roughness and composition can be also determined. Measurements based on these principles have been performed for a long time; the ellipsometry method was adapted to work on interfaces and thin layers relatively recently[23]. The theory describing the physics of light reflexion from a thin film/substrate system is complicated and analytical formulae are not derived for general use; nevertheless, instrument specific simple formulae are usually available for data interpretation.

4.2.6. Surface Plasmon Resonance

SPR is based on the Kretschmann theory of the resonance of surface plasmons, originally published in 1971[24]. The method was established and theoretically reinforced in 1997[25]. However, it has become an effective tool of biophysics only recently, with the introduction of the absorption configuration[26] where the surface bound layers of the studied material interact with – and absorb at resonance of – evanescent waves. In this technique, the sample has to be deposited onto a substrate of a very thin gold layer on a smooth glass carrier. A laser beam is then shone to the back of the sample through the glass carrier, and the intensity of the reflexion of this light is measured (Figure 4.5). It is known that the reflexion of light does not happen entirely on the very interface of materials of different refraction index: a small amount of light, the so called evanescent wave will "penetrate" the surface. This penetration results in an interaction and energy transfer from the light beam into the interface, through exciting surface plasmons, collective oscillating modes of electrons on the interface. When the angle of incidence of the laser beam is scanned around the total reflexion, there is an angle where the light is not transmitted but not reflected: the energy coupling into the material is maximal through the resonance of surface plasmons. Hence the name. The analytical potential of this phenomenon lays in the fact that, if this penetration depth is more than the thickness of the layer of material forming the interface, and layers of other materials follow the first one, the evanescent wave will necessarily interact with those materials, too. The angle of total reflection, and, consistently, the angle for the measured minimal intensity will change with the introduction of different material qualities. Depending on what do we know about the materials, layer thickness, density and mass can be determined. Since the measurements are quick, dynamics of the surface processes can be also studied. We should realise the SPR measurements by themselves are often a special application of biomimetic membrane systems, since phospholipid coated sample chips are used to study the dynamics and reactions of membrane bound proteins.
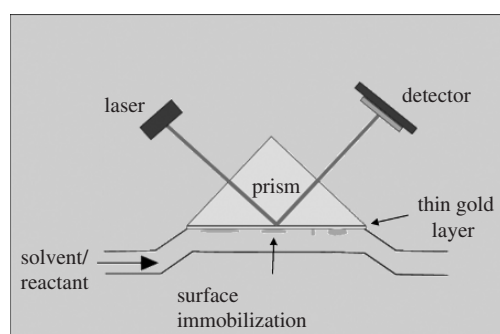

FIGURE 4.5. The schematics of surface plasmon resonance.

4.3.   Coverage and Mass

In order to characterize a supported membrane, the first things to measure are the geometrical properties. We are interested in the surface coverage: if it is a monolayer or a multilayer, wheter it is continuous or fragmented and, in case vesicles were used for the deposition, if it is fused or not. Practically, we have two choices to perform such measurements: by obtaining average characteristics over a large area by a macroscopic (or, rather, non-Hi-Res, since the vertical resolution can still be in the nanometer range) method or by AFM imaging. There are advantages and disadvantages associated with either choice.

We can measure average thickness by Ellipsometry and SPR. Although both methods are sensitive to very small changes, quantification of absolute values is problematic. We should remember that the methods are based on optical properties; hence, a small amount of material that cause a large change in the extinction coefficient, such as metal ions, might generate a more intensive signal than an otherwise several thousand times larger protein. This also means, of course, that the incorporation of such ions can be easily monitored, which on the other hand is a serious challenge for any other methods discussed here.

Ellipsometry, in particular, is frequently used to measure thickness of thin layers. There are not many works, however, of using this method for the characterization of biomimetic membranes. A few recent example include the in- or ex-situ characterization of supported membrane deposition[27−29] and a study of the hydrolysis of phospholipid membranes[30] (Figure 4.6). As a supporting method, ellipsometry can be very valuable. However, since our forcus is on the comprehensive characterization of the biomimic membranes, and methods that can provide such results, we do not discuss the theory and the interpretation of the ellipsometry results in detail.

SPR has its strengths in the in situ measurements of the immobilization and the reactions of surface confined biosystems. The measurement of a data point
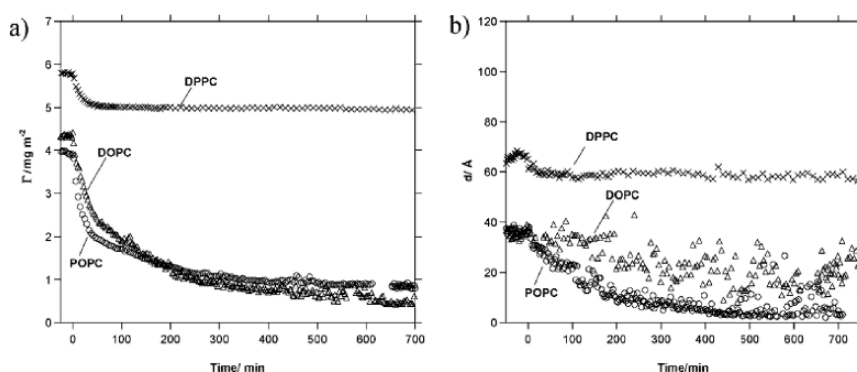

FIGURE 4.6. Ellipsometry measurement of changes in (a) surface excess and (b) bilayer thickness during hydrolysis of DOPC, POPC, and DPPC supported bilayers. Reprinted with permission from Vacklin et al.[30]. Copyright (2005) American Chemical Society.

is instantaneous, at least, compared to the dynamics of the biological processes it is used to study. Two different experimental designs are commonly used: absolute (single channel) or relative measurements. When monitoring the changes in a single data channel when performing e.g. membrane deposition *in situ*, a saturation curve can be recorded. There are formulas (that we do not discuss here) to relate the SPR signal to the thickness and/or dielectric properties of the sample; a persisting problem is, however, the lack of information about the specimen, which renders the quantitative interpretation amiguous. The situation is even more complex if the surface coverage is not complete; in order to estimate the amount of discontinuities, account for multilayer-formation or the amount of non-ruptured vesicles, the saturation curves by themselves are not sufficient. It is more convenient therefore to perform comparative measurements, where one data channel provides a reference signal, which can be a sample deposited *via* a standard protocol *in situ*, or a reference sample characterized by other (e.g. imaging) methods. With either experimental design, reliable qualitative data can be collected[31]. SPR is also a useful tool to characterize membrane insertion of biomolecules; for example, membrane binding[32] and membrane disruption[33] by antimicrobial peptides was studied this way (Figure 4.7).

The kinetics of membrane deposition can be also measured with QCM. A comparison of parallel SPR and the QCM measurements (Figure 4.8) highlights the differences between the two methods. The vesicle adhesion to the surface prior to rupture, invisible on the SPR record, results in a strong signal of QCM frequency shifts. This difference arises since the QCM directly measures the mass deposited onto the sensor. To interpret the QCM measurements as mass change, the Sauerbrey equation is used:

$$\Delta f = -\frac{2f_0^2}{A\sqrt{\rho_q \mu_q}} \Delta m \tag{1}$$

where Δf is the measured frequency shift, f_0 is the original resonance frequency of the cystal, A is the active area of the crystal, ρ_q and μ_q are the density and shear modulus of quartz, 2.648 g/cm^3 and 2.947*10^{11} g/cm*s^2, respectively, while Δm is the mass change. Higher (odd) harmonics are more sensitive to small mass changes than the fundamental resonance. And, measuring the energy dissipated into the sample, a qualitative measure of the viscoelastic properties of the deposited layer can be recorded.

Besides of simply monitoring the amount of membrane mass, by correlating the dissipation to the frequency shift, it can be identified whether the vesicles are ruptured on the surface or not. While the intact vesicles carry a significant mass, their viscosity doesn't differ much from that of the water or buffer solution[34]. Furthermore, enzymatic degradation of vesicles[35] and membranes (Figure 4.9;[36]) can be easily studied. In general, a feasible extension of this method is the study of the incorporation and reactions of membrane proteins. In contrast to the optical methods, QCM would not be the right tool to monitor metal ion incorporation (although it is not absolutely impossible); however, its high sensitivity to small mass changes makes it an ideal tool to measure the incorporation of small
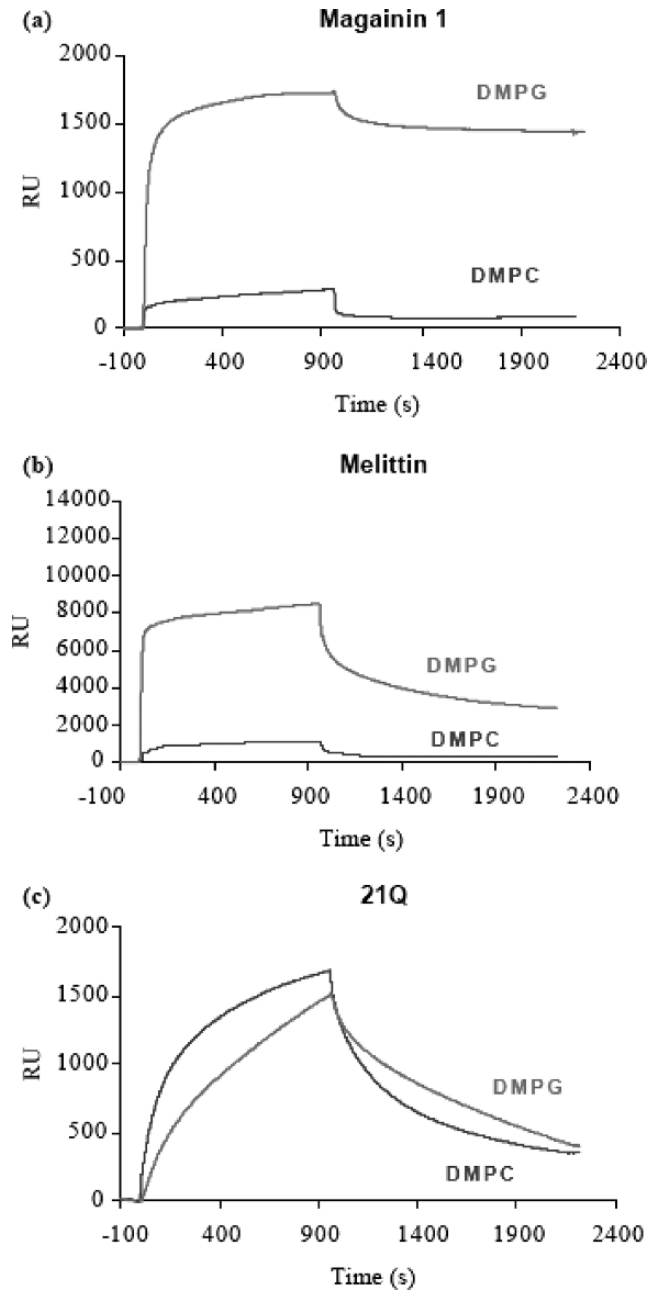
FIGURE 4.7. Membrane binding of antimicrobial peptides, recorded with SPR. Comparative peptide sensorgrams for the binding of (a) magainin 1, (b) melittin and (c) 21Q (des 22–25-melittin) to DMPC and DMPG. Peptide concentration 50 μM. Reprinted from Biochimica et Biophysica Acta 1512, Mozsolits H, Wirth HJ, Werkmeister J, Aguilar MI, Analysis of antimicrobial peptide interactions with hybrid bilayer membrane systems using surface plasmon resonance, 64–76, Copyright (2001), with permission from Elsevier[32].
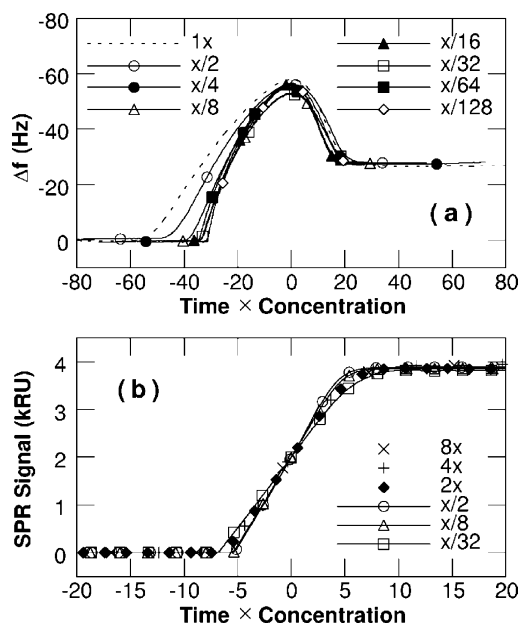
FIGURE 4.8. Vesicle deposition of phospholipid membranes: adsorption vs exposure for different vesicle concentrations. (a) QCM and (b) SPR data are shown for adsorption from solutions with concentrations ranging from x/128 to 8x where x is the reference concentration of 126 ng/ml (164 mM) of lipid in buffer. . Note the initial peak on (a): the QCM measures the sum weight of the vesicles before rupturing and fusing on the surface. The SPR shows only the fused membrane (b). Reprinted figure with permission from[95] as follows: Keller CA, Glasmastar K, Zhdanov VP, Kasemo B, Physical Review Letters 84 , 5443–5446, 2000. Copyright (2000) by the American Physical Society.

organic molecules, which in turn would not initiate measurable change in optical properties.

Morphology of the membrane structure is frequently characterized by direct imaging such as AFM[37−50]. The morphology maps provides a regiment of information. In the imaged surface area, the exact rate of coverage can be determined. The thickness of the membrane revealed in the morphology and it is thus possible to distinguish between different phases, raft formation, and identify multilayer formation directly (Figure 4.10). The coherence of the membrane is also revealed. It is often observed that holes open in the middle of otherwise homogeneous areas[50], and small islands of few hundred nanometers of diameter patches sit on top. Unopened vesicles, often trapped on the top of the membrane can be also imaged. And, AFMs have the resolution to image membrane inserted structures: ionchannels, proteins and peptides as well as macromolecular biosensor structures and their conformation, function and interaction[51−65]. As of yet, however, it does not have the speed of capturing fast dynamical processes, thus any kinetical measurements are limited to minute-scale events, or rather, steady states thereof.
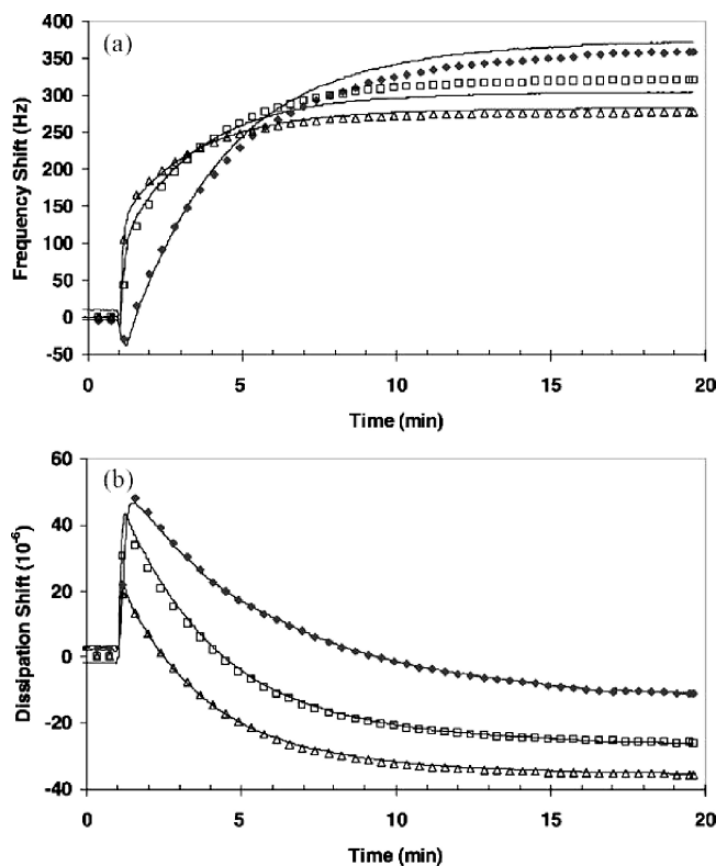
FIGURE 4.9. Hydrolysis of a triolein membrane. QCM-D data obtained at pH 10 without Ca2+ using1.0 μgml^{-1} Lipoprime at 30°C. Frequency (a) and dissipation responses (b) of 5MHz (□), 15MHz (♦), and 25MHz (Δ) are shown. The response amplitudes were normalised by dividing with their corresponding overtone number, i.e. 1, 3, and 5. For better visualisation, only every 15th data point is plotted, and the time of enzyme addition is aligned to t = 1 min. Lines are the corresponding modelled responses. Reprinted from Chemistry and Physics of Lipids 125, Snabe T, Petersen SB: Lag phase and hydrolysis mechanisms of triacylglycerol film lipolysis, 69–82. Copyright (2003), with permission from Elsevier[36].

It is thus the advantage of the optical methods to measure fast (second scale) dynamics.

We have thus demonstrated that the capability, and ease, to perform dynamical measurements justify the use of optical and QCM methods. Ellipsometry and SPR are very sensitive to optically active specimen such as metal ions, whereas the QCM is able to monitor the immobilization/surface kinetics of small molecules. We conclude that high resolution imaging will be the ultimate tool to look at the fine details of membrane structure and properties.
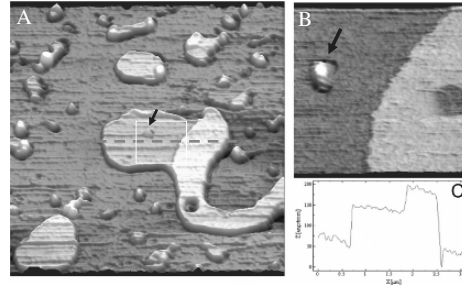
FIGURE 4.10. A) topographical image of vesicle-deposited phospholipid membrane on a mica surface. The image was recorded in a physiological buffer solution. A hight section along the dash line (C) confirms the superposition of two bilayers. An unopened vesicle can be seen incorporated into the membrane (arrow) as it can be seen on the zoom picture (B) taken at a later time point on the area demarcated by the white rectangle. The membranes display dynamical behaviour: during the time passed between the two measurement, a section of the upper membrane on panel (A) developed several holes (one visible on (B)). Pictures courtesy of K. Hall and M-I Aguilar, Department of Biochemistry, Monash University, Victoria, Australia.

4.4.   Morphology and Mechanical Properties

4.4.1.   Imaging and a Few Common Artefacts

In this section, we will be talking mostly about AFM. The theories discussed below, however, describe general physical phenomena; thus the formalism introduced here will be applicable for other methods which use/measure similar quantities. Surface force apparatus, for instance, is built on the same probe-surface interaction model, while QCM utilizes the oscillation theory similar to that of the AFM probe.

We have seen in the previous section that average surface coverage, layer thickness and mass can be measured with other methods. AFM can provide with similar results, however, at the state of the art, AFM captures only steady-states of dynamic processes. We have to recognise this disadvantage compared to the above discussed methods; it is better to perform AFM measurements on a static or equilibrial system than during dynamical changes. Nevertheless, AFM was granted with the trust of biologists and biophysicists with the recognition of the given limitations[66,67].

After this disconcerting introduction, let us focus on the advantages of using AFM for the characterization of biomimetic membranes. First of all, AFM is an imaging method; the thickness, coverage and surface roughness of the system can be directly measured, moreover, seen. But there is more to learn from a 3D representation of the surface. On Figure 4.10, different phases of a low coverage, vesicle-deposited membrane are depicted. Small unilamellar vesicles adhere to the surface, where they initially retain globular form, mostly due to their small size. Laplace's law describes that, for a given surface tension, the

pressure in a vessel is inversely proportional to the radius of the vessel, that is, a smaller radius of curvature results in a larger pressure difference. In practical terms, it means the radial force towards the centre of the bubble is much higher than the surface forces which work on flattening the vesicle; thus, the small vesicles remain spherical. When the vesicles fuse on the surface, however, the radius increases, and the surface forces become stronger than the radial force, the vesicle takes up a donut shape first, than flatten and finally collapse. A collapsed vesicle usually undergoes a rearrangement to form a single bilayer membrane patch on the surface. These membrane patches can also fuse upon heat treatment and form a continuous membrane. These steps can be easily followed by AFM imaging. The size and distribution of the individual vesicles, the rate of fusion and collapse can be monitored and the dynamics of membrane deposition can be assessed as a quality control of the membrane deposition. Furthermore, once the membrane was formed, AFM offers a direct way to measure the surface coverage, identifying the density, average size and nature (e.g. circular or meandering) of the discontinuities. AFM images can identify unfused vesicles and secondary bilayers on top of the primary membrane surface. The thickness of the memrane can be dirrectly measured from the images, although quantitative height measurements on the nanometer scale need more than a section analysis, as we will see below.

The first problem arises when it is not clear whether the basal plane observed on an image is the substrate, a single bilayer or a multiple bilayer structure. From the surface morphology, distinguishing between an atomically flat mica and a membrane surface is often not possible. Two solutions are available: to obtain an atomic resolution image and identify whether the lattice constant of the substrate material matches the periodicity on the image, or to perform a force dissection.

Force dissection uses the AFM tip as a "power tool". It is basically a mechanical etching performed by either pushing the tip hard against the surface or oscillating it at a high amplitude (often with a "ringing" feedback, referred to as acoustic dissection) while scanning the surface with a high scan rate. The result is a rectangular hole in the membrane, which reaches all the way to the substrate surface. By imaging this hole, the thickness of the membrane can be measured. The tip usually becomes contaminated during dissection, accordingly, any further high resolution work requires a new probe.

Thus, the deposition efficiency and the quality of the membrane can be easily assessed with AFM. However, the main reason for using the imaging technique is to study the processes to which the biomimetic membrane serves as substrate: protein binding, incorporation, aggregation as well as conformation and polymerization. This means, however, high resolution imaging, still considered black magic by many, and inconsistant, misleading and unreliable by others. Such judgements reflect the lack of good summarizing works on the physics of the imaging on nanometer scale.

In routine operation, in a physiological solution (a low concentration aqueous buffer) AFMs can easily capture images of 500 nm lateral scan size with

512×512 pixell resolution. Evidently, this means that the size of a data pixell is about 1 nm. The objects of interest: peptides, proteins are a few nanometers in size; with this resolution, they can be seen, but cannot be analysed. Higher resolution imaging, however, is influenced and limited by numerous factors, the first and most obvious of which is the tip convolution. An average AFM tip has an apex radius of 10–50 nm with a 60–70 degrees cone angle. This is significantly larger than the structures we intend to resolve. Consistently, if the sample surface is considered a rigid boundary, that is, no compression can happen, nor any morphology change whatsoever, the contour of the tip is convoluted from the contour of the sample. In practical terms, while the height of the objects stay correct, the lateral dimensons extend significantly and the geometry becomes rounded. While deconvolution algorithms are often used to improve such images, there is no way to tell the exact shape of the sample where the morphology prohibits direct tip access, such as at vertical steps and narrow holes. A simple solution of this problem would be the application of sharper probes with high aspect ratio, such as ion-beam etched silica tips or electronbeam deposited amorphous carbon "whiskers" or "stings". Some initial assumptions are, however, misleading. The sample surface, in the determining majority of cases, cannot be treated as a rigid envelope. The tip does deform the surface upon contact, in both elastic and non-elastic manner. When the maximal force exerted by the probe upon imaging, the "imaging force", exceeds what the toughness of the substrate can tolerate, imaging damage occurs. The description of the force interaction needs some deeper insight to the physics of AFM operation, as we will see below. Nevertheless, the damage caused by the tip can be also simply related to the contact area: the same force acting on smaller area can cause more damage. Accordingly, sharper tips pose a higher risk of surface destruction. It is also obvius that, if the surface is indeed deformed upon contact with the tip, the contour measured by the AFM is a result of a complex interaction where the softer surface areas might appear as lower morphology. However, it also means that a relatively blunt tip can provide a surprisingly accurate surface tracking, when sensing a step in the change of the surface properties – e.g. running over "empty space" at a step – of the sample. The probe shape is therefore an important parameter, and it is indeed desired to use sharper tips, however, one needs to keep in mind that the selection is also a trade-off where the improvement of the resolution can easily end in surface damage.

The significance of the imaging force is increasing in case of tapping mode imaging. Originally invented to reduce the lateral (shear) forces, this mode might pose a higher risk to sensitive surfaces such as biomimetic membranes, even though it is practically the only method favoured for high resolution bioimaging. The imaging problem can be understood by simply considering a tip repeatedly hitting – or tapping – the surface with a certain frequency (as it happens during tapping mode operation). On large scale, recording a picture in a reasonable time – that is, 1–10 minutes – means the tip is scanned relatively fast over the sample, and thus the individual "taps" by the tip happen well apart. Using the same frame capture rate, for higher resolution pictures the range is soon reached

the contact areas of the the consequent impacts start to overlap. Eventually, at the highest resolution where the non-destructive treatment of a delicate sample would be the most important, the tip will end up hammering the same area at an ultrasonic frequency. Thus the destructive effect of this local sonication needs to be understood and minimized for imaging at small scan scales. In addition, system instabilities, caused by non-linear tip-surface interactions can also result in transient increase of the exerted force, causing loss of image quality and, potentially, surface damage.

From the application point of view, it seems plausible to reduce the effect of local sonication by simply increasing the distance between, and decreasing the force of, the individual impacts, that is, establishing faster scanning with smaller amplitudes. However, the scan speed is limited by the bandwidth of the hardware and the probe, while the reduction of the probe amplitude is reported to cause a number of imaging artefacts of unknown origin. Furthermore, there is no quick fix for the system instabilities. Thus, distortion-free high resolution imaging might not be considered black magic, and treated with scepticism, without a reason. However, a closer look at the imaging procedure provides us with simple answers and guidelines.

4.4.2. Surface Forces and Continuum Mechanics; AFM Simulation

The modeling and simulation of AFM imaging is an active research field, where the major goals are to provide a theoretical background for the interpretation of high resolution imaging, to propose novel means of data substraction, including new working modes, and to explain the phenomenological observations about the dynamical behaviour of the machines. The model of an AFM system can be subsequentially compiled from the model of the probe, the tip-surface interaction, the control signal (amplitude) detection, the feedback mechanism, and the scanning along an arbitrary surface structure. The probe is commonly treated as a massless spring (spring constant: D) with an effective mass (m) at the end. A system of this kind is considered a linear harmonic oscillator, with a natural (circular) frequency given by $\omega_0 = sqrt(D/m)$. If this resonator is exposed to environmental damping, and it is driven by an actuator, the equation of motion takes the form

$$m\frac{d^2 x}{dt^2} = -Dx - \eta\frac{dx}{dt} + F_0 \sin \omega t \tag{2}$$

where x is the distance along the trajectory of the oscillation, η is the damping and F_0 is the periodic drive force with ω (circular) frequency. The solution of this differential equation is a sinusoidal periodic motion

$$x(t) = A \sin(\omega t + \delta) \tag{3}$$

with an amplitude given by

$$A = \frac{a_o}{\sqrt{(\omega_0^2 - \omega^2)^2 + 4\beta^2\omega^2}} \tag{4}$$

where $a_0 = F_0/m$ and $\beta = \eta/2m$, and the phase lag between the drive and the oscillator is

$$tg\delta = \frac{2\beta\omega}{\omega_0^2 - \omega^2} \tag{5}$$

Eq. 4, when plotted against the drive frequency, is near zero except for a peak around the natural frequency ω_0, called the resonance curve (Figure 4.11). Accordingly, the tapping mode AFM probe has to be driven close to the natural frequency – or resonance frequency – to have measureble amplitude. The phase lag δ (Eq. 5) also exhibits resonance properties: it undergoes a 180 deg change in the proximity of the resonance frequency, with a steep slope (see Figure 4.11). Both the phase and the amplitude of the oscillation are sensitive to small changes in the parameters of the oscillator; both are also sensitive to the introduction of an external force field, such as the tip-surface interaction. Thus both can be used to establish a feedback to maintain constant probe-surface distance. There are indications that the probe exhibits a more complex behaviour even in the absence of an external field, and so different treatment such as the continuummechanical description of the cantilever beam would be more approprite 68. Nevertheless, for the majority of the studies the linear massless spring is a sufficient model.
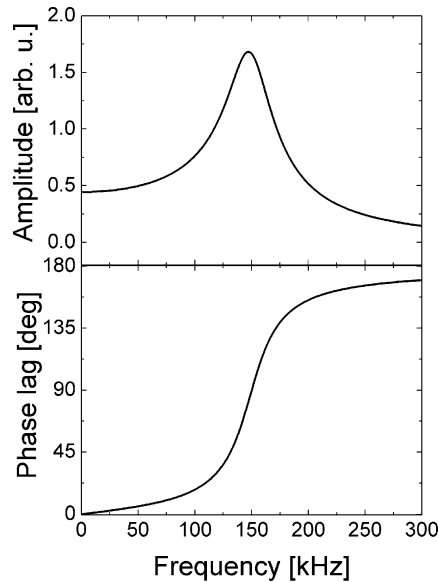

FIGURE 4.11. Amplitude and phase resonance curves for an ideal driven harmonic oscillator.

During tapping mode operation, the probe is moved into the proximity of the surface where the tip taps the sample at the end of its trajectory in each period. Consistently, the tip is moving inside - or rather, in and out - of the force field of the surface. The physical description of the probe interacting with the surface, however, is far more complicated than that of the oscillator by itself. The above solution is valid only for the absence of external forces. In case of the AFM simulation therefore the differential equation 2 has to be completed with an interaction force term. The modelling of this interaction is where the theoretical works choose different paths.

Common practice is to divide the tip-surface interaction to the effects of non-contact and contact forces. For demonstration purposes, the sample surface is treated as an uncompressible hard envelope and different non-contact interactions, such as Coulombic (electrostatic) attraction/retraction, van der Waals or capillary attraction forces. This approach might succeed in demonstrating the principles of operation, and thus often appears in user's manuals of commercial instruments. It fails, however, to explain many aspects of high resolution imaging which is our major focus in this book, hence we proceed to the more accurate models. It appears that the contact part of the interaction is more important for the accuracy of the measurements than the non-contact forces. With a second thought, it is quite obvious that forces with the steepest spatial slope would have the determining influence on the probe oscillation; in case of short range interactions, such forces appear in or near contact. It is common to assume therefore van der Waals forces for the non-contact interaction[69] while in mechanical contact with the surface different continuummechanics apply. We should understand that in this case both repulsive and attractive forces appear, and the deformation of the interacting objects also becomes significant. The validity of a model can be evaluated by examining a force-distance curve, which can be recorded *via* an SFA – or an AFM. Since the force interaction also reveals the physical properties of the sample, the following discussion will highlight in turn some aspects of the physical characterization of biomimetic membranes, an other key topic in this chapter. AFM approach-retract (force) curves, in particular, are frequently used to calculate the elasticity – Young's modulus – of a sample. Since the literature is divided about the interpretation of these force curves, we have one more reason to discuss the available interaction models. We should mention that a few authors deduced remarkable results from a very simple approach, where the surface was treated as a linear spring and the attractive contact forces were either neglected[70,71] or included as a constant contact adhesion[72]. In the first work, it was shown that the tip-surface interaction is nonlinear and thus, at an "unlucky" set of parameters, chaotic behaviour can occur. It was also observed that the phase image collected parallel to dynamic (tapping mode) operation is an independent information channel, revealing surface properties like elasticity. In the second work, the authors conclude that, contrary to the consensual presumption, the amplitude of the tapping mode probe is more sensitive to attractive than to repulsive forces and show that this sensitivity can lead to instabilities such as a non-linear amplitude-distance curve. In practical terms it means that the same

probe amplitude can occur in more than one distance from the surface and a surface perturbation can result in switching between these positions. Such sudden non-topographical steps are often seen during AFM imaging. This work also identifies the probe (free) amplitude, the setpoint and the drive frequency as the key parameters determining the behaviour of the probe. This was later confirmed by a number of works using complex interaction models. Both works conclude, however, that the validity of this approach is limited and better tip-surface interaction model is needed. In consecutive works by others, different continuum mechanical models are applied. Since the same formalism can be used to interpret force curve data, in the followings we give a brief overview of the continuum mechanics theories. A very good discussion can be found also in[73].

Continuum mechanics are used to describe the contact of two microscopic bodies. The classical theory of contact deformation was introduced by Hertz in 1881[74]. He found the following relationship between the radius of the contact area of two bodies pressed against each othe with P load:

$$r^3 = \frac{3}{4}(k_1 + k_2)\frac{R_1 R_2}{R_1 + R_2}P \tag{6}$$

where R_1 and R_2 are the radii of curvature while k_1 and k_2 are the elastic constants of the two bodies:

$$k_i = \frac{1 - \nu_i^2}{E_i} \tag{7}$$

where ν is the Poisson ratio and E is the Young's modulus. We introduce the products $R = (R_1 * R_2)/(R_1 + R_2)$ and $K = 3/4(k_1 + k_2)$ (note: K is also often defined as the reciprocal of this formula) the reduced radius of curvature and the reduced elastic modulus, respectively. The displacement of the points of the two interacting bodies far from the contact (which do not deform under the load) as a function of the load is then

$$d^3 = \frac{K^2 P^2}{R} \tag{8}$$

Obviously, in this model the separation of the surfaces does not require force, and the contact area under zero load is a point of zero radius. Experimental evidence, however, contradicts these aspects of the Hertz theory. It was shown even before the introduction of high resolution surface characterizing tools that the separation of the surfaces does require a certain force, and that the contact radius is larger than zero under zero external load. It is easy to see that attractive surface forces must be responsible for this effect. A modification of the Hertz theory was suggested by Derajaguin, Müller and Toporov (DMT theory,[75]) where the normal load was corrected with the effect of adhesion. Thus Eq. 6 and Eq. 8 take the following forms:

$$r^3 = RK(P + 2\pi R\varpi) \tag{9}$$

and

$$d^3 = \frac{K^2}{R}(P + 2\pi R \varpi) \tag{10}$$

where ϖ is the work of adhesion. Thus the force needed to separate the two bodies is now

$$P_0 = -2\pi R \varpi \tag{11}$$

This model works well on stiff surfaces and for low adhesion which usually mean small contact radii. Further experimental evidence suggests, however, that the contact radius is not zero even for the separation of the surfaces. This "neck formation" is negligible for stiff surfaces, but becomes significant for materials like phospholipid membranes. Further adjustments to the model are needed. A modification of the Hertz theory for compliant materials and high adhesion is the JKRS model[76]. It includes not only compressive (Hertzian) but also tensile stresses, which appear at the edge of the contact area. Without discussing the details of the derivation of the theory, which can be found in[76] and a number of textbooks, Eq. 6 of the Hertzian theory becomes

$$r^3 = RK(P + 3\pi\varpi R + \sqrt{6\pi\varpi RP + (3\pi\varpi R)^2}) \tag{12}$$

where in parenthesis there is a the corrected Hertzian load. It can be seen that, in case if the surface energy is zero, Eq. 12 reverts to Eq. 6. The displacement of the bodies under varying normal load can be derived from

$$d = \frac{r^2}{R} \tag{13}$$

We can easily deduce that the break-away force needed to separate the two surfaces is

$$P_0 = -\frac{3}{2}\pi\varpi R \tag{14}$$

In case of two unlike surfaces, in our case the AFM probe tip and e.g. a phospholipid membrane, the work of adhesion is $\varpi = (\gamma_1 \gamma_2)^{1/2}$ where γ_1 and γ_2 are the surface energies of the two bodies. It can be seen that, if the AFM is used to record an approach-retract – that is, force versus distance – curve, the slope of the contact repulsive interaction is described by Eq. 13 while the breakaway point can be given by Eq. 14. Thus, when the physical properties of the probe tip (apex radius, surface energy, Young's modulus and Poisson ratio) are known, the mechanical properties of the sample can be easily determined. We will return to this problem later.

The JKRS model applies for compliant materials and high adhesion, but it assumes only elastic deformation. In case of contemporaneous plastic deformation, and especially for dynamic case, it might underestimate the interaction

forces. Furthermore, since in the JKRS theory there are no forces between the surfaces where they are not in contact, infinite stresses occur around the connective neck. There is a model that accounts for these problems but it provides no analytical solution[77,78], therefore ignored by AFM modelling groups. A good compromise came as an extension of the Dugdale theory, which treats the separation of contacting bodies by assuming an adhesion zone ahead of a crack which fails at its strength. This is the Maugis continuum mechanics[79,80] which provides an analytical solution for the spatial function of the interaction force, converging into the DMT and JKRS theories for stiff surfaces with low adhesion and compliant surfaces with high adhesion, respectively. The solution is given in the form of parametric equations (which explains why is this theory not favoured for force curve analysis). A generalized variable includes the physical properties of the interacting bodies:

$$\lambda = \frac{2.06}{\xi_0} \left(\frac{K^2 \varpi^2 R}{\pi} \right)^{\frac{1}{3}} \tag{15}$$

where R, K and ϖ are the same as above, while ξ_0 is the equlibrium interatomic distance. λ includes all the parameters determining the free energy of the surface, thus, changes in the material quality will appear as different lambdas. The role of this parameter is to establish the transition from the DMT to the JKRS condition. The parametric equations are

$$\frac{\lambda \overline{A}}{2} \left[\sqrt{m^2 - 1} + (m^2 - 2) \arctan \sqrt{m^2 - 1} \right]$$
$$= 1 - \frac{4\lambda^2 \overline{A}}{3} \left[1 - m + \sqrt{m^2 - 1} \arctan \sqrt{m^2 - 1} \right]$$
$$\overline{\Delta} = \overline{A}^2 - \frac{4\lambda \overline{A}}{3} \sqrt{m^2 - 1}$$
$$\overline{P} = \overline{A}^3 - \lambda \overline{A}^2 \left[\sqrt{m^2 - 1} + m^2 \arctan \sqrt{m^2 - 1} \right] \tag{16}$$

where we can recognize the analogues of the Hertzian load versus contact radius and contact radius versus displacement functions. The normalized variables are the radius of the contact area, the load and the normal displacement (penetration depth):

$$\overline{A} = \frac{r}{\left(\pi K \varpi R^2 \right)^{1/3}} \tag{17}$$

$$\overline{P} = \frac{P}{\pi \varpi R} \tag{18}$$

$$\overline{\Delta} = \frac{d}{\left(\pi^2 \varpi^2 K^2 R \right)^{1/3}} \tag{19}$$

and $m = c/a$ with c being the width of the annular region at the outer edge of the contact radius where adhesive forces are assumed. The analytical solution

of these equations is a force-distance curve, which is highly accurate for a wide range of materials. Force curves calculated with the DMT and JKRS models, and the transition established by the Maugis formalism are shown on Figure 4.12. Thus, this is a theory well suited for the study of the effect of the surface properties on the AFM imaging.

Returning to the modeling of the tapping mode imaging, the next problem is the solution of Eq. 2. For complex models the nonlinearity often prohibits the analitical solution, thus numerical methods are needed. Furthermore, while most of the works seek a stable (equilibrial) solution, the dynamical behaviour of the probe - the transient response to surface perturbations - will significantly influence the maximal exerted force and the accuracy of surface tracing. It is thus feasible to solve Eq. 2 for the trajectory of the probe tip, and simulate the AFM amplitude detection mechanism. AFMs measure probe amplitude mostly either by integrating the detector signal (RMS) or by lock-in (frequency filtering) method. The amplitude signal is used in the feedback model, which is usually a simple PID control:

$$\Delta Z = Ps + I \int s dt + D \frac{\partial s}{\partial t} \tag{20}$$

where P, I and D are user selectable parameters, $s = A_{setpoint} - A_{measured}$ is the control signal and ΔZ is the correction of the tip-surface distance needed to restore the setpoint amplitude. Here the AFM model is complete.
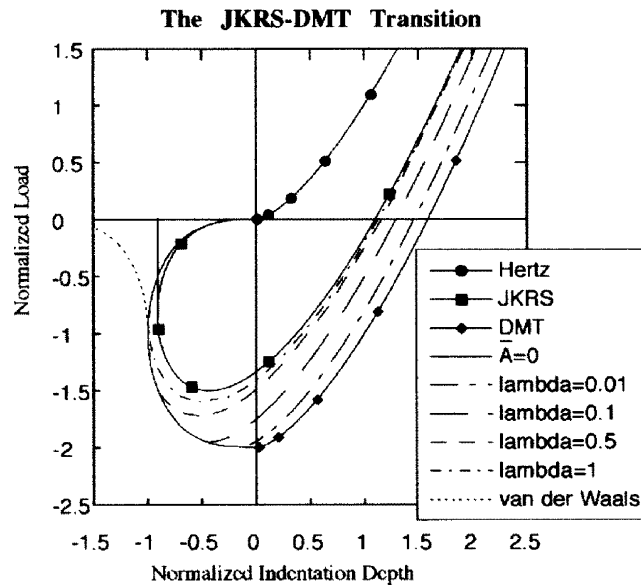

FIGURE 4.12. A comparison of the DMT and JKRS force curves, and the transition achieved by using Maugis continuum mechanics. Reprinted with permission from N. A. Burnham et al.: *How does a tip tap?*[13] Copyright IOP Publishing Limited 1997.

AFM simulations were carried out by numerous authors e.g.[13,81−91], with a wide range of varying complexity. These works were mostly focused on the identification of a sole parameter having the largest influence on the imaging process. It was shown that the complex interaction scheme can cause contrast artifacts[84], and that the "tapping" is sometimes "hammering" due to unexpectedly high imaging forces[85]. The cantilever dynamics were also intensively studied, showing that the tip has both stable and unstable motions when in intermittent contact with the surface[86] and that the correct description of the cantilever beam bending goes beyond the linear spring approach[68,87]. Based on above detailed models, the possibility of substracting information about the physical properties of the sample – analytical imaging – was frequently discussed. Patterns in phase imaging were interpreted as maps of elasticity[82], charge distribution 4 and energy dissipation[89,90]. It was shown that resonant harmonics of the cantilever oscillation, when a torsional mode matches a harmonic of the natural frequency of the beam, exhibit exceptional sensitivity for the sample properties[88]. It was recently noted that surface energy can influence the elasticity measurements performed with AFM[91].

Due to the overwhelming number of – sometimes contradictory – works, we attempt to briefly summarize the properties of the tapping mode AFM imaging as they are known so far. As we will see, the theory here provides us with explanation of, and solution for, most of the common imaging problems.

The first and most important question is the amount of force exerted on the sample during imaging, the minimization of which is of key importance for biosamples. When imaging a phospholipid membrane, it is common to observe that the object suddenly disappear in the middle of the picture, or by the second scan of the same area. Even if such drastical changes do not occur, the membrane tends to change shape and decompose upon repeated imaging. This is consistent with too high imaging force, which damages – or simply rips off – the membrane from the surface.

The impact of one "tap" of the tip, the *equilibrial* force, is a function of the following imaging parameters: the oscillating amplitude of the tip far from the surface (free amplitude), the setpoint amplitude (that is, the amplitude of the probe during operation), and the frequency of the oscillation. Also determining are the properties of the sample and the probe: the surface energy, elasticity, charge distribution and radius of curvature. One would think that only the radius of the tip apex matters; when looking at the parameters of Eq. 6, however, it is obvious that the reduced radius of curvature is a product of the radii of both the sample and the tip. These parameters determine the force exerted on the sample upon scanning over a featureless surface. When the probe encounters a sudden change in the morphology or the physicochemical properties of the surface, however, the response to these perturbations result in a *transient* force which is often much higher than the equilibrial force. It is a function of the quality factor of the probe, the scanning speed and the feedback parameters.

Since we are bound to accept the material properties of the sample, the equilibrial force has to be controlled by the imaging parameters. Let us first

look at the probe as a physical system. While the conventional wisdom refers to the cantilever spring constant as the deremining factor for the force, it is true only for the static case. For dynamics, it is the impact of the tip – which can be represented with the effective mass as we have discussed above – that determines the force. A practical, and, I assume, well known example is a folded sheet of paper that can break a pencil if it impacts with high enough momentum. With a simple model, let us imagine the following scene: the probe is a linear harmonic oscillator as we have described above, with the trajectory traced by the tip given with Eq. 3. The time derivative – velocity – of this form is a harmonic cosine function with the constant multiplicator $A\omega$, which is the maximal velocity of the probe, and it is a function of the maximal amplitude and the frequency of the oscillation. Since the resonance frequency depends on the spring constant of the cantilever, it does indeed influence the force, but not directly: softer cantilevers resonate at lower frequencies. However, as we will see below, working with low frequencies has its disadvantages, too. But returning to the model, the cosine function indicates that the momentary velocity is zero at the maximal displacement of the mass, accordingly, the momentary momentum is also zero. Thus, if the tip just touches the surface at the end of its trajectory, from this model no force is expected. If the probe is moved closer to the surface, however, the momentum at impact will increase rapidly, as determined by

$$I = mA\omega\cos(\omega t + \delta) \qquad (21)$$

where the tip-surface distance z is included through the argument of the cosine which we know is equal to *arcsin(A/z)*. Thus, the free amplitude A and the setpoint – A/z – are the two key parameters which need to be optimised. To minimize the imaging force, the smallest possible amplitude is desired, with a setpoint amplitude as close to the free amplitude as possible. Considering the real probe-surface interaction, the solution is less simple: Eq. 2 has to be solved for an additional force term which includes non-contact forces and a contact mechanical model as discussed before. In general, the conclusions drawn from the simple reasoning above would abide the scrutiny, however, other factors have to be also considered. The presence of the attractive non-contact forces allows for system settings when the probe does not physically touch the surface. In this "zero force" case, however, changes in material quality on the surface appear as morphological differences[14]. The same is true for low free amplitude tapping, especially on compliant surfaces, when the contact attractive forces have the most significant influence on the probe amplitude. Furthermore, the energy of the low amplitude oscillation is often not enough to break the tip away from a sample of high adhesion, thus leading to instabilities. The AFM hardware is an other limiting factor: too small free amplitudes, especially in combination with too high feedback amplitudes, would fall into the range where the discrete steps of the A/D converter are reached. One more argument against too high setpoint amplitudes is that the dynamical range of the probe amplitude has to be symmetrical for a stable feedback, that is, the increase in the amplitude when stepping down a step has to be comparable to the effect of stepping up. This

problem, however, belongs to the topic of imaging accuracy and artefacts, which we will discuss later.

Now let us return to the primitive model we employed to discuss the equilibrial imaging force. So far we have only considered a harmonic solution of Eq. 2. The complete solution, however, includes the term

$$y = Ae^{-\beta t} \sin(\omega_1 t - \varphi_0) \tag{22}$$

where y is the trajectory of the tip, ϕ_0 is the initial phase lag, and $\omega_1 = sqrt(\omega_0^2 - \beta^2)$ and we have defined A and β before as the maximal amplitude and the damping coefficient, respectively. This equation describes an exponentially decaying sinusoidal motion. Thus, any perturbation to the system which changes the amplitude and/or the phase lag would generate a transient term Eq. 22 in addition to the periodic term Eq. 3. The probe reaches the equilibrial amplitude under the new conditions that perturbated the system after the decay of the transient term. Since our original assumption was an immediate change, we have to consider what changes does this term bring into the picture we have about the operation of the machine. It is obvious that the inclusion of the transient amplitude into the feedback mechanism would lead to improper reaction to the surface structures, and, eventually, instability and imaging artefacts. Thus, the sampling frequency of the feedback cannot be higher than the reciprocal of the time constant of a typical transient (or, rather, it is desired to reduce the transient length). It is also obvious that the force exerted on the surface during the transient will be higher than the equilibrial force; thus, to assess the risk of sample damage, means of characterizing the expected transients are needed. The quality factor of the sample is an often used descriptor. It was originally defined as the ratio of the drive and the response amplitude but usually determined from the quotient of the width of the amplitude resonance curve and the resonance frequency. Lowering the quality factor decrease the transient length significally, allowing faster scanning; it does, however, also decrease the sensitivity of the probe, and increase the initial force. Higher quality factor probes, on the other hand, exhibit higher sensitivity, but the accompanying long decay extends the region of transient force and thus, in average, might cause surface damage; and the lengthy transient obviously limits the scanning speed.

After the exerted force, the second important property of an AFM is the accuracy of the imaging. While the accuracy of the piezoelectric scanners, the means and limits of closed loop operation and calibration have been discussed in numerous sources, our discussion will focus on less obvious phenomena: the inherent nonlinearities and artefacts of the probe. As it was briefly mentioned before, the dynamical range of the amplitude response is key to generate sufficient control signal for the feedback to approach or retract the probe. It has not been discussed, however, whether the probe is able to follow the morphology changes: the amplitude transfer efficiency. Basically, this is the measure of the ability of the probe amplitude to follow a sinusoidal modulation of a certain frequency. A plot of this parameter against the frequency of the modulation is called the transfer function of the probe. Since the interaction is nonlinear,

however, the transfer efficiency also depends on the amplitude, not only the frequency, of the modulation. This can be better characterized by using describing function (which is practically the transfer function of a nonlinear system and has to be separated due to a definition mismatch). Nevertheless, the describing function of the tapping mode AFM probe is usually linear, close to a 1:1 transfer until it reaches a corner frequency after which it has a fast decay. The frequency range of the linear amplitude transfer is called the bandwith. In practical terms, the bandwith shows the limits of the adaptation capability of the oscillating probe: a perturbation which have a spatial frequency beyond the corner frequency, such as a vertical step on the surface, cause the probe amplitude to lag behind the topography change and thus leads to inaccurate height measurements. Without discussing the details, we should point out that the frequency range of a perturbation is dependent on the scan speed. Accordingly, a telltale sign of the bandwith limited behaviour is if the measured height of a periodic object, like a test grid, is a function of the scan velocity. We have to compromise in a scan speed which provides consistent measurements, and which is often much lower than the theoretical linear velocity range of the AFM scanner.

An other source of height artifacts, as briefly mentioned before, is found in the surface properties. Attractive forces as well as elastic deformation of the sample can cause incorrect height measurements. As introduced with the JKRS model, and further elaborated in the Maugis theory, the separation of the probe from the surface happens at a non-zero contact radius, that is, a "neck" is formed which suddenly breaks at its strength. The length of this neck is a function of the strength of the adhesion and the surface stiffness and elasticity. Soft elastic surfaces exhibiting high adhesion can "hang on" to the probe for a surprisingly long time before separation, and thus extending the influence of the surface on the probe amplitude. Depending on the combination of parameters, this can lead to positive height artefact of up to 50% magnitude as observed experimentally. On the other hand, a similar sample without high adhesion would merely "give way" to the probe, thus causing a negative height artefact. Furthermore, in case of nanometer size objects, the change in the sample curveture by itself can cause a significant height measurement error (usually negative deviation for small sample radii), especially for low free amplitude imaging.

Finally, we should mention the phenomenon of contrast inversion. If the oscillating probe is pushed against the surface, the amplitude usually decays linearly with the distance (after a brief "rounded" range) and reaches zero once the energy of the drive dissipates into the surface altogether. In case of above-mentioned compliant, elastic samples exhibiting high adhesion (that is, high surface tension), this approach curve might become nonlinear. Since biological membranes typically fall into this category, we should understand the effect that such material properties make on the behaviour of the probe. Visually, a shoulder or a peak is formed on the approach curve. If this peak appears at the far end, after engaging the surface, the probe can work at higher setpoints than the free amplitude. After a large surface perturbation, however, it is possible for the probe to find the same amplitude on other side of the peak; this being a

positive slope, the feedback would generate an inverted image: higher structures would appear lower. This is an instable working condition and usually ends in loosing the surface. If the peak appears on the slope, the inverted range is usually too short for even temporary stable operation, thus the other possibility is for the probe to fall on the same amplitude on a negative slope but a certain distane away farther from (or closer to) the surface, thus recording a step artefact parallel to the scan direction.

With this, we reached the end of the discussion of probe behaviour and imaging artefacts. The "black magic" component of the imaging was explained in simple physical models and the four determining system parameters: the free amplitude, setpoint, the scan velocity and the operating frequency were identified, the careful and sensible control of which is sufficient to optimize the imaging most of the time. Furthermore, and more importantly, this reasoning highlighted the importance of careful analysis in the interpretation of the images to avoid premature conclusions.

4.4.3. Mechanical Properties

The theoretical overview presented in the previous section does not only support the modelling of the probe-surface interaction, but also provide with a list of key surface properties which determine the interactions of biological – or biomimetic – membrane surfaces with any foreign objects *in vivo* and *in vitro*. In particular, changes in the elasticity and surface tension (or surface energy) of the membrane can be diagnostic of structural chages, material incorporation or chemical alteration as well as mechanical stress and strain. As we have seen, the simple way of mesuring these properties is pushing a probe of known physical properties and geometrical shape against the sample surface and retracting until it breaks away, while recording the force acting between the probe and the sample. The slope of the curve can be used to calculate the elastic modulus based on either of the continuum mechanic models discussed above. It can be seen that Eq. 8, 10 and Eq. 13 describe the penetration depth as a function of normal load. The selection of the theory determines the accuracy of the measurement; there is no convention, however, about which model has to be used. When looking at the retracting curve, the maximal adhesion force, or "rupture" force, can be used to determine the surface energy. It is assumed that the JKRS theory gives the best estimation of the adhesion forces on a phospholipid membrane, thus Eq. 14 has to be used. For more accurate measurements, the complete interaction force, including the contact and non-contact components, can be fitted to the approach-retract curve. It can be seen that, for compliant surfaces, this curve has a hysteresis. When the attractive (e.g Van der Waals) non-contact forces become strong enough to cause a small protrusion of the surface, the attractive force suddenly increases with the decreasing distance and thus the probe "jumps to contact" with the surface. This jump is usually small. When retracting the probe, however, the adhesion keeps the two bodies in contact until a stretched neck is formed which suddenly breaks at the maximal adhesion force, after which the

probe finds itself at a certain distance from the surface, where the Van der Waals attraction is much lower. The hysteresis represented by the difference between the jump to contact and the rupture point, and the discontinuity of the force-distance function makes a perfect fit of the interaction model problematical. The best match can be reached by applying the Maugis model which includes the nonlinear behaviour. The applicability of a certain model is, however, also the function of the means and accuracy of the measurement.

Surface force apparatus was invented to record force-distance curves, and it has the highest precision. It has a major disadvantage, however: it performs a "blind" measurement, between two points predetermined by the geometry of the instrument. For everyday measurements, therefore, it is more convenient to use the AFM as a force measurement tool[96]. After recording a picture, and selecting the points of interest, AFM can perform a simple approach and retract curve, while the primary input channel, the bending of the cantilever, is plotted against the distance (Figure 4.13). Since the cantilever bending is directly proportional to the normal load, the force-distance curve is instantly generated. These measurements are typically used to measure surface properties of a wide range of materials including lipid membranes[97−102] but it can be used to measure interactions of membrane inserted proteins with antibodies, proteins and peptides as well. Furthermore, AFMs can also perform force curve mapping, called force volume imaging, when at each raster point of an image it collects a statistical number of force curves. Thus, after averaging, each raster point can be represented by e.g. its elasticity or maximal adhesion. After comparing this map to the surface morphology, and performing the corrections for the surface geometry (as we have seen, the maximal adhesion force is the function of the curvature of the surface), an accurate map of these properties can be achieved and used to distinguish different materials on the related topography.

The accuracy of these measurements is a function of the accuracy of the probe parameters we use for data analysis. Whereas most AFM probes come with a nominal value and an error range for the radius of curvature and the spring constant, the actual values of the individual probe properties can be way off compared to the nominated range. It is important therefore to determine these parameters with independent measurements.

The tip shape can be determined by using standard calibration samples. These are usually test grids with factory-guaranteed geometry. Step grids can be used to measure the radius of curvature in one direction; pin grids provide with a convolution picture of the whole tip apex. Measuring the spring constant is far more complicated. Whereas more than a dozen different methods exist, based on comparative studies[103, 104] four are considered the most accurate. These are the added mass[105], the reference cantilever[106], the thermal fluctuation[107] and the Sader model[19]. The first one uses a set of different – calibrated – masses which have to be attached to the cantilever one-by-one, and the changes in resonance frequency have to be measured. Since, from the simple relationship $\omega_0 = sqrt(D/m)$ the resonance frequency is a simple function of the mass of the
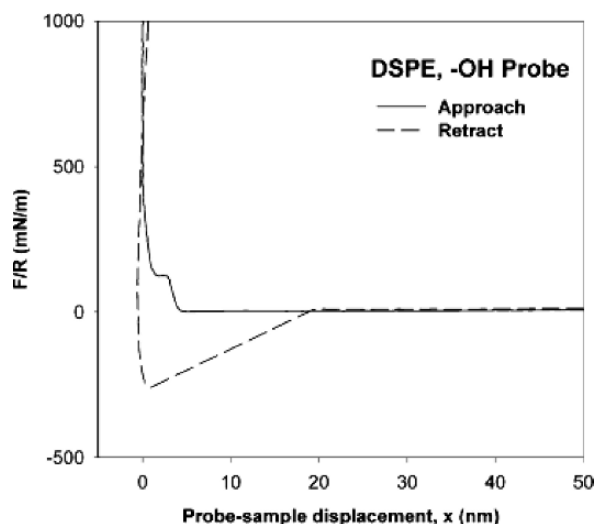
FIGURE 4.13. Normalized AFM force curve measured on a Langmuir-Blodgett DSPE lipid film. The AFM tip was hydrophobically coated. This representation is used to measure adhesion. Reprinted with permission from Schneider et al.[102] Copyright (2003) American Chemical Society.

oscillator, plotting the square of the frequency against the reciprocal of the added mass will define a line with the slope D, that is, the spring constant.

The reference cantilever method uses a previously calibrated beam. If the unknown probe is pushed against this beam (Figure 4.14), the unknown spring constant D_1 can be calculated from the formula

$$D_1 = D_0 \frac{Z - N}{N \cos \varphi} \qquad (23)$$

where Z is the (arbitrary) vertical travel of the base of the standard beam (in nm), D_0 is the spring constant of the standard beam, N is the *calibrated* deflection (in nm) of the unknown cantilever after Z vertical displacement of the reference lever, and ϕ is the attachment angle of the unknown cantilever (typically 6 degrees). The ratio Z/N is the inverse of the slope of the force – distance curve in the contact regime. A major disadvantage of this and the added mass method is the involvement of complicated and time consuming micropositioning tasks.

The thermal fluctuation method is based on the simple condition that, in equilibrium, the kinetic energy transfer to the cantilever by colliding gas particles equals the Boltzmann energy of the gas:

$$\frac{1}{2} D \langle x^2 \rangle = \frac{1}{2} k_B T \qquad (24)$$

where $\langle x^2 \rangle$ is the mean square of the thermal fluctuation of the cantilever beam, k_B is Boltzmann's constant and T is the ambient temperature in Kelvins.
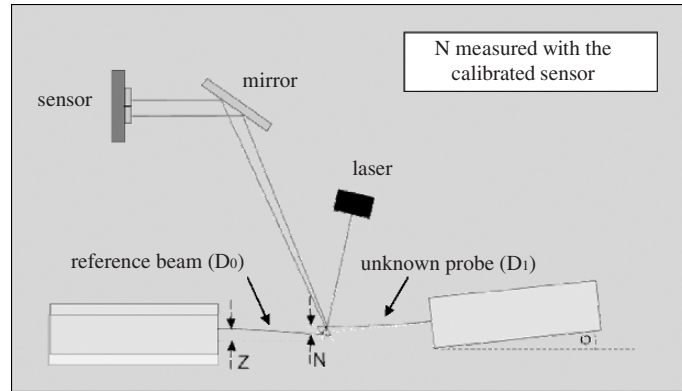
FIGURE 4.14. The experimental setup used to measure the spring constant of an "unknown" probe with the reference beam method[106].

Integrating the thermal fluctuations of the cantilever over a wide range, the spring constant can be simply determined[107]. The method is very sensitive to the accuracy of the calibration of the detector signal – cantilever displacement relationship.

The Sader method is an extension of the geometrical method originally proposed by Cleveland et al.[105]: after measuring the resonance frequency of the cantilever (from e.g. the thermal spectrum) the spring constant can be calculated based on the cantilever geometry and published data of Young's modulus and Poisson ratio. This was a simple but not too accurate approach. Sader extended this method with the measurement of the quality factor and the inclusion of the fluid dynamics of the environment; for details see[19]. At the time of the writing of this book, a calculator is available on Sader's home page.

It is still recommended to use at least two different calibration methods; however, comparative studies suggest that the advanced thermal fluctuation[108] and the Sader method provide the most consistent and accurate results[103, 104].

Finally we should discuss the possibility to substract physical properties from phase images. In the theoretical overview above we have established the formalism to describe the trajectory of the tip of the AFM probe during inter-action with the surface while driven with a sinusoidal signal. For modelling purposes, this trajectory is treated as the sensor signal which is assumed to be a harmonic periodic motion (this assumption is not always true, but it does not influnce the results) and the amplitude of this motion is determined similarly to the way the AFM calculates the probe amplitude. The same approach can be used to calculate the phase lag between the drive and the response signal. Whereas there is no analytical solution of the equation of motion, there is no dircet formula to relate phase lag to any surface properties. It can be derived, however, from a series of calculations and displayed graphically.

There are numerous works attempting to interpret the phase images as charge distribution, energy dissipation, spring constant, elastic modulus or adhesion; in a

controlled environment, when only one parameter is changing, each interpretation might be true. It was shown, for example, that membranes of different charges can be clearly distinguished[4]. The same effect can be explained, however, with the surface energy or Young's modulus difference between the phospholipid and the mica substrate. This difference can be used, on the other hand, to determine whether a membrane patch sits on the substrate or on top of an other membrane layer. The ambiguity in the identification of the key parameter, however, cannot be easily avoided; for the general case, numerical simulation is the only solution. Since this field is not yet fully explored, we leave this matter for the reader's consideration.

4.5.   A Brief Outlook

Here we finished the discussion of the imaging and analytical apparatus available for high resolution characterization of biomimetic membranes. As a final conclusion, we should briefly highlight the perspectives in the methodology. A typical application of a biomimetic membrane system is the study of protein processes such as membrane insertion/incorporation, aggregation, environment-dependent conformation as well as charge transfer properties, channel/pore formation, ion conductivity, selectivity and gating. The characterization of these systems is thus aimed at the membrane inserted proteins rather than the membrane itself (a few typical examples of imaging membrane inserted proteins are Figure 4.1 and Figure 4.15). There are numerous works on imaging membrane inserted proteins, fewer of which looked at protein function *in situ*. So far, the best results have been achieved on the characterization of medium to large size transmembrane channels, since it is relatively easy to morphologically distinguish the open and a closed conformation[7,8,10,93,94] and thus observe the effect of e.g. ionic perturbations directly. The potential of the methods discussed above, and the morphological imaging in particular, is to extend the in-situ studies to smaller proteins and peptides as well as to more complex biological/biochemical processes such as the mechanism and dynamics of fibre formation. The averaging methods like QCM, SPR or Ellipsometry are often applied to characterize such processes; imaging methods, however, have been neglected so far. Importantly, imaging is the only way to *show* the molecular scale events and thus confirm hypothetical mechanisms and identify individual variations in biological processes. Morphological analysis can also provide structural information about the native hydrated state of the proteins, complementary to the electronmicroscopy and electron crystallography methods that work only on dehydrated, crystalline samples. With the gathering mass of information on the imaging process and the extensive hardware development, AFM based methods are expected to gain full recognition among the routine tools of the nanotechnology of biological and biomimetic systems.
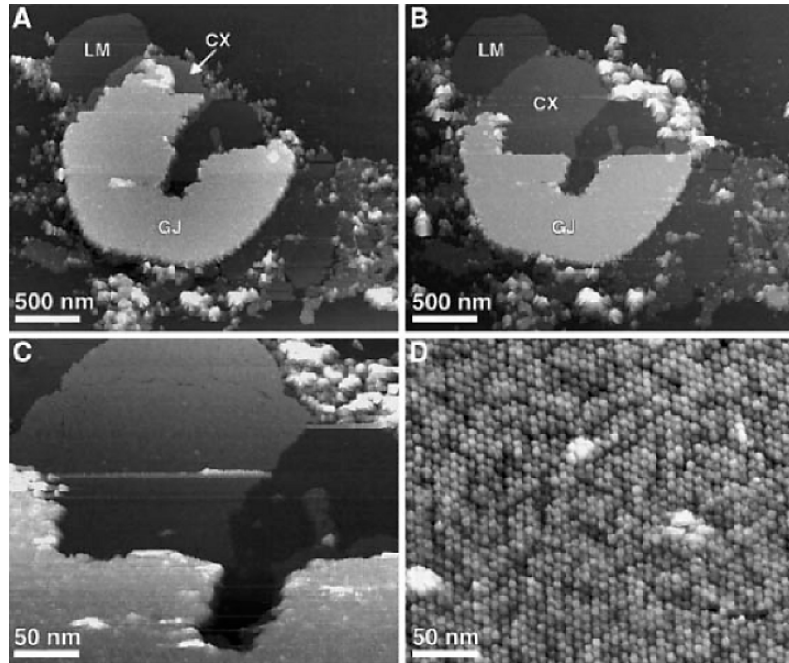
FIGURE 4.15. AFM imaging of a plaque of 26 kDalton protein gap junction structures (GJ) surrounded by a lipid membrane (LM) in buffer solution. Gap junctional hemichannels are exposed in a small area (CX) on A) and a larger area after force dissection on B). C), D) show the extracellular surfaces of the exposed hemichannels in different magnifications. Reprinted by permission from EMBO Journal[10], copyright (2002) Macmillan Publishers Ltd.

References

1. G. Binnig, C. Quate, Ch. Gerber, *Phys. Rev. Lett.* **56**, (1986) 930.
2. C. Ionescu-Zanetti, A. Mechler, S. A. Carter and R. Lal, *Adv. Mat.* **16** (5) (2004) 385–389.
3. Q. Zhong, D. Inniss, K. Kjoller and V. B. Elings *Surf. Sci. Lett.* **290** (1993) L688.
4. D. M. Czajkowsky, M. J. Allen, V. Elings and Z. Shao *Ultramicroscopy* **74,** (1998) 1.
5. G. Friedbacher, H. Fuchs, *Pure Appl. Chem.* **71** (7), (1999) 1337.
6. A. Philippsen, W. Im, A. Engel, T. Schirmer, B. Roux and D. J. Müller, *Biophys. J.* **82** (2002) 1667.
7. J.Thimm, A. Mechler, H. Lin, S. Rhee, R. Lal, *J Biol. Chem.* **280** (2005) 10646–10654.
8. R. Lal and S. A. John *Am. J. Physiol.* **266** (1) (1994) C1.
9. G Schitter, R. W. Stark, A. Stemmer, *Ultramicroscopy* **100**, (3–4), (2004) 253.
10. D. J. Muller, G. M. Hand, A. Engel and G. E. Sosinsky, *EMBOJ* **21,** (14), (2002) 3598.

11. P. Heszler, K. Révész, C.T. Reimann, Á. Mechler and Z. Bor, *Nanotechnology* **11**, (2000) 37.

12. J. Tamayo, A. D. L. Humphris and M. J. Miles *Appl. Phys. Lett.* **77** (2000) 582.

13. N. A. Burnham, O. P. Behrend, F. Oulevey, G. Gremaud, P-J. Gallo, D. Gourdon, E. Dupas, A. J. Kulik, H. M. Pollock, G. A. D. Briggs, *Nanotech.* **8** (2), (1997) 67.

14. Á. Mechler, J. Kokavecz, P. Heszler, R. Lal, *Appl. Phys. Lett.* **82** (21), (2003)3740.

15. J. Kokavecz, P. Heszler, Z. Toth, Á. Mechler, *Appl. Surf. Sci.* **210** (1–2), (2003) 123.

16. Á. Mechler, J. Kokavecz, P. Heszler, *Mater. Sci. Eng.* C **15** (1–2), (2001) 29.

17. B. Anczykowski, J.P. Cleveland, D. Krüger, V. Elings, H. Fuchs, *Appl. Phys. A* **66** (1998) S885.

18. J Kokavecz, Z. L. Horváth, Á. Mechler, Appl. Phys. Lett. **85,** (15), (2004) 3232.

19. J. E. Sader,*J. Appl. Phys*. **84**, (1), (1998) 64.

20. J. H. Kindt, J. B. Thompson, M. B. Viani, P. K. Hansma, *Rev. Sci. Inst.***73**, (6), (2002) 2305.

21. J. H. Kindt, J. B. Thompson, G. T. Paloczi, M. Michenfelder, B. L. Smith, G. Stucky, D. E. Morse, and P. K. Hansma, *Mat. Res. Soc. Symp*. **620** (2000) M4.2.1.

22. G. Sauerbrey, *Z. Phys.***155** (1959) 206.

23. D. Denengel *Chem. Ing. Technik* **45** (1973) 1107–1109.

24. E. Kretschmann, *Z. Phys.* **241** (1971) 313–324.

25. Z. Salamon, H. A. Macleod and G. Tollin, *Biochim. Biophys. Acta* **1331** (1997) 117–129.

26. K. Kurihara and K. Suzuki, *Anal. Chem.***74** (2002) 696–701.

27. M. Benes, D. Billy, A. Benda, H. Speijer, M. Hof and W. T. Hermens, *Langmuir* **20** (2004) 10129–10137.

28. G. Siegal, C. Abletshauser, A. Malmsten and D. Klussendorf, *Desalination* **143** (2002) 407–414.

29. N. M. Rao, A. L. Plant, V. Silin, S. Wight and S. W. Hui, *Biophys. J.***73** (1997) 3066–3077.

30. H. P. Vacklin, F. Tiberg, G. Fragneto, R. K. Thomas, *Biochemistry* **44** (2005) 2811–2821.

31. H. Mozsolits and M-I Aguilar, *Biopolymers* **66** (2002) 3–18.

32. H. Mozsolits, H. J. Wirth, J. Werkmeister and M. I. Aguilar, *Biochim. Biophys. Acta*, **1512** (2001) 64.

33. K. Hall, H. Mozsolits, M-I. Aguilar, *Lett. Peptide Sci.* **10** (2003) 475–485.

34. R. Richter, A. Mukhopadhyay and A. Brisson, *Biophys. J.* **85** (2003) 3035–3047.

35. P. H. Justesen, T. Kristensen, T. Ebdrup, D. Otzen, *J. Coll. Int. Sci*. 279 (2004) 399–409.

36. T. Snabe, S. B. Petersen *Chem. Phys. Lipids* **125** (2003) 69–82.

37. L. K. Tamm, C. Bohm, J. Yang, Z. F. Shao, J. Hwang, M. Edidin and E. Betzig, *Thin Solid Films* **285** (1996) 813–816.

38. Y. Fang and J. Yang, *Biochim. Biophys. Acta* **1324** (1997) 309–319.

39. S. M. Stephens and R. A. Dluhy, *Microchim. Acta* **S14** (1997) 455–457.

40. T. M. Winger and E. L. Chaikof, *Langmuir***14** (1998) 4148–4155.

41. L. K. Nielsen, J. Risbo, T. H. Callisen and T. Bjornholm, *Biochim. Biophys. Acta* **1420** (1999) 266–271.

42. Z Y. Tang, W. G. Jing and E. K. Wang, *Langmuir* **16** (2000) 1696–1702.

43. J. A. Last, T. A. Waggoner and D. Y. Sasaki, *Biophys. J.* **81** (2001) 2737–2742.

44. L. Wang, Y. H. Song, X. J. Han, B. L. Zhang and E. K. Wang, *Chem. Phys. Lipids* **123** (2003) 177–185.

45. F Tokumasu, A, J. Jin, G. W. Feigenson and J. A. Dvorak, *Biophys. J.* **84** (2003) 2609–2618.
46. Y. Ohta, S. Yokoyama, H. Sakai and M. Abe, *Coll. Surf. B* **34** (2004) 147–153.
47. T. Spangenberg, N. F. de Mello, T. B. Creczynski-Pasa, A. A. Pasa and H. Niehus, Phys. *Status Solidi A* **201** (2004) 857–860.
48. J. H. Tong and T. J. McIntosh, *Biophys. J.* **86** (2004) 3759–3771.
49. J. D. Green, L. Kreplak, C. Goldsbury, X. L. Blatter, M. Stolz, G. S. Cooper, A. Seelig, J. Kist-Ler and U. Aebi,*J. Mol. Biol.* **342** (2004) 877–887.
50. K. E. Kirat, L. Lins, R. Brasseur and Y. F. Dufrene, *Langmuir***21** (2005) 3116–3121.
51. D. M. Czajkowsky, S. T. Sheng and Z. F. Shao, *J. Mol. Biol.* **276** (1998) 325–330.
52. N. C. Santos, E. Ter-Ovanesyan, J. A. Zasadzinski, M. Prieto and M. A. R. B. Castanho, *Biophys. J.* **75** (1998) 1869–1873.
53. H. Lin, Y. W. J. Zhu and R. Lal, *Biochem.* **38** (1999) 11189–11196.
54. E. M. Erb, X. Y. Chen, S. Allen, C. J. Roberts, S. J. B. Tendler, M. C. Davies and S. Forsen, *Anal. Biochem.* **280** (2000) 29–35.
55. H. X. You, L. Yu and X. Y. Qi, *FEBS Lett.* **503** (2001) 97–102.
56. P. E. Milhiet, M. C. Giocondi, O. Baghdadi, F. Ronzon, C. Le Grimellec and B. Roux, *Single Molecules* **3** (2002) 135–140.
57. N. Fang and V. Chan, *Biomacromolecules***4** (2003) 1596–1604.
58. J. P. Rieu, F. Ronzon, C. Place, F. Dekkiche, B. Cross and B. Roux, *Acta Biochimica Polonica* **51** (2004) 189–197.
59. M. A. Hussain and C. A. Siedlecki, *Micron* **35** (2004) 565–573.
60. R. Tero, M. Takizawa, Y. J. Li, M. Yamazaki and T. Urisu, *Appl. Surf. Sci.* **238** (2004) 218–222.
61. J. Murray, J. Cuccia, A. Ianoul, J. J. Cheetham and L. J. Johnston,*Chembiochem* **5** (2004) 1489–1494.
62. A. Zebrowska and P. Krysinski, *Langmuir* **20** (2004) 11127–11133.
63. I. Ohtsuka and S Yokoyama, *Chem. Pharmaceutical Bulletin* **53** (2005) 42–47.
64. A. Berquand, N. Fa, Y. F. Dufrene and M. P. Mingeot-Leclercq, *Pharmaceutical Research* **22** (2005) 465–467.
65. X. M. Liang, G. Z. Mao and K. Y. S. Ng, *J. Coll. Interf. Sci.* **285** (2005) 360–372.
66. Z. F. Shao, J. Mou, D. M. Czajkowsky, J. Yang and J. Y. Yuan, *Advances in Physics* **45** (1996) 1–86.
67. N. C. Santos and M. A. R. B. Castanho,*Biophys. Chem.* **107** (2004) 133–149.
68. B. A. Todd, S. J. Eppell, and F. R. Zypman, *Appl. Phys. Lett.* **79** (2001) 1888.
69. J. N. Israelachvili, *Intermolecular and surface forces*, Academic Press, London (1985).
70. J. P. Spatz, S. Sheiko, M. Möller, R. G. Winkler, O. Marti, Nanotech. **6**, (1995) 40.
71. R. G. Winkler, J. P. Spatz, S. Sheiko, M. Möller, R. Reineker, O. Marti, Phys. Rev. B **54** (1996) 8908.
72. A. Kühle, A. H. Sørensen, J. Bohr, *J. Appl. Phys.* **81**, (1997) 6562.
73. X. Shi and Y-P Zhao, *J. Adhesion Sci. Technol.* **18** (1), (2004) 55.
74. H. Hertz, *J Reine Angew. Math.* **92** (1881) 156.
75. B. V. Derjaguin, V. M. Muller, YU. P. Toporov,*J. Coll. Int. Sci.* **53** (2), (1975) 314.
76. K. L. Johnson, K. Kendall, A. D. Roberts, *Proc. R. Soc. A* **324**, (1971) 301.
77. V. M. Müller, V. S. Yushenko, B. V. Derjaguin,*J. Coll. Int. Sci.* **77**, (1980) 91.
78. B. D. Hughes, L. R. White,*J. Mech. Appl. Math.* **32**, (1979) 445.
79. D. Maugis, *J. Coll. Int.* Sci. **150**, (1992) 243.

80. D. Maugis, B. Gauthier-Manuel, *J. Adh. Sci.* Tech. **8**, (1994) 1311.
81. B. Anczykowski, D. Krüger, H. Fuchs, *Phys. Rev. B* **53**, (1996) 15485
82. R. G. Winkler, J. P. Spatz, S. Sheiko, M. Möller, R. Reineker, O. Marti, *Phys. Rev. B* **54** (1996) 8908.
83. R. Garcia and A. S. Paulo, *Phys. Rev. B* **60**, (1999) 4961.
84. A. Kühle, A. H. Sørensen, J. B. Zandbergen, and J. Bohr, *Appl. Phys. A* **66**, (1998) S329.
85. O. P. Behrend, F. Oulevey, D. Gourdon, E. Dupas, A. J. Kulik, G. Gremaud, and N. A. Burnham, *Appl. Phys. A* **66**, (1998) S219.
86. R. Garcia and A. S. Paulo, Phys. Rev. B **61** (2000) 13381.
87. M. Gauthier, N. Sasaki, and M. Tsukada, *Phys. Rev. B* **64** (2001) 085409.
88. O. Sahin, C. F. Quate, O. Solgaard, and A. Atalar, *Phys. Rev. B* **69** (2004) 165416.
89. R. Garcia, J. Tamayo, and A. S. Paulo, Surf. *Interface Anal.* **27** (1999) 312.
90. J. P. Cleveland, B. Anczykowski, A. E. Schmid, and V. B. Elings, *App. Phys. Lett* **72**, (1998) 2613.
91. S. Cuenot, C. Fretigny, S. Demoustier-Champagne, and B. Nysten, *Phys. Rev. B* **69** (2004) 165410.
92. M. Csiszár, A. Szûcs, M. Tölgyesi, Á. Mechler, J. B. Nagy and M. Novák, *J. Electroanal. Chem.* **497** (2001) 69.
93. D. J. Müller, D. Fotiadis, S. Scheuring, S. A. Müller and A. Engel *Biophys. J.* **76** (1999) 1101–1111.
94. T. Meier, U. Matthey, F. Henzen, P. Dimroth, D. J. Müller, *FEBS Letters* **505** (2001) 353–356.
95. C. A. Keller, K. Glasmästar, V. P. Zhdanov and B. Kasemo, *Phys. Rev. Lett.* **84** (2000) 5443–5446.
96. M. Benz, T. Gutsmann, N. H. Chen, R. Tadmor and J. Israelachvili, *Biophys. J.* 86 (2004) 870–879.
97. Y. F. Dufrene, T. Boland, J. W. Schneider, W. R. Barger and G. U. Lee, *Faraday Discussions* **111** (1998) 79–94.
98. L. Zhang, R. Vidu, A. J. Waring, R. I. Lehrer, M. L. Longo and P. Stroeve, *Langmuir* **18** (2002) 1318–1331.
99. T. Kaasgaard, O. G. Mouritsen and K. Jorgensen, *FEBS Lett.* **515** (2002) 29–34.
100. P. Desmeules, M. Grandbois, V. A. Bondarenko, A. Yamazaki and C. Salesse, *Biophys. J.* **82** (2002) 3343–3350.
101. N. Maeda, T. J. Senden and J. M. di Meglio, *Biochim. Biophys. Acta* **1564** (2002) 165–172.
102. J. Schneider, W. Barger and G. U. Lee, *Langmuir* **19** (2003) 1899–1907.
103. R. Levy and M. Maaloum, *Nanotechnology* **13** (2002) 33–37.
104. N. A. Burnham, X. Chen, C. S. Hodges, G. A. Matei, E. J. Thoreson, C. J. Roberts, M. C. Davies and S. J. B. Tendler, *Nanotechnology* **14** (2003) 1.
105. J. P. Cleveland, S. Manne, D. Bocek and P. K. Hansma, *Rev.Sci. Instrum* **64** (1993) 403–5.
106. C. T. Gibson, G. S. Watson and S. Myhra *Nanotechnology* **7** (1996) 259–62.
107. J. L. Hutter and J. Bechhoefer *Rev. Sci. Instrum.* **64** (1993) 1868–73.
108. H-J. Butt and M. Jaschke *Nanotechnology* **6** (1995) 1–7.

5
Biomimetic Membranes in Biosensor Applications

Till Böcking and J. Justin Gooding

5.1.   Introduction

Biosensors are portable analytical devices designed to be used by the general public, directly in the field without any specific training or without requiring any processing steps.[1,2] For a portable analytical device to achieve this goal, which essentially means there cannot be any sample preparation step, requires the device to have exquisite selectivity for the target analyte because invariably complex samples such as blood will have a myriad of other compounds present. To achieve this specificity biosensors borrow from nature using the recognition molecules of living things such as enzymes, antibodies, peptides or DNA. Thus a biosensor comprises a biorecognition molecule integrated with a signal transducer to give a reagentless analytical device (see Figure 5.1). The signal transducer determines the extent of the biorecognition event and converts it into an electronic signal which can be outputted to the end user. Common transducers include amperometric electrodes, optical waveguides or mass sensitive piezo-electric crystals. The final biosensor is a solid-state device which is exposed to a solution sample and hence the biorecognition reaction is an interfacial reaction. The classic example of a biosensor is the glucose monitors used by diabetics where the biorecognition molecule is the enzyme glucose oxidase and the transducer is an electrode (Figure 5.2).

To produce a solid-state device which incorporates biorecognition molecules over a signal transducer requires the immobilisation of the biorecognition molecule. Thus the immobilisation step must maintain the biorecognition molecule close to the signal transducer whilst retaining the activity of the biological molecule and ideally stabilising the biological molecule. Immobilisation must also maintain accessibility of the biorecognition molecule to the target analyte which, in the case of large analytes such as bacteria, means the recognition molecules must project out into solution. Frequently immobilisation will perturb the thermodynamics of binding between the biorecognition molecule and the target analyte and hence minimisation of this pertubation is also desirable.
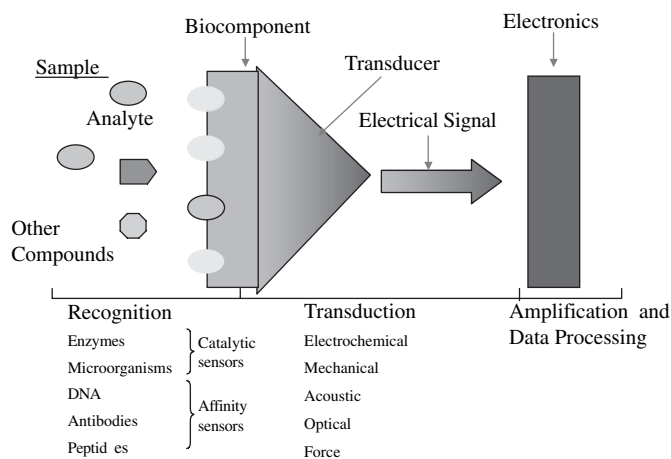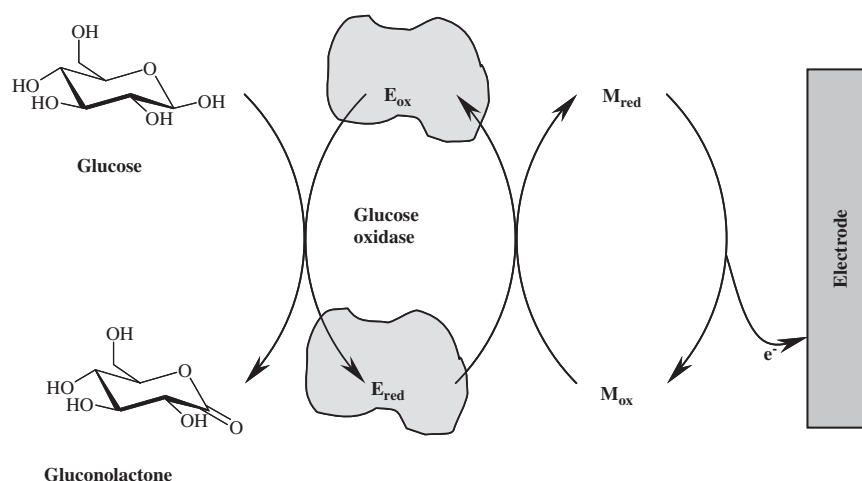
FIGURE 5.1. A schematic of a biosensor.

FIGURE 5.2. The enzyme reaction scheme for a glucose biosensor which allows transduction of the extent of glucose in a sample via the current produced at the electrode. E_{ox} refers to the catalytically active oxidised form of the enzyme, E_{red} is the inactive reduced form, M_{ox} is an oxidant which reoxidises the enzyme and M_{red} is the reduced form of this species which diffuses to the electrode where it is reoxidised and gives a current which is outputted to the end user.

The thermodynamics of binding determines the affinity of the biorecognition molecule for the target analytes which has implications for both the selectivity and detection limit of the biosensor. Coupled with all these demands on the immobilisation step when fabricating a biosensor is that non-specific interactions between the biosensing interface and the sample solution must also be minimised.

As a consequence of the requirements the biosensing interface must fulfil for an effective biosensor to be developed, interfacial design for biosensors has been an active area of research[3−7]. The demanding criteria a biosensing interface must satisfy are similar criteria that interfaces in biological systems often face. In biological systems selective adsorption of a species to an interface or transport of a species across an interface must be achieved despite the presence of many other species in the environment. Thus, in a similar way to mimicking biological recognition the mimicking of biological interfaces for the fabrication of biorecognition interfaces for biosensing applications is a logical step. Furthermore, it is at the cell surface (that is the cellular membrane) that many of the important interactions in biology occur, and many biorecognition molecules only function effectively when immersed within a phospholipid membrane[8]. Therefore using biomimetic membranes to fabricate biosensing interfaces affords opportunities to develop novel biosensors which otherwise would not be possible.

This chapter will focus on the use of biomimetic membranes in biosensing applications. The intention is not to be an exhaustive review of the extensive research into developing biosensors using biomimetic membranes but rather to highlight some of the important developments and important advantages of biomimetic membranes in biosensing. It will be focused on bilayer lipid membranes (BLMs), technologies which are compatible with developing a portable analytical device and where detection of a target analyte is the objective of the published work. As a consequence, research which employs lab based instruments for monitoring binding kinetics, such as some of the surface plasmon resonance instruments which are often referred to as a biosensor, will not be considered in detail. Similarly nor will the large body of research on functionalising novel biomimetic membranes with proteins for understanding biological interactions which occur at membranes[8−10].

5.2.   Biosensors

5.2.1.   Classes of Biosensors

Biosensors can be subdivided into two classes based on the type of biorecognition molecule. Catalytic biosensors employ enzymes and microorganisms as the biorecognition molecule which catalyses a reaction involving the analyte to give a product. Common analytes for catalytic biosensors are small organic molecules like glucose or lactate. As products are generated in the enzyme reaction, typically transduction is achieved by detecting one of these products. The glucose biosensors provide an example of how this class of biosensor typically allows detection of an analyte in a complex sample without requiring any user intervention. In a glucose biosensor all the end user is required to do is prick their finger and place a droplet of blood on the test strip. Within a minute the biosensor has displayed the glucose content of the blood despite blood containing a plethora of other biochemicals, proteins and cells. The glucose

biosensor achieves this using the enzyme glucose oxidase immobilised in a polymer layer over an electrode (Figure 5.2). β-D-Glucose which is exposed to the sensing interface is oxidised by the enzyme to gluconolactone and the enzyme is reduced in the process. A co-substrate, M_{ox}, which in nature is oxygen, reoxidises the enzyme back to its catalytic oxidised form. The reduced form of the co-substrate M_{red}, hydrogen peroxide in natural systems, then diffuses to the electrode where it is oxidised. As the amount of M_{red} is related to the amount of glucose in the sample, the current is also indicative on the concentration of the analyte[11]. In most commercial devices M_{ox} and M_{red} are a redox mediating species such as the ferrocene/ferrocinium couple or ferro/ferricyanide.

The other category of biosensors is **affinity biosensors**. Biorecognition molecules commonly used in affinity biosensors include antibodies, DNA, peptides and lectins. Affinity biosensors are characterised by a binding event between the biorecognition molecule and the analyte (the affinity reaction) often with no further reaction occurring. Hence the challenge then becomes transducing the biorecognition event. Transduction of affinity biosensors has been achieved using labelled species and using label free approaches. If transduction is achieved using labelled species the principles are very similar to an immunoassay with the amount of analyte detected being inferred from the amount of label which binds to the interface. The most common transducers for detecting labelled species are optical where an optically active label is detected[12−14] or electrochemical where the label is electroactive[13,15]. Label-free methods most frequently involve evanescent wave based optical methods such as surface plasmon resonance[16−18] or use mass sensitive acoustic wave devices[19,20] which monitor molecules binding to, or desorbing from, a transducer surface. Any change in species adsorbed to this surface will give a response. In the case of both label and label free methods one of the key factors which limits biosensor performance is non-specific binding. The problem of non-specific binding highlights the importance of inter-facial design in a biosensor[6,21] and solving this problem is where biomimetic membranes possess considerable potential for biosensing applications.

5.2.2.   *Why Biomimetic Membranes for Biosensing Applications?*

The commercial and analytical success of the glucose biosensor demonstrates that biosensors can realise their promise of being portable analytical devices which can be used by the general public. However there are only few other examples (pregnancy test kits, cholesterol monitors) of this class of technology making a serious impact on our daily lives. The reasons for the lack of widespread use of biosensors can be related to a few key challenges which have dogged their widespread development.

1. The first is simply one of market size. Glucose is the largest market for enzymatic sensors which currently sits at around 5 billion US dollars per annum[22]. The consequence of the lack of large markets is that any new

biosensing technology that is developed needs to be generic; that is can be applied to a number of different analytes without a significant change in the technology. The evidence for the merits of a generic approach is the success of the gene chips marketed by a number of companies which in many ways can be thought of as biosensors. The ability to have many different sequences of DNA analysed on a single chip surface made it viable for a single chip to cost thousands of US dollars when the technology became commercially available. It is of no coincidence that possibly the next big success of the biosensing world could be the AMBRI Ion channel biosensor[23,24]. The AMBRI ion channel biosensors is technology that can be applied to a large number of different analytes. We shall return to the AMBRI device later.

2. The second stumbling block is one of reproducible mass fabrication of the biosensors. For example the deposition of polymer layers containing the biorecognition molecule over the transducer with sufficient precision in their thickness to give a reproducible device continues to be a significant challenge[11,25]. The reason why production of highly reproducible devices is required is, for a user intervention free device, calibration of each device by the end-user is not a viable option. One of the main directions in research to overcome the problem of reproducibility, at least for affinity sensors, is to use self-assembly of monolayers[3,5,6] or BLMs[26,27] on the transducer surface to which the biorecognition molecule is anchored to or immersed within.

3. Selectivity of the biosensor response continues to be a challenge. This is despite the biorecognition molecules being highly specific for the target analyte. The lack of specificity is invariably a consequence of the poor selectivity of the method of transduction. With electrochemical devices which measure a current, the interference comes from other species in the sample reacting directly at the electrode surface at the same potential as the product of the enzyme reaction that is detected[28]. With the vast majority of other transduction methods such as surface plasmon resonance,[14] acoustic wave devices,[19,29] impedance spectroscopy (EIS)[30] and labelling methods selectivity of the biosensor response is compromised by non-specific adsorption to the biosensing interface.

4. Analytical methods are invariably being pushed to lower limits of detection and biosensors are no exception. Typically the detection limit is largely determined by the activity of the biorecognition molecule in catalytic biosensors or the affinity constant of binding in affinity biosensors. As a consequence the immobilisation protocol must limit any decrease in activity of catalytic molecules and any restriction in the availability of the biorecognition molecule to the analyte in solution. Other issues which influence the sensitivity are the sensitivity of the transducer and non-specific binding which contributes a background signal to the specific analytical signal.

5. Robustness of the device is the final key challenge facing researchers developing biosensors. Lack of robustness issues can relate to the entire biosensing interface or to the stability of the biological molecule after immobilisation. In the case of particularly fragile biomolecules one strategy to provide stability

in a biosensing interface is to immerse the biomolecule in an environment similar to which it is found and in the case of membrane bound biomolecules this means immobilising the biomolecules in a biomimetic membrane.

So how do biomimetic bilayer membranes overcome some of these challenges to biosensor development? Many of these stumbling blocks are an issue of interfacial design; the design of the biorecognition interface integrated with the signal transducer. What biomimetic membranes provide is a generic approach to modifying the transducer surface which can be applied to many different types of biomolecules[8,31]. The fact that biomimetic bilayer membranes are formed by self-assembly to give essentially a single plane where the biorecognition reaction occurs could be a solution to the problem of reproducibility[32]. The continuous nature of the membranes means that the underlying transducer surface is protected from the environment of the sample which restricts direct access of interferences to the transducer surface but does not necessarily overcome the problem of non-specific adsorption. Finally the fact that the biomimetic membranes are mimicking a natural environment in which many biorecognition molecules can be found means that the affinity constant between the biorecognition molecule and the target analyte may not be significantly perturbed by being immobilised.

Additional advantages of biomimetic membranes are that they afford biosensing opportunities not available using other approaches with regards to transduction methods and the range of biorecognition molecules that can be used. An example of unique transduction methods is the ion channel biosensor which is discussed in detail below[23,24]. The ion channel biosensor uses a transfer of ions through a biomimetic membrane as the method of transducing a biorecognition reaction, an approach only possible with a biomimetic membrane. In the case of many membrane receptors the molecules typically possess significant hydrophobic domains and therefore have a different tertiary structure in solution relative to a membrane. Changes in the tertiary structure will naturally influence the affinity and specificity of the biorecognition molecule for the target analyte. In the case of such biorecognition molecules, immobilisation within a biomimetic membrane is the only viable option for the development of a biosensor. This is particularly the case with complex membrane proteins which dimerise or oligomerise within a membrane[8]. The combination of these two advantages provide a unique class of biosensors based on biomimetic membranes which can mimic the mode of action of a toxin or other cell surface binding molecule in a natural system. Perhaps the most explored example of this approach is the detection of cholera toxin which enters cells via binding to the ganglioside GM_1 on the cell surface[8,33−36]. The ganglioside is incorporated as part of the lipid membrane either as a liposome or on the flat surface of a transducer.

Based on the above discussion of the challenges facing the development of biosensors and the possible solutions provided by biomimetic membranes, one may come to the conclusion that this is the only viable path to follow in developing new biosensors. This is in fact not the case because of the limitation of biomimetic membranes. The key limitation is one of lack of

robustness. Suspended lipid bilayers are rarely stable for more than 8 hours[37]. As a consequence considerable research effort has gone into methods of fabricating supported and tethered bilayers[8,10,38−42]. These biomimetic membranes are still reasonably complicated to fabricate reliably and a question mark still exists over their long term storage and hydration for re-use (although it should be noted such issues appear to have been dealt with by AMBRI in the commercialisation of their technology[43]). As there are possibly simpler and more robust methods for fabricating biosensors interfaces which have a similar level of control over interfacial design, the use of biomimetic membranes for the fabrication of biosensors should be limited to devices where the biomimetic membrane renders a distinct advantage over simpler methods of fabricating a biosensor. Such advantages are discussed above and include when a biomimetic membrane is the only option for immobilisation of the biorecognition molecule, when the biorecognition molecule gives optimal binding affinity to the analyte and when the biomimetic membrane produces a novel method of transducing the biorecognition event with performance advantages over other methods.

In the following sections we will outline the architectures of various biomimetic membranes followed by some of the advances using these systems in biosensors.

5.3.   Biomimetic Membranes for Biosensor Applications

Biomimetic membranes can be classified according to how they are made and how they are supported. Common subdivisions are vesicles or liposomes, suspended ("free-standing") BLMs where the bilayer is formed across an aperture in a septum separating two aqueous solutions, and supported planar BLMs where the bilayers are stabilised on solid supports. The discussion of sensors based on vesicles will be largely restricted to a few examples where the vesicles have been immobilised on the sensor surface. Free standing BLMs have been used extensively as model membranes[44,45] and for analytical applications[27] but have insufficient long term mechanical stability to be viable as portable biosensing devices. Despite a number of recent advances towards forming more robust free standing BLMs across micro-machined apertures[46−49] and microporous supports[50−55] these approaches will not be discussed in detail. Integration of the bilayer with a solid surface provides far greater stability than a free standing BLM and thus the majority of biomimetic membrane based biosensors employ supported BLMs. One can distinguish three basic types of supported BLMs:

1. Hybrid BLMs (hBLMs) are formed by depositing a monolayer of lipids onto a hydrophobic surface (for example a SAM).
2. Solid supported "floating" BLMs (sBLMs) are deposited onto a hydrophilic substrate and stabilised by physical interactions (mainly electrostatic) between bilayer and substrate surface.
3. Tethered BLMs (tBLMs) are stabilised by anchoring all or a number of lipids in the bottom half of the lipid bilayer (bottom leaflet) via hydrophilic spacers or polymers to the substrate.

A large body of research has been carried out to establish the methods for the reproducible formation of supported bilayer systems with structural and electrical properties approaching those of biological membranes. In this context, the desirable electrical properties indicative of a solvent- and defect-free BLM are determined by the alkyl chain region of the bilayer with a capacitance close to $\sim 10^{-2}$ F m^{-2} (= 1 μF cm^{-2}) and a high resistance of $\sim 10^3$ Ω m^2 (= 10 MΩ cm^2)[56,57]. We will briefly discuss the architectures of the different types of supported BLMs with respect to their suitability for biosensor applications since these technologies underpin the development of some of the most elegant and promising biomimetic membrane based biosensors.

5.3.1. Hybrid Bilayer Lipid Membranes (Supported Lipid Monolayers)

Hybrid BLMs (Figure 5.3a) are asymmetrical structures, in which a lipid monolayer (serving as the upper leaflet) is deposited onto a hydrophobic surface, such as a SAM of alkylthiols on gold[64] or a polymer film with hydrophobic side-chains[59−61]. The advantages of hBLMs lie in their facile and reproducible formation and mechanical robustness with lifetimes of several weeks[65]. Hybrid BLMs can be formed by interaction of lipid vesicles with hydrophobic surfaces, whereby the packing density of the lipid monolayer depends on the quality of the underlying SAM[66]. They are suitable for the detection of interactions occurring at the membrane surface. Since hBLMs are not separated from the substrate by an aqueous region, they are unsuitable for incorporating integral membrane proteins with large hydrophilic domains. Thus, in biosensor design hBLMs generally serve to anchor biorecognition elements on the transducer surface, similar to immobilisation schemes using SAMs. The potential advantage of using hBLM for this purpose over SAMs is that the biorecognition elements are reasonably mobile (as the lipids to which they are attached can diffuse in the plane of the membrane) and may thus re-orient to maximise interactions with analytes in the solution.

5.3.2. Solid Supported "Floating" Bilayer Lipid Membranes

BLM supported on solid substrates (Figure 5.3b) are generally assembled by adsorption and fusion of vesicles on clean, hydrophilic surfaces such as mica, glass, or other oxide surfaces. Alternatively formation can be achieved by Langmuir-Blodgett (vertical) transfer of a lipid monolayer from the solution-air interface to the substrate (bottom leaflet) followed by deposition of the top leaflet by either Langmuir-Schaefer (horizontal) transfer[67,68] or vesicle fusion[67] The membrane interacts with the surface via electrostatic, hydration and van der Waals forces[69]. In these systems, the bilayer is separated from the substrate by a thin film of water ($\sim$10-20 Å)[70−72]. Although the lubricating water film
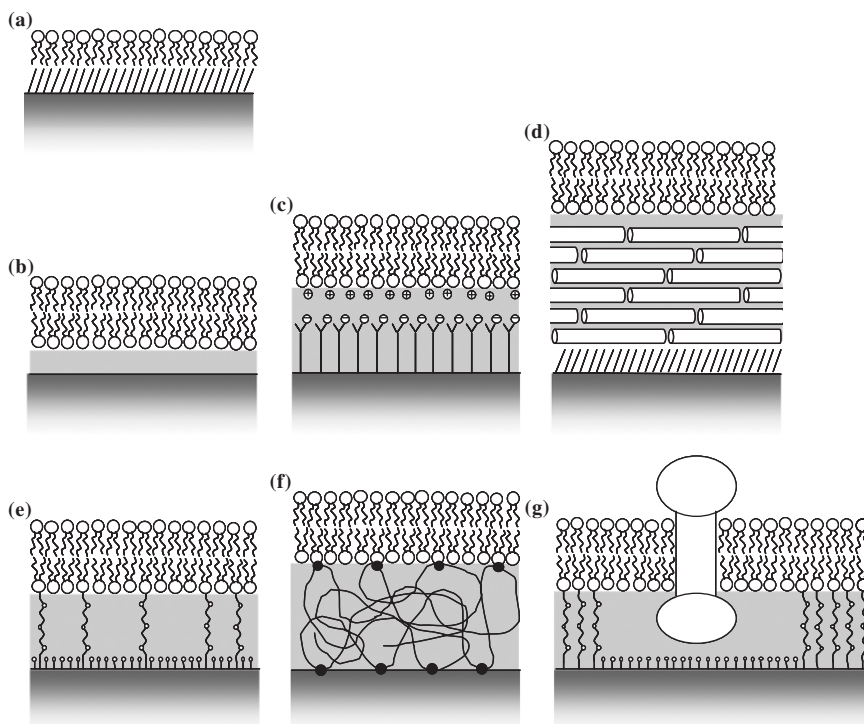
FIGURE 5.3. Architectures of supported BLMs. (a) Hybrid BLM: Deposition of a lipid monolayer onto a hydrophobic alkyl monolayer or a hydrophobic brush by unrolling of vesicles or Langmuir-Blodgett transfer leads to the formation of a hBLM. These model systems are robust and suitable for probing interaction occurring at the membrane surface. (b-d) Solid supported "floating" bilayers can be formed by vesicle adsorption or Langmuir-Blodgett techniques (or a combination of both) on hydrophilic substrates and interact by electrostatic, hydration and long-range van der Waals forces with the substrate. (b) Solid supported BLM formed directly on a hard surface float on a thin film of water, so that the bilayer is maintained in the fluid state. Transmembrane proteins incorporated into this type of sBLM are generally immobilised on the surface. (c) A hydrophilic SAM screens the coupling between substrate and bilayer. The SAM can for example consist of carboxy- or hydroxy-terminated alkyl-thiols on gold or a peptide with terminal carboxy-function.[58] (d) Alternatively a "soft" polymer cushion such as dextran or cellulose can be deposited onto the solid substrate. The example presented here depicts a thin hydrated cellulose film.[59−63] (e-g) Tethered BLM: There are two main strategies for covalently linking a "tethered" bilayer to a solid support: (e) using hydrophilic (low molecular weight) spacer molecules and (f) using a hydrophilic polymer cushion to tether lipids in the bottom leaflet to the surface. The region between the surface and the bilayer is hydrated and fulfils several functions: The aqueous region serves to separate the bilayer from the solid support (which reduces the lipid-substrate interactions) to maintain a structure resembling a biological membrane with lateral mobility of lipids and allows the incorporation of proteins. It also provides an aqueous reservoir for ions, e.g. to ensure

(*Continued*)

maintains the long range fluidity of the membrane,[73,74] the interactions between the lipid headgroups and the substrate restrict the lateral diffusion of lipids[73,75]. The aqueous layer between bilayer and surface is too small to accommodate large hydrophilic domains of integral proteins if these are to be incorporated for biosensing applications. Further, proteins can also interact strongly with the oxide surface, which leads to loss of lateral mobility or even denaturation[63,76]. Since the bilayer is merely physically adsorbed, it can easily be detached from the surface[41] and the strength of the interaction depends on pH and salt concentration, which have to be maintained within a certain range. Solid supported membranes have a comparatively high defect density and low self-healing properties as judged by their electrical properties. It has been suggested that the low electrical resistance of sBLMs (in comparison to free standing BLMs) is due to the reduced density of lipids in the bilayer after transfer to the solid substrate[77].

Solid supported membranes provide crucial model systems for studying adhesion and signalling between cells of the immune system[78]. Furthermore, recent advances in micropattern formation in sBLMs hold great promise for developing laboratory based membrane microarrays[69]. However, the disadvantages of sBLMs discussed above, in particular the relative instability and the insufficient aqueous reservoir between the bilayer and the surface, may limit the utility of these systems for biosensors.

A strategy to improve the stability of sBLMs to make them more suitable transducer coatings in biosensors consists of polymerisation of diene-functionalised lipid monomers[79]. The polymerised membrane can be dried out and rehydrated while maintaining reasonably good anti-fouling properties[80] and supports the functional incorporation of the membrane photoreceptor rhodopsin[81]. The disadvantage of polymerisation is of course that the membrane components are no longer free to diffuse.

To reduce the lipid-substrate interactions, composite systems have been developed, in which the bilayer is supported on a SAM terminated with polar or charged head groups (Figure 5.3c) or on a hydrophilic soft polymer cushion[42] (Figure 5.3d) such as an ultrathin layer of dextran[82] or cellulose[59−61]. Cell-adhesion molecules incorporated into sBLMs on cellulose cushions showed long range lateral mobility, which demonstrated the biocompatibility of the cellulose films[63]. Polymer cushions can either be covalently linked to the substrate[82] or physisorbed. The formation of stable sBLMs on physisorbed polymer cushions is

FIGURE 5.3. *(Continued)* the proper function of ion channels and to allow measurement of the movement of ions through channels in the bilayer. (e) Monolayers of lipid derivatives attached to hydrophilic spacers and terminated with a surface reactive group are assembled on the surface. The density of tethered lipids can be adjusted by including a larger number of small hydrophilic molecules to serve as lateral spacers. Approaches to achieve such structures are based on thiol-gold chemistry, silane-oxide coupling and ligand-receptor interactions. (f) The tBLM is anchored to a soft polymer cushion. Different approaches are based on lipopolymers ("top-down") and coupling of lipid layers to polymer cushions ("bottom-up"). (g) A patterned bilayer consisting of regions of tethered bilayer and regions of untethered bilayer above a hydrophilic SAM.

dependent on the balance of the interaction forces between the different components in the system as well as on the method used to deposit the bilayer[83,84].

5.3.3. *Tethered Bilayer Lipid Membranes*

In tBLM systems the bilayer is covalently attached to the solid support via hydrophilic tethers (Figure 5.3e) or polymer cushions (Figure 5.3f). The hydrated tether region or polymer cushion also serves to "decouple" the bilayer from the substrate, i.e. to screen the interactions of the lipids with the underlying solid substrate.

5.3.3.1.   Surface Attachment via Low Molecular Weight Tethers

The most successful biomimetic membrane based biosensors have so far been based on tBLMs in which a number of lipids in the bottom leaflet are anchored to the sensor surface via low molecular weight tethers (Figure 5.3e). These tethers are designed to allow the formation of an aqueous region between lipid bilayer and the substrate, which can accommodate the extra- or intracellular domains of transmembrane proteins and provides an ionic reservoir required for ion channel function. For this purpose tethered lipids generally consist of three segments: (1) a functional group for immobilisation on the solid substrate on one end, (2) a hydrophilic spacer defining the aqueous reservoir region and (3) the lipid inserting into the membrane on the other end.

The most common strategy for tBLM formation relies on the chemisorption of lipid derivatives with sulfhydryl or disulfide moieties ("thiolipids") to gold surfaces. In the first step a SAM is deposited onto the gold substrate from a solution containing thiolipid. In the second step the bilayer is completed by vesicle adsorption or by solvent-dilution techniques.* Alternatively, tBLM formation on bare gold surfaces can be initiated by adsorption of thiolipid containing micelles[85−87] or vesicles[88].

Other chemistries for the anchoring of bilayers applicable to a wider range of substrates (such as gold and oxide surfaces) rely on the non-covalent interaction of tagged lipids with functionalised surfaces. For example, lipid films have been immobilised via the reversible complex formation between oligo-histidines and metal ion chelator groups[89−91]. Recently, a protocol was reported for the coupling of biotinylated vesicles on streptavidin coated glass and aluminium oxide surfaces followed by fusion of the vesicles to form continuous streptavidin-supported bilayers[92−94]. Interestingly, streptavidin-supported bilayers could be reconstituted on microporous aluminium oxide electrodes whereby the bilayer extended into the pores[92]. The large internal surface area of porous substrates and the intimate mixing between sample and transducer surface in such structures could be exploited for sensors with high sensitivity.

---

* In the solvent-dilution technique a solution of lipids in a water miscible solvent is placed onto the thiolipid SAM. Dilution of the solvent by rapid addition of water results in the formation of the tBLM.

Instead of employing tethered lipids, biomimetic membranes can also be anchored via the protein component. This approach was first demonstrated by attaching biomimetic membranes[95] or cell membrane fragments[96] via biotinylated transmembrane receptors to avidin coated surfaces. Recently protein-tethered BLM were also formed by binding histidine tagged transmembrane proteins to surface bound metal ion chelators[91,97−99]. There are two advantages of these protein-tethered BLMs with regards to assembling biosensor and high-throughput screening platforms: Firstly, the proteins are uniformly oriented in the bilayer. Secondly, the tBLM can be assembled directly from cell homogenates without the need for protein purification[96].

The overall quality of the tBLM with respect to the fluidity and lateral mobility of lipids, structural integrity and its resulting electrical properties (and therefore its applicability for biosensing) is dependent on the interplay of all components in the system, including the chemical structure and length of the hydrophilic tether,[100] the chemical structure of the membrane forming lipids (see Section 5.3.3.2) as well as surface roughness of the underlying substrate[101−103]. The tether must allow decoupling of the bilayer from the substrate and formation of an ionic reservoir. The spacer unit of the tether often contains an oligo(ethylene glycol) (OEG) moiety. Early work indicated that tBLM anchored via short OEG spacers (n=1-3) were insufficiently decoupled from the surface[87] Raguse et al.[104] found that increasing the size of the aqueous reservoir by using longer polar tethers or by decreasing the surface density of tethered lipids with diluents resulted in improved properties of the ionic reservoir for biosensing. An alternative approach to the polyethylene glycol based tethers is the use of short peptides to support BLMs, which has been studied extensively by Knoll and co-workers[105−111]. The peptide supported tBLM supported the functional incorporation of proteins such as H^+-ATP synthase[105,106] and cytochrome c oxidase[109] but were generally associated with poor electrical properties.

5.3.3.2.   Phytanyl Lipid Derivatives for Highly Insulating Membranes

Most commonly, the sulphur functionalised lipid species ("thiolipids"), which link the tBLM to the gold surface, are derivatives of glycerophospholipids or in some instances derivatives of cholesterol[112−115] The resulting tBLMs showed relatively poor electrical properties: The membrane resistance was often orders of magnitude lower (for example see references 86, 103, 112, 116, 117) than that observed for free-standing BLM ($\sim$10 MΩ cm^2), which severely limited the ability to use changes in conduction through membrane channels as part of a transduction method for biosensors. It has been shown that SAMs of phytanylthiols provide better barrier properties than SAMs of straight alkylthiols.[118] This probably has its origin in the different phase behaviour of the chains. Due to the branched alkyl chains, phytanyl based monolayers remain in the liquid-crystalline state with "self-healing" properties, whereas alkyl monolayers are in the crystalline state and exhibit domain boundaries and crystal

defects.[118] In a number of tBLMs prepared from glycerophospholipid derivatives the lipid chains of the tethered leaflet are also found to be in the crystalline state, especially for saturated lipids (e.g.[87]), and this may account for some of the reduction in membrane resistance.

Cornell and co-workers have developed an ion channel switch biosensor based on a highly insulating tBLMs containing various phytanyl lipid species (Figure 5.4) some of which are anchored on gold electrodes via sulfur-gold bonds[23,24,119−122] (see Section 5.5.2 for details of the transduction method employed in the biosensor). The tethering components include lipids spanning the entire membrane as well as lipids residing in the bottom leaflet attached to polar tethers composed of oligo(ethylene glycol) units. To adjust the density of tethers short chain disulfides are co-adsorbed onto the gold surface during SAM formation to serve as lateral spacers. All lipid species contain phytanyl chains. The chemical composition of the tBLM is thus reminiscent of the cell membrane of prokaryotic organisms from the domain Archaea, which can grow in habitats with extreme temperatures, pH values and salt concentrations. Phytanyl lipids and membrane-spanning amphiphile species play an important role in stabilising the cell membrane under these conditions. These tBLMs were found to be stable over several months[23,123].

Recently the groups of Vogel[124] and of Knoll[101,102] independently reported tBLMs composed of a SAM of tethered phytanyl lipid derivatives on gold and an upper leaflet containing 1,2-diphytanoyl-sn-glycero-3-phosphocholine. Most importantly, the electrical properties of both biomimetic membranes closely resembled those of biomembranes with a capacitance of 6-7 mF m^{-2} and a
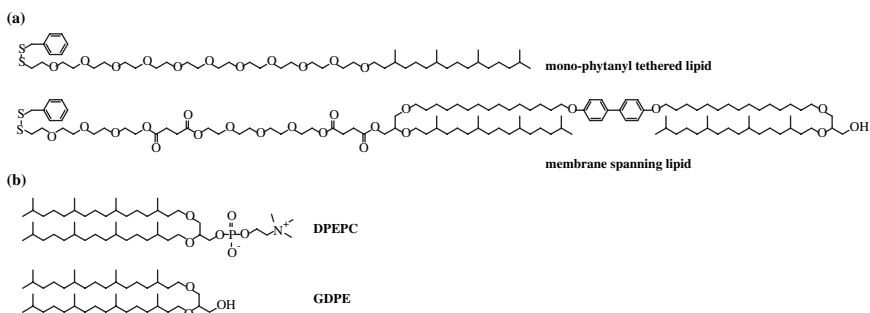
FIGURE 5.4. Chemical structures of a selection of phytanyl lipid species for formation of fluid and electrically insulating tBLMs.[100] (a) Tethered species linking the BLM to the gold substrate and forming an aqueous reservoir between the electrode and the bilayer. The tethering component with a single phytanyl chain inserted into the bottom (or inner) leaflet of the bilayer is typically used in a large excess over the membrane-spanning lipid. The properties of the reservoir region and the stability of the tBLM are improved by using ether linkages for the inner layer tethering components instead of ester linkages (which are prone to hydrolysis). (b) The remaining phytanyl lipids constituting the bilayer are untethered species such as glycerol diphytanyl ether phosphatidylcholine (DPEPC) and glycerol diphytanyl ether (GDPE).

resistance several orders of magnitude higher than values for glycerophospholipid based tBLMs.[116] The membrane resistance of the system developed by Vogel and co-workers (7 MΩ cm^2) was sufficient to observe the closure of a few individual ion channels inserted into this highly insulating tBLM using EIS. The excellent insulating properties of the tBLM by Knoll and co-workers (18-71 MΩ cm^2) were attributed not only to the superior insulating properties of the phytanyl lipids but also to the ultra-smooth template-stripped gold substrate used in these studies, which ensured the perfect supramolecular alignment of the lipid derivatives[101,102]. A similar conclusion with regard to surface roughness was drawn in a study comparing the electrical properties of thiolipid BLM on rough polycrystalline surfaces to those on mercury drop electrodes[103].

5.3.3.3. Surface Attachment via Functionalised Polymers

A number of strategies have been developed for the assembly of polymer supported tBLMs.[41] In the "top-down" concept, the lipid/lipopolymer mixture is pre-organised at the solution-air interface and then transferred onto the solid support. The "bottom-up" approach consists of a layer-by-layer deposition. First the polymer cushion is deposited onto the substrate followed by anchoring a lipid monolayer containing reactive anchor lipids on the polymer cushion. The third approach relies on self-assembly of a monolayer of lipopolymers with surface reactive side-chains for formation on the surface.[125−128] In all three approaches the bilayer is completed by transfer of the upper leaflet from the solution-air interface or by vesicle spreading.

Recent advances have shown that by choosing the appropriate polymer and fine-tuning its properties (such as the chain-length) one can fabricate tBLMs stabilised by covalent linkages at the bilayer-polymer and polymer-substrate interfaces with a high lateral mobility of lipids[129−131] and incorporated proteins.[129,131] Further these tBLMs can exhibit improved self-healing characteristics when compared to sBLMs on solid substrates.[129] These developments show the potential of polymer based tBLMs for the functional incorporation of membrane proteins, which may enable fundamental studies of interactions occurring at cell surfaces as well as biosensing platforms.

5.3.4.   Laterally Structured Bilayer Lipid Membranes

Micropatterning of supported bilayer systems is of great interest for manufacturing arrays of different recognition elements to allow the detection of multiple analytes in one device and to identify possible interferences. Furthermore, membrane microarrays hold great promise for high-throughput screening for example of compounds binding to transmembrane receptors.

The large body of work on patterned solid supported ("floating") BLMs has been reviewed by Groves and Boxer.[69] Supported BLMs can be partitioned into discrete corrals of fluid membrane by diffusion barriers. Techniques

include patterning of existing sBLMs by scratching the substrate, micro-contact printing of discrete patches of membrane, and pre-patterning (eg by photolithography) of the substrate with barrier materials followed by sBLM formation. In a recent development vesicles modified with oligonucleotides were captured on corrals of sBLMs bearing the complementary oligonucleotide sequence to prepare self-sorting arrays of mobile tethered vesicles;[132−134] this technology could provide a route for preparing arrays of integral membrane proteins.

Native biomembranes can also be selectively deposited onto ultrathin cellulose films micropatterned by deep UV photolithography or by stamping of protein barriers.[135] In both cases erythrocyte ghosts were shown to adhere and fuse only to the cellulose micropatterns to form supported bilayers.

Laterally structured tBLMs consisting of untethered regions embedded in a matrix of tethered bilayer (Figure 5.3g) can be formed on SAMs patterned by micro-contact printing,[114,115] photolithography[116] or demixing of different lipid species before transfer to the substrate.[87] Transmembrane proteins and ionophores are largely confined to the untethered regions. Micro-patterned tBLMs prepared by micro-contact printing with square domains ($15 \times 15 \ \mu m^2$) of untethered bilayer showed an increased leakage of current through the tethered regions of the bilayer[114,115] thus degrading the sensitivity for potential biosensors based on modulation of the membrane conductance. Heyse et al.[116] incorporated the transmembrane photo-receptor rhodopsin into the untethered regions of a tBLM patterned by photolithography and monitored its activation using one-dimensional imaging SPR, which demonstrated the potential for screening G-protein coupled receptors in this system. Stripe micropatterns can be formed in polymer supported tBLMs as a result of phase separation in a monolayer of lipid and lipopolymer during transfer onto a glass surface.[136] Spreading of vesicles onto the monolayer leads to stripes in the μm range of unsupported and polymer tethered bilayers. Interestingly, transmembrane receptors partition into the lipopolymer tethered region, presumably because the polymer layer can provide an aqueous reservoir sufficient for the incorporation of transmembrane proteins.

5.4.   Catalytic and Affinity Biosensors Fabricated using Supported Bilayer Lipid Membranes

5.4.1.   Catalytic Biosensors based on Supported BLMs

Several oxidase enzyme based biosensors on supported lipid bilayer membranes have been reported.[137−141] The sBLM of these systems is often formed by cutting a polymer coated metal wire (such as stainless steel, platinum or silver) while immersed into a lipid solution. The lipid coated tip of the wire is then immersed into an electrolyte solution upon which a sBLM assembles on the electrode surface.[142] Catalytic sBLM biosensors typically work in a similar

way. As shown in Figure 5.2 and the accompanying text for glucose oxidase, in the presence of oxygen oxidase enzymes react with the substrate and produce hydrogen peroxide which can be detected at an underlying electrode. In enzyme electrodes based on supported BLMs typically the enzyme is conjugated to the BLM using avidin-biotin coupling. Thus the enzyme is conjugated with biotin and incorporated within the BLM are some biotinylated phospholipids. As avidin and streptavidin have 4 binding sites for biotin molecules, avidin links the enzyme to the bilayer and the enzyme. Reaction of the enzyme with the substrate produces hydrogen peroxide which diffuses through the BLM to the underlying electrode. The rate of diffusion of the H_2O_2 through the BLM has been shown to be sensitive to the lipid composition of the BLM.[143] The resultant enzyme biosensor is sensitive, although no more sensitive than enzyme electrodes where the enzyme is attached to a SAM modified electrode,[144] but suffers from the same interference problems as most enzyme electrodes. The interference problem comes from other electroactive species in solution diffusing through the BLM and reacting at the electrode at the potential required to oxidise the hydrogen peroxide. Incorporation of the electron carrier Tetracyanoquinodimethane into the BLM can reduce the potential of detection to +0.15 V (from +0.65 V for sBLM without electron carrier) which partially solves the interference problem.[138] Another approach to reducing the problem of electroactive interferences has been to deposit a thin film of Nafion (containing ferrocene as electron relays to allow electrons to efficiently reach the underlying electrode) onto the platinum electrode before formation of the BLM.[137]

Other enzymes have also been integrated with supported BLMs in a similar manner to glucose oxidase include xanthine oxidase,[145] acetylcholine esterase, choline oxidase[141] and urease.[146] However, the enzyme based BLM biosensors discussed thus far face similar problems to other enzyme electrodes and have the additional drawbacks of the fragility and poor storage stability of the BLM without the BLM adding any distinct advantage or alternative method of transducing the biorecognition event. An exception is a study by Nikolelis and Siontorou[147] where urea, acetylcholine and penicillin have al been detected using a supported BLM incorporated within a flow injection apparatus. The BLM was formed on a microfilter support using the monolayer folding technique; enzymes were simply added to the lipid monolayer before bilayer formation. Reaction between the enzymes and the substrates produce hydronium ions which are believed to lead to a change in the electrostatic field and the phase structure of the BLM. The result is a transient current in the picoampere range which is linearly dependent on substrate concentration. A drawback of the system was that the sBLM was only stable for 10 min in air, preventing storage of the device in a dry state. To improve the stability of the lipid layer and allow storage in air the same flow injection system was used more recently in conjunction with a lipid film encased in a methacrylate polymer and modified with enzyme (acetylcholine esterase)[148] or an artificial receptor for neurotransmittors[149]; however, these systems would no longer be regarded as biomimetic membranes because the lipid films probably consist of a multilayer of lipid.[150]

5.4.2. Affinity Biosensors

5.4.2.1. Immunosensors based on Supported BLMs

There is relatively little work on supported lipid bilayer membranes for the detection of the binding of an antigen to its antibody (immune complex formation). Early work using free-standing BLM with adsorbed proteins showed a rapid transient reduction in impedance upon addition of the corresponding specific antigen or antibody.[151] Similarly, an increase in capacitance and decrease in conductance was measured by cyclic voltammetry for a simple supported BLM system formed from a mixture of lipids and hepatitus B antigens on stainless steel electrodes when hepatitus B antibodies were added to the solution.[152] In a more sophisticated system antibodies directed against the herbicide 2,4-dichlorophenoxyacetic acid (2,4-D)[153,154] or anti-human IgE antibodies[154] were anchored to the surface of sBLMs using biotin-avidin coupling and formation of the immune complex was again detected by a change in conductance and capacitance (as well as an increase in the elasticity modulus of the bilayer system). The mechanism underlying the changes of the electrical and mechanical properties in these systems upon formation of the immune complex is not well understood but thought to be induced by conformational changes of the immune complex.[154] The 2,4-D system highlighted a deficiency in the use of sBLMs for immunosensing. The authors reported in the same study that lower detection limits were achieved using a liposome immunoassay.[154] Furthermore, a simple immunosensor based on the same transduction method as the above sBLM system (ie electrical impedance spectroscopy) composed of an electrode modified with a thiol SAM and 2,4-D antibodies also exhibited a lower limit of detection.[155] This latter study highlights the importance of using biomimetic membranes for biosensing applications only when there is a distinct advantage over other approaches.

5.4.2.2. DNA Modified BLMs

Supported phosphatidylcholine bilayers on silver electrodes modified with single stranded probe DNA have been used for the detection of DNA hybridisation based on the change in its electrical properties upon duplex formation with target DNA.[156,157] Single stranded DNA with a C_{16}alkyl tail was incorporated into the upper phospholipid leaflet. This caused an increase of the ion current through the bilayer[156,157] due to structural changes caused by the adsorption of the lipid linked single stranded DNA to the surface of the lipid membrane.[158] Hybridisation of the complementary strand to the probe DNA causes a reversal of this effect due to the duplex desorbing from the surface of the lipid monolayer.[157,158] Unfortunately the sensor could not discriminate between similar sequences as partially complementary strands also gave a response.

5.4.2.3. Detection of Toxins using Hybrid BLMs, Supported BLMs and Vesicles

Charych et al.[159] developed a colourimetric sensor for the detection of receptor-ligand binding based on a hBLM consisting of a polydiacetylene (PDA) lipid
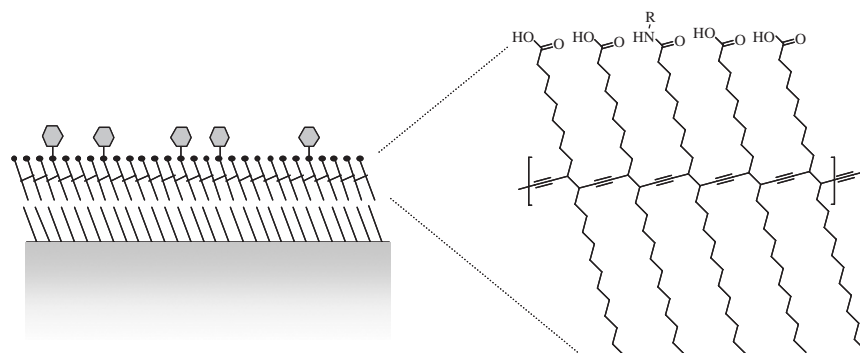
FIGURE 5.5. Schematic of the colourimetric hBLM based sensor consisting of hydrophobic SAM and polydiacetylene layer modified with biorecognition molecules. The structure of the polydiacetylene lipid layer is shown on the right. Adapted from Charych et al.[159]

layer deposited onto a octadecylsilane SAM (Figure 5.5). The PDA upper leaflet (formed by UV mediated polymerisation of diacetylenic lipid monomers) appears blue in colour. Binding of a virus to specific ligands attached to the bilayer caused a colour change from blue to red. The mechanism by which the colour change occurs is not completely understood but is believed to be due to an irreversible conformational change of the conjugated polymer backbone.[160] The sensing principle has been exploited in a number of studies using PDA vesicles modified with recognition molecules to detect influenza virus[161] or cholera toxin.[35] Biomimetic vesicles containing PDA and natural lipids have been used to monitor lipase activity[162,163] membrane active antibacterial peptides,[164] specific ions,[163,165] antibodies in solution[166] and bacterial pore forming toxin.[167] Strictly speaking the colourimetric system based on polydiacetylene lipids is not classified as a biosensor which is defined as a solid state device where a biorecognition component is integrated with a signal transducer. Here the transducer is the human eye.

Photopolymerisation of supported BLM composed of diacetylene-containing phospholipid yielded bilayers resistant toward detergent solubilisation or exposure to air.[168] Patterned bilayers could be fabricated by photolithography. The unexposed (monomeric) regions of the bilayer could subsequently be removed and the empty areas filled with a new lipid bilayer. The resulting structure consists of areas of supported BLM incorporated into the matrix of polymerised bilayer. Unfortunately it was found that the polymerisation proceeded heterogeneously possibly resulting in a reorganisation of the lipid film.

The recognition molecule GM1 was also used in an electrochemical biosensor for enterotoxin[169,170] and cholera toxin[34] employing lipid vesicles[169,170] or other lipid microstructures[34] adsorbed onto electrode surfaces. Apart from diacetylene lipids and ganglioside GM_1 the lipid structures also contained ferrocene labelled lipids. Ferrocene molecules, which are not in the immediate proximity of the electrode, would normally be regarded as too far from the electrode to be

oxidised or reduced. However, all ferrocene molecules could be interrogated electrochemically in this system due to electron hopping from ferrocene to ferrocene (Figure 5.6). Binding of enterotoxin or cholera toxin interrupted the electron-hopping pathway and a reduced current was observed. A reduced signal on binding of an analyte is usually disfavoured as false positives are more likely.

Cheng and co-workers[171,172] recently reported the preparation of sBLMs with strong resistance to air-dry damage. The bilayers were formed by fusion of positively charged ethylphosphocholine vesicles on the surfaces of poly(dimethylsiloxane) microchannels. Fluorescence recovery after photo-bleaching experiments showed a relatively high mobility of the ethylphospho-choline lipids in the sBLM, which does not change after drying and rehydrating
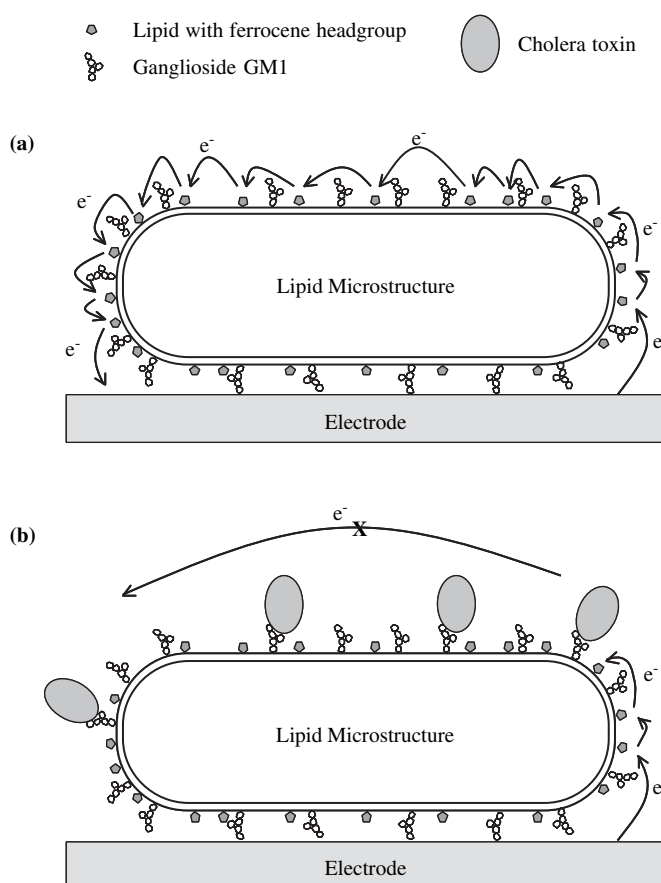
FIGURE 5.6. A schematic of the proposed mechanism for redox microstructure sensor. (a) without binding of analyte electrons can hop from one ferrocene to another whilst if cholera binds (b) the hopping pathway is blocked. Adapted from Cheng et al.[34]

of the membrane. A microflow immunoassay for the detection of cholera toxin was demonstrated by incorporation of ganglioside GM1 into the sBLMs, binding of the toxin and detection using a primary and fluorescently labelled secondary antibody.

The same recognition molecule was used by Cooper and co-workers[173] where phosphatidylcholine vesicles containing 0.1 to 2% of ganglioside GM_1 were captured on a hydrogel surface derivatised with lipophilic alkyl chain anchors. The specific binding of the cholera toxin to the vesicles was monitored via surface plasmon resonance. The dissociation constant (K_D) of the GM_1-cholera toxin binding equilibrium determined from the SPR data for serial dilutions of cholera toxin was very similar to the K_D in solution. The similarity of the K_D is important as it indicates that a lipid bilayer environment can allow the anchoring of certain biorecognition molecules with minimal disruption of the binding equilibrium. This is contrary to many other methods of immobilisation of biomolecules where the surface limits configurational freedom of the biomolecule and adversely affects the affinity between the biomolecular partners with a resultant increase in detection limit.

Swanson and co-workers[174–177] have used the multivalent character of cholera toxin to allow multiple ganglioside GM_1 to bind to the same toxin in a fluorescent biosensor (Figure 5.7). The gangliosides are labelled with either a donor or an acceptor. Binding of cholera toxin brings the donor and acceptor closer together which increases the amount of Fluorescence Resonance Energy Transfer (FRET). As a result decreased donor fluorescence and increased acceptor fluorescence is observed upon binding. An increase in sensitivity could be achieved through two-tiered energy transfer.[177] Here the emission spectrum of the donor does not overlap with the absorption spectrum of the acceptor with the advantage of a large decrease in background fluorescence due to exclusive excitation of the donor. An intermediate (also linked to GM1) is incorporated into the system to bridge the gap between the donor and the acceptor. All of these sensing principles rely on a key feature of biomimetic membranes: Formation of multivalent cholera toxin- GM1 complexes is dependent on the fluidity of the lipid bilayer to allow for lateral diffusion of GM1.[178] The optical transduction scheme could be adapted for the detection of other multivalent analytes. Compared with the commonly
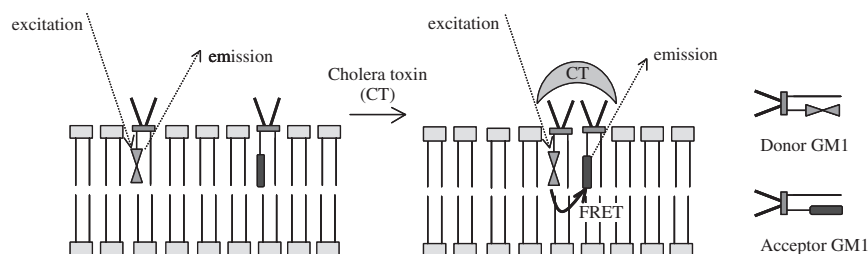
FIGURE 5.7. A schematic of the optical transduction scheme of the binding of multivalent proteins such as cholera toxin. Adapted from Song et al.[174]

used enzyme-linked immunosorbent assay (ELISA), the method showed similar sensitivity and selectivity with the added advantage of a fast response (within minutes) in a single step.[174] The possibility of developing portable biosensors was demonstrated by assembly of the phospholipid bilayer with optically tagged GM1 on planar optical waveguides.[174] The method was also adapted for (laboratory-based) flow cytometry whereby the sensing bilayers were supported on glass microspheres.[177] Using flow cytometry the detection sensitivity was improved to less than 10 pM and the method also provided kinetic information of the multivalent binding.

5.4.3. General Remarks on Supported BLMs for Biosensing Applications

The vast majority of biosensors described above which employ supported BLMs for biosensing applications are essentially using the supported BLM as an alternative method of immobilising biorecognition molecules over a transducer rather than exploiting any particular feature of the bilayers. Thus, if the issues regarding biosensor development discussed in section 5.2.2 are considered then few of these criteria are satisfied and from a commercial perspective most of the ideas discussed above are not viable. That is not to say the work is without merit as these studies have taught us a considerable amount about the strengths and limitations of using biomimetic membranes for biosensors.

Biomimetic membranes supported on polymers or hydrogels can have unacceptable levels of non-specific binding which has been attributed to the proteins and small molecules binding at sites where there are defects in the biomimetic membrane.[8] The presence of defects in the bilayer highlights another potential shortcoming of supported BLMs, especially on hard surfaces such as electrodes. The bilayers on these surfaces can be polycrystalline or amorphous in nature and thus do not have the same fluidity as a natural membrane. Furthermore the defects also arise because at a molecular level many of these surface are exceedingly rough.[179] As a consequence the lateral organisation of the bilayers due to van der Waals forces between the phospholipid tails can be disturbed.[125,180]

With the fragility of membranes and the challenges in manufacturing and storing the membranes we believe the use of biomimetic membranes is only viable if they provide a distinct advantage over other methods of immobilising biomolecules either (1) with regards to biomolecule function or (2) by providing alternative methods of transducing the biorecognition reactions. Some strategies discussed in this section utilise specific properties of biomembranes, for example by exploiting the lateral mobility of membrane lipids to enable polyvalent interactions. Both of these advantages are elegantly demonstrated by the biosensors based on ion channel gating described in the following section.

5.5.   Membrane Biosensors Based on Ion Channel Gating

5.5.1.   Signal Transduction via Ion Channels

The principle behind signal transduction at the cellular level via gated ion channels has been successfully adapted for the development of extremely sensitive BLM based biosensors. In cellular signal transduction the ion channels are in the closed state until the appropriate stimulus (binding of the ligand or change in the membrane potential) leads to opening of the channel and subsequent movement of ions through the channel pore. The use of ion channel gating in biosensing is particularly attractive because of the intrinsic amplification of the ligand binding. In a sensor the ion channel acts as a switch, the current is switched on (or off) by opening (or closing) of channels in the presence of analyte, which can be detected by an increase (or decrease) of the conductance. This sensing principle was initially demonstrated in a number of studies using free-standing BLM. For example, glutamic acid could be detected by an increase in the ion current through glutamate receptor ion channels incorporated into the BLM.[181] Cells contain a large number of ligand-gated ion channels which can be exploited for detection of their respective ligands. However, for the development of a generic ion channel based biosensor strategies are required that allow the incorporation of sites for the specific binding and subsequent switching of channel activity by new analytes. In an early approach the selectivity of nicotinic acetylcholine receptors in free-standing BLM were tailored by attachment of bispecific antibodies.[182,183] Crosslinking of the antibodies attached to the channel in the presence of the antigen analyte led to blocking of the ion channels. More recent strategies for conferring ligand specificity onto ion channels (natural and synthetic) are presented below.

5.5.1.1.   Criteria for the Biomimetic Membrane

The development of a suitable biomimetic membrane is the key requirement for commercially viable and highly sensitive biosensors. The membrane should fulfil the following requirements: (1) The bilayer should be fluid and provide a biomimetic environment for the functional incorporation of the channel molecules. This includes a sufficient aqueous region between the bilayer and the electrode. (2) The membrane should be robust and preferably stable when stored dry. (3) The bilayer should form a highly insulating layer (i.e., extremely low conductivity) as to allow the measurement of the ion current through a few or even single ion channels. This is important for achieving a low limit of detection and also essential for miniaturisation of the sensor.

These requirements can be met by a number of tethered BLM systems that closely resemble natural lipid membranes. Fabrication of these systems is discussed in Section 5.3.3. The extensive literature on the development of tBLMs by self-assembly highlights the difficulties in tuning the properties of the bilayer

components to obtain high quality bilayers with all of the desired features. Thus, the fabrication involves substantial effort in the design and synthesis of a considerable number of complex compounds. However, once the correct composition has been identified, formation of the tBLM can be achieved by self-assembly in a relatively fast and reproducible fashion.

5.5.1.2. Measurement of Membrane Conductance

The electrical properties of tethered BLM systems (with and without incorporated ion channels) are routinely determined by electrical impedance spectroscopy.[30,184] Impedance measurements are carried out by injecting a small alternating current of known frequency and small amplitude into the system and measuring the amplitude and phase difference of concomitant electrical potential that develops across it. The equivalent parallel conductance and capacitance may then be determined. In a system with electrically distinct regions the impedance (and hence the equivalent parallel conductance and capacitance) disperses with frequency. The impedance of supported bilayers is usually measured using a three electrode set-up: (1) the substrate supporting the bilayer, (2) a counter electrode in the electrolyte solution to inject current and (3) a reference electrode in the electrolyte solution to measure the voltage that develops across the system. Since the substrate supporting the bilayer serves as an electrode to inject current as well to measure the voltage, the measurement always includes the contributions due to the properties of the substrate and the interfacial regions formed at the substrate-solution interface (electrical double layer) in addition to the contributions from the solution and the bilayer itself. The capacitative and conductive properties of the different regions may be determined by fitting the impedance data to an equivalent circuit model. Each of the electrically different regions dominates in a different frequency regime. The properties of a highly insulating bilayer dominate in the lower frequency regime and hence the conductance of a BLM based biosensor should be monitored at those frequencies.

5.5.1.3. Gating of Ion Channels Incorporated into Tethered BLMs

Vogel and co-workers developed an immunosensor based on a synthetic ligand-gated ion channel (SLIC), which consists of a ligand-binding and a pore forming region. In the first study the SLIC was attached to the gold electrode via a thiolated peptide spacer, followed by self-assembly of a tethered thiolipid bilayer.[117] The gating of the channel by binding of a ligand (in this case an antibody) resulted in an increase of membrane resistance measured by EIS. The response of this type of immunosensing device was limited by the insufficient electrical resistance of the tBLM itself. To overcome this problem high resistance tBLMs composed of phytanyl lipids were utilised in a later study.[124] Incorporation of the SLIC increased the membrane conductance. Subsequent selective binding of the antibody decreased the conductance as a function of antibody concentration. The authors were able to detect the closing of a few individual channels.

Ligand-mediated modulation of channel activity has also been shown for the bacterial receptor protein OmpF incorporated into tBLMs by the micelle dilution technique.[185,186] OmpF is the receptor for the antibacterial toxin *colicin N*. Binding of the toxin closes the ion channel, which was determined by EIS. In a similar study, mutant OmpF containing a single cysteine was immobilised on gold followed by self assembly of the tBLM using a novel thiolipid for the bottom leaflet and 1,2-diphytanoyl-sn-glycero-3-phosphocholine (DPhyPC) or 1,2-dioleoyl-sn-glycero-3-phosphocholine (DOPC) for the top leaflet but the proteolipid layer had too many defects to achieve high sensitivity detection of the ligand.[187]

5.5.1.4.   Gating of Ion Channels Incorporated into Membranes on a Sensor Chip

Schalkhammer and co-workers have developed a variety of sensor chips with integrated membrane supports fabricated by thin-film techniques and photolithography for amperometric biosensors based on the modulation of membrane conductance.[188−190] The sensor chip shown in Figure 5.8 contains a supported BLM on a thin hydrogel layer separating two buffer-filled compartments. The phospholipid bilayer contains membrane-spanning bola-amphiphiles for improved robustness. Membrane spanning bis-gramicidin channels incorporated into the BLM allow a constant ionic current through the membrane separating the aqueous compartments. Binding of analyte to a ligand covalently coupled to the ion channel leads to a reduction of the measured current. Because the buffer-filled compartments provide a large ionic reservoir in both sides of the membrane the measurement can be carried out using direct current without the saturation effects observed for systems with a small ionic reservoir between the bilayer and the electrode. In a variation of the device the membrane support consists of an electropolymer deposited directly onto the electrode. In this case the BLM is tethered to the polymer support via hydrophilic spacers. The sensor has been applied to the detection of DNA sequences from the herpes virus. Unfortunately the sensor design is not yet suitable for applications in the field because the membrane displayed insufficient stability.

5.5.2.   Taking Biosensors a Step Further: The AMBRI Ion Channel Switch Biosensor

The excellent performance of these membranes certainly comes as no surprise after the seminal work of Cornell and co-workers in developing the AMBRI biosensor (Figure 5.9).[23,24,43,100,104,123,191−194] The recognition interface is comprised of a lipid bilayer which is anchored to an underlying gold electrode using alkanethiol chemistry. The lipid bilayer contains 10 or more components including the bacterial peptide gramicidin A, which forms dimeric ion channels by alignment of monomers in the two leaflets of the bilayer. Gramicidin A molecules in the bottom leaflet of the tBLM are immobilised via tethers on the gold substrate while those in the upper layer can diffuse freely.

a)
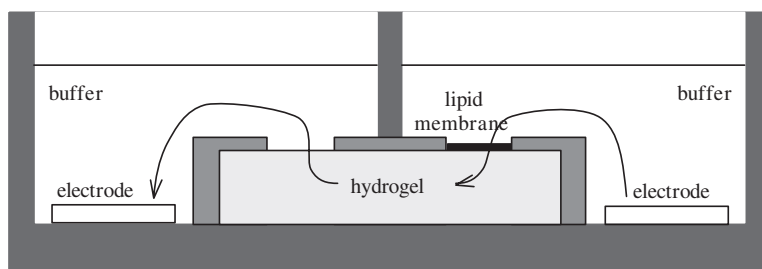
b)
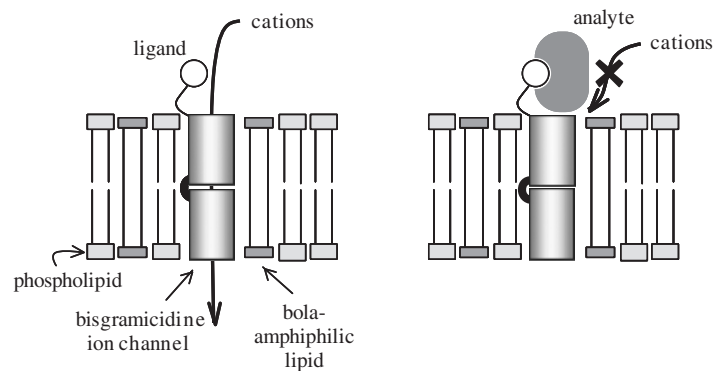
c)
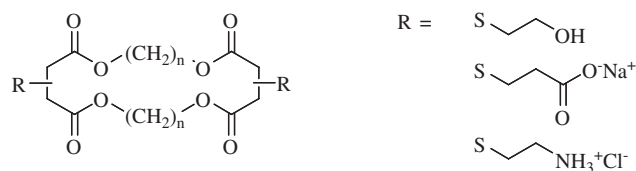
FIGURE 5.8. (a) Scheme of the sensor chip. The lipid membrane is formed on the hydrogel inside a hydrophobic frame produced by photolithography. The arrows indicate the flow of the ionic current. (b) Scheme of the sensor membrane containing phospholipids, membrane-spanning bola-amphiphilic lipids and stable bis-gramicidin channels formed by covalent head-to-head dimerisation of two monomers. The channel is modified with a binding site for the analyte. In the absence of the analyte the channel is permanently open allowing flow of cations across the membrane (shown on the left). The biorecognition event leads to a conformational change in the modified channel leading to a reduction of the ionic current (shown on the right). (c) Structure of the bola-amphiphilic lipids and a selection of hydrophilic headgroups. Adapted from Anrather et al.[190]
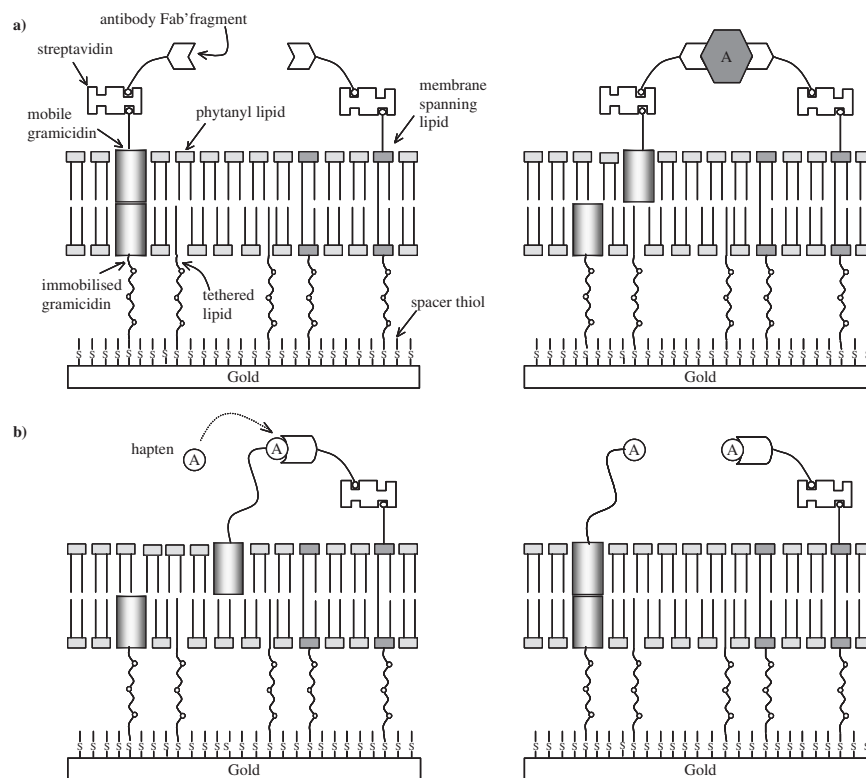
FIGURE 5.9. The ion channel biosensor based on a tethered lipid bilayer developed by AMBRI.[23] (a) Schematic of the two-side sandwich assay. The sensor membrane consists of tethered lipids and spacer thiols, which define an ionic reservoir under the bilayer composed of phytanyl lipids. Incorporated within the lower part of the bilayer are immobilised gramicidin molecules, which are bound to the electrode with a thiol. Mobile gramicidin molecules with pendant biotin groups are incorporated in the upper leaflet. Membrane spanning lipids, also with pendant biotin, span across both halves of the bilayer. Biotinylated antibody fragments are attached to both the mobile gramicidin molecules and the membrane spanning lipids using streptavidin as a molecular building block. When there is no analyte (left) present the mobile gramicidin molecules can move laterally in the upper leaflet of the bilayer. In this "open" state the mobile gramicidin molecules can form channels with immobile ones resulting in a large conductance of the membrane. When the analyte cross-links the two Fab antibody fragments (right), the gramicidin molecules in the upper leaflet can no longer diffuse freely and the ion channels are closed resulting in a decrease of the conductance. (b) Schematic of the competitive assay. The general architecture of the tBLM is the same as in (a) with the following changes: The mobile gramicidin molecules in the top leaflet are modified with a hapten, which binds to the hapten specific antibody attached membrane spanning lipids. Thus, in the absence of analyte (left) the gramicidin molecules in the upper leaflet are unable to diffuse laterally to form open ion channels. Analyte (hapten) added to the sensor (right) displaces the hapten-linked gramicidin, allowing it to diffuse freely and form ion channels with the immobilised gramicidin molecules in the lower leaflet resulting in an increase of conductance.

In one variant, the two-side sandwich assay, Gramicidin A molecules in the upper layer are derivatised with antibody Fab' fragments. In addition, antibody Fab' fragments are immobilised on the membrane surface via membrane spanning lipids. In the presence of the analyte the conductivity of the channels is "switched off" when the free diffusion of gramicidin A in the top leaflet is restricted by crosslinking the antibody Fab' fragment on the Gramicidin molecule and that immobilised on the membrane surface. This type of assay requires a large analyte (such that two antibodies can bind to it) and has been demonstrated for the detection of proteins (such as thyroid stimulating hormone) and bacteria (such as *E. coli*).

The competitive assay is designed for the detection of small molecules and has been demonstrated for the cardiac glycoside digoxin. Here digoxin molecules are tethered to the gramicidin molecules in the upper leaflet of the bilayer. In the absence of analyte conductance is turned off as the tethered digoxin binds to immobilised antibody Fab' fragments on the membrane surface. When analyte (digoxin) is present in the solution it competes for binding to the antibody and can uncouple the gramicidin molecules in the upper leaflet. Intermittent formation of ion channels as the freed gramicidin molecules diffuse freely in the upper lipid layer leads to an overall increase in the membrane conductance.

Recently the same type of tBLM has also been used for the functional incorporation of alamethicin channels and used for the detection of amiloride based inhibitors.[194] Others have investigated the ion channel switch biosensor for detecting sequences of DNA.[195] In this study the gramicidin molecules in the upper leaflet and the membrane spanning lipids were modified with oligonucleotides complementary to different regions of the target DNA strand. Duplex formation of the oligonucleotides with the respective complementary stretch on the target DNA resulted in the switching off of the ion channels. Addition of DNAse, an enzyme that digests double stranded DNA, released the gramicidin molecule allowing free diffusion and resulting in an increase of the conductance.

The elegance of biosensors is that they exploit biology's approach to selectively recognising specific molecules in a matrix containing many other things by using biological recognition molecules. Implicit in the preceding discussion is that biomimetic membranes go one step further and provide an opportunity to not only use biological molecules for recognition but to keep them in a biological type environment. The AMBRI biosensor takes this a step further. The particularly elegant aspects of this design are firstly it utilises not only biological molecules for detection but also mimics cellular approaches to transduction. In the authors' opinions the ion channel biosensor is probably the most important development in the entire biosensing field in the last 20 years. The fact that the development of the AMBRI biosensor took more than 10 years and many millions of dollars perhaps demonstrates the capital costs involved in at least the development of commercialisable biomimetic membrane based biosensors.

Added to the elegance of the concept of the ion channel biosensor is that is meets many of the challenges to biosensor development discussed in section 5.2.2. The transduction method is reasonably generic for affinity biosensors. The interface is made by self-assembled and should be reasonably reproducible. The interface will resist non-specific adsorption and even if there is some non-specific adsorption, provided it does not block access to the membrane or disrupt the membrane structure it will not affect the transduction mechanism. Because binding of the analyte to the sensor effectively switches on or off the ion channels the biosensor has exquisite sensitivity. Finally the only question is one of robustness. The AMBRI sensing chip is a "one-shot" device, which partially obviates this problem and makes it compatible with the requirements of regulatory authorities anyway. Their patent portfolio[43] also demonstrates that they have developed methodologies for drying and rehydrating the membranes as well as storing them. Having satisfied the requirements of a biosensor it is of no surprise that the release of the AMBRI biosensor onto the market place appears imminent.

5.6.   Concluding Remarks

This chapter has been written from the perspectives of what the possibilities are for using biomimetic membranes for biosensing applications and the issues that must be faced. The large amount of research into biomimetic membranes which has already been conducted clearly demonstrates the complexity of the systems but also the incredible opportunities biomimetic membranes afford not just with regards to portable analytical devices but as a research tool to understand biological membrane processes. It is the complexity of the biomimetic membrane systems which is behind our thesis that biomimetic membrane should only be used in biosensing applications when there are distinct advantages over other approaches to fabricating biosensors. The more recent work on tethered bilayers has however demonstrated some key advantages of biomimetic membranes for biosensing applications and also demonstrated that the fabrication of devices based on this technology has the potential to be commercially viable. As a consequence we are excited about the future of biomimetic membranes for the development of biosensors. The fabrication and stabilisation of tethered BLMs seems to be approaching a sufficient level of understanding for researchers to begin exploiting them for the myriad of unique biosensing opportunities these systems provide.

References

1. E. A. H. Hall, *Biosensors* (Open University Press, Buckingham, 1990).
2. D. R. Thevenot, K. Toth, R. A. Durst, and G. S. Wilson, Electrochemical Biosensors: Recommended Definitions and Classification, *Analytical Letters* **34**, 635–659 (2001).

3. T. Wink, S. J. vanZuilen, A. Bult, and W. P. vanBennekom, Self-Assembled Monolayers for Biosensors, *Analyst* **122**, R43-R50 (1997).

4. S. V. Rao, K. W. Anderson, and L. G. Bachas, Oriented Immobilization of Proteins, *Mikrochimica Acta* **128**, 127–143 (1998).

5. S. Flink, F. C. J. M. van Veggel, and D. N. Reinhoudt, Sensor Functionalities in Self-Assembled Monolayers, *Advanced Materials* **12**, 1315–1328 (2000).

6. J. J. Gooding, F. Mearns, W. R. Yang, and J. Q. Liu, Self-Assembled Monolayers into the 21(St) Century: Recent Advances and Applications, *Electroanalysis* **15**, 81–96 (2003).

7. N. K. Chaki, and K. Vijayamohanan, Self-Assembled Monolayers as a Tunable Platform for Biosensor Applications, *Biosensors & Bioelectronics* **17**, 1–12 (2002).

8. M. A. Cooper, Advances in Membrane Receptor Screening and Analysis, *Journal of Molecular Recognition* **17**, 286–315 (2004).

9. A. L. Ottova, and H. Ti Tien, Self-Assembled Bilayer Lipid Membranes: From Mimicking Biomembranes to Practical Applications, *Bioelectrochemistry and Bioenergetics* **42**, 141–152 (1997).

10. S. Heyse, T. Stora, E. Schmid, J. H. Lakey, and H. Vogel, Emerging Techniques for Investigating Molecular Interactions at Lipid Membranes, *Biochimica Et Biophysica Acta* **1376**, 319–338 (1998).

11. E. A. H. Hall, J. J. Gooding, and C. E. Hall, Redox Enzyme Linked Electrochemical Sensors: Theory Meets Practice, *Mikrochimica Acta* **121**, 119–145 (1995).

12. C. L. Baird, and D. G. Myszka, Current and Emerging Commercial Optical Biosensors, *Journal of Molecular Recognition* **14**, 261–268 (2001).

13. E. Mallat, D. Barcelo, C. Barzen, G. Gauglitz, and R. Abuknesha, Immunosensors for Pesticide Determination in Natural Waters, *Trac-Trends in Analytical Chemistry* **20**, 124–132 (2001).

14. *Optical Biosensors: Present and Future,* edited by F. S. Ligler, C. A. Rowe-Taitt (Elsevier, Amsterdam, 2002).

15. P. Skladal, Advances in Electrochemical Immunosensors, *Electroanalysis* **9**, 737–745 (1997).

16. T. Weimar, Recent Trends in the Application of Evanescent Wave Biosensors, *Angewandte Chemie-International Edition* **39**, 1219-+ (2000).

17. Z. Salamon, H. A. Macleod, and G. Tollin, Surface Plasmon Resonance Spectroscopy as a Tool for Investigating the Biochemical and Biophysical Properties of Membrane Protein Systems. Ii: Applications to Biological Systems, *Biochimica Et Biophysica Acta* **1331**, 131–152 (1997).

18. Z. Salamon, H. A. Macleod, and G. Tollin, Surface Plasmon Resonance Spectroscopy as a Tool for Investigating the Biochemical and Biophysical Properties of Membrane Protein Systems. I: Theoretical Principles, *Biochimica Et Biophysica Acta* **1331**, 117–129 (1997).

19. C. K. O'Sullivan, and G. G. Guilbault, Commercial Quartz Crystal Microbalances – Theory and Applications, *Biosensors & Bioelectronics* **14**, 663–670 (1999).

20. A. Janshoff, H.-J. Galla, and C. Steinem, Piezoelectric Mass-Sensing Devices as Biosensors-an Alternative to Optical Biosensors?, *Angewandte Chemie, International Edition* **39**, 4004–4032 (2000).

21. A. Akkoyun, and U. Bilitewski, Optimisation of Glass Surfaces for Optical Immunosensors, *Biosensors & Bioelectronics* **17**, 655–664 (2002).

22. J. D. Newman, and A. P. F. Turner, Home Blood Glucose Biosensors: A Commercial Perspective, *Biosensors & Bioelectronics* **20**, 2435–2453 (2005).

23. B. A. Cornell, V. L. B. Braach-Maksvytis, L. G. King, P. D. J. Osman, B. Raguse, L. Wieczorek, and R. J. Pace, A Biosensor That Uses Ion-Channel Switches, *Nature* **387**, 580–583 (1997).

24. B. A. Cornell, Membrane-Based Biosensors, *Optical Biosensors*, 457–495 (2002).

25. J. J. Gooding, M. Hammerle, and E. A. H. Hall, An Enzyme Electrode with Response Independent of the Thickness of the Enzyme Layer, *Sensors and Actuators B-Chemical* **34**, 516–523 (1996).

26. A. L. Ottova, and H. T. Tien, Supported Planar Lipid Bilayers (Blms) as Biosensors, *Journal of Surface Science and Technology* **16**, 115–148 (2000).

27. M. Trojanowicz, Analytical Applications of Planar Bilayers Lipid Membranes, *Membrane Science and Technology Series* **7**, 807–845 (2003).

28. M. Zhao, D. B. Hibbert, and J. J. Gooding, Solution to the Problem of Interferences in Electrochemical Sensors Using the Fill-and-Flow Channel Biosensor, *Analytical Chemistry* **75**, 593–600 (2003).

29. B. A. Cavic, G. L. Hayward, and M. Thompson, Acoustic Waves and the Study of Biochemical Macromolecules and Cells at the Sensor-Liquid Interface, *Analyst* **124**, 1405–1420 (1999).

30. H. G. L. Coster, T. C. Chilcott, and A. C. F. Coster, Impedance Spectroscopy of Interfaces, Membranes and Ultrastructures, *Bioelectrochemistry and Bioenergetics* **40**, 79–98 (1996).

31. M. Trojanowicz, Miniaturized Biochemical Sensing Devices Based on Planar Bilayer Lipid Membranes, *Fresenius' Journal of Analytical Chemistry* **371**, 246–260 (2001).

32. J. J. Gooding, E. A. H. Hall, and D. B. Hibbert, From Thick Films to Monolayer Recognition Layers in Amperometric Enzyme Electrodes, *Electroanalysis* **10**, 1130–1136 (1998).

33. C. A. Rowe-Taitt, J. J. Cras, C. H. Patterson, J. P. Golden, and F. S. Ligler, A Ganglioside-Based Assay for Cholera Toxin Using an Array Biosensor, *Analytical Biochemistry* **281**, 123–133 (2000).

34. Q. Cheng, S. M. Zhu, J. Song, and N. Zhang, Functional Lipid Microstructures Immobilized on a Gold Electrode for Voltammetric Biosensing of Cholera Toxin, *Analyst* **129**, 309–314 (2004).

35. J. J. Pan, and D. Charych, Molecular Recognition and Colorimetric Detection of Cholera Toxin by Poly(Diacetylene) Liposomes Incorporating G(M1) Ganglioside, *Langmuir* **13**, 1365–1367 (1997).

36. S. Ahn-Yoon, T. R. DeCory, and R. A. Durst, Ganglioside-Liposome Immunoassay for the Detection of Botulinum Toxin, *Analytical and Bioanalytical Chemistry* **378**, 68–75 (2004).

37. H. T. Tien, and A. L. Ottova, The Lipid Bilayer Concept and Its Experimental Realization: From Soap Bubbles, Kitchen Sink, to Bilayer Lipid Membranes, *Journal of Membrane Science* **189**, 83–117 (2001).

38. W. Knoll, F. Yu, T. Neumann, S. Schiller, and R. Naumann, Supramolecular Functional Interfacial Architectures for Biosensor Applications, *Physical Chemistry Chemical Physics* **5**, 5169–5175 (2003).

39. A. L. Ottova, and H. T. Tien, Supported Planar Blms (Lipid Bilayers). Formation, Methods of Study, and Applications, *Interfacial Catalysis*, 421–459 (2003).

40. E. K. Sinner, and W. Knoll, Functional Tethered Membranes, *Current Opinion in Chemical Biology* **5**, 705–711 (2001).

41. W. Knoll, C. W. Frank, C. Heibel, R. Naumann, A. Offenhausser, J. Ruhe, E. K. Schmidt, W. W. Shen, and A. Sinner, Functional Tethered Lipid Bilayers, *Reviews in Molecular Biotechnology* **74**, 137–158 (2000).

42. E. Sackmann, and M. Tanaka, Supported Membranes on Soft Polymer Cushions: Fabrication, Characterization and Applications, *Trends in Biotechnology* **18**, 58 –64 (2000).

43. B. Raguse, R. J. Pace, L. G. King, B. Cornell, and V. L. Braach-Maksvytis, Self-Assembly of Sensor Membranes, WO9701092, 1997.

44. A. Ottova-Leitmannova, and H. T. Tien, Bilayer Lipid Membranes: An Experimental System for Biomolecular Electronic Devices Development, *Progress in Surface Science* **41**, 337–445 (1992).

45. A. Ottova, V. Tvarozek, J. Racek, J. Sabo, W. Ziegler, T. Hianik, and H. T. Tien, Self-Assembled Blms: Biomembrane Models and Biosensor Applications, *Supramolecular Science* **4**, 101–112 (1997).

46. M. Eray, N. S. Dogan, L. J. Liu, A. R. Koch, D. F. Moffett, M. Silber, and B. J. Vanwie, Highly Stable Bilayer-Lipid Membranes (Blms) Formed on Micro-fabricated Polyimide Apertures, *Biosensors & Bioelectronics* **9**, 343–351 (1994).

47. T. D. Osborn, and P. Yager, Formation of Planar Solvent-Free Phospholipid Bilayers by Langmuir-Blodgett Transfer of Monolayers to Micromachined Apertures in Silicon, *Langmuir* **11**, 8–12 (1995).

48. S. D. Ogier, R. J. Bushby, Y. Cheng, S. D. Evans, S. W. Evans, A. T. A. Jenkins, P. F. Knowles, and R. E. Miles, Suspended Planar Phospholipid Bilayers on Micro-machined Supports, *Langmuir* **16**, 5696–5701 (2000).

49. Y. Cheng, R. J. Bushby, S. D. Evans, P. F. Knowles, R. E. Miles, and S. D. Ogier, Single Ion Channel Sensitivity in Suspended Bilayers on Micromachined Supports, *Langmuir* **17**, 1240–1242 (2001).

50. M. Mayer, J. K. Kriebel, M. T. Tosteson, and G. M. Whitesides, Microfabricated Teflon Membranes for Low-Noise Recordings of Ion Channels in Planar Lipid Bilayers, *Biophysical Journal* **85**, 2684–2695 (2003).

51. B. Schuster, and U. B. Sleytr, S-Layer-Supported Lipid Membranes, *Reviews in Molecular Biotechnology* **74**, 233–254 (2000).

52. B. Schuster, D. Pum, M. Sara, O. Braha, H. Bayley, and U. B. Sleytr, S-Layer Ultrafiltration Membranes: A New Support for Stabilizing Functionalized Lipid Membranes, *Langmuir* **17**, 499–503 (2001).

53. B. Schuster, S. Weigert, D. Pum, M. Sara, and U. B. Sleytr, New Method for Generating Tetraether Lipid Membranes on Porous Supports, *Langmuir* **19**, 2392–2397 (2003).

54. G. Favero, A. D'Annibale, L. Campanella, R. Santucci, and T. Ferri, Membrane Supported Bilayer Lipid Membranes Array: Preparation, Stability and Ion-Channel Insertion, *Analytica Chimica Acta* **460**, 23–34 (2002).

55. G. Favero, L. Campanella, A. D'Annibale, R. Santucci, and T. Ferri, Mixed Hybrid Bilayer Lipid Membrane Incorporating Valinomycin: Improvements in Preparation and Functioning, *Microchemical Journal* **74**, 141–148 (2003).

56. C. Karolis, H. G. L. Coster, T. C. Chilcott, and K. D. Barrow, Differential Effects of Cholesterol and Oxidized-Cholesterol in Egg Lecithin Bilayers, *Biochimica Et Biophysica Acta* **1368**, 247–255 (1998).

57. H. G. L. Coster, The Physics of Cell Membranes, *Journal of Biological Physics* **29**, 363–399 (2003).

58. C. Peggion, F. Formaggio, C. Toniolo, L. Becucci, M. R. Moncelli, and R. Guidelli, A Peptide-Tethered Lipid Bilayer on Mercury as a Biomimetic System, *Langmuir* **17**, 6585–6592 (2001).

59. H. Sigl, G. Brink, M. Seufert, M. Schulz, G. Wegner, and E. Sackmann, Assembly of Polymer/Lipid Composite Films on Solids Based on Hairy Rod Lb Films, *European Biophysics Journal* **25**, 249–259 (1997).

60. H. Hillebrandt, G. Wiegand, M. Tanaka, and E. Sackmann, High Electric Resistance Polymer/Lipid Composite Films on Indium-Tin-Oxide Electrodes, *Langmuir* **15**, 8451–8459 (1999).

61. H. Hillebrandt, M. Tanaka, and E. Sackmann, A Novel Membrane Charge Sensor: Sensitive Detection of Surface Charge at Polymer/Lipid Composite Films on Indium Tin Oxide Electrodes, *Journal of Physical Chemistry B* **106**, 477–486 (2002).

62. M. Tanaka, S. Kaufmann, J. Nissen, and M. Hochrein, Orientation Selective Immobilization of Human Erythrocyte Membranes on Ultrathin Cellulose Films, *Physical Chemistry Chemical Physics* **3**, 4091–4095 (2001).

63. S. Goennenwein, M. Tanaka, B. Hu, L. Moroder, and E. Sackmann, Functional Incorporation of Integrins into Solid Supported Membranes on Ultrathin Films of Cellulose: Impact on Adhesion, *Biophysical Journal*, 646–655 (2003).

64. A. L. Plant, Supported Hybrid Bilayer Membranes as Rugged Cell Membrane Mimics, *Langmuir* **15**, 5128–5135 (1999).

65. A. L. Plant, M. Gueguetchkeri, and W. Yap, Supported Phospholipid/Alkanethiol Biomimetic Membranes: Insulating Properties, *Biophysical Journal* **67**, 1126–1133 (1994).

66. V. I. Silin, H. Wieder, J. T. Woodward, G. Valincius, A. Offenhausser, and A. L. Plant, The Role of Surface Free Energy on the Formation of Hybrid Bilayer Membranes, *Journal of the American Chemical Society* **124**, 14676–14683 (2002).

67. E. Kalb, S. Frey, and L. K. Tamm, Formation of Supported Planar Bilayers by Fusion of Vesicles to Supported Phospholipid Monolayers, *Biochimica Et Biophysica Acta* **1103**, 307–316 (1992).

68. L. K. Tamm, and H. M. McConnell, Supported Phospholipid Bilayers, *Biophysical Journal* **47**, 105–113 (1985).

69. J. T. Groves, and S. G. Boxer, Micropattern Formation in Supported Lipid Membranes, *Acc Chem Res* **35**, 149–157 (2002).

70. T. M. Bayerl, and M. Bloom, Physical Properties of Single Phospholipid Bilayers Adsorbed to Micro Glass Beads. A New Vesicular Model System Studied by Deuterium Nuclear Magnetic Resonance, *Biophysical Journal* **58**, 357–362 (1990).

71. S. J. Johnson, T. M. Bayerl, W. Weihan, H. Noack, J. Penfold, R. K. Thomas, D. Kanellas, A. R. Rennie, and E. Sackmann, Coupling of Spectrin and Polylysine to Phospholipid Monolayers Studied by Specular Reflection of Neutrons, *Biophysical Journal* **60**, 1017–1025 (1991).

72. V. Kiessling, and L. K. Tamm, Measuring Distances in Supported Bilayers by Fluorescence Interference-Contrast Microscopy: Polymer Supports and Snare Proteins, *Biophysical Journal* **84**, 408–418 (2003).

73. L. K. Tamm, Lateral Diffusion and Fluorescence Microscope Studies on a Monoclonal Antibody Specifically Bound to Supported Phospholipid Bilayers, *Biochemistry* **27**, 1450–1457 (1988).

74. J. T. Groves, N. Ulman, and S. G. Boxer, Micropatterning Fluid Lipid Bilayers on Solid Supports, *Science* **275**, 651–653 (1997).

75. R. Merkel, E. Sackmann, and E. Evans, Molecular Friction and Epitactic Coupling between Monolayers in Supported Bilayers, *Journal de Physique* **50**, 1535–1555 (1989).

76. J. Salafsky, J. T. Groves, and S. G. Boxer, Architecture and Function of Membrane Proteins in Planar-Supported Bilayers: A Study with Photosynthetic Reaction Centers, *Biochemistry* **35**, 14773–14781 (1996).

77. G. Wiegand, N. Arribas-Layton, H. Hillebrandt, E. Sackmann, and P. Wagner, Electrical Properties of Supported Lipid Bilayer Membranes, *Journal of Physical Chemistry B* **106**, 4245–4254 (2002).

78. J. T. Groves, and M. L. Dustin, Supported Planar Bilayers in Studies on Immune Cell Adhesion and Communication, *J Immunol Methods* **278**, 19–32 (2003).

79. E. E. Ross, L. J. Rozanski, T. Spratt, S. Liu, D. F. O'Brien, and S. S. Saavedra, Planar Supported Lipid Bilayer Polymers Formed by Vesicle Fusion. 1. Influence of Diene Monomer Structure and Polymerization Method on Film Properties, *Langmuir* **19**, 1752–1765 (2003).

80. E. E. Ross, T. Spratt, S. Liu, L. J. Rozanski, D. F. O'Brien, and S. S. Saavedra, Planar Supported Lipid Bilayer Polymers Formed by Vesicle Fusion. 2. Adsorption of Bovine Serum Albumin, *Langmuir* **19**, 1766–1774 (2003).

81. V. Subramaniam, I. D. Alves, G. F. Salgado, P. W. Lau, R. J. Wysocki, Jr., Z. Salamon, G. Tollin, V. J. Hruby, M. F. Brown, and S. S. Saavedra, Rhodopsin Reconstituted into a Planar-Supported Lipid Bilayer Retains Photoactivity after Cross-Linking Polymerization of Lipid Monomers, *Journal of the American Chemical Society* **127**, 5320–5321 (2005).

82. G. Elender, M. Kuehner, and E. Sackmann, Functionalization of Si/Sio$_2$ and Glass Surfaces with Ultrathin Dextran Films and Deposition of Lipid Bilayers, *Biosensors & Bioelectronics* **11**, 565–577 (1996).

83. J. Majewski, J. Y. Wong, C. K. Park, M. Seitz, J. N. Israelachvili, and G. S. Smith, Structural Studies of Polymer-Cushioned Lipid Bilayers, *Biophysical Journal* **75**, 2363–2367 (1998).

84. J. Y. Wong, J. Majewski, M. Seitz, C. K. Park, J. N. Israelachvili, and G. S. Smith, Polymer-Cushioned Bilayers. I. A Structural Study of Various Preparation Methods Using Neutron Reflectometry, *Biophysical Journal* **77**, 1445–1457 (1999).

85. H. Lang, C. Duschl, M. Graetzel, and H. Vogel, Self-Assembly of Thiolipid Molecular Layers on Gold Surfaces: Optical and Electrochemical Characterisation, *Thin Solid Films* **210/211**, 818–821 (1992).

86. H. Lang, C. Duschl, and H. Vogel, A New Class of Thiolipids for the Attachment of Lipid Bilayers on Gold Surfaces, *Langmuir* **10**, 197–210 (1994).

87. C. Duschl, M. Liley, H. Lang, A. Ghandi, S. M. Zakeeruddin, H. Stahlberg, J. Dubochet, A. Nemetz, W. Knoll, and H. Vogel, Sulfur-Bearing Lipids for the Covalent Attachment of Supported Lipid Bilayers to Gold Surfaces: A Detailed Characterization and Analysis, *Materials Science & Engineering, C: Biomimetic Materials, Sensors and Systems* **C4**, 7–18 (1996).

88. A. Sevin-Landais, P. Rigler, S. Tzartos, F. Hucho, R. Hovius, and H. Vogel, Functional Immobilisation of the Nicotinic Acetylcholine Receptor in Tethered Lipid Membranes, *Biophysical Chemistry* **85**, 141–152 (2000).

89. U. Rädler, J. Mack, N. Persike, G. Jung, and R. Tampe, Design of Supported Membranes Tethered Via Metal-Affinity Ligand-Receptor Pairs, *Biophysical Journal* **79**, 3144–3152 (2000).

90. T. Stora, Z. Dienes, H. Vogel, and C. Duschl, Histidine-Tagged Amphiphiles for the Reversible Formation of Lipid Bilayer Aggregates on Chelator-Functionalized Gold Surfaces, *Langmuir* **16**, 5471–5478 (2000).

91. P. Rigler, W.-P. Ulrich, and H. Vogel, Controlled Immobilization of Membrane Proteins to Surfaces for Fourier Transform Infrared Investigations, *Langmuir* **20**, 7901–7903 (2004).

92. V. Proux-Delrouyre, J.-M. Laval, and C. Bourdillon, Formation of Streptavidin-Supported Lipid Bilayers on Porous Anodic Alumina. Electrochemical Monitoring of Triggered Vesicle Fusion, *Journal of the American Chemical Society* **123**, 9176–9177 (2001).

93. V. Proux-Delrouyre, C. Elie, J.-M. Laval, J. Moiroux, and C. Bourdillon, Formation of Tethered and Streptavidin-Supported Lipid Bilayers on a Microporous Electrode for the Reconstitution of Membranes of Large Surface Area, *Langmuir* **18**, 3263–3272 (2002).

94. A. Berquand, P.-E. Mazeran, J. Pantigny, V. Proux-Delrouyre, J.-M. Laval, and C. Bourdillon, Two-Step Formation of Streptavidin-Supported Lipid Bilayers by Peg-Triggered Vesicle Fusion. Fluorescence and Atomic Force Microscopy Characterization, *Langmuir* **19**, 1700–1707 (2003).

95. C. Bieri, O. P. Ernst, S. Heyse, K. P. Hofmann, and H. Vogel, Micropatterned Immobilization of a G Protein-Coupled Receptor and Direct Detection of G Protein Activation, *Nature Biotechnology* **17**, 1105–1108 (1999).

96. K. L. Martinez, B. H. Meyer, R. Hovius, K. Lundstrom, and H. Vogel, Ligand Binding to G Protein-Coupled Receptors in Tethered Cell Membranes, *Langmuir* **19**, 10925–10929 (2003).

97. F. Giess, M. G. Friedrich, J. Heberle, R. L. Naumann, and W. Knoll, The Protein-Tethered Lipid Bilayer: A Novel Mimic of the Biological Membrane, *Biophysical Journal* **87**, 3213–3220 (2004).

98. M. G. Friedrich, F. Giess, R. Naumann, W. Knoll, K. Ataka, J. Heberle, J. Hrabakova, D. H. Murgida, and P. Hildebrandt, Active Site Structure and Redox Processes of Cytochrome C Oxidase Immobilised in a Novel Biomimetic Lipid Membrane on an Electrode, *Chemical Communications (Cambridge, United Kingdom)*, 2376–2377 (2004).

99. K. Ataka, F. Giess, W. Knoll, R. Naumann, S. Haber-Pohlmeier, B. Richter, and J. Heberle, Oriented Attachment and Membrane Reconstitution of His-Tagged Cytochrome C Oxidase to a Gold Electrode: In Situ Monitoring by Surface-Enhanced Infrared Absorption Spectroscopy, *Journal of the American Chemical Society* **126**, 16199–16206 (2004).

100. G. Krishna, J. Schulte, B. A. Cornell, R. J. Pace, and P. D. Osman, Tethered Bilayer Membranes Containing Ionic Reservoirs: Selectivity and Conductance, *Langmuir* **19**, 2294–2305 (2003).

101. S. M. Schiller, R. Naumann, K. Lovejoy, H. Kunz, and W. Knoll, Archaea Analogue Thiolipids for Tethered Bilayer Lipid Membranes on Ultrasmooth Gold Surfaces, *Angewandte Chemie, International Edition* **42**, 208-211 (2003).

102. R. Naumann, S. M. Schiller, F. Giess, B. Grohe, K. B. Hartman, I. Kaercher, I. Koeper, J. Luebben, K. Vasilev, and W. Knoll, Tethered Lipid Bilayers on Ultraflat Gold Surfaces, *Langmuir* **19**, 5435–5443 (2003).

103. P. Krysinski, A. Zebrowska, A. Michota, J. Bukowska, L. Becucci, and M.R. Moncelli, Tethered Mono- and Bilayer Lipid Membranes on Au and Hg, *Langmuir* **17**, 3852–3857 (2001).

104. B. Raguse, V. Braach-Maksvytis, B. A. Cornell, L. G. King, P. D. J. Osman, R. J. Pace, and L. Wieczorek, Tethered Lipid Bilayer Membranes: Formation and Ionic Reservoir Characterization, *Langmuir* **14**, 648–659 (1998).

105. R. Naumann, A. Jonczyk, R. Kopp, J. van Esch, H. Ringsdorf, W. Knoll, and P. Graeber, Incorporation of Membrane Proteins in Solid-Supported Lipid Layers, *Angewandte Chemie, International Edition in English* **34**, 2056–2058 (1995).

106. R. Naumann, A. Jonczyk, C. Hampel, H. Ringsdorf, W. Knoll, N. Bunjes, and P. Graeber, Coupling of Proton Translocation through Atpase Incorporated into Supported Lipid Bilayers to an Electrochemical Process, *Bioelectrochemistry and Bioenergetics* **42**, 241–247 (1997).

107. N. Bunjes, E. K. Schmidt, A. Jonczyk, F. Rippmann, D. Beyer, H. Ringsdorf, P. Graeber, W. Knoll, and R. Naumann, Thiopeptide-Supported Lipid Layers on Solid Substrates, *Langmuir* **13**, 6188–6194 (1997).

108. E. K. Schmidt, T. Liebermann, M. Kreiter, A. Jonczyk, R. Naumann, A. Offenhausser, E. Neumann, A. Kukol, A. Maelicke, and W. Knoll, Incorporation of the Acetylcholine Receptor Dimer from Torpedo Californica in a Peptide Supported Lipid Membrane Investigated by Surface Plasmon and Fluorescence Spectroscopy, *Biosensors & Bioelectronics* **13**, 587–591 (1998).

109. R. Naumann, E. K. Schmidt, A. Jonczyk, K. Fendler, B. Kadenbach, T. Liebermann, A. Offenhausser, and W. Knoll, The Peptide-Tethered Lipid Membrane as a Biomimetic System to Incorporate Cytochrome C Oxidase in a Functionally Active Form, *Biosensors & Bioelectronics* **14**, 651–662 (1999).

110. R. Naumann, T. Baumgart, P. Graber, A. Jonczyk, A. Offenhausser, and W. Knoll, Proton Transport through a Peptide-Tethered Bilayer Lipid Membrane by the H($^+$)-Atp Synthase from Chloroplasts Measured by Impedance Spectroscopy, *Biosensors & Bioelectronics* **17**, 25–34 (2002).

111. T. Baumgart, M. Kreiter, H. Lauer, R. Naumann, G. Jung, A. Jonczyk, A. Offenhausser, and W. Knoll, Fusion of Small Unilamellar Vesicles onto Laterally Mixed Self-Assembled Monolayers of Thiolipopeptides, *Journal of Colloid and Interface Science* **258**, 298–309 (2003).

112. L. M. Williams, S. D. Evans, T. M. Flynn, A. March, P. F. Knowles, R. J. Bushby, and N. Boden, Kinetics of the Unrolling of Small Unilamellar Phospholipid Vesicles onto Self Assembled Monolayers, *Langmuir* **13**, 751–757 (1997).

113. Y. Cheng, N. Boden, R. J. Bushby, S. Clarkson, S. D. Evans, P. F. Knowles, A. Marsh, and B. Mills, Attenuated Total Reflection Fourier Transform Infrared Spectroscopic Characterization of Fluid Lipid Bilayers Tethered to Solid Supports, *Langmuir* **14**, 839–844 (1998).

114. A. T. A. Jenkins, R. J. Bushby, N. Boden, S. D. Evans, P. F. Knowles, Q. Liu, R. E. Miles, and S. D. Ogier, Ion-Selective Lipid Bilayers Tethered to Microcontact Printed Self-Assembled Monolayers Containing Cholesterol Derivatives, *Langmuir* **14**, 4675–4678 (1998).

115. A. T. A. Jenkins, N. Boden, R. J. Bushby, S. D. Evans, P. F. Knowles, R. E. Miles, S. D. Ogier, H. Schoenherr, and G. J. Vancso, Microcontact Printing of Lipophilic Self-Assembled Monolayers for the Attachment of Biomimetic Lipid Bilayers to Surfaces, *Journal of the American Chemical Society* **121**, 5274–5280 (1999).

116. S. Heyse, O. P. Ernst, Z. Dienes, K.-P. Hofmann, and H. Vogel, Incorporation of Rhodopsin in Laterally Structured Supported Membranes: Observation of Transducin Activation with Spatially and Time-Resolved Surface Plasmon Resonance, *Biochemistry* **37**, 507–522 (1998).

117. S. Terrettaz, W.-P. Ulrich, R. Guerrini, A. Verdini, and H. Vogel, Immunosensing by a Synthetic Ligand-Gated Ion Channel, *Angewandte Chemie, International Edition* **40**, 1740–1743 (2001).

118. V. Braach-Maksvytis, and B. Raguse, Highly Impermeable "Soft" Self-Assembled Monolayers, *Journal of the American Chemical Society* **122**, 9544–9545 (2000).

119. C. J. Burns, L. D. Field, J. Morgan, B. J. Petteys, J. Prashar, D. D. Ridley, K. R. A. S. Sandanayake, and V. Vignevich, Components for Tethered Bilayer Membranes: Synthesis of Hydrophilically Substituted Phytanol Derivatives, *Australian Journal of Chemistry* **54**, 431–438 (2001).

120. A. Bendavid, C. J. Burns, L. D. Field, K. Hashimoto, D. D. Ridley, K.R. Sandanayake, and L. Wieczorek, Solution- and Solid-Phase Synthesis of Components for Tethered Bilayer Membranes, *Journal of organic chemistry* **66**, 3709–3716 (2001).

121. C. J. Burns, P. Culshaw, L. D. Field, M. Islam, J. Morgan, B. Raguse, D. D. Ridley, L. Wieczorek, M. Wilkinson, and V. Vignevich, Synthesis of New Components for Tethered Bilayer Membranes and Preliminary Surface Characterization, *Australian Journal of Chemistry* **52**, 1071–1075 (1999).

122. C. J. Burns, L. D. Field, K. Hashimoto, B. J. Petteys, D. D. Ridley, and K. R. A. S. Sandanayake, A Convenient Synthetic Route to Differentially Functionalized Long Chain Polyethylene Glycols, *Synthetic Communications* **29**, 2337–2347 (1999).

123. B. A. Cornell, G. Krishna, P. D. Osman, R. D. Pace, and L. Wieczorek, Tethered-Bilayer Lipid Membranes as a Support for Membrane-Active Peptides, *Biochemical Society transactions* **29**, 613–617 (2001).

124. S. Terrettaz, M. Mayer, and H. Vogel, Highly Electrically Insulating Tethered Lipid Bilayers for Probing the Function of Ion Channel Proteins, *Langmuir* **19**, 5567–5569 (2003).

125. J. Spinke, P. Yager, H. Wolf, M. Liley, H. Ringsdorf, and W. Knoll, Polymer-Supported Bilayer on a Solid Substrate, *Biophysical Journal* **63**, 1667–1671 (1992).

126. C. Erdelen, L. Haeussling, R. Naumann, H. Ringsdorf, H. Wolf, J. Yang, M. Liley, J. Spinke, and W. Knoll, Self-Assembled Disulfide-Functionalized Amphiphilic Copolymers on Gold, *Langmuir* **10**, 1246–1250 (1994).

127. P. Theato, and R. Zentel, Stabilization of Lipid Bilayers on Surfaces through Charged Polymers, *Journal of Macromolecular Science, Pure and Applied Chemistry* **A36**, 1001–1015 (1999).

128. P. Theato, and R. Zentel, Formation of Lipid Bilayers on a New Amphiphilic Polymer Support, *Langmuir* **16**, 1801–1805 (2000).

129. M. L. Wagner, and L. K. Tamm, Tethered Polymer-Supported Planar Lipid Bilayers for Reconstitution of Integral Membrane Proteins: Silane-Polyethyleneglycol-Lipid as a Cushion and Covalent Linker, *Biophysical Journal* **79**, 1400–1414 (2000).

130. C. A. Naumann, O. Prucker, T. Lehmann, J. Ruehe, W. Knoll, and C. W. Frank, The Polymer-Supported Phospholipid Bilayer: Tethering as a New Approach to Substrate-Membrane Stabilization, *Biomacromolecules* **3**, 27–35 (2002).

131. O. Purrucker, A. Foertig, R. Jordan, and M. Tanaka, Supported Membranes with Well-Defined Polymer Tethers-Incorporation of Cell Receptors, *ChemPhysChem* **5**, 327–335 (2004).

132. C. Yoshina-Ishii, and S. G. Boxer, Arrays of Mobile Tethered Vesicles on Supported Lipid Bilayers, *Journal of the American Chemical Society* **125**, 3696–3697 (2003).

133. C. Yoshina-Ishii, G. P. Miller, M. L. Kraft, E. T. Kool, and S. G. Boxer, General Method for Modification of Liposomes for Encoded Assembly on Supported Bilayers, *Journal of the American Chemical Society* **127**, 1356–1357 (2005).

134. C. M. Ajo-Franklin, C. Yoshina-Ishii, and S. G. Boxer, Probing the Structure of Supported Membranes and Tethered Oligonucleotides by Fluorescence Interference Contrast Microscopy, *Langmuir* **21**, 4976–4983 (2005).

135. M. Tanaka, A. P. Wong, F. Rehfeldt, M. Tutus, and S. Kaufmann, Selective Deposition of Native Cell Membranes on Biocompatible Micropatterns, *Journal of the American Chemical Society* **126**, 3257–3260 (2004).

136. O. Purrucker, A. Foertig, K. Luedtke, R. Jordan, and M. Tanaka, Confinement of Transmembrane Cell Receptors in Tunable Stripe Micropatterns, *Journal of the American Chemical Society* **127**, 1258–1264 (2005).

137. M. Trojanowicz, and A. Miernik, Bilayer Lipid Membrane Glucose Biosensors with Improved Stability and Sensitivity, *Electrochimica Acta* **46**, 1053–1061 (2001).

138. M. Snejdarkova, M. Rehak, M. Babincova, D. F. Sargent, and T. Hianik, Glucose Minisensor Based on Self-Assembled Biotinylated Phospholipid Membrane on a Solid Support and Its Physical Properties, *Bioelectrochemistry and Bioenergetics* **42**, 35–42 (1997).

139. M. Snejdarkova, M. Rehak, and M. Otto, Design of a Glucose Minisensor Based on Streptavidin-Glucose Oxidase Complex Coupling with Self-Assembled Biotinylated Phospholipid Membrane on Solid Support, *Analytical Chemistry* **65**, 665–668 (1993).

140. T. Hianik, M. Snejdarkova, V. I. Passechnik, M. Rehak, and M. Babincova, Immobilization of Enzymes on Lipid Bilayers on a Metal Support Allows Study of the Biophysical Mechanisms of Enzymic Reactions, *Bioelectrochemistry and Bioenergetics* **41**, 221–225 (1996).

141. M. Rehak, M. Snejdarkova, and T. Hianik, Acetylcholine Minisensor Based on Metal-Supported Lipid Bilayers for Determination of Environmental Pollutants, *Electroanalysis* **9**, 1072–1077 (1997).

142. H. T. Tien, and Z. Salamon, Formation of Self-Assembled Lipid Bilayers on Solid Substrates, *Bioelectrochemistry and Bioenergetics* **22**, 211–218 (1989).

143. M. Otto, M. Snejdarkova, and M. Rehak, Hydrogen Peroxide/Oxygen Biosensor Based on Supported Phospholipid Bilayer, *Analytical Letters* **25**, 653–662 (1992).

144. J. J. Gooding, and D. B. Hibbert, The Application of Alkanethiol Self-Assembled Monolayers to Enzyme Electrodes, *Trac-Trends in Analytical Chemistry* **18**, 525–533 (1999).

145. M. Rehak, M. Snejdarkova, and M. Otto, Application of Biotin-Streptavidin Technology in Developing a Xanthine Biosensor Based on a Self-Assembled Phospholipid Membrane, *Biosensors & Bioelectronics* **9**, 337–341 (1994).

146. T. Hianik, Z. Cervenanska, T. Krawczynski vel Krawczyk, and M. Snejdarkova, Conductance and Electrostriction of Bilayer Lipid Membranes Supported on Conducting Polymer and Their Application for Determination of Ammonia and Urea, *Materials Science & Engineering, C: Biomimetic Materials, Sensors and Systems* **C5**, 301–305 (1998).

147. D. P. Nikolelis, and C. G. Siontorou, Bilayer Lipid Membranes for Flow Injection Monitoring of Acetylcholine, Urea, and Penicillin, *Analytical Chemistry* **67**, 936–944 (1995).

148. D. P. Nikolelis, M. G. Simantiraki, C. G. Siontorou, and K. Toth, Flow Injection Analysis of Carbofuran in Foods Using Air Stable Lipid Film Based Acetyl-cholinesterase Biosensor, *Analytica Chimica Acta* **537**, 169–177 (2005).

149. D. P. Nikolelis, C. G. Siontorou, G. Theoharis, and I. Bitter, Flow Injection Analysis of Mixtures of Dopamine, Adrenaline and Ephedrine in Human Biofluids Using Stabilized after Storage in Air Lipid Membranes with a Novel Incorporated Resorcin[4]Arene Receptor, *Electroanalysis* **17**, 887–894 (2005).

150. D. P. Nikolelis, and M. Mitrokotsa, Stabilized Lipid Film Based Biosensor for Atenolol, *Biosensors & Bioelectronics* **17**, 565-572 (2002).

151. J. del Castillo, A. Rodriguez, C. A. Romero, and V. Sanchez, Lipid Films as Transducers for Detection of Antigen-Antibody H and Enzyme-Substrate Reactions, *Science* **153**, 185–188 (1966).

152. L. G. Wang, Y. H. Li, and H. T. Tien, Electrochemical Transduction of an Immunological Reaction Via S-Blms, *Bioelectrochemistry and Bioenergetics* **36**, 145–147 (1995).

153. T. Hianik, V. I. Passechnik, L. Sokolikovi, M. Snejdarkova, B. Sivak, M. Fajkus, S. A. Ivanov, and M. Franek, Affinity Biosensors Based on Solid Supported Lipid Membranes. Their Structure, Physical Properties and Dynamics, *Bioelectrochemistry and Bioenergetics* **47**, 47–55 (1998).

154. T. Hianik, M. Snejdarkova, L. Sokolikova, E. Meszar, R. Krivanek, V. Tvarozek, I. Novotny, and J. Wang, Immunosensors Based on Supported Lipid Membranes, Protein Films and Liposomes Modified by Antibodies, *Sensors and Actuators, B: Chemical* **B57**, 201–212 (1999).

155. I. Navratilova, and P. Skladal, The Immunosensors for Measurement of 2, 4-Dichlorophenoxyacetic Acid Based on Electrochemical Impedance Spectroscopy, *Bioelectrochemistry* **62**, 11–18 (2004).

156. C. G. Siontorou, D. P. Nikolelis, P. A. E. Piunno, and U. J. Krull, Detection of DNA Hybridization Using Self-Assembled Bilayer Lipid Membranes (Blms), *Electroanalysis* **9**, 1067–1071 (1997).

157. U. J. Krull, D. P. Nikolelis, S. C. Jantzi, and J. Zeng, Electrochemical Detection of Hybridization of DNA Oligomers of Mixed Base Sequence by Surface-Stabilized Bilayer Lipid Membranes, *Electroanalysis* **12**, 921–925 (2000).

158. J. Zeng, D. P. Nikolelis, and U. J. Krull, Mechanism of Electrochemical Detection of DNA Hybridization by Bilayer Lipid Membranes, *Electroanalysis* **11**, 770–773 (1999).

159. D. H. Charych, J. O. Nagy, W. Spevak, and M. D. Bednarski, Direct Colorimetric Detection of a Receptor-Ligand Interaction by a Polymerized Bilayer Assembly, *Science* **261**, 585–588 (1993).

160. R. Jelinek, and S. Kolusheva, Polymerized Lipid Vesicles as Colorimetric Biosensors for Biotechnological Applications, *Biotechnology Advances* **19**, 109–118 (2001).

161. A. Reichert, J. O. Nagy, W. Spevak, and D. Charych, Polydiacetylene Liposomes Functionalized with Sialic-Acid Bind and Colorimetrically Detect Influenza-Virus, *Journal of the American Chemical Society* **117**, 829–830 (1995).

162. R. Jelinek, S. Okada, S. Norvez, and D. Charych, Interfacial Catalysis by Phospholipases at Conjugated Lipid Vesicles: Colorimetric Detection and Nmr Spectroscopy, *Chemistry & Biology* **5**, 619–629 (1998).

163. S. Rozner, S. Kolusheva, Z. Cohen, W. Dowhan, J. Eichler, and R. Jelinek, Detection and Analysis of Membrane Interactions by a Biomimetic Colorimetric Lipid/Polydiacetylene Assay, *Analytical Biochemistry* **319**, 96-104 (2003).

164. S. Kolusheva, L. Boyer, and R. Jelinek, A Colorimetric Assay for Rapid Screening of Antimicrobial Peptides, *Nature Biotechnology* **18**, 225–227 (2000).

165. S. Kolusheva, T. Shahal, and R. Jelinek, Cation-Selective Color Sensors Composed of Ionophore-Phospholipid-Polydiacetylene Mixed Vesicles, *Journal of the American Chemical Society* **122**, 776–780 (2000).

166. S. Kolusheva, R. Kafri, M. Katz, and R. Jelinek, Rapid Colorimetric Detection of Antibody-Epitope Recognition at a Biomimetic Membrane Interface, *Journal of the American Chemical Society* **123**, 417–422 (2001).

167. G. Ma, and Q. Cheng, Vesicular Polydiacetylene Sensor for Colorimetric Signaling of Bacterial Pore-Forming Toxin, *Langmuir* **21**, 6123–6126 (2005).

168. K. Morigaki, H. Schoenherr, C. W. Frank, and W. Knoll, Photolithographic Polymerization of Diacetylene-Containing Phospholipid Bilayers Studied by Multimode Atomic Force Microscopy, *Langmuir* **19**, 6994–7002 (2003).

169. Q. Cheng, T. Z. Peng, and R. C. Stevens, Signaling of Escherichia Coli Enterotoxin on Supramolecular Redox Bilayer Vesicles, *Journal of the American Chemical Society* **121**, 6767–6768 (1999).

170. T. Z. Peng, Q. Chen, and R. C. Stevens, Amperometric Detection of Escherichia Coli Heat Labile Enterotoxin by Redox Diacetylenic Vesicles on a Sol-Gel Thin Film Electrode, *Analytical Chemistry* **72**, 1611–1617 (2000).

171. K. S. Phillips, and Q. Cheng, Microfluidic Immunoassay for Bacterial Toxins with Supported Phospholipid Bilayer Membranes on Poly(Dimethylsiloxane), *Analytical Chemistry* **77**, 327–334 (2005).

172. K. S. Phillips, Y. Dong, D. Carter, and Q. Cheng, Stable and Fluid Ethylphosphocholine Membranes in a Poly(Dimethylsiloxane) Microsensor for Toxin Detection in Flooded Waters, *Analytical Chemistry* **77**, 2960–2965 (2005).

173. M. A. Cooper, A. Hansson, S. Lofas, and D. H. Williams, A Vesicle Capture Sensor Chip for Kinetic Analysis of Interactions with Membrane-Bound Receptors, *Analytical Biochemistry* **277**, 196–205 (2000).

174. X. D. Song, and B. I. Swanson, Direct, Ultrasensitive, and Selective Optical Detection of Protein Toxins Using Multivalent Interactions, *Analytical Chemistry* **71**, 2097–2107 (1999).

175. D. Kelly, K. M. Grace, X. Song, B. I. Swanson, D. Frayer, S. B. Mendes, and N. Peyghambarian, Integrated Optical Biosensor for Detection of Multivalent Proteins, *Optics Letters* **24**, 1723-1725 (1999).

176. X. Song, J. Shi, and B. Swanson, Flow Cytometry-Based Biosensor for Detection of Multivalent Proteins, *Analytical Biochemistry* **284**, 35–41 (2000).

177. X. Song, J. Shi, J. Nolan, and B. Swanson, Detection of Multivalent Interactions through Two-Tiered Energy Transfer, *Analytical Biochemistry* **291**, 133-141 (2001).

178. R. Wang, J. Shi, A. N. Parikh, A. P. Shreve, L. Chen, and B. I. Swanson, Evidence for Cholera Aggregation on Gm1-Decorated Lipid Bilayers, *Colloids and Surfaces, B: Biointerfaces* **33**, 45–51 (2004).

179. D. Losic, J. G. Shapter, and J. J. Gooding, Influence of Surface Topography on Alkanethiol Sams Assembled from Solution and by Microcontact Printing, *Langmuir* **17**, 3307–3316 (2001).

180. C. Duschl, and W. Knoll, Structural Characterization of Langmuir-Blodgett Multilayer Assemblies by Plasmon Surface Polariton Field-Enhanced Raman-Spectroscopy, *Journal of Chemical Physics* **88**, 4062–4069 (1988).

181. H. Minami, M. Sugawara, K. Odashima, Y. Umezawa, M. Uto, E. K. Michaelis, and T. Kuwana, Ion Channel Sensors for Glutamic-Acid, *Analytical Chemistry* **63**, 2787–2795 (1991).

182. S. R. Reiken, B. J. VanWie, H. Sutisna, D. F. Moffett, A. R. Koch, M. Silber, and W. C. Davis, Bispecific Antibody Modification of Nicotinic Acetylcholine Receptors for Biosensing, *Biosensors & Bioelectronics* **11**, 91–102 (1996).

183. M. Eray, N. S. Dogan, S. R. Reiken, H. Sutisna, B. J. Van Wie, A. R. Koch, D. F. Moffett, M. Silber, and W. C. Davis, A Highly Stable and Selective Biosensor Using Modified Nicotinic Acetylcholine Receptor (Nachr), *BioSystems* **35**, 183–188 (1995).

184. H. G. L. Coster, and T. C. Chilcott in: *Surface Chemistry and Electrochemistry of Membranes,* edited by T. Smith Sorensen (Marcel Dekker, Inc., New York, Basel, 1999).

185. T. Stora, J. H. Lakey, and H. Vogel, Ion-Channel Gating in Transmembrane Receptor Proteins: Functional Activity in Tethered Lipid Membranes, *Angewandte Chemie, International Edition* **38**, 389–392 (1999).

186. Q. Hong, S. Terrettaz, W. P. Ulrich, H. Vogel, and J. H. Lakey, Assembly of Pore Proteins on Gold Electrodes, *Biochemical Society transactions* **29**, 578–582 (2001).

187. S. Terrettaz, W.-P. Ulrich, H. Vogel, Q. Hong, L. G. Dover, and J. H. Lakey, Stable Self-Assembly of a Protein Engineering Scaffold on Gold Surfaces, *Protein Science* **11**, 1917–1925 (2002).

188. M. Smetazko, C. Weiss-Wichert, M. Saba, and T. Schalkhammer, New Synthetic, Bolaamphiphilic, Macrocyclic Lipids Forming Artificial Membranes, *Supramolecular Science* **4**, 495–501 (1997).

189. T. Schalkhammer, and F. Pittner, Membranes and Membrane DNA/RNA Sensors, WO9720203, 1997.

190. D. Anrather, M. Smetazko, M. Saba, Y. Alguel, and T. Schalkhammer, Supported Membrane Nanodevices, *Journal of Nanoscience and Nanotechnology* **4**, 1–22 (2004).

191. G. E. Woodhouse, L. G. King, L. Wieczorek, and B. A. Cornell, Kinetics of the Competitive Response of Receptors Immobilized to Ion-Channels Which Have Been Incorporated into a Tethered Bilayer, *Faraday Discussions* **111**, 247–258 (1999).

192. G. Woodhouse, L. King, L. Wieczorek, P. Osman, and B. Cornell, The Ion Channel Switch Biosensor, *Journal of Molecular Recognition* **12**, 328–334 (1999).

193. G. Krishna, J. Schulte, B. A. Cornell, R. Pace, L. Wieczorek, and P. D. Osman, Tethered Bilayer Membranes Containing Ionic Reservoirs: The Interfacial Capacitance, *Langmuir* **17**, 4858–4866 (2001).

194. P. Yin, C. J. Burns, P. D. J. Osman, and B. A. Cornell, A Tethered Bilayer Sensor Containing Alamethicin Channels and Its Detection of Amiloride Based Inhibitors, *Biosensors & Bioelectronics* **18**, 389–397 (2003).

195. S. W. Lucas, and M. M. Harding, Detection of DNA Via an Ion Channel Switch Biosensor, *Analytical Biochemistry* **282**, 70–79 (2000).

About the Contributors

Loïc J. Blum received the Doctorat de spécialité (1983) in Biochemistry and the Doctorat d'Etatès Sciences (1991) from the Université Claude Bernard-Lyon 1. He is presently Professor of Biochemistry and Biotechnology at the same University and is involved in the development of Nanobiotechnologies related topics (biosensors, bioanalytical micro and nano systems, biochips and biomimetic membranes). He is the head of both the Laboratoire de Génie Enzymatique et Biomoléculaire (LGEB) and the CNRS research unit EMB2 (Enzymes Membranes Biologiques et Biomimétiques, UMR 5013). Since 1983 author or co-author of 130 articles and book chapters, co-editor of a book on Biosensors (*Biosensor Principles and Application*, Marcel Dekker, 1991), author of a book on *Bio- and Chemi-Luminescent Sensors* (World Scientific, 1997). He is also Member of the Editorial Board of international journals: *Analytical Letters, Journal of Cellular and Molecular Medicine, Sensors, Biosensors & Bioelectronics (from 2007).*

Till Böcking is a Postdoctoral Research Associate at the School of Chemistry and School of Physics at the University of New South Wales. After obtaining a degree in Biology researching lipid oxidation in cell membranes, he completed a PhD project under the supervision of Prof. Hans Coster and Prof. Kevin Barrow at the University of New South Wales aimed at assembling biofunctional layers on silicon surfaces with a particular focus on tethered lipid bilayers. His research interests include surface modification by self-assembly to fabricate biorecognition interfaces and substrates for studying cell-surface interactions.

Agnès Girard-Egrot is biochemist by training, with a MS degree from the University of Nancy in France. During her PhD supervised by Prof. P. Coulet at the University of Lyon, where she is currently Associate Professor, she started studies on supramolecular assemblies and biomimetic membranes using the Langmuir-Blodgett technique, with more than twenty publications and two book chapters as of today, including the June 2003 *Langmuir* cover. She is a regular referee for this Journal and others, with an emphasis on biomimetic layers subjects. Through partnership with teams from two French Universities as well as Italian, Australian, and Chinese institutes, she is a member of the Nano2life international network.

J. Justin Gooding is Professor of Chemistry and the leader of the Laboratory for Nanoscale Interfacial Design at The University of New South Wales. He obtained a DPhil from Oxford University under the guidance of Prof Richard Compton before becoming a post-doctoral research associate at the Institute of Biotechnology at Cambridge University. In 1997 he returned to his native Australia as a Vice-Chancellor Post-Doctoral Research Fellow at the University of New South Wales before taking up an academic position in 1998. His research interests are in molecular level modification of surfaces using self-assembled monolayers which has led to an interest in bilayers on solid surfaces. He also leads research programs on electron transfer kinetics, electroanalytical chemistry, biosensors and biomaterials.

Donald Martin has formal training in optometry, biomedical engineering and electrophysiology (postdoctoral). He was the first Australian recipient of the Bausch&Lomb International Travel Award (1982) and his postdoctoral training was at Sydney University by winning the inaugural Medical Foundation Post-Doctoral Fellowship (1988–91). He worked with Prof Irving Fatt at the University of California (Berkeley) and he has had academic and research positions at The University of NSW, St Vincents Hospital and UTS, in addition to being a R&D consultant in contact lenses to Johnson&Johnson and Bausch&Lomb (U.S.A.). The results of his research are reported in more than 70 publications in several international journals, including *The Lancet*, and have led to patents for a novel diagnostic system for diabetic retinopathy and a novel non-invasive drug delivery system.

Don initiated the formation of the Australian research network in nanobiotechnology called *OzNano₂Life* (www.ambafrance-au.org/oznano2life). He is regularly invited to participate in international delegations in nanobiotechnology by the Australian government. He is an Executive Board Member of the Australian French Association for Science and Technology (AFAS NSW). He was invited to organise and chair panel discussions on nanobiotechnology for the Annual Conference of the Biotechnology Industry Organisation (BIO) in 2003, 2004 and 2005. He is on the editorial board for 2 international journals in nanobiosciences. His contributions to science and technology are recognised formally in the Hansard records of the NSW Parliament.

Adam Mechler received his PhD at the University of Szeged (Hungary) in Physics. Before joining the School of Chemistry at Monash University (Australia) in 2004, he spent three years at the University of California Santa Barbara (USA), and completed sabbaticals at the Uppsala University (Sweden), the Foundation of Research and Technology Hellas (Greece), and the University of Technology Sydney (UTS, Australia). He won prestigious fellowships including NATO Advanced Postdoctoral Fellowship and Monash Fellowship and has ongoing research collaborations with Melbourne, La Trobe, UTS and Uppsala Universities. His major research interest is the characterization and control of biomolecular surface processes as well as relevant surface synthesis and architecture aiming at sensor applications. His research relies in a large part on morphological characterization with atomic force microscopy, the theory of which he has also extensively studied. Dr. Mechler's works have been published in several international journals including Physical Review B, Applied Physics Letters, Nanotechnology and Advanced Materials, and have attracted more than 60 citations to date.

Stella M. Valenzuela completed her PhD studies in Immunology and Molecular Biology at the Centre for Immunology, St Vincent's Hospital and The University of New South Wales, Sydney, Australia. She received the "Young Investigator Award" for her PhD project which lead to the discovery of 2 novel proteins, the chloride intracellular ion channel protein (CLIC-1), and the cytokine, macrophage

inhibitory cytokine-1 (MIC-1). Since receiving her PhD, she has held research positions at St Vincent's Hospital, Sydney, the University of New South Wales and the University of Technology Sydney. In 2003 she was appointed Lecturer in Medical Sciences and Bionanotechnology at the University of Technology Sydney, Australia. Dr Valenzuela's research interests are in the areas of ion channel biology and bionanotechnology. She has been an active participant in the OzNano$_2$Life Network, and is a member of the UTS Institute for Nanoscale Technology. When not working on her research, her interests are travelling and spending time with her family.

Index